ansa-Metallocene based *normal* and *expanded* Calixpyrroles and Calixphyrins: Syntheses, Spectral and Structural Characterization

THESIS SUBMITTED TO
THE UNIVERSITY OF KERALA
FOR THE DEGREE OF
DOCTOR OF PHILOSOPHY
IN CHEMISTRY
UNDER THE FACULTY OF SCIENCE

By

RAMAKRISHNAN S.

PHOTOSCIENCES AND PHOTONICS SECTION
CHEMICAL SCIENCES AND TECHNOLOGY DIVISION
NATIONAL INSTITUTE FOR INTERDISCIPLINARY SCIENCE AND TECHNOLOGY (NIIST-CSIR)
TRIVANDRUM – 695 019
KERALA, INDIA

2011

DECLARATION

I hereby declare that the Ph.D. thesis entitled "***ansa*-Metallocene based *normal* and *expanded* Calixpyrroles and Calixphyrins: Syntheses, Spectral and Structural Characterization**" is an independent work carried out by me at the Photosciences and Photonics Section, Chemical Sciences and Technology Division, National Institute for Interdisciplinary Science and Technology (NIIST-CSIR), Trivandrum, under the supervision of Dr. A. Srinivasan and it has not been submitted elsewhere for any other degree, diploma or title.

In keeping with the general practice of reporting scientific observations, due acknowledgement has been made wherever the work described is based on the findings of other investigators.

Ramakrishnan S.

April 1, 2011

CERTIFICATE

This is to certify that the work embodied in the thesis entitled "***ansa*-Metallocene based *normal* and *expanded* Calixpyrroles and Calixphyrins: Syntheses, Spectral and Structural Characterization**" has been carried out by Mr. Ramakrishnan S. under my supervision and guidance at the Photosciences and Photonics Section, Chemical Sciences and Technology Division, National Institute for Interdisciplinary Science and Technology (NIIST-CSIR), Trivandrum and the same has not been submitted elsewhere for a degree.

Dr. A. Srinivasan
(Thesis Supervisor)

ACKNOWLEDGEMENTS

It is with immense pleasure, I express my gratitude and deep sense of indebtedness to Dr. A. Srinivasan, my research supervisor, for suggesting the research problem and also for his encouragement, inspiring guidance and timely advice throughout the course of this work.

I profoundly thank Dr. M. L. P. Reddy, Scientist, Inorganic Chemistry Section, for his constant discussion, encouragement and care.

I am highly grateful to Prof. M. V. George for his encouraging interactions and suggestions.

I owe my sincere thanks to Dr. Suresh Das, Director, NIIST-CSIR and former directors, Prof. T. K. Chandrashekar and Dr. B. C. Pai for providing me the laboratory facilities to carry out this research work.

My sincere thanks are due to Dr. A. Ajayaghosh, Dr. K. R. Gopidas, Dr. D. Ramaiah and Dr. K. George Thomas, Scientists of the Photosciences and Photonics Section for the suggestions and support leading to the completion of this work.

I extend my gratitude to Dr. G. Vijay Nair, Dr. Mangalam S. Nair, Dr. K. V. Radhakrishnan, Dr. R. Luxmi Varma, Dr. A. Jayalekshmy, Scientists of the Organic Chemistry Section for their timely help in the initial stages of this research work.

I express my heartfelt thanks to Dr. Babu Varghese, IIT-Chennai and Dr. E. Suresh, CSMCRI-Bhavnagar for their fruitful help in carrying out the Single Crystal X-ray Structural Analysis.

I thank sincerely Dr. V. G. Anand, Assistant Professor, IISER, Pune for his help rendered during the course of this work.

I express my sincere thanks to Dr. S. Gokulnath who taught me all the basic principles of lab chemistry with extreme patience, Dr. V. Prabhuraja, Dr. J. Sreedhar Reddy, Dr. Rajneesh Misra and Dr. Rajeev Panwar for their encouragement and support.

I wholeheartedly extend my thanks to Research Scholars of our group Ms. K. S. Anju, Ms. P. Divia, Mr. Ajesh P. Thomas, Ms. K. C. Gowri Sreedevi, Ms. P. S. Salini, Ms. M. G. Derry Holaday, Mr. R. Sabarinathan, Ms. M. Suchithra, and all the former and present members of Photosciences and Photonics Section and Organic Chemistry Section for their co-operation and timely help.

All my friends at NIIST, IIT-Chennai, CSMCRI-Bhavnagar and NISER-Bhubaneswar are acknowledged for their support.

I am thankful to Ms. Saumini Mathew, Mr. Adarsh, Mr. Preethanuj for NMR, Dr. Moni, IIT-Chennai for ^{13}C NMR spectra, Ms. S. Viji for FAB-mass, Mr. Deepak for IR-spectra, Ms. Sarada Nair and Mr. Robert Philip for general help.

I am obliged to all my teachers for their help and encouragement at different stages of my life.

K. J. Jerly Sir and Dr. Mahesh Hariharan are immensely acknowledged for introducing me to the world of chemistry.

I am deeply grateful to my family for their constant love and care.

Finally, UGC, CSIR and DST are highly acknowledged for the financial support.

Ramakrishnan S.

Contents

List of Tables

List of figures

List of Abbreviations

$BF_3.OEt_2$	borontrifluoride diethyletherate
Cbz	benzyl carbamate
CCD	cambridge crystallographic data
$CDCl_3$	deuterated chloroform
COSY	correlation spectroscopy
Cp	cyclopentadienyl
CSA	cystamine
DDQ	2,3-dichloro-5,6-dicyano-1,4-benzoquinone
DMSO	dimethylsulphoxide
EtOAc	ethyl acetate
FAB	fast atomic bombardment
FT-IR	fourier transformation infra red
$LiAlH_4$	lithium aluminium hydride
MSA	methanesulphonic acid
NBS	N-bromosuccinimide
NMR	nuclear magnetic resonance
ROMP	ring opening metathesis polymerization
2,3,2-tet	N,N'-bis(2-aminoethyl)-1,3-propanediamine
TFA	trifluoroacetic acid
TFCP	*meso*-tetraferrocenylcalix[4]pyrrole
THF	tetrahydrofuran
TLC	thin layer chromatography

TMEDA	N,N,N’,N’-Tetramethylethylenediamine
TMS	tetramethylsilane
p-TSA	*para*-toluene sulphonic acid
UV	ultraviolet

PREFACE

Supramolecular assemblies with cyclic structures, particularly pyrrole receptors, have attracted considerable attention due to their potential application in the areas of host–guest chemistry, molecular recognition and catalysis. Amongst various receptors, calixpyrroles contains only sp^3 hybridized *meso* carbons whereas calixphyrins contain a mixture of both sp^2 and sp^3 hybridized *meso* carbon bridges. Calixpyrroles function as anion binding receptors where as calixphyrins can bind with both cations and anions. On the other hand, *ansa*-ferrocene type bridged pyrrolic systems, metallocene appended porphyrins, *meso*-ferrocenyl calixpyrroles and calixphyrins have been found to be suitable for anionic guests, multiple electron transfer reactions and molecular electronic devices. However, incorporating metallocenes into the backbone of the fully/partially conjugated macrocycles are rare.

The compounds of metallocenes with interannular bridge have emerged as an important area in the field of *ansa*-metallocenes. Most of the examples reported in the literature mainly contains either single, double or more elements as a bridge which connects the two cyclopentadienyl rings of the metallocene, forms the basis of the first chapter. However, our work is mainly concentrated on the introduction of heteroaromatic rings mainly pyrrole, thiophene and furan rings as the interannular bridge which connects the two cyclopentadienyl rings of the metallocenes mainly ferrocene and ruthenocene which results in the formation of pyrrole based macrocycles which can be called as *ansa*-metallocene-based calixpyrroles and calixphyrins.

The second chapter deals with the syntheses, spectral and structural characterization of precursors mainly 1,1'-metallocenyl-bis(*gem*-diaryl/arylalkyl/ cyclohexyl/dialkylhydroxy)methane and 1,1'-metallocenyl-bis-(*gem*-diaryl/arylalkyl/

cyclohexyl/dialkylpyrrolyl)methane. The 1,1'-ferrocene diols were synthesized from the reaction of 1,1'-bis-lithiated salt of ferrocene with various ketones ranging from diaryl, arylalkyl, cyclohexyl to dialkyl ketones. The acid-catalyzed condensation of these diols and pyrrole resulted in the formation of 1,1'-ferrocenyl dipyrromethanes. All these precursors were characterized by the standard spectroscopic techniques like FAB-mass, ^{1}H NMR and finally confirmed by single crystal X-ray diffraction analysis. The same synthetic methodology has been exploited in the next higher metallocene such as ruthenocene.

The third chapter deals with the syntheses, spectral and structural characterization of *ansa*-ferrocene-based *normal* calixpyrroles. Here, the *meso*-dialkyldipyrromethane acts as the interannular bridge between the two cyclopentadienyl rings of ferrocene, incorporating metallocene in the mainframe work of calixpyrroles in an *ansa* type way. These macrocycles were synthesized by the acid catalysed condensation of 1,1'-ferrocenyldipyrromethanes with the respective ketones. All these new macrocycles were characterized by the standard spectroscopic techniques like FAB-mass, ^{1}H NMR and finally confirmed by single crystal X-ray diffraction analysis. The final macrocycles adopt partial 1,2-alternate conformation in the solid state. The structural analysis clearly shows that these macrocycles retain the parent calix[4]pyrrole behaviour. By using similar synthetic methodology, the same chemistry has been further extended to next higher metallocene, such as, ruthenocene and observed the similar trend.

Incorporation of metallocenes in the main framework of calixphyrins based macrocycles forms the subject of the fourth chapter. *p*-TSA catalysed condensation of 1,1'-ferrocenyldiaryldipyrromethanes with the electron withdrawing and electron donating aryl-aldehydes followed by oxidation with DDQ results in the formation of

ansa-ferrocene-based *normal* calixphyrins. By changing the aryl substituted 1,1'-ferrocenyl precursor to alkyl substituted, apart from *normal* calixphyrins, *expanded* calixphyrins were also obtained. All these new macrocycles were characterized by the standard spectroscopic techniques like FAB-mass, ^{1}H NMR and finally confirmed by single crystal X-ray diffraction analysis. Since, they bear analogy to both calixpyrroles and porphyrins, which can be called as calix[*n*]metallocenyl[*m*]phyrins where n = 1, 2 and m = 2, 4. In addition to this, the role of aryl *vs.* alkyl is also highlighted to explain the formation of *expanded* macrocycles. Similar results were obtained with the next higher metallocene, such as ruthenocene.

In addition to pyrrole, the fifth chapter is concerned with the introduction of one more heterocyclic ring mainly thiophene and furan in the above mentioned macrocycles which results in the formation of *ansa*-ferrocene-based core-modified *expanded* calixpyrroles and calixphyrins. All the new macrocycles were characterized by standard spectroscopic analysis and further confirmed by single crystal X-ray analysis. From the single crystal X-ray structural analyses, it is clear that *ansa*-ferrocene-based calix[2]pyrrole[1]thiophene adopts 1,3-alternate conformation in the solid state and retains the parent calix[4]pyrrole behaviour whereas *ansa*-ferrocene-based calix[2]phyrin[1]thiophene is partially planar.

Chapter 1

ansa-Metallocenes

1.1 Introduction

The discovery of ferrocene [Kealy and Pauson 1951, Miller *et al*. 1952] and the elucidation of its bis-pentahapto sandwich structure 60 years ago [Wilkinson *et al*. 1952, Fischer and Pfab 1952] have resulted in one of the most important developments in modern organometallic chemistry mainly in bis-cyclopentadienyl-transition metal and lanthanide metal compounds. Related metallocene structures have been extended to multinuclear compounds having Cp ligands, half-sandwich type compounds, more importantly, the cyclopentadienyl ring can be modified in a virtually limitless number of ways in order to influence the electronic properties, steric and co-ordination environment of the metal. A very popular modification to the metallocene ligand framework is the inclusion of a linking group between the two cyclopentadienyl rings of the same metallocene, called an interannular bridge (Chart 1.1).

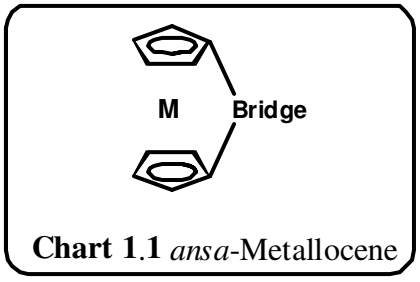

Chart 1.1 *ansa*-Metallocene

Complexes with this feature were originally called as metallocenophanes and this term is still applied mainly to bridged metallocene complexes of the Group 8 metals. However, the name '*ansa*-metallocene' is now more commonly used in reference to bent-metallocene complexes of the early transition metals, lanthanides and main group metals. The term *ansa*-

metallocene (*ansa* being Greek for "handle" meaning bent handle, attached at both ends) was coined by Lüttringhaus and Kullick to describe alkylidene-bridged ferrocenes, which was developed in the 1950's [Lüttringhaus and Kullick 1958, Lüttringhaus and Kullick 1961]. Brintzinger and co-workers pioneered the design and syntheses of these complexes [Smith *et al*. 1979, Wild *et al*. 1982, Wild *et al*. 1985, Wochner *et al*. 1985]. *Ansa*-metallocenes have recently been investigated in two main areas: as olefin polymerization catalysts with the early transition metals like zirconium at metal center [McKnight and Waymouth 1998, Dahlmann *et al*. 1999, Coates 2000], and as the basic monomer unit in organometallic polymers prepared by ring-opening polymerization with the late transition metal incorporated as the metal center [Mizuta *et al*. 2000, Archer 2001]. In the former case, the metal center is strongly bonded to the Cp ring; in contrast, in the latter case, the metal center is relatively weakly co-ordinated with the carbon rings and hence the ligands are very labile. *Ansa*-metallocenes made a huge splash in the polymer industry with the report by Kaminsky and Brintzinger that C2-symmetric *ansa*-zirconocene complexes activated by methylalumoxane produce highly isotactic polypropylene [Kaminsky *et al*. 1985]. A plethora of *ansa*-metallocene complexes of the Group 4 metals, the Group 3 metals, and the lanthanide metals have since been developed, largely for their application as alkene polymerization catalysts, catalyst models [Brintzinger *et al*. 1995, Kaminsky 1998, Hlatky 1999] and also as catalysts for asymmetric synthetic organic transformations. Some *ansa*-metallocenes are active in Ziegler-Natta catalysis, although none are used commercially [Wang 2006]. The introduction of a bridge, spanning both Cp rings prevents internal cyclopentadienyl rotation and increases the rigidity of the molecule, which has been exploited in homogeneous Ziegler-Natta catalysis. Furthermore, *ansa*-bridging can be used

for the generation of highly strained, ring tilted metallocenes, thereby offering a possibility to influence their electronic structure [Pudelski *et al*. 1995].

Often *ansa*-metallocenes are described in terms of the angle defined by the two Cp rings. In titanocene dichloride, this angle is 58.5˚ whereas in the *ansa*-titanocene $Me_2Si(C_5H_4)_2TiCl_2$, the angle is 51.2˚ [Bajgur *et al*. 1985]. The bridge on these *ansa*-metallocenes plays a very important role in the application of these compounds in catalysis and also in organic synthesis. These bridges affect the activity and stereoselectivity of these catalysts mainly by steric effect and electronic effect [Shapiro 2002].

1.2 Types of *ansa*-metallocenes

1.2.1 Atom bridged *ansa*-metallocenes

There are series of atom bridged *ansa*-metallocene such as single atom bridged, two atom bridged, three and long atom bridged, double bridged metallocene etc.

1.2.1.1 Single atom bridged metallocenes

Different kind of single atom bridged metallocenes are silicon, carbon, germanium, tin, phosphorus and boron bridged ones. The first single element bridged *ansa*-ferrocene compound **1** (Figure 1.1) was synthesized by Osborne and whiteley in 1975 [Osborne and

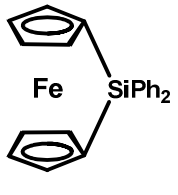

1

Figure 1.1. Silicon bridged *ansa*-ferrocene

whiteley 1975], where they have incorporated silicon in the bridging position. The most commonly studied single atom bridged *ansa*-metallocenes are dimethylsilylene bridged *ansa*-zirconocene **2** (Figure 1.2). Silylene bridged zirconocene are more efficient than the

corresponding hafnocene and titanocene catalysts in olefin polymerization [Stehling *et al*. 1994]. The main types of carbon bridged metallocenes are isopropylene bridged *ansa*-zirconocene **3** (Figure 1.2) [Dang *et al*. 1999], cycloalkylidene bridged highly active and thermally stable *ansa*-titanocene [Xu *et al*. 2001, Wang *et al*. 2005]. There are only a few examples for germanium bridged compounds of which the most commonly used are dimethylgermylene bridged zirconocene **4** (Figure 1.2) [Spaleck *et al*. 1990, Tian *et al*. 2001, Xu *et al*. 2002]. Among the single atom bridged metallocene catalysts, boron atom bridged ones **5** (Figure 1.2) are the most exploited mainly due to its lewis acidic nature [Reetz *et al*. 1999, Shapiro 2001, Braunschweig *et al*. 2003, Ashe III *et al*. 2004, Shapiro *et al*. 2004].

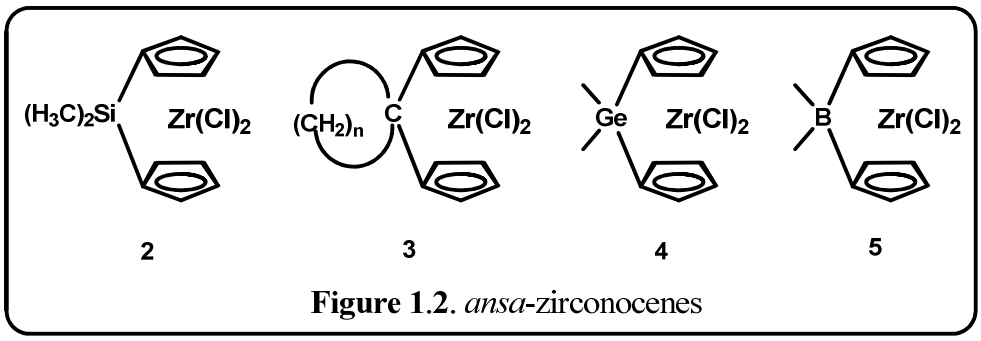

Figure 1.2. *ansa*-zirconocenes

Müller and co-workers reported the synthesis and structural characterization of first aluminium-bridged sandwich compound of *ansa*-ferrocene **6** (Figure 1.3) [Schachner *et al*. 2005]. Manners and co-workers elucidated the synthesis and characterization of the first examples of strained metallocenophanes **7-9** (Figure 1.3) with late transition metals particularly Nickel, Palladium and Platinum in the bridge. These are strained, unexpectedly electron-rich species containing square-planar d^8 centers. The synthesis was done by reaction of the corresponding $[MCl_2(P\textit{n}\text{-}Bu_3)_2]$ [M = Ni, Pd, and Pt] with dilithioferrocene.tmeda [Whittell *et al*. 2008, Matas *et al*. 2010]. Müller and co-workers also reported the synthesis and characterization of polyferrocene with gallium in bridging positions by the polymerization of Galla[1]ferrocenophane **10** [Bagh *et al*. 2010].

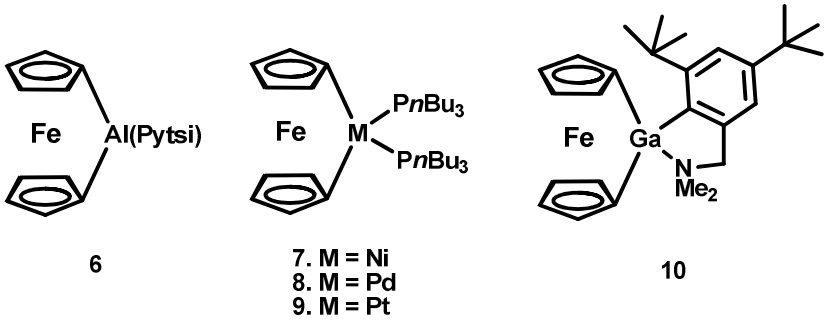

6 7. M = Ni 8. M = Pd 9. M = Pt 10

Figure 1.3. Metal atom bridged *ansa*-ferrocene

The single atom bridged [1]-ferrocenophanes shown in figure 1.4 with main-group elements in the bridging position are known in the literature from group 16 (S **11**, Se **12**) [Pudelski *et al*. 1995, Rulkens *et al*. 1997], 15 (P **13**, As **14**) [Stoeckli-Evans *et al*. 1980, Osborne *et al*. 1980, Seyferth and Withers 1982, Butler *et al*. 1983], 14 (Si **1**, Ge **15)** [Osborne and Whiteley 1975, Foucher *et al*. 1992, Stoeckli-Evans *et al*. 1980, Osborne *et al*.

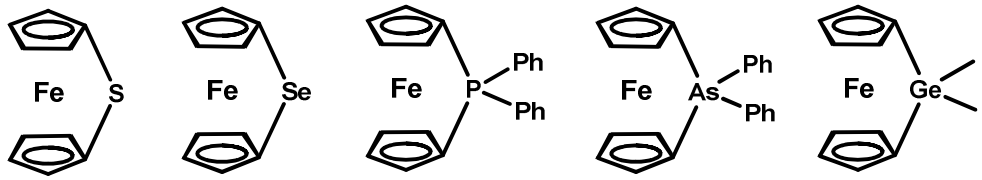

11 12 13 14 15

Figure 1.4. Group 14, 15, 16 elements bridged *ansa*-ferrocene

1980, Foucher *et al*. 1994, Rulkens *et al*. 1996, Jäkle *et al*. 1998] and 13 (B) elements [Braunschweig *et al*. 1997, Berenbaum *et al*. 2000], with the [1]boraferrocenophanes being the most recent examples in this series. The first *ansa*-zirconocenes with aluminum **16** or gallium **17** (Figure 1.5) in bridging positions were synthesized by Müller and co-workers in 2010 [Lund *et al*. 2010]. They have also done the polymerization using gallium-bridged zirconocenophane.

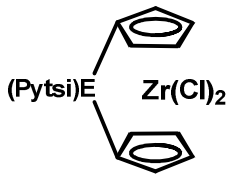

16. E = Al
17. E = Ga

Figure 1.5. Group 13 elements bridged *ansa*-zirconocene

1.2.1.2 Two atom bridged metallocenes

The two atom bridged *ansa*-metallocenes are ethylidene bridged zirconocene complex **18** (Figure 1.6) [Jin *et al*. 1998, Lee *et al*. 1998, Lee *et al*. 2002]. Wrackmeyer and co-workers reported the two tin atom bridged *ansa*-ferrocene **19** (Figure 1.6) [Herberhold *et*

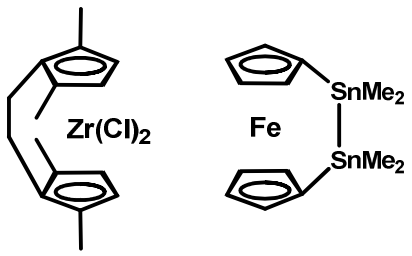

18 **19**

Figure 1.6. Two atoms bridged *ansa*-metallocene

al. 1996]. Manners and co-workers reported the cleavage of bridging C-C bonds of group 8 dicarba[2]metallocenophanes in the melt at elevated temperatures and performed detailed studies of this novel reactivity to gain insight into the mechanism of thermal ROP observed in related derivatives [Herbert *et al*. 2010].

1.2.1.3 Three atom bridges

Three atom and longer bridges (Figure 1.7) are not much exploited due to its less rigidity and less stereochemical control in catalytic reactions and organic synthetic reactions. The most commonly used are *ansa*-titanocene based trimethylene bridged systems **20** [Davis and Bernal 1971, Dormund *et al*. 1976, Schnutenhaus and Brintzinger 1979]. Wrackmeyer and co-workers reported the three tin atom bridged *ans*a-ferrocene **21** [Herberhold *et al*. 1996]. The stereoisomers of disiloxane-bis(1-indenyl)-*ansa*-ferrocene **22** were prepared by the reaction of disiloxane-bis-1,3-inden-1'-yl anion with $FeCl_2$; the diastereomers were separated by column chromatography and recrystallized from *n*-heptane [Amako *et al*. 2005]. These isomers were also characterized by ^{1}H, ^{13}C, and ^{29}Si NMR and IR spectroscopy. The *ansa*-ferrocene with 1,1'-polysilyl unit **23** was reported and studied the Si-Si insertion chemistry.

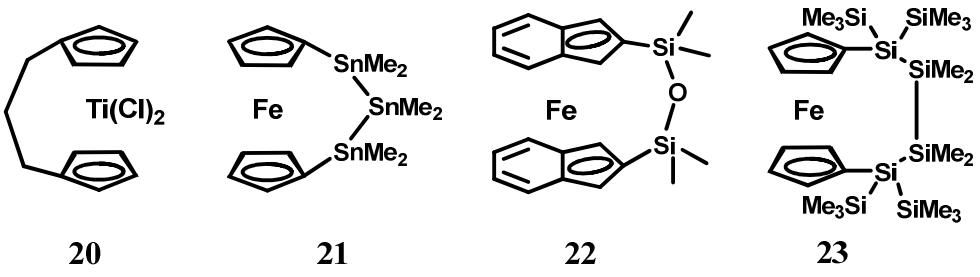

Figure 1.7. Three or higher atoms bridged *ansa*-metallocene

The *ansa*-ferrocene with a 1,1'-tetramethyldisilanylene bridge has been studied to some extent with respect to Si-Si insertion chemistry [Finckh *et al*. 1992, Finckh *et al*. 1993, Peckham *et al*. 1995, Wagner *et al*. 2007]. Despite the presence of sterically demanding SiMe substituents on the cyclopentadienyl rings, these compounds were found to undergo thermal ring-opening polymerization at 170˚C to produce very soluble, high molecular weight poly(ferrocenylsilane).

1.2.2 Functional groups bridged *ansa*-metallocenes

A large variety of metallocene-functionalized macrocyclic ligands in an *ansa* type way have been reported, including crown ethers as well as polyaza- and polythiamacrocycles, Schiff-base and mixed-donor ligand systems, with various binding motifs of the metallocene functional groups. The *ansa*-metallocene ligand has inspired the design of related bridged ligand frameworks. These include cyclopentadienyl-type ring systems tethered to amine [Jäkle *et al*. 1996], amide [McKnight and Waymouth 1998], alkoxide [Rieger 1991, Chen *et al*. 1997], ether [Qian *et al*. 1998], phosphine [Kettenback and Butenschön 1990], phosphide [Kunz *et al*. 2001], arene ligands [Deckers *et al*. 2000] and interannular-bridged bis(η^6-arene) [Elschenbroich *et al*. 1997], bis(dicarbollide) [Varadarajan *et al*. 1992], and bis(boratabenzene) [Ashe *et al*. 2001] transition metal complexes.

1.2.2.1 *ansa*-Ferrocene based Crown Ethers

ansa-Ferrocene based crown ethers are shown in Figure 1.8. In 1986, Saji showed that *ansa*-ferrocene crown ether molecule **24** [Saji 1986] which could be used as an electrochemical sensor for alkali metal cations via a mixture of through space and bond interactions, where two of the co-ordinating oxygen atoms are attached to the ferrocenyl cyclopentadienyl ring. Gokel and co-workers reported a ferrocene cryptand molecule **25** in which an aza crown ether acts as a bridge between two cyclopentadienyl rings of the ferrocene, which is used for the selective complexation with alkali metal ions mainly sodium ions and transition metal ions exclusively silver ions [Medina *et al*. 1992]. A different type of *ansa*-ferrocenyl crown ether moiety **26** was reported which also showed selectivity towards Na^+ and Li^+ ions [Plenio and Diodone 1995]. Hall and Chu have used cyclic voltammetry method to investigate the co-ordination of alkaline earth and lanthanide metal

cations by a series of ferrocene cryptands such as compound **27** [Hall and Chu 1995]. Plenio and Aberle reported the synthesis and metal complexes of oxa ferrocene cryptand **28** [Plenio and Aberle 1998].

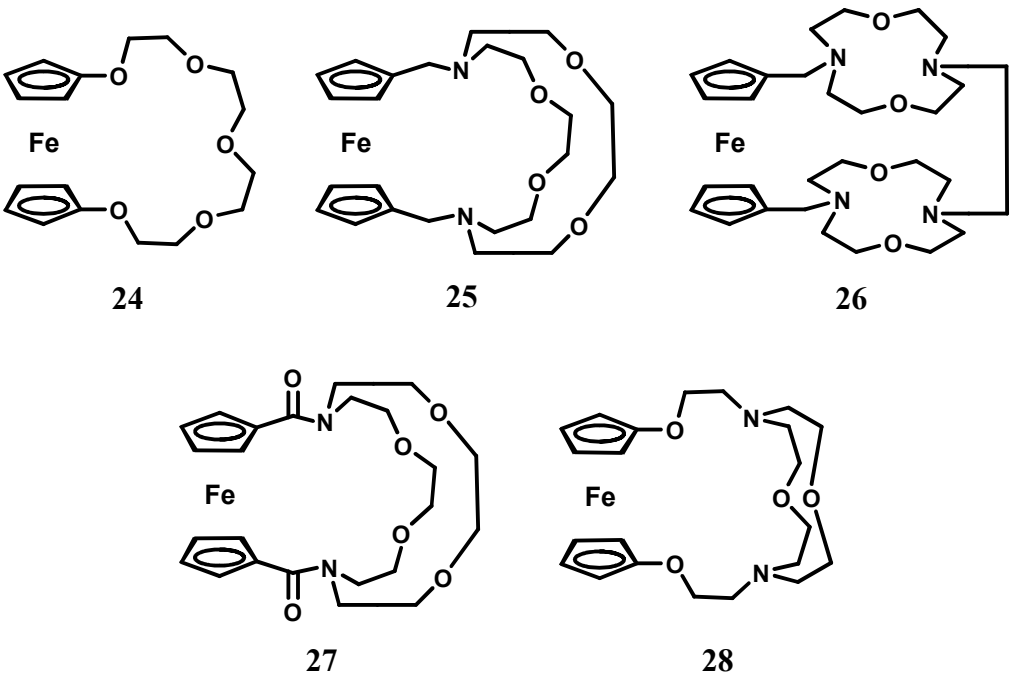

Figure 1.8. *ansa*-ferrocene based crown ethers

1.2.2.2 *ansa*-Ferrocene based Ruthenium Bipyridyl Complex

Compound **29** (Figure 1.9) contains multiple redox centers such as redox-active ruthenium bipyridyl moiety in addition to a ferrocenyl group [[b]Beer *et al*. 1997]. In the presence of chloride anions, the amide substituted bipyridyl reduction wave is shifted cathodically by 40 mV whereas the ferrocene–ferrocenium redox couple is shifted cathodically by 60 mV. The cathodic shift is therefore observed for both redox centers in this receptor species.

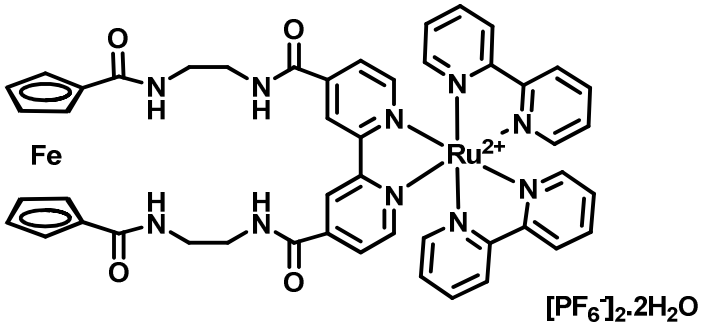

29

Figure 1.9. *ansa*-ferrocene based ruthenium bipyridyl complex

1.2.2.3 *ansa*-Ferrocene with Pyrazabole Bridges

Wagner and co-workers reported a variety of stereorigid *ansa*-ferrocene derivatives, where one such derivative **30** is shown in Figure 1.10. Such derivatives were established by B-N adduct formation [Jäkle *et al*. 1996]. These compounds were obtained by the reaction of 1,1'-diborylferrocene with selected pyrazole derivatives. The introduction of pyrazabole bridge did not have any effect on the ferrocene core.

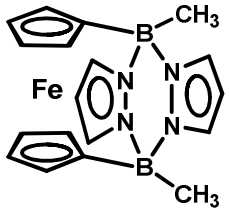

30

Figure 1.10. *ansa*-ferrocene with pyrazabole bridge

1.2.2.4 *ansa*-(alkenyl)-Ferrocene

Tilley *et al* reported the vinylene-bridged *ansa*-ferrocene complex **31** (Figure 1.11) which was synthesized by the McMurry coupling of 1,1'-ferrocenedicarbaldehyde [Buretea and Tilley 1997]. The ring opening metathesis polymerization of this strained metallocene afforded poly(ferrocenylenevinylene) as an insoluble orange solid which has a conductivity of 10^{-3} $ohm^{-1}cm^{-1}$ after doping with iodine. By the ring-closing metathesis reaction of 1,1'-

diallylmetallocene using Grubb's complex $RuCl_2$-(=CHPh)$(PCy_3)_2$, Ogasawara and co-workers reported a variety of but-2-ene bridged metallocene **32** (Figure 1.11) [Ogasawara *et al*. 2002].

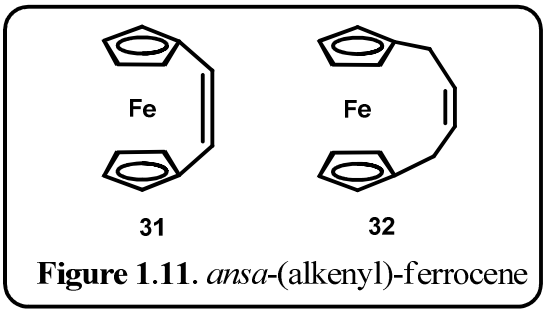

Figure 1.11. *ansa*-(alkenyl)-ferrocene

1.2.2.5 *ansa*-Ferrocene with both Trisulfide and Hydrocarbon Straps

Rauchfuss reported another kind of *ansa*-ferrocene **33** (Figure 1.12) in which the cyclopentadienyl rings are linked via two different straps [Brandt *et al*. 1998]. One strap contains the trisulfide linkage and the other strap is a hydrocarbon part. These two different straps acted as inter annular bridges.

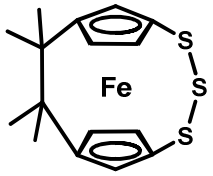

33

Figure 1.12. Trisulfide and Hydrocarbon bridged *ansa*-ferrocene

1.2.2.6 *ansa*-Ferrocene-based Bipyridine Boronium Bridges

Wagner *et al* reported the synthesis and structural characterization of *ansa*-ferrocene complex **34** (Figure 1.13) in which 2,2'-bipyridylboronium substituents [Ding *et al*. 2001, Ma *et al*. 2002] acts as a linking group between the two cyclopentadienyl rings. Electronic communication between the two 2,2'-bipyridylboronium substituents was observed suggesting the reduced forms to be partially delocalized redox intermediates.

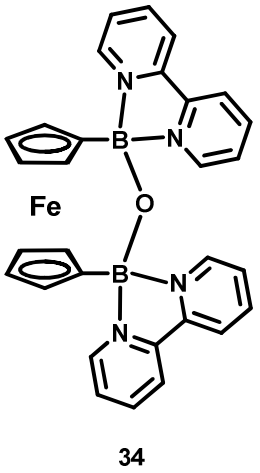

34

Figure 1.13. Bipyridine boron bridged *ansa*-ferrocene

1.2.2.7 *ansa*-Ferrocene-based Peptide macrocycles

Kraatz and co-workers reported *ansa*-ferrocene-based peptide **35** (Figure 1.14), which was formed by the reaction of ferrocene dicarboxylic acid with peptide cystamines at high dilutions [Chowdhury *et al*. 2004]. These macrocycles possess disulfide containing cystamine $(CSA)_2$ linkages. These systems exhibit H-bonding of the amide NH in solution as shown by their temperature dependent NMR spectra. This macrocycle also displays intramolecular N---O cross-ring H-bonding in the solid state involving the amino acids proximal to the ferrocene.

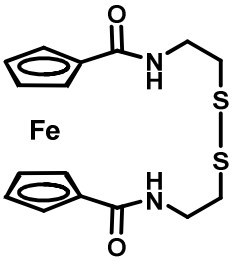

35

Figure 1.14. Peptide based *ansa*-ferrocene

1.2.2.8 Cyclam derived-*ansa*-Ferrocenes

Beer *et al*. have recently reported *ansa*-ferrocene based cyclams and the selective electrochemical recognition of sulfate over phosphate and phosphate over sulfate by using these polyaza ferrocene macrocyclic receptors in aqueous solution [[a]Beer *et al*. 1999]. The reaction of 1,1'-ferrocene-bis(methylenepyridinium) salt with 1,4,8,11-tetraazacyclotetradecane-5,12-dione, followed by $LiAlH_4$ reduction resulted in the formation of FcCyclam **36** (Figure 1.16) [Plenio *et al*. 2001]. Metal complexes of FcCyclam with M^{2+} = Co^{2+}, Ni^{2+}, Cu^{2+}, and Zn^{2+} were synthesized from FcCyclam and the respective metal triflates. The synthesis, structural, electrochemical, and spectroscopic characterization of cyclam-derived ferrocene containing macrocycle **37** (Figure 1.15) was mainly based on schiff-base condensation of 2,3,2-tet [2,3,2-tet = N,N'-bis(2-aminoethyl)-1,3-propanediamine] with 1,1'-diformylmetallocene, and their $Fe^{2+/3+}$, Co^{2+}, Ni^{3+}, Cu^{2+}, and Zn^{2+} complexes [Comba *et al*. 2005].

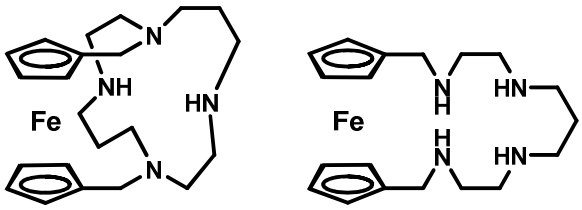

36 37

Figure 1.15. *ansa*-ferrocenyl cyclams

1.2.2.9 *ansa*-(carbene)-Ferrocenes

Bielawski *et al* described a novel carbene architecture that contains a 1,1' disubstituted ferrocene moiety **38** (Figure 1.16) and demonstrated its ability to engage in unique electronic interactions with co-ordinated transition metals [Khramov *et al*. 2008]. The transition-metal complexes of novel N-aryl and N-alkyl diaminocarbenes were incorporated to the 1,1'-disubstituted ferrocene moiety. The electrochemistry of ferrocene

was utilized to confirm long-range, but significant, electronic communication between the Fe center in the redox-active carbenes and co-ordinated transition metals. Streubel and co-workers reported the synthesis of diaminophosphanebridged [5]ferrocenophane bis(carbene complex) **39** (Figure 1.16) and performed the preliminary studies on ring opening reactions that afforded the first bis(2H-azaphosphirene complex) together with a trinuclear 1,1'-ferrocenediyl-bridged complex bearing a 2,3-dihydro-1,2,3-azadiphosphete and a nitrile ligand [Helten *et al*. 2010].

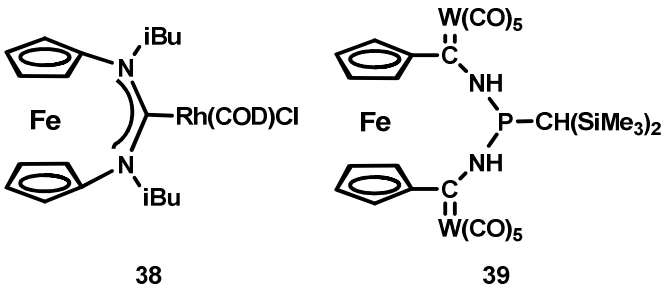

38 39

Figure 1.16. *ansa*-(carbene)-ferrocene

1.2.2.10 *ansa*-(selenyl)-Ferrocene

The synthesis, complexation and characterization of the novel macrocyclic polyselenaferrocenophane **40** (Figure 1.17) such as 1,5,9,13-tetraselena[13]ferrocenophane [Jing *et al*. 2010] was recently reported. This potentially tetradentate ligand can bind in either a planar or folded conformation, forming stable complexes. The Ag(I) cation forms 1-D polymer $\{[AgL](PF_6)\}_n$ due to its large ionic radius.

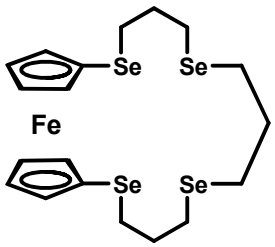

40

Figure 1.17. *ansa*-(selenyl)-ferrocene

1.3 Other metallocenes: Non-iron [n]Metalloarenophanes [Braunschweig and Kupfer 2010]

Over the last five years, there was a tremendous development in the field of *ansa*-metallocenes other than ferrocene which have not been derived from bis(cyclopentadienyl) metal complexes and mainly those based on $[M(\eta^6\text{-}C_6H_6)_2]$ (where M is V, Cr, or Mo), $[Mn(\eta^5\text{-}C_5H_5)(\eta^6\text{-}C_6H_6)]$, and $[M(\eta^5\text{-}C_5H_5)(\eta^7\text{-}C_7H_7)]$ (where M is V or Cr) (Figure 1.18).

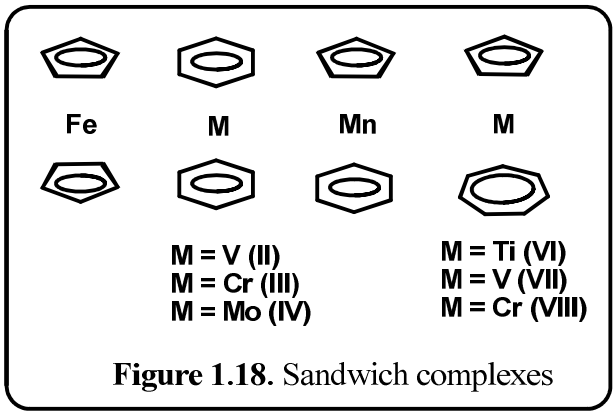

Figure 1.18. Sandwich complexes

The reason for the predominance of ferrocene is closely connected to its high stability, cheap availability, and well-established dimetalation, which enables a straightforward access to ring-substituted and *ansa*-type derivatives. The first examples of *ansa* other than cyclopentadienyl rings were reported by Elschenbroich and co-workers in 1990 [Elschenbroich *et al*. 1990], where they reported the synthesis, structural characterization, and reactivity of the tilted bis(arene) metal complexes $[(C_6H_5)_2Si(\eta^6\text{-}C_6H_5)_2]M$, (M = V, Cr, Mo) **41-43** (Figure 1.19). Ragogna and co-workers have recently been able to incorporate the cyclobutadienyl moiety into a strained [2]cobaltoarenophane **44** for the first time [Chadha *et al*. 2007]. The enhanced reactivity of either the bond between the carbocyclic ligands and the bridging element(s), or that between the bridging elements, or that between the metal and one of the carbocyclic ligands results in the strained character of these kind of *ansa* complexes. These organometallic compounds were mainly used in ring opening

polymerization [Hultzsch *et al*. 1995], diboration reactions [Braunschweig *et al*. 2006, Bauer *et al*. 2010], bis-silylation of propyne [Braunschweig and Kupfer 2007] etc.

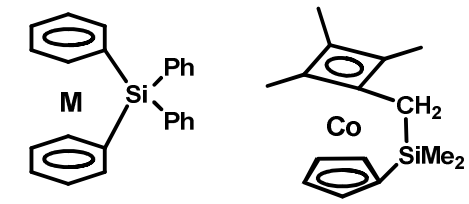

41. M = V (II)
42. M = Cr (III)
43. M = Mo (IV)

44

Figure 1.19. Metalloarenophanes

1.4 Conclusion and present work

The compounds of metallocenes with interannular bridge have emerged as an important area in the field of *ansa*-metallocenes. Most of the above mentioned examples mainly contain either single, double or more elements as bridges, functionalizable moiety which connects the two cyclopentadienyl rings of the metallocene. So, the first chapter is dealt with *ansa*-metallocenyl derivatives. Our work is mainly concentrated on the introduction of heteroaromatic rings mainly pyrrole, thiophene and furan as the interannular bridge that connects the two cyclopentadienyl rings of the metallocenes mainly ferrocene and ruthenocene in an *ansa* type way which results in the formation of heteroaromatic rings based macrocycles which can be called as *ansa*-metallocene-based calixpyrroles and calixphyrins.

The second chapter deals with the syntheses, spectral and structural characterization of the precursors mainly 1,1'-metallocenyl-bis-(*gem*-diaryl/alkylaryl/cyclohexyl/ dialkylhydroxy)methane and 1,1'-metallocenyl-bis-(*gem*-diaryl/alkylaryl/cyclohexyl/ dialkylpyrrolyl)methane. The 1,1'-ferrocene diols were synthesized from the reaction of 1,1'-bis-lithiated salt of ferrocene with various ketones ranging from diaryl to arylalkyl to

cyclohexyl to dialkyl ketones. $BF_3.OEt_2$ catalyzed condensation of these diols with pyrrole resulted in the formation of 1,1'-ferrocenyl dipyrromethanes. All these 1,1'-ferrocenyl diols and dipyrromethanes were clearly characterized by the standard spectroscopic techniques like FAB-mass, ^{1}H NMR and finally by single crystal X-ray diffraction analyses. Similar starting material synthesis is further extended to the next higher metallocene such as ruthenocene.

The third chapter is concerned with the syntheses, spectral and structural characterization of *ansa*-ferrocene-based *normal* calixpyrroles. Here, the *meso* alkylaryl/cyclohexyl/dialkyl dipyrromethane acts as the interannular bridge between the two cyclopentadienyl rings of ferrocene. Or in other words, our work is also related with the modification in the main frame work of calixpyrroles and hence we were successful in incorporating metallocene in the mainframe work of calixpyrroles in an *ansa* type way. These macrocycles were synthesized by the acid catalysed condensation of 1,1'-ferrocenyldipyrromethanes with the respective ketones. All these new macrocycles were characterized by the standard spectroscopic techniques like FAB-mass, ^{1}H NMR and finally by single crystal X-ray diffraction analysis. They adopt partial 1,2-alternate conformation in the solid state. The structural analysis clearly shows that these macrocycles retain the parent calix[4]pyrrole behaviour. The similar chemistry has been further extended to the next higher metallocene, ruthenocene.

Incorporation of metallocenes in the main framework of calixphyrin based macrocycles is the subject of the fourth chapter. *p*-TSA catalysed condensation of 1,1'-ferrocenyldiaryldipyrromethanes with the electron withdrawing and electron releasing aldehydes followed by oxidation with DDQ results in the formation of *ansa*-metallocene-based *normal* calixphyrins. By changing the aryl substituted precursor to alkyl substituted

one, apart from *normal* calixphyrins, *expanded* calixphyrins were also obtained. All these new macrocycles were clearly characterized by the standard spectroscopic techniques like FAB-mass, ^{1}H NMR and finally by single crystal X-ray diffraction analysis. Since they bear analogy to both calixpyrroles and porphyrins, which can be called as calix[*n*]metallocenyl[*m*]phyrins where n = 1, 2 and m = 2, 4. In addition to this, the role of aryl *vs* alkyl is also highlighted to explain the formation of higher macrocycles.

In addition to pyrrole, the fifth chapter is concerned with the introduction of one more heterocyclic ring mainly thiophene and furan in the above mentioned macrocycles, which results in the formation of *ansa*-metallocene-based core-modified *expanded* calixpyrroles and calixphyrins. All the new macrocycles were characterized by standard spectroscopic methods and further confirmed by single crystal X-ray analysis. From the single crystal X-ray structural analyses, it is clear that *ansa*-ferrocene-based calix[2]pyrrole[1]thiophene adopts 1,3-alternate conformation in the solid state and retains the parent calix[4]pyrrole behaviour whereas *ansa*-ferrocene-based calix[2]phyrin[1]thiophene is partially planar.

Chapter 2

General Experimental Methods and Techniques

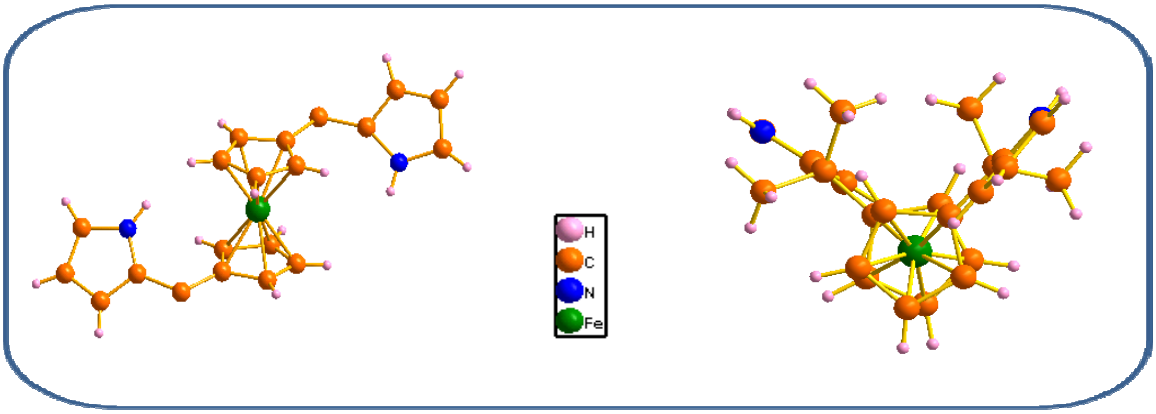

2.1 Abstract

All the general experimental procedures and the important physico-chemical techniques employed in the course of investigation are outlined in this chapter. The syntheses, spectral and structural characterization of the precursor mainly 1,1'-metallocenyl-bis-(gem-diaryl/alkylaryl/cyclohexyl/dialkylpyrrolyl)methane have been clearly explained. The other starting materials like 1,1'-metallocenyl-bis-(gem-diaryl/alkylaryl/cyclohexyl/dialkylhydroxy)methane, 2,5-thiophene/furan diols and 5,5-(alkylaryl/cyclohexyl/dialkyl)dipyrromethane have been synthesized according to the literature procedure. The structures of 1,1'-ferrocenyl-bis-(gem-diphenylpyrrolyl)methane and 1,1'-ferrocenyl-bis-(gem-dimethylpyrrolyl)methane were finally confirmed by single crystal X-ray structural analyses. The crystal studies clearly shows that the pyrrole rings are trans to each other with respect to the ferrocene ring and the side view further confirms that the terminal pyrrole units are perpendicular to the ferrocenyl unit and facing opposite to each other. Due to C–H---pyrrolic π-cloud and pyrrolic N-H---pyrrolic π-cloud interactions, these molecules generate one-dimensional array in the solid state. The same synthetic methodology has been exploited in the next higher metallocene such as ruthenocene.

2.2 Chemicals for Syntheses

Common solvents used for syntheses were purified according to known procedures [Vogel]. Pyrrole, thiophene and furan were procured from Aldrich chemicals USA, were distilled before use. Trifluoroacetic acid (TFA), Borontrifluoride diethyletherate ($BF_3.OEt_2$), *p*-toluenesulphonic acid (*p*-TSA), 1.6 M *n*-BuLi, 4-tolualdehyde, 4-anisaldehyde, 4-nitrobenzaldehyde, 4-cyanobenzaldehyde, 2,3,4,5,6-pentafluorobenzaldehyde, DDQ, Ruthenocene and deuterated solvents were procured from Aldrich, USA and used as received. Ferrocene, chloranil and N,N,N',N'-Tetramethylethylenediamine which was distilled over KOH before use, ferrocene and chloranil were procured from S.D.Fine Chem, India.

2.3 Physico-Chemical Techniques

The details of the instruments used for characterization and evaluation of spectroscopic data are given below.

Electronic absorption spectra were recorded with Perkin Elmer–Lambda 25 UV-Visible spectrophotometer. NMR spectra were recorded with Bruker 300 MHz or 500 MHz machine with $CDCl_3$ as solvent. Chemical shifts were expressed in parts per million (ppm) relative to TMS. FAB mass spectra were obtained on a JEOL SX-120/DA6000 spectrometer using argon (6 KV, 10 mA) as the FAB gas. The melting points were measured on a JSGW melting point apparatus and were not optimized. Cyclic Voltammetric and differential pulse Voltammetric studies were done on a CHI model 620B CV apparatus, CH instruments, Inc. interfaced to computer. A three electrode system consisting of platinum working electrode and commercially available saturated calomel electrodes, reference electrode and a platinum

mesh counter electrode were used. The reference electrode was separated from the bulk of the solution by a fritted glass bridge filled with the solvent/supporting electrolyte mixture. Half wave potentials were measured as the average of anodic and cathodic peak potentials.

2.4 X-ray Structure Determinations

X-ray diffraction studies were carried out using Bruker axs kappa Apex II single crystal x-ray diffractometer equipped with graphite mono-chromated Mo(Kα) (λ= 0.7107 Å) radiation and CCD detector. Crystals were cut to suitable size under nitrogen and immediately mounted on a glass fiber using cyanoacrylate adhesive. The unit cell parameters were determined from 36 frames measured (0.5˚ phi-scan) from three different crystallographic zones and using the method of difference vectors. The intensity data were collected with an average four-fold redundancy per reflection and optimum resolution (0.75 Å). The intensity data collection, frames integration, LP correction and decay correction were done using SAINT-NT (version 6.0) software. Empirical absorption correction (multi-scan) was performed using SADABS (1999) program. The structures were solved using SIR92 program. The structures were refined using SHELXL-97 program [Altomare *et al*. 1993, Blessing 1995, Bruker 1999, Bruker 2004, Farrugia 1997, Farrugia 1999, Sheldrick 1997, Spek 2003]. All the non-hydrogen atoms were refined with anisotropic displacement parameters. In all structures discussed in this thesis, most of the hydrogen atoms could be located in the difference Fourier map. However, the hydrogen atoms whose positions could be assigned geometrically were constrained to those positions and were given riding model refinement. The treatment of other hydrogen atoms during refinement, are discussed in the respective chapters. The hydrogen bonding interactions were generated by Diamond Software [Brandenburg].

X-ray quality single crystals for the compounds were grown using appropriate solvent mixtures by vapour diffusion method. The single crystal X-ray diffraction data of some crystals were collected on a Bruker AXS Kappa Apex 2 CCD diffractometer at 293(2) K and some other crystals were collected on a Bruker SMART Apex diffractometer equipped with CCD area detector at 100(2) K. Both the above diffractometers were equipped with graphite monochromated Mo(Kα) radiation (λ = 0.71073 Å). The crystal structure of all the compounds were solved by direct methods, as included in SHELXTL program package [Altomare *et al*. 1993, Blessing 1995, Bruker 1999, Bruker 2004, Farrugia 1997, Farrugia 1999, Sheldrick 1997, Spek 2003]. The structures of all the compounds were refined by full-matrix least squares refinement on F^2 [SHELXL-97 1998]. All non hydrogen atoms were refined anisotropically. All the hydrogen bonding interactions were generated with the help of Diamond software [Brandenburg].

2.5 Syntheses of Precursors

The syntheses of various precursors in this thesis are shown in Scheme 2.1-2.4. The synthesis and experimental details are given for important precursors which are used for the synthesis of macrocycles described in this thesis.

2.5.1 Syntheses of 1,1'-metallocenyl-bis-(*gem*-diaryl/alkylaryl/cyclohexyl/ dialkylhydroxy)methane (1 - 7) [Carroll *et al*. 1994]

The precursors for the target macrocycles which has been explained in the next three chapters, such as, diols **1 - 7** were synthesized from the reaction of 1,1'-bis-lithiated salt of ferrocene with various ketones (Scheme 2.1), yielded 20 – 80% of the diols (Table 2.1) [Carroll *et al*. 1994].

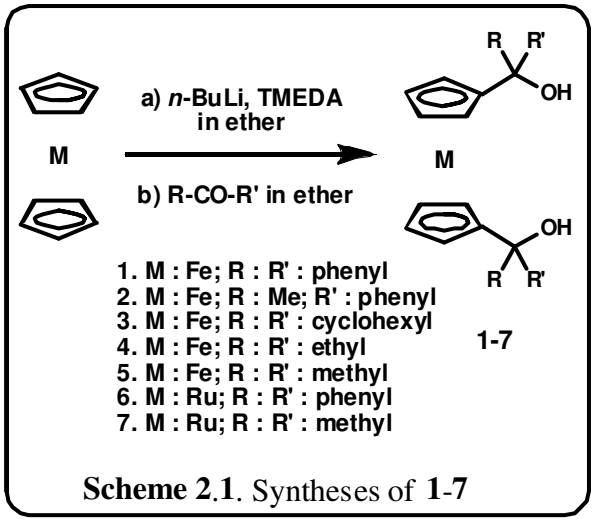

Scheme 2.1. Syntheses of **1-7**

Table 2.1. Yields of 1,1'-metallocenyl diols

no.	M	R	R^1	yield (%)
1	Fe	C_6H_5	C_6H_5	71.5
2	Fe	CH_3	C_6H_5	11
3	Fe	cyclohexyl		19.4
4	Fe	C_2H_5	C_2H_5	21
5	Fe	CH_3	CH_3	23
6	Ru	C_6H_5	C_6H_5	67
7	Ru	CH_3	CH_3	21.5

2.5.2 Syntheses and Spectral analyses of 1,1'-metallocenyl-bis-(*gem*-diaryl/alkyl aryl/cyclohexyl/dialkylpyrrolyl)methane (8 - 14) [Ramakrishnan and Srinivasan 2007]

The hitherto unknown 1,1'-ferrocenyl-bis-(*gem*-diaryl/alkylaryl/cyclohexyl/ dialkylpyrrolyl)methane **8 - 12** were obtained by the $BF_3.OEt_2$ catalyzed condensation of pyrrole and diols **1 - 5** in 63 – 80% yield (Scheme 2.2) (Table 2.2). The synthetic methodology adopted here was entirely different from the work reported by Sessler and co-workers, where they generated the 1,1'-ferrocenyl dipyrromethane from the isomeric mixture of cyclopentadienyl functionalized pyrroles [Scherer *et al*. 1998].

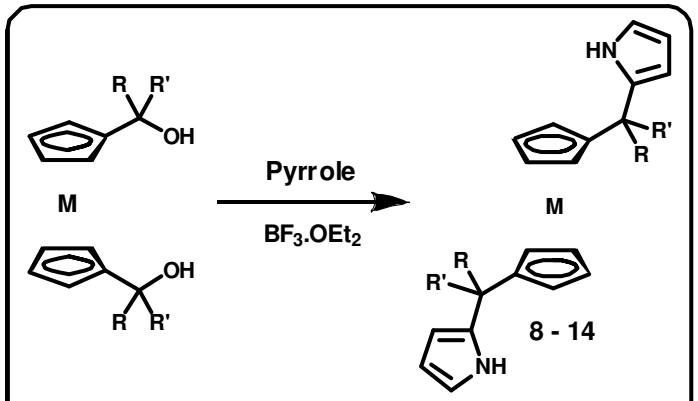

8. M : Fe; R : R' : phenyl
9. M : Fe; R : Me; R' : phenyl
10. M : Fe; R : R' : cyclohexyl
11. M : Fe; R : R' : ethyl
12. M : Fe; R : R' : methyl
13. M : Ru; R : R' : phenyl
14. M : Ru; R : R' : methyl

Scheme 2.2. Syntheses of **8** - **14**

Table 2.2. Yields of 1,1'-metallocenyl dipyrromethanes

no.	M	R	R'	yield (%)
8	Fe	C_6H_5	C_6H_5	80.3
9	Fe	CH_3	C_6H_5	63.6
10	Fe	cyclohexyl		80
11	Fe	C_2H_5	C_2H_5	68
12	Fe	CH_3	CH_3	65
13	Ru	C_6H_5	C_6H_5	81
14	Ru	CH_3	CH_3	68

The FAB mass spectral analysis of **8 - 12** predicted the exact composition of the starting materials. The ^{1}H NMR analysis of **8 - 12** (Figure 2.1) in $CDCl_3$ shows signals corresponding to half the linear chain, suggesting the symmetrical nature in which the pyrrole rings are opposite to each other. The ferrocenyl protons of **8 - 12** resonated as a set of two singlets between 3.74 and 4.15 ppm. The α-pyrrolic protons of **8 - 12** resonated as a singlet at 6.69, 6.61, 6.67, 6.74 and 6.48 ppm whereas β-pyrrolic protons resonated as a set of multiplet between 6.17 to 6.01 ppm and another set as a singlet at 6.02 to 5.85 ppm

respectively. The NH protons of **8 - 12** appeared as a broad singlet at 8.66, 7.64, 7.93, 8.97 and 7.76 ppm.

a)

b)

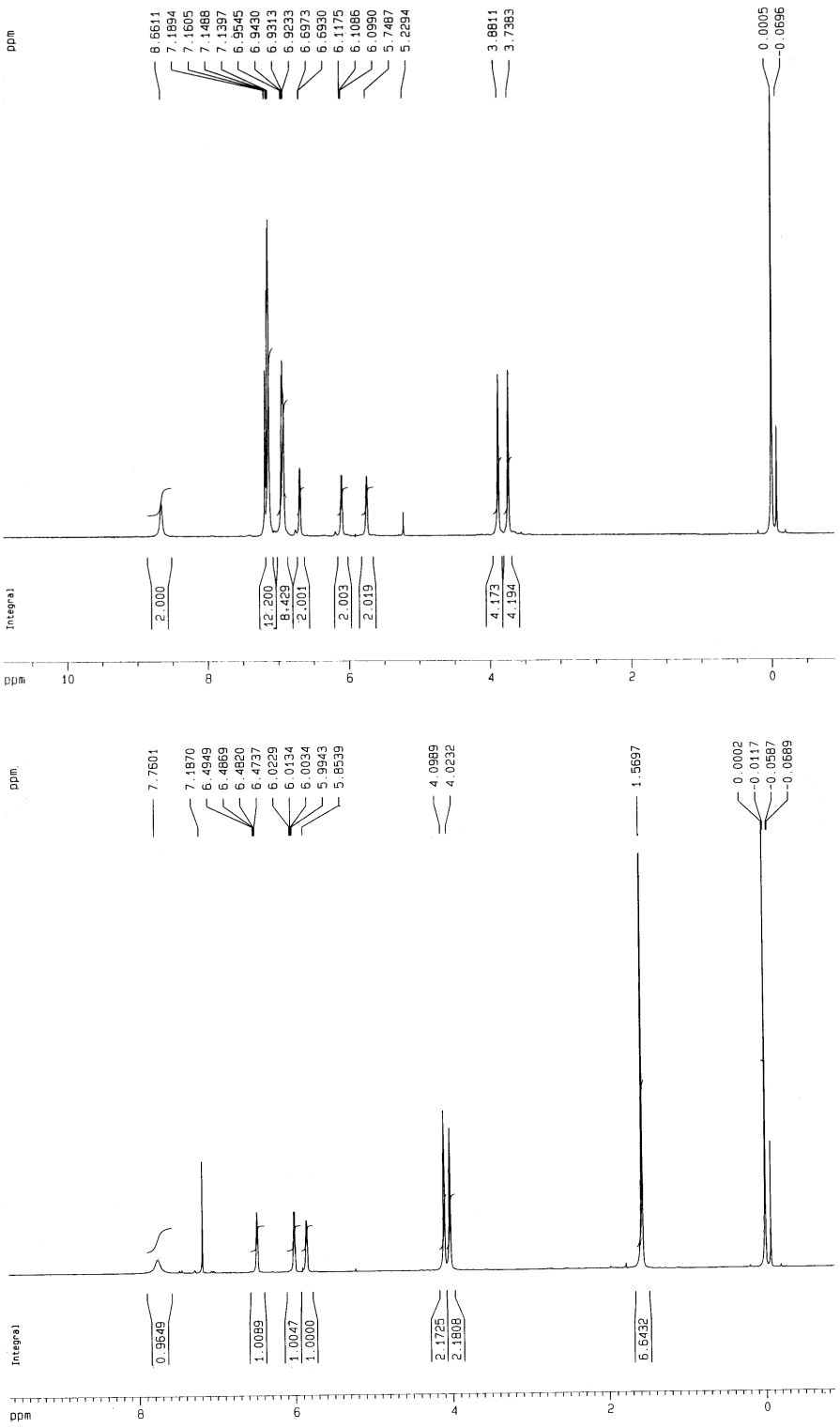

Figure 2.1. ^{1}H NMR spectra of a) **8** and b) **12** in $CDCl_3$

The structures of **8** [Ramakrishnan and Srinivasan 2007] and **12** [Ramakrishnan *et al*. 2010] were finally confirmed from single crystal X-ray diffraction analysis (Table 2.3) as shown in Figure 2.2. The structure of **8** clearly shows that the pyrrole rings are *trans* to each other with respect to the ferrocene ring and the dihedral angles between two planes (1 and 2; 3 and 4) are 56.47 and 49.89˚, respectively. The side view further confirms that the terminal pyrrole units are perpendicular to the ferrocenyl unit and facing opposite to each other, thus showing that the molecule adopts a helical twist in the solid state. This twisting of the molecule avoids the formation of linear polymeric products during the condensation process,

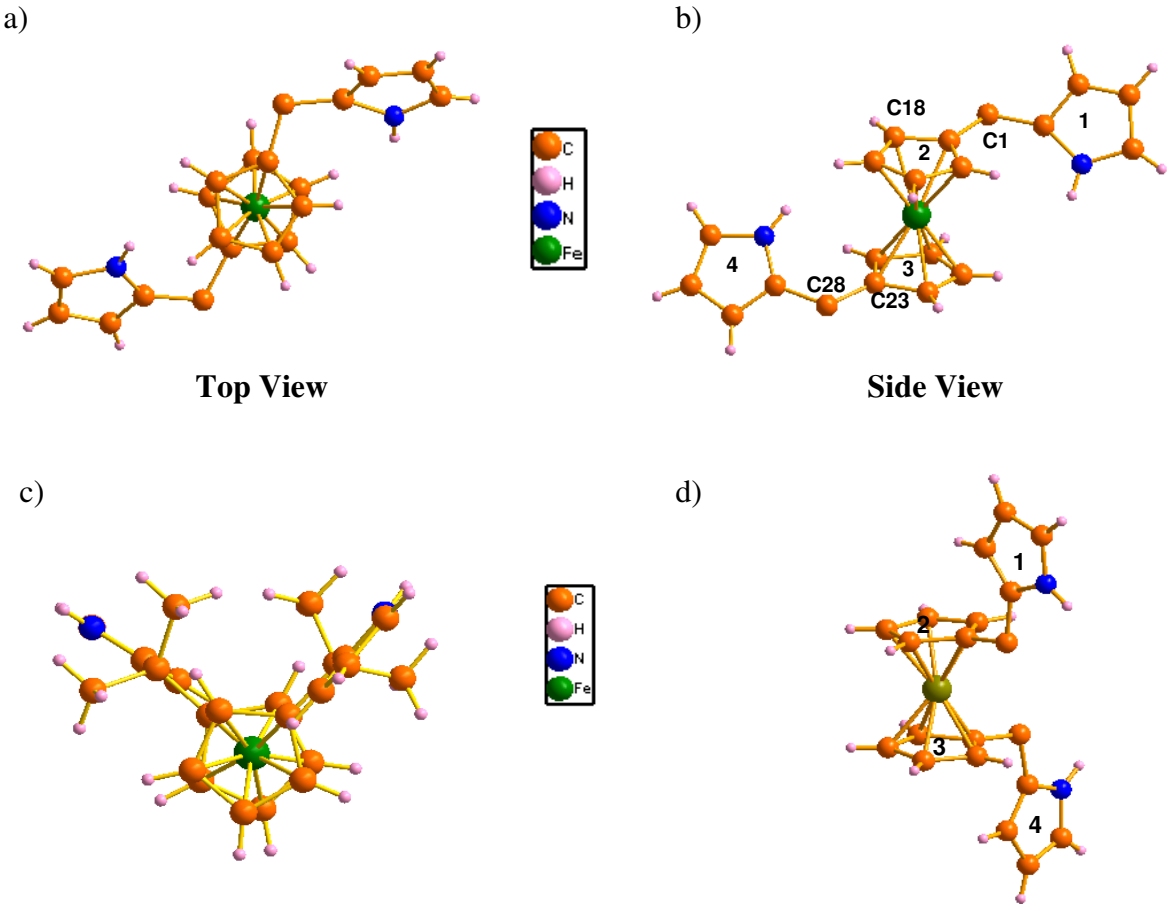

Figure 2.2. Single crystal X-ray structures of **8** (a,b) and **12** (c,d). The *meso* groups in the top and side views are omitted for clarity.

thus supporting the so-called helical effect involved in the formation of the macrocycles [Franck 1982, Tietze *et al*. 1993, Sessler *et al*. 1995].

The pyrrolic rings in **8** and **12** are *trans* to each other, with the dihedral angles between the pyrrole and ferrocene units (plane 1, 2 and 3, 4) in **8** are 49.90 and 56.47˚ (Figure 2.2b), whereas the respective angles in **12** (Figure 2.2d) are 87.57 and 88.96˚, which are 37.67 and 32.49˚ higher than **8**. This suggests that the pyrrolic units in **12** are arranged almost perpendicular to the ferrocene plane which are highly flexible and there is more freedom for rotation. In **8**, there are three C–H---pyrrolic π-cloud interactions observed between two molecules, with two inter and one intra molecular interactions with the distances and angles: (i) C42–H42---N2(π): 2.69 Å, 154˚; (ii) C16A–H16A---N1(π): 2.82 Å, 147˚ and (iii) C15–H15---N1(π): 2.79 Å, 135˚; which forms a one-dimensional array (Figure 2.3a). A similar such array is observed in **12**, where the *meso*-methyl C–H from one molecule (C19–H19c---N1(π)) and ferrocenyl C–H from the third molecule (C1–H1---N1(π)) interacts with the second molecule pyrrolic π-cloud, with distances and angles of 2.74 Å, 155˚ and 2.86 Å, 172˚ (Figure 2.3b and 2.3c). The intermolecular distance between the two closest pyrrolic π clouds in **8** is 8.76 Å (Figure 2.3a) and the respective distance in **12** is 5.07 and 4.93 Å (Figure 2.3b and 2.3c) which are 3.69 and 3.83 Å lower than **8**. Apart from Figure 2.3b and 2.3c, **12** also generates another 1-D array which is formed between the pyrrolic N-H of one of the molecules with the pyrrolic π-cloud of another molecule with the distance and angle of N1-H1A…N2(π) are 2.93 Å and 174˚.

a)

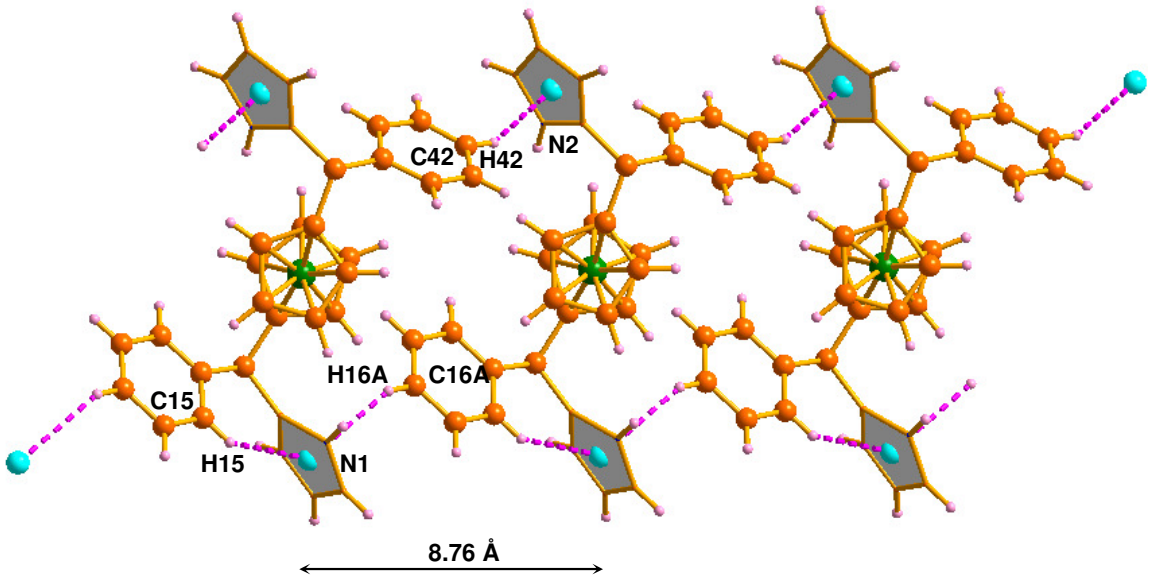

b)

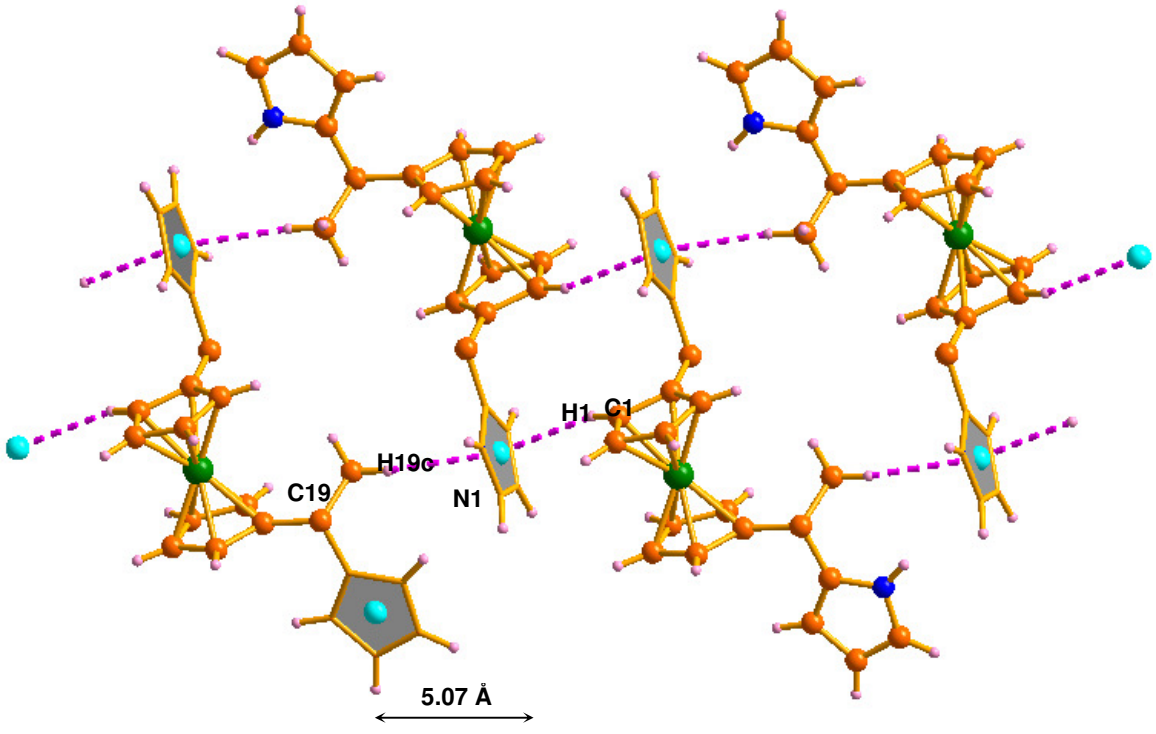

c)

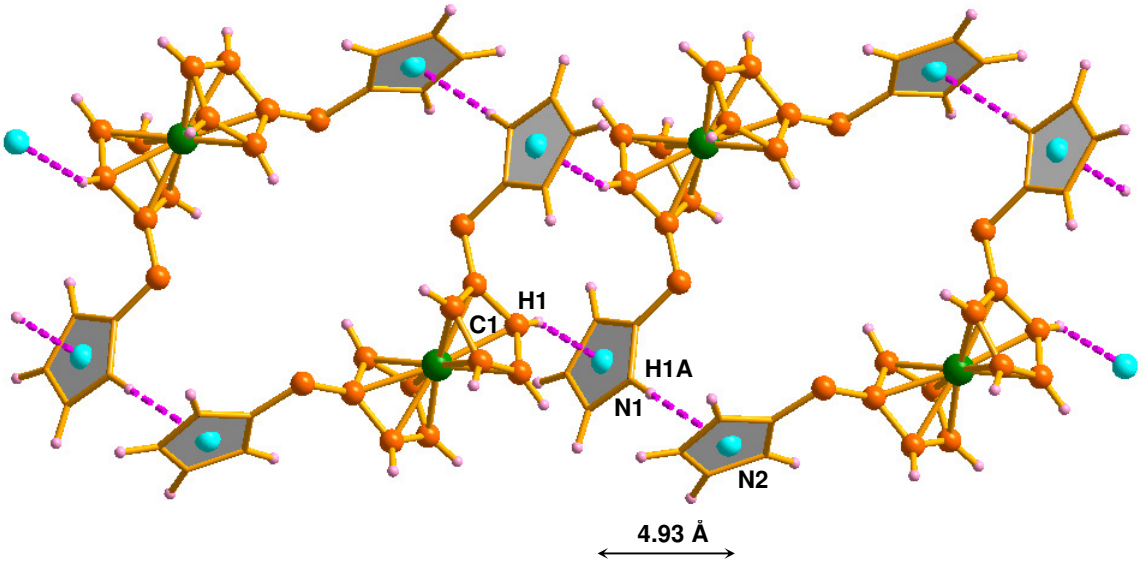

Figure. **2.3**. Single crystal X-ray structures and analyses of **8** and **12**. a) 1-D array of **8**. (b) and (c) are two different 1-D arrays of **12**. The groups which are not involved in the hydrogen bonding interactions are omitted for clarity.

The similar synthetic methodology has been employed for the next higher metallocene such as ruthenocene. 1,1'-bislithiated salt of ruthenocene upon treatment with ketones like benzophenone and acetone (Scheme 2.1) yielded the respective diols **6** and **7** in 67 and 21.5% yield respectively. $BF_3.OEt_2$ catalysed condensation of these diols with pyrrole (Scheme 2.2) yielded the respective 1,1'-ruthenocenyl dipyrromethanes **13** and **14**.

2.5.3 Syntheses of 2,5-thiophene/furan diols (15 – 17) [Ulman and Manassen 1975, Chadwick and Willbe 1977, Ulman and Manassen 1979, Srinivasan *et al*. 1998, [a]Srinivasan *et al*. 1999, [b]Srinivasan *et al*. 1999]

The syntheses of 2,5-bis(dimethylhydroxymethyl)thiophene **15** and furan **16** and 2,5-

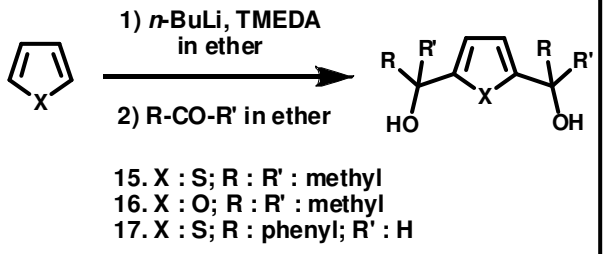

Scheme 2.3. Syntheses of **15** - **17**

bis(phenylhydroxymethyl)thiophene **17** is summarized in Scheme 2.3.

2.5.4. Syntheses of 5,5-(alkylaryl/cyclohexyl/dialkyl)dipyrromethane (18 – 21) [Sobral *et al*. 2003]

The syntheses of 5,5-(alkylaryl/cyclohexyl/dialkyl)-dipyrromethane are summarized in Scheme 2.4.

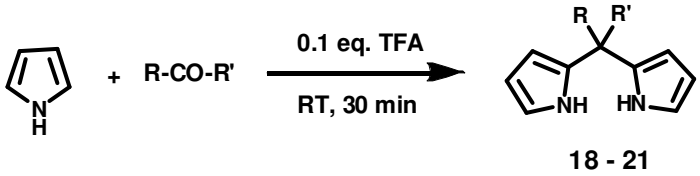

Scheme 2.4. Syntheses of **18** - **21**

2.6 Experimental Section

Synthesis of 1,1'-bis(diphenylhydroxymethyl)ferrocene (1):

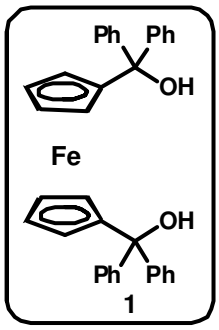

Ferrocene (2 g, 10.8 mmol) was dissolved in 60 mL dry ether under N_2 atm in a dry 250 mL round bottomed flask followed by the addition of TMEDA (5 mL, 32.4 mmol). 18 mL of *n*-Butyl Lithium was added drop wise to the above solution and allowed to stir at room temperature for 90 min. Then the reaction mixture was refluxed for 4 hr after which it is allowed to come to room temperature. Benzophenone (5 g, 27 mmol) in 30 mL dry ether was added dropwise to the above reaction mixture at 0˚C and allowed to stir for further 2 hr. The reaction mixture was quenched with 100 mL of saturated NH_4Cl solution. The organic layer was extracted with ether and dried over anhydrous sodium sulphate. The solvent was removed by vacuum distillation. The fraction eluted with EtOAc : petroleum ether (10 : 90)

by silica gel column chromatography (silica gel 100 – 200 mesh) was identified as yellow solid **1**. Yield = 4.25 g, 71.5%. ^{1}H NMR (300 MHz, $CDCl_3$, 298 K) : δ = 7.18 (s, 20H, phenyl CH), 4.09 (s, 4H, ferrocenyl CH), 3.89 (s, 4H, ferrocenyl CH); FAB mass (m/z) : Calcd for $C_{36}H_{30}FeO_2$: 550.16; Found : 550.29.

Synthesis of 1,1'-bis(methylphenylhydroxymethyl)ferrocene (**2**):

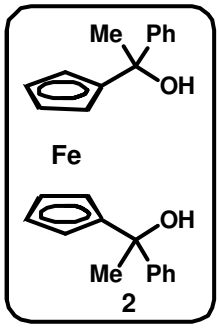

The above procedure was followed by using acetophenone (3.16 mL, 27 mmol) in 30 mL dry ether. The fraction eluted with EtOAc : petroleum ether (5 : 95) was identified as yellow solid **2**. Yield = 0.5 g, 11%. ^{1}H NMR (300 MHz, $CDCl_3$, 298 K) : δ = 7.46-7.18 (m, 10H, phenyl CH), 4.37-3.95 (m, 8H, ferrocenyl CH), 1.88 (s, 3H, methyl CH), 1.78 (s, 3H, methyl CH); FAB mass (m/z) : Calcd for $C_{26}H_{26}FeO_2$: 426.13; Found : 425.79.

Synthesis of 1,1'-bis(cyclohexylhydroxymethyl)ferrocene (**3**):

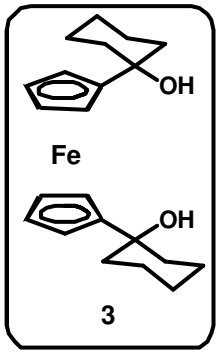

The above procedure was followed by using cyclohexanone (2.8 mL, 27 mmol) in 30 mL dry ether. The diol **3** was separated by silica gel column chromatography (silica gel 100 – 200 mesh) (5 : 95, EtOAc : petroleum ether) as a yellow solid. Yield = 0.8 g, 19.4%. ^{1}H NMR (300 MHz, $CDCl_3$, 298 K) : δ = 4.21-4.2 (t, 4H, ferrocenyl CH), 4.15-4.14 (t, 4H, ferrocenyl CH), 2.94 (brs, 2H, hydroxyl OH), 1.86 (m, 6H, cyclohexyl CH), 1.74-1.66 (m, 6H, cyclohexyl CH). 1.2-1.1 (m, 4H, cyclohexyl CH), 0.88-0.83 (m, 4H, cyclohexyl CH); FAB mass (m/z) : Calcd for $C_{22}H_{30}FeO_2$: 382.16; Found : 382.59.

Synthesis of 1,1'-bis(diethylhydroxymethyl)ferrocene (**4**):

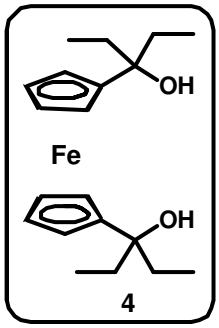

The above procedure was followed by using 3-pentanone (5.4 mL, 54 mmol) in 30 mL dry ether. The diol **4** was separated by silica gel column chromatography (silica gel 100 – 200 mesh) (5 : 95, EtOAc : petroleum ether) as a yellow solid. Yield = 0.8 g, 21%. ^{1}H NMR (300 MHz, $CDCl_3$, 298 K) : δ = 4.16-4.15 (d, J = 3 Hz, 8H, ferrocenyl CH), 2.87 (brs, 2H, hydroxyl OH), 1.85-1.73 (m, 4H, CH_2-H), 1.69-1.57 (m, 4H, CH_2-H), 0.84-0.79 (t, 12H, methyl CH); FAB mass (m/z) : Calcd for $C_{20}H_{30}FeO_2$: 358.16; Found : 358.09.

Synthesis of 1,1'-bis(dimethylhydroxymethyl)ferrocene (**5**):

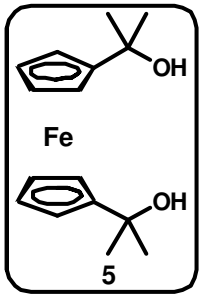

The above procedure was followed by using dry acetone (10 mL, 130 mmol). The diol **5** was separated by silica gel column chromatography (silica gel 100 – 200 mesh) (10 : 90, EtOAc : petroleum ether) as a yellow solid. Yield = 0.75 g, 23%. ^{1}H NMR (300 MHz, $CDCl_3$, 298 K) : δ = 4.14-4.13 (t, 4H, ferrocenyl CH), 4.09-4.08 (t, 4H, ferrocenyl CH), 3.55 (brs, 2H, hydroxyl OH), 1.06 (s, 12H, methyl CH); FAB mass (m/z) : Calcd for $C_{16}H_{22}FeO_2$: 302.10; Found : 302.23.

Synthesis of 1,1'-bis(diphenylhydroxymethyl)ruthenocene (**6**):

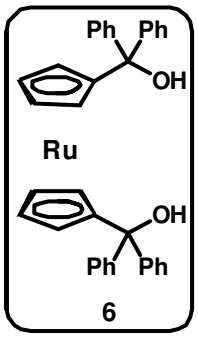

The above procedure was followed by using ruthenocene (0.9 g, 4 mmol) and benzophenone (1.8 g, 10 mmol) in 20 mL dry ether. The diol **6** was separated by silica gel column chromatography (silica gel 100 – 200 mesh) (10 : 90, EtOAc : petroleum ether) as a white solid. Yield = 1.6 g, 67%. ^{1}H NMR (300 MHz, $CDCl_3$, 298 K) : δ = 7.35 (m, 20H, phenyl CH), 4.23 (s, 8H, ruthenocenyl CH); FAB mass (m/z) = Calcd for $C_{36}H_{30}RuO_2$: 596.13; Found : 596.52.

Synthesis of 1,1'-bis(dimethylhydroxymethyl)ruthenocene (**7**):

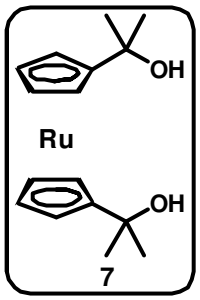

The above procedure was followed by using ruthenocene (2 g, 8.7 mmol) and dry acetone (3.2 mL, 43.5 mmol). The diol **7** was separated by silica gel column chromatography (silica gel 100 – 200 mesh) (10 : 90, EtOAc : petroleum ether) as a yellow solid. Yield = 0.65 g, 21.5%. ^{1}H NMR (300 MHz, $CDCl_3$, 298 K) : δ = 4.31 (s, 8H, ruthenocenyl CH), 3.66 (brs, 2H, hydroxyl OH), 1.17 (s, 12H, methyl CH); FAB mass (m/z) : Calcd for $C_{16}H_{22}RuO_2$: 348.07; Found : 348.59.

Synthesis of 1,1'-bis(diphenylpyrrolylmethyl)ferrocene (**8**):

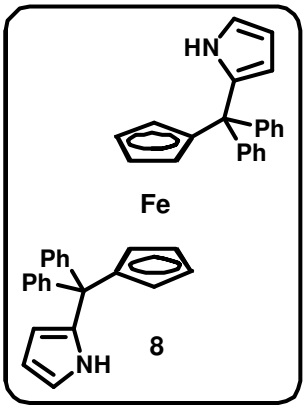

1,1'-bis(diphenylhydroxymethyl)ferrocene (**1**) (1.5 g, 2.73 mmol) and pyrrole (7.6 mL, 109.1 mmol) were stirred under N_2 atm for 10 min at room temperature. $BF_3.OEt_2$ (0.04 mL, 0.273 mmol) was added to the above mixture and the solution was stirred at room temperature for further 1h under dark conditions. Then it is quenched with 75 mL dichloromethane. The product was filtered and thoroughly washed with petroleum ether to remove excess pyrrole and the resultant yellow residue was identified as **8**. Yield = 1.42 g, 80.3%; m.p : 230˚C; ^{1}H NMR (300 MHz, $CDCl_3$, 298 K) : δ = 8.66 (brs, 2H, pyrrole NH), 7.19-7.14 (m, 12H, phenyl CH), 6.95-6.92 (m, 8H, phenyl CH), 6.69 (s, 2H, *α*-pyrrole CH), 6.10 (q, 2H, *β*-pyrrole CH), 5.75 (s, 2H, *β*-pyrrole CH), 3.88 (s, 4H, ferrocenyl CH), 3.74 (s, 4H, ferrocenyl CH); ^{13}C NMR (100 MHz, $CDCl_3$, 298 K) : δ = 54.70, 70.61, 70.85, 97.48, 108.03, 108.47, 109.98, 116.44, 117.98, 126.85, 127.65, 129.64, 136.64, 148.00; FT-IR (CH_2Cl_2) : 3428.57, 2917.58, 1637.87, 1486.99, 1262.03, 1019.20 cm^{-1}; FAB-MS (m/z) : Calcd for $C_{44}H_{36}FeN_2$: 648.22; Found : 648.

Synthesis of 1,1'-bis(methylphenylpyrrolylmethyl)ferrocene (9):

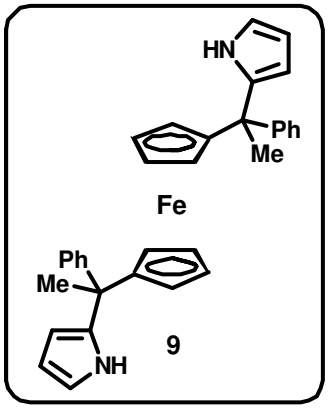

The above procedure was followed by using 1,1'-bis(methylphenylhydroxymethyl)ferrocene (**2**) (0.5 g, 1.2 mmol) and pyrrole (3.3 mL, 47 mmol). The crude product was purified by silica gel column chromatography (100 – 200 mesh). The fraction eluted with EtOAc : petroleum ether (3 : 97) was identified as pale yellow solid **9**. Yield = 0.4 g, 63.6%; m.p : 164˚C; ^{1}H NMR (300 MHz, $CDCl_3$, 298 K) : δ = 7.64 (brs, 2H, pyrrole NH), 7.18 (m, 10H, phenyl CH), 6.99 (m, 4H, phenyl CH), 6.61 (s, 2H, *α*-pyrrole CH), 6.13 (t, 2H, *β*-pyrrole CH), 5.96 (s, 2H, *β*-pyrrole CH), 3.99 (s, 4H, ferrocenyl CH), 3.90 (t, 3H, ferrocenyl CH), 3.82 (s, 1H, ferrocenyl CH), 1.94 (s, 6H, methyl CH); ^{13}C NMR (100 MHz, $CDCl_3$, 298 K) : δ = 28.77, 43.29, 68.30, 68.35, 68.41, 68.47, 68.86, 69.02, 98.12, 105.66, 107.46, 115.99, 126.09, 139.64, 148.80; FT-IR (CH_2Cl_2) : 3436.18, 2979.86, 1593.98, 1492.47, 1444.84, 1366.28, 1265.28, 1025.07 cm^{-1}; FAB-MS (m/z) : Calcd for $C_{34}H_{32}FeN_2$: 524.19; Found : 524.06.

Synthesis of 1,1'-bis(cyclohexylpyrrolylmethyl)ferrocene (10):

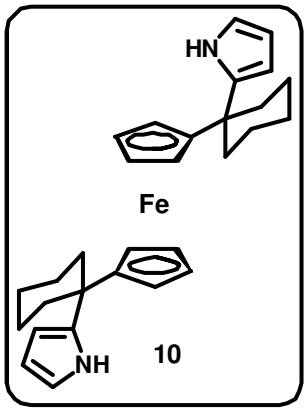

The above procedure was followed by using 1,1'-bis(cyclohexylhydroxymethyl)ferrocene (**3**) (0.8 g, 2.1 mmol) and pyrrole (5.8 mL, 84 mmol). The crude product was purified by silica gel column chromatography (100 – 200 mesh). The fraction eluted with EtOAc : petroleum ether (3.5 : 96.5) was identified as pale yellow solid **10**. Yield = 0.8 g, 80%; m.p : 145˚C; ^{1}H NMR (300 MHz, $CDCl_3$, 298 K) : δ = 7.93 (brs, 2H, pyrrole NH), 6.67 (s, 2H, *α*-pyrrole CH), 6.15 (d, J = 2.73 Hz, 2H, *β*-pyrrole CH), 6.02 (s, 2H, *β*-pyrrole CH), 3.97 (s, 4H, ferrocenyl CH),

3.84 (s, 4H, ferrocenyl CH), 2.23 (d, J : 13.3 Hz, 4H, cyclohexyl CH), 1.77 (m, 5H, cyclohexyl CH), 1.42 (m, 6H, cyclohexyl CH), 1.23 (m, 3H, cyclohexyl CH), 0.88 (m, 2H, cyclohexyl CH); ^{13}C NMR (100 MHz, $CDCl_3$, 298 K) : δ = 22.46, 22.86, 23.45, 26.75, 27.85, 28.45, 29.50, 35.15, 36.17, 38.26, 42.57, 64.75, 65.17, 67.17, 68.19, 69.15, 128.45, 137.75, 147.56; FT-IR (CH_2Cl_2) : 3428.94, 3093.40, 2929.48, 1591.23, 1443.09, 1264.77, 1031.13 cm^{-1}; FAB-MS (m/z) : Calcd for $C_{30}H_{36}FeN_2$: 480.22; Found : 480.75.

Synthesis of 1,1'-bis(diethylpyrrolylmethyl)ferrocene (**11**):

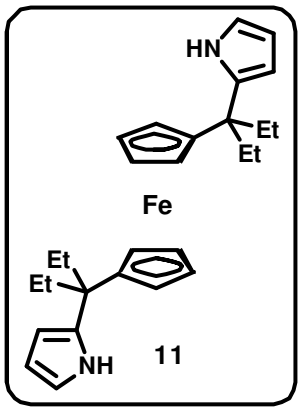

The above procedure was followed by using 1,1'-bis(diethylhydroxymethyl)ferrocene (**4**) (0.8 g, 2.2 mmol) and pyrrole (6.2 mL, 88.8 mmol). The crude product was purified by silica gel column chromatography (100 – 200 mesh). The fraction eluted with EtOAc : petroleum ether (3.5 : 96.5) was identified as pale yellow solid **11**. Yield = 0.68 g, 68%; m.p : 122˚C; ^{1}H NMR (300 MHz, $CDCl_3$, 298 K) : δ = 8.97 (brs, 2H, pyrrole NH), 6.74 (s, 2H, *α*-pyrrole CH), 6.17 (d, J : 2.45 Hz, 2H, *β*-pyrrole CH), 6.02 (s, 2H, *β*-pyrrole CH), 4.15 (s, 4H, ferrocenyl CH), 3.93 (s, 4H, ferrocenyl CH) , 1.87 (m, 8H, ethyl CH), 0.7 (t, 12H, ethyl CH); ^{13}C NMR (100 MHz, $CDCl_3$, 298 K) : δ = 9.21, 32.07, 41.99, 67.92, 68.68, 106.28, 107.45, 115.86, 136.31; FT-IR (CH_2Cl_2) : 3426.77, 3097.84, 2967.48, 2877.34, 1556.44, 1463.89, 1082.47, 1036.45, 827.36, 786.10 cm^{-1}; FAB-MS (m/z) : Calcd for $C_{28}H_{36}FeN_2$: 456.22; Found : 456.74.

Synthesis of 1,1'-bis(dimethylpyrrolylmethyl)ferrocene (**12**):

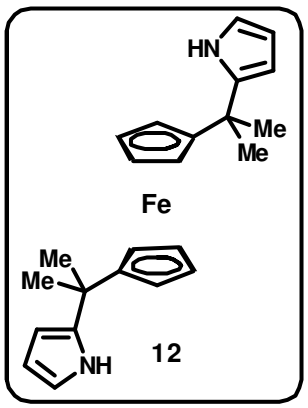

The above procedure was followed by using 1,1'-bis(dimethylhydroxymethyl)ferrocene (**5**) (0.88 g, 2.91 mmol) and pyrrole (8 mL, 116.6 mmol). The crude product was purified by silica gel column chromatography (100 – 200 mesh). The fraction eluted with EtOAc : petroleum ether (3 : 97) was identified as yellow solid **12**. Yield = 0.76 g, 65%; m.p : 108˚C; ^{1}H NMR (300 MHz, $CDCl_3$, 298 K) : δ = 7.76 (brs, 2H, pyrrole NH), 6.48 (q, 2H, *α*-pyrrole CH), 6.01 (q, 2H, *β*-pyrrole CH), 5.85 (s, 2H, *β*-pyrrole CH), 4.09 (s, 4H, ferrocenyl CH), 4.02 (s, 4H, ferrocenyl CH), 1.56 (s, 12H, methyl CH); ^{13}C NMR (100 MHz, $CDCl_3$, 298 K) : δ = 29.98, 34.24, 68.25, 68.32, 99.37, 102.71, 107.77, 115.57, 140.86; FT-IR (CH_2Cl_2) : 3417.58, 2917.58, 1594.01, 1262.03, 1119.38, 1023.36 cm^{-1}; FAB-MS (m/z) : Calcd for $C_{24}H_{28}FeN_2$: 400.16; Found : 400.18.

Synthesis of 1,1'-bis(diphenylpyrrolylmethyl)ruthenocene (**13**):

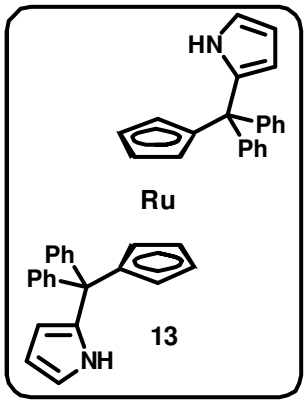

The above procedure was followed by using 1,1'-bis(diphenylhydroxymethyl)ruthenocene (**6**) (1 g, 1.7 mmol) and pyrrole (5 mL, 68 mmol). The product was filtered and thoroughly washed with petroleum ether to remove excess pyrrole and resultant white residue was identified as **13**. Yield = 0.95 g, 81%; m.p : 194˚C; ^{1}H NMR (300 MHz, $CDCl_3$, 298 K) : δ = 9.23 (brs, 2H, pyrrole NH), 7.21 (m, 12H, phenyl CH), 7.01 (m, 8H, phenyl CH), 6.70 (t, 2H, *α*-pyrrole CH), 6.10 (t, 2H, *β*-pyrrole CH), 5.58 (t, 2H, *β*-pyrrole CH), 4.39 (s, 4H, ruthenocenyl CH), 4.24 (s, 4H, ruthenocenyl CH); ^{13}C NMR (100 MHz, $CDCl_3$, 298 K) : δ = 73.66, 74.27, 100.76, 107.54, 109.51, 115.81, 126.45, 127.24, 129.23, 147.89; FT-IR (CH_2Cl_2) : 3433.77,

2923.07, 1593.98, 1259.29, 1116.63, 1027.70 cm^{-1}; FAB-MS (m/z) : Calcd for $C_{44}H_{36}RuN_2$: 694.19; Found : 694.10.

Synthesis of 1,1'-bis(dimethylpyrrolylmethyl)ruthenocene (**14**):

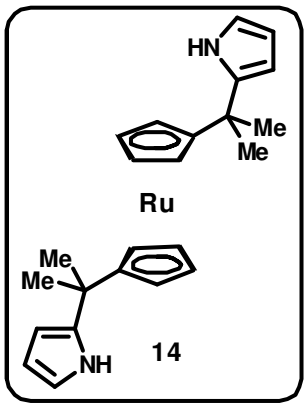

14

The above procedure was followed by using 1,1'-bis(dimethylhydroxymethyl)ruthenocene (**7**) (0.8 g, 2.31 mmol) and pyrrole (6.4 mL, 92.2 mmol). The crude product was purified by silica gel column chromatography (100 – 200 mesh). The fraction eluted with EtOAc : petroleum ether (3 : 97) was identified as yellow solid **14**. Yield = 0.70 g, 68%; m.p : 108˚C; ^{1}H NMR (300 MHz, $CDCl_3$, 298 K) : δ = 7.70 (brs, 2H, pyrrole NH), 6.4 (q, 2H, *α*-pyrrole CH), 5.98 (q, 2H, *β*-pyrrole CH), 5.81 (s, 2H, *β*-pyrrole CH), 4.03 (s, 4H, ruthenocenyl CH), 3.99 (s, 4H, ruthenocenyl CH), 1.63 (s, 12H, methyl CH); ^{13}C NMR (100 MHz, $CDCl_3$, 298 K) : δ = 30.08, 34.68, 68.40, 68.21, 99.89, 101.92, 108.05, 115.03, 141.19; FT-IR (CH_2Cl_2) : 3416.98, 2918.03, 1592.98, 1263.87, 1120.40, 1021.98 cm^{-1}; FAB-MS (m/z) : Calcd for $C_{24}H_{28}RuN_2$: 446.13; Found : 446.74.

Synthesis of 2,5-bis(dimethylhydroxymethyl)thiophene (**15**):

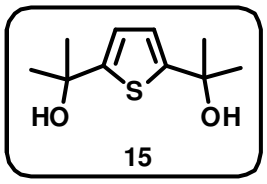

15

Thiophene (0.95 mL, 12 mmol) was dissolved in 30 mL dry ether under N_2 atm followed by the addition of TMEDA (5.4 mL, 36 mmol). 22 mL of *n*-Butyl Lithium was added drop wise to the above solution and allowed to stir at room temperature for 90 min. Then the reaction mixture was refluxed for 4 hr after which it is allowed to come to room temperature. Dry Acetone (4.4 mL, 60 mmol) was added drop wise to the above reaction mixture at 0°C and allowed to stir for further 2 hr. The reaction mixture was quenched with 100 mL of saturated NH_4Cl solution. The organic layer was extracted with ether and dried over anhydrous sodium sulphate. The

solvent was removed by vacuum distillation. The diol **15** was separated by silica gel column chromatography [(silica gel 100 – 200 mesh), (4 : 96, EtOAc : petroleum ether)] as a white solid. Yield = 0.275 g, 11.5%. ^{1}H NMR (300 MHz, $CDCl_3$, 298 K) : δ = 6.78 (s, 2H, thiophene CH), 2.13-2.08 (m, 2H, hydroxyl OH), 1.65 (s, 12H, methyl CH). FAB mass (m/z) : Calcd for $C_{10}H_{16}SO_2$: 200.09; Found : 200.65.

Synthesis of 2,5-bis(dimethylhydroxymethyl)furan (**16**):

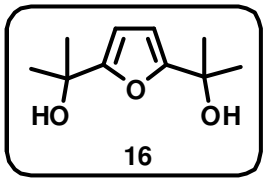

16

Furan (1.06 mL, 14 mmol) was dissolved in 30 mL dry ether under N_2 atm followed by the addition of TMEDA (4.5 mL, 30 mmol). 16 mL of *n*-Butyl Lithium was added drop wise to the above solution and allowed to stir at room temperature for 90 min. Then the reaction mixture was refluxed for 4 hr after which it is allowed to come to room temperature. Dry Acetone (5 mL, 70 mmol) was added drop wise to the above reaction mixture at 0 ℃ and allowed to stir for further 2 hr. The reaction mixture was quenched with 100 mL of saturated NH_4Cl solution. The organic layer was extracted with ether and dried over anhydrous sodium sulphate. The solvent was removed by vacuum distillation. The diol **16** was separated by silica gel column chromatography [(silica gel 100 – 200 mesh), (4 : 96, EtOAc : petroleum ether)] as a white solid. Yield = 0.29 g, 11%. ^{1}H NMR (300 MHz, $CDCl_3$, 298 K) : δ = 6.09 (s, 2H, furan CH), 2.69 (brs, 2H, hydroxyl OH), 1.56 (s, 12H, methyl CH). FAB mass (m/z) : Calcd for $C_{10}H_{16}O_3$: 184.11; Found : 184.35.

Synthesis of 2,5-bis(phenylhydroxymethyl)thiophene (**17**):

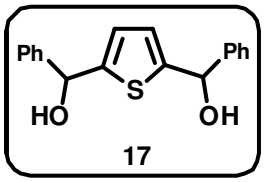

17

Thiophene (0.95 mL, 12 mmol) was dissolved in 30 mL dry ether under N_2 atm followed by the addition of TMEDA (5.4 mL, 36 mmol). 22 mL of *n*-Butyl Lithium was added drop wise to the above solution and allowed to stir at room temperature for 90 min. Then the reaction mixture was refluxed

for 4 hr after which it is allowed to come to room temperature. Benzaldehyde (3.7 mL, 36 mmol) in 20 mL dry ether was added drop wise to the above reaction mixture at 0°C and allowed to stir for further 2 hr. The reaction mixture was quenched with 100 mL of saturated NH_4Cl solution. The organic layer was extracted with ether and dried over anhydrous sodium sulphate. The solvent was removed by vacuum distillation. The diol **17** was separated by silica gel column chromatography [(silica gel 100 – 200 mesh), (4 : 96, EtOAc : petroleum ether)] as a white solid. Yield = 0.27 g, 8%. ^{1}H NMR (300 MHz, $CDCl_3$, 298 K) : δ = 7.38 – 7.32 (m, 4H, phenyl CH), 7.28 – 7.18 (m, 6H, phenyl CH), 6.6 (s, 2H, thiophene CH), 5.86 (s, 2H, *meso* CH), 2.26 (brs, 2H, hydroxyl OH) FAB mass (m/z) : Calcd for $C_{18}H_{16}O_2S$: 296.09; Found : 296.58.

Synthesis of 5-methyl-5-phenyldipyrromethane (**18**):

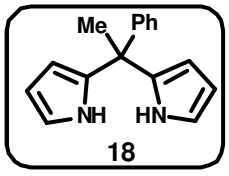

18

A solution of acetophenone (3 mL, 25 mmol) and pyrrole (8.7 mL, 125 mmol) was degassed by bubbling with N_2 for 10 min and then trifluoroacetic acid (0.4 mL, 5 mmol) was added. The solution was stirred for 30 min at room temperature. The mixture was diluted with CH_2Cl_2 (50 mL), then washed with 0.1 N aq. NaOH, water and dried over anhydrous sodium sulphate. The solvent was removed by vacuum distillation. The resulting dark brown oil was purified by silica gel column chromatography (silica gel 100 – 200 mesh), (8 : 92, EtOAc : petroleum ether) and the first moving fraction was identified as **18** as white solid. Yield = 3.4 g, 57.6%. ^{1}H NMR (300 MHz, $CDCl_3$, 298 K): δ = 7.77 (brs, 2H, pyrrolyl NH), 7.17-7.3 (m, 2H, phenyl CH), 7.13-7.07 (m, 3H, phenyl CH), 6.66-6.65 (d, J = 1.2 Hz, 2H, α-pyrrolyl CH), 6.18-6.15 (q, 2H, β-pyrrolyl CH), 5.97 (s, 2H, β-pyrrolyl CH), 2.05 (s, 3H, methyl CH). FAB mass (m/z) : Calcd for $C_{16}H_{16}N_2$: 236.13; Found : 236.07.

Synthesis of 5,5-cyclohexyldipyrromethane (**19**):

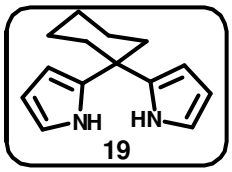

19

A solution of cyclohexanone (1.05 mL, 10.2 mmol) and pyrrole (14.1 mL, 204 mmol) was degassed by bubbling with N_2 for 10 min and then trifluoroacetic acid (0.16 mL, 2.04 mmol) was added. The solution was stirred for 30 min at room temperature. The mixture was diluted with CH_2Cl_2 (50 mL) then washed with 0.1 N aq. NaOH, water and dried over anhydrous sodium sulphate. The solvent was removed by vacuum distillation. The resulting dark brown oil was purified by silica gel column chromatography [(silica gel 100 – 200 mesh), (3 : 97, EtOAc : petroleum ether)] and the first moving fraction was identified as **19** as white solid. Yield = 0.76 g, 35%. ^{1}H NMR (300 MHz, $CDCl_3$, 298 K): δ = 7.69 (brs, 2H, pyrrolyl NH), 6.59-6.58 (d, J = 1.25 Hz, 2H, α-pyrrolyl CH), 6.14-6.12 (m, 2H, β-pyrrolyl CH), 6.05-6.03 (d, 2H, β-pyrrolyl CH), 1.77 (m, 4H, cyclohexyl CH), 1.42 (m, 6H, cyclohexyl CH). FAB mass (m/z) : Calcd for $C_{14}H_{18}N_2$: 214.15; Found : 214.69.

Synthesis of 5,5-diethyldipyrromethane (**20**):

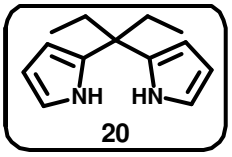

20

A solution of 3-pentanone (1.23 mL, 12 mmol) and pyrrole (16 mL, 240 mmol) was degassed by bubbling with N_2 for 10 min and then trifluoroacetic acid (0.18 mL, 2.3 mmol) was added. The solution was stirred for 30 min at room temperature. The mixture was diluted with CH_2Cl_2 (50 mL), then washed with 0.1 N aq. NaOH, water and dried over anhydrous sodium sulphate. The solvent was removed by vacuum distillation. The resulting dark brown oil was purified by silica gel column chromatography [(silica gel 100 – 200 mesh), (1 : 99, EtOAc : petroleum ether)] and the first moving fraction was identified as **20** as white solid. Yield = 1.21 g, 50%. ^{1}H NMR (300 MHz, $CDCl_3$, 298 K): δ = 7.65 (brs, 2H, pyrrolyl NH), 6.57 (s, 2H, α-pyrrolyl CH),

6.11 (s, 4H, β-pyrrolyl CH), 1.95-1.91 (q, 4H, CH_2 H), 0.7-0.67 (t, 6H, methyl CH). FAB mass (m/z) : Calcd for $C_{13}H_{18}N_2$: 202.15; Found : 202.77.

Synthesis of 5,5-dimethyldipyrromethane (**21**):

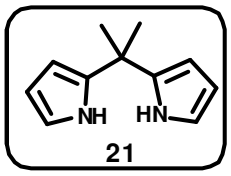

21

A solution of acetone (4 mL, 53 mmol) and pyrrole (18 mL, 260 mmol) was degassed by bubbling with N_2 for 10 min and then trifluoroacetic acid (0.8 mL, 10.4 mmol) was added. The solution was stirred for 30 min at room temperature. The mixture was diluted with CH_2Cl_2 (75 mL), then washed with 0.1 N aq. NaOH, water and dried over anhydrous sodium sulphate. The solvent was removed by vacuum distillation. The resulting brown oil was purified by silica gel column chromatography [(silica gel 100 – 200 mesh), (5 : 95, EtOAc : petroleum ether)] and the first moving fraction was identified as **21** as white solid. Yield = 1.17 g, 13%. ^{1}H NMR (300 MHz, $CDCl_3$, 298 K) : δ = 7.66 (brs, 2H, pyrrolyl NH), 6.59-6.58 (d, J = 1.25 Hz, 2H, α-pyrrolyl CH), 6.13-6.08 (m, 4H, β-pyrrolyl CH), 1.63 (s, 6H, methyl CH). FAB mass (m/z) : Calcd for $C_{11}H_{14}N_2$: 174.12; Found : 174.10.

2.7 Crystal data

Table 2.3. Crystallographic data for **8** and **12**

Parameters	**8**	**12**
Solvent of crystallization	CH_2Cl_2 / Pentane	$CHCl_3$ / Heptane
Empirical formula	$C_{44}H_{36}FeN_2$	$C_{24}H_{28}FeN_2$
M_w	648.60	400.33
T [K]	293(2)	293(2)
λ [Å]	0.71073	0.71073
Crystal system	Triclinic	Triclinic
Space group	P-1	P-1
a[Å]	8.7609(4)	7.3633(3)
b[Å]	10.2902(5)	12.0119(5)
c[Å]	18.3852(8)	12.4506(6)
α [°]	101.069(2)	105.413(2)
β [°]	100.895(2	95.925(2)
γ [°]	92.606(3)	106.768(2)
V[Å^3]	1591.54(13)	996.98(8)
Z, ρ_{calcd} [Mg m^{-3}]	2, 1.353	2, 1.334
μ ($Mo_{K\alpha}$) [mm^{-1}]	0.510	0.767
F (000)	680	424
Crystal size [mm]	0.30 × 0.20 × 0.20	0.30 × 0.20 × 0.20
θ range for data collection [°]	1.15 to 22.26	1.73 to 33.64
Limiting indices	$-9 \le h \le 9$ $-10 \le k \le 10$ $-19 \le l \le 19$	$-11 \le h \le 10$ $-18 \le k \le 18$ $-19 \le l \le 19$
Reflections collected	22632	27755
Refinement method	Full-matrix least-squares on F^2	Full-matrix least-squares on F^2
Data / restraints / parameters	3988 / 27 / 394	7805 / 0 / 248
Goodness-of- fit on F^2	1.048	1.099
Final R indices[I>2σ(I)]	R1 = 0.0908, wR2 = 0.2375	R1 = 0.0391 wR2 = 0.1006
R indices (all data)	R1 = 0.1563, wR2 = 0.2562	R1 = 0.0619 wR2 = 0.1221
Largest $\Delta\rho$[e Å^{-3}]	1.055 and -0.884	0.776 and -0.250

Chapter 3

ansa-Metallocene-based *normal* Calixpyrroles

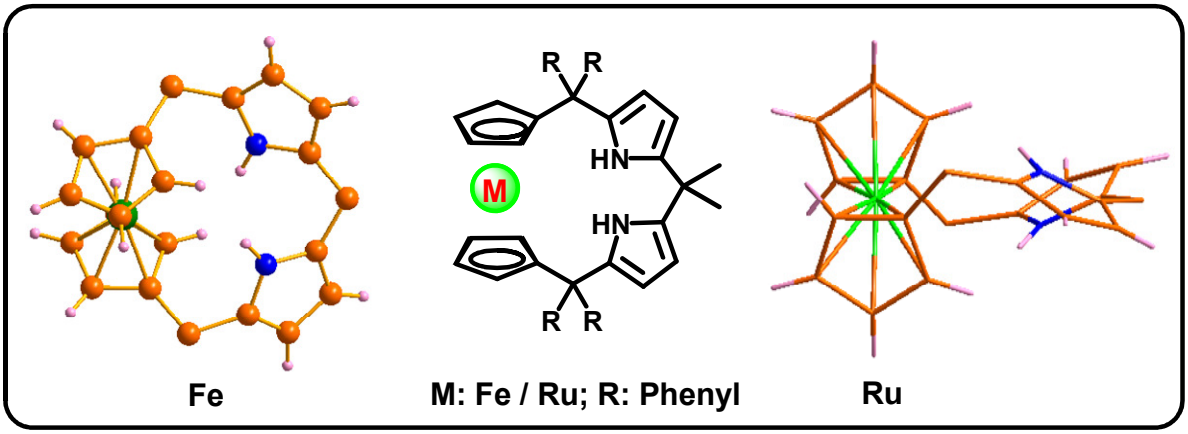

3.1 Abstract

The syntheses, spectral and structural characterization of ansa-metallocene based normal calixpyrroles are described in the concerned chapter. Metallocene units are incorporated into the backbone of the calixpyrrole frame work for the first time in an ansa type way. Acid catalysed condensation of 1,1'-ferrocenyl-bis-(gem-diaryl/alkylaryl/cyclohexyl/dialkylpyrrolyl)methane with the respective ketones or 1,1'-ferrocenyl-bis-(gem-diaryl/alkylaryl/cyclohexyl/dialkylhydroxy)methane with the respective 5,5-(alkylaryl/cyclohexyl/dialkyl)dipyrromethane yielded ansa-ferrocene based normal calixpyrroles in approximately moderate yields. One of the reason for the low yield is that, acidification of the ferrocenyl dipyrromethane occurs which is very much evident from the TLC analysis. The absence of two α-CH protons in the pyrrolic rings, which are observed in 1,1'-ferrocenyldipyrromethane, proved by ^{1}H and ^{1}H - ^{1}H COSY spectral analysis of the macrocycle and the correlation between the pyrrolic NH with β-CH protons suggests the formation of the macrocycle. The pyrrole rings in 1,1'-ferrocenyldipyrromethane rotate in clockwise and anticlockwise directions and condense with ketones in the presence of acid catalyst to form the macrocycle. The confirmation of the proposed structure of the macrocycles has finally come from the single-crystal X-ray structural analysis. The side view of the macrocycle clearly shows that both the pyrrole rings in the macrocycle adopts partial 1,2-alternate conformation in the solid state which shows that the macrocycles retains the parent calix[4]pyrrole behavior in the solid state. The chemistry is further extended into the next higher metallocene, such as, ruthenocene and observed the same trend as that of the ferrocenyl derivative.

3.2 Introduction

The calixpyrrole **1** (Figure 3.1) (*meso*-octasubstituted porphyrinogens) is a venerable class of macrocycles, which are colorless and not naturally occurring, was first synthesized by Baeyer in 1886 by condensing pyrrole and acetone in the presence of an acid (Scheme 3.1) [Baeyer 1886]. Indeed, subsequent to the work of Baeyer, Dennstedt and Zimmermann also studied this reaction, using 'chlorzink' as the acid catalyst [Dennstedt and Zimmerman 1887, Dennstedt 1890].

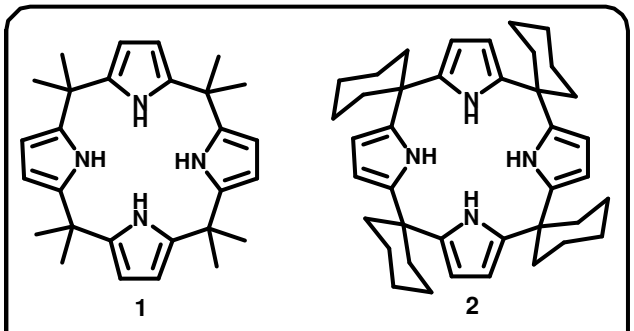

Figure 3.1. Structure of calix[4]pyrrole

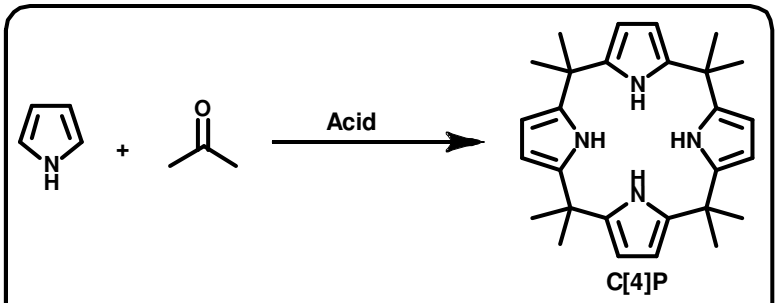

Scheme 3.1. Synthesis of calix[4]pyrrole

Thirty years later, during the first world war, chelintzev and tronov repeated these reactions and proposed a cyclic tetrameric structure for calix[4]pyrrole [[a]Chelintzev and Tronov 1916, [b]Chelintzev *et al*. 1916] and the name α, β, γ, δ–octamethylporphinogen to these macrocycle was given by Fischer [Fischer and Orth 1934]. They have carried out several other reactions which included acid catalysed condensation of pyrrole, acetone and

ethyl methyl ketone, which yielded a small quantity of single calix[4]pyrrole configurational isomer. Additionally, ethyl methyl ketone and acetone were co-condensed with pyrrole forming a mixed *meso*-hexamethyldiethyl calix[4]pyrrole of unknown structure. In 1950s, Rothemund and Gage used methanesulphonic acid as the acid catalyst, obtained an improved yield and clearly proved its structure [Rothemund and Gage 1955]. In early 1970s, Brown *et al*. reported a refined procedure in which they condensed cyclohexanone with pyrrole in a 1 : 1 ratio in the presence of acid to produce tetraspirocyclohexyl calix[4]pyrrole **2** (Figure 3.1) [Brown *et al*. 1971], a compound which was earlier reported by Chelintzev, Tronov and Karmanov in 1916, in decent yield.

3.3 Synthetic methods

3.3.1 Modification at the *C*-rim

Series of *C*-rim substituted calix[4]pyrrole are known in the literature which is shown in Figure 3.2. Substitution of the *β*-pyrrolic hydrogen by different groups comes under modification at the *C*-rim of the calixpyrrole. One of the earlier reports on the *C*-rim substitution was given by Sessler and co-workers where they treated **1** with 4 equiv of *n*-butyl lithium followed by the addition of ethyl bromoacetate resulted in mono-or poly alkylation **3a** and **3b** at the *β*–pyrrolic sites. They also synthesized *β*-octabromo-*meso*-octamethylcalix[4]pyrrole **3c** by the reaction of **1** with NBS in dry THF under reflux conditions. Due to the electron-withdrawing nature of bromine, **3c** has more affinity towards anions when compared with parent **1** [[a]Gale *et al*. 1997, [a]Sessler *et al*. 2000]. Subsequently they synthesized and studied the anion binding properties of *β*-octafluoro-*meso*-octamethylcalix[4]pyrrole **3d** [[b]Anzenbacher *et al*. 2000, Levitskaia *et al*. 2003, Sessler *et al*.

2009, Gale *et al*. 2010]. By suitably changing the synthetic procedures, different β-mono substituted derivatives like ester **3e**, acid **3f**, iodo **3g**, formyl **3h** and protected alcohol derivatives **3i** were also been prepared [[c]Anzenbacher *et al*. 2000].

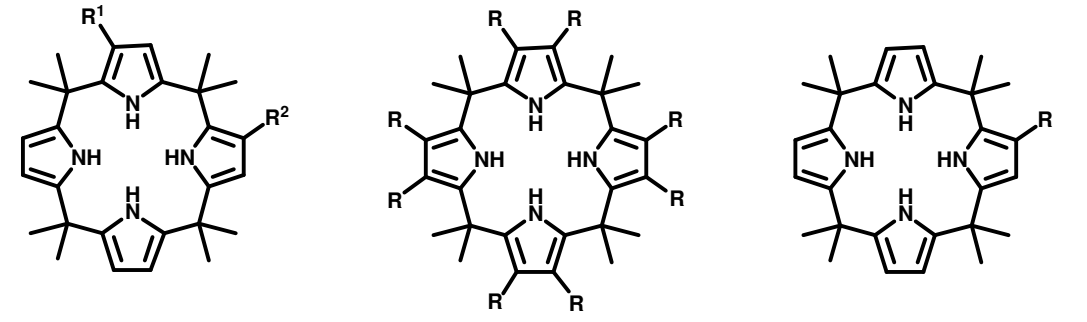

Figure 3.2. Structure of *C*-rim substituted calix[4]pyrrole

3.3.2 Modification at the N-rim

Takata and co-workers reported a synthetic procedure in which the treatment of calix[4]pyrrole **1** with sodium hydride and methyl iodide in the presence of 18-crown-6 ether in THF resulted in the substitution of N-hydrogen by a methyl moiety, thereby resulting in

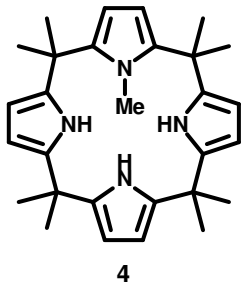

Figure 3.3. Structure of N-rim substituted calix[4]pyrrole

the modification at the N-rim **4** takes place (Figure 3.3) [Furusho *et al*. 1998]. Depending on the equiv of the methyl iodide used, mono, di, tri and tetra N-substituted calix[4]pyrroles can also be obtained.

3.3.3 Modification at the *meso* position

The acid catalysed condensation of different ketones with pyrrole resulted in *meso*-functionalized calix[4]pyrroles [Sessler *et al*. 1996]. *mes*o-Mono-amine functionalized calix[4]pyrrole **5** (Figure 3.4) was obtained by the $BF_3.OEt_2$ catalysed condensation of Cbz-protected 3-aminoacetophenone, 3-pentanone and pyrrole followed by deprotection using Pd-C [[a]Anzenbacher *et al*. 2000].

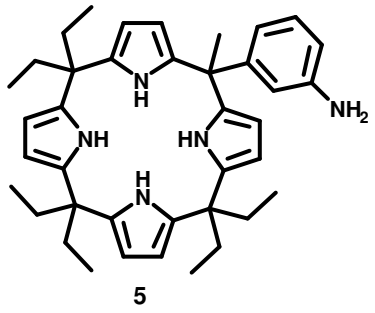

5

Figure 3.4. Structure of *meso* mono-amine functionalized calix[4]pyrrole

3.4 Structural studies

Forty years later after the Rothemund's structural proposal, the X-ray structure determination of this compound revealed the alternating conformations of the pyrrole rings in the solid state [[a]Gale *et al*. 1996] with vicinal pyrrole rings pointing in opposite directions (Figure 3.5a) These macrocycles can adopt a variety of conformations according to the following stability order: 1,3-alternate > partial cone > 1,2-alternate > cone (Figure 3.6), both in the gas phase and in CH_2Cl_2 [Wu *et al*. 2001].

a) b)

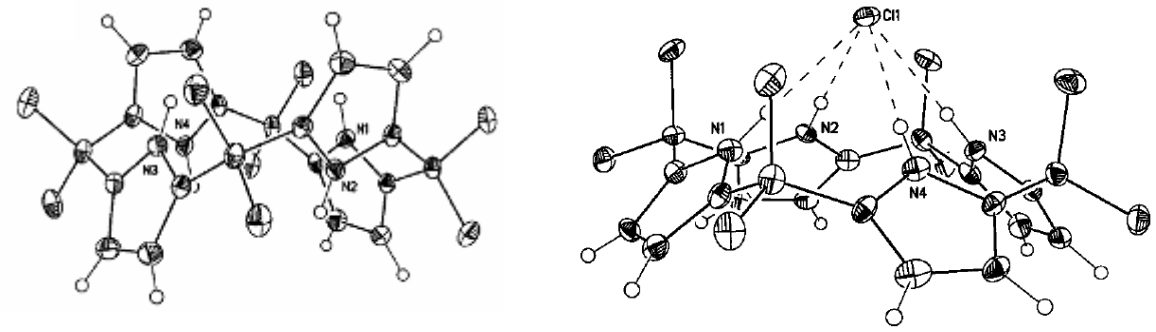

Figure 3.5. Crystal Structure of a) **1** and b) **1** + Cl^-

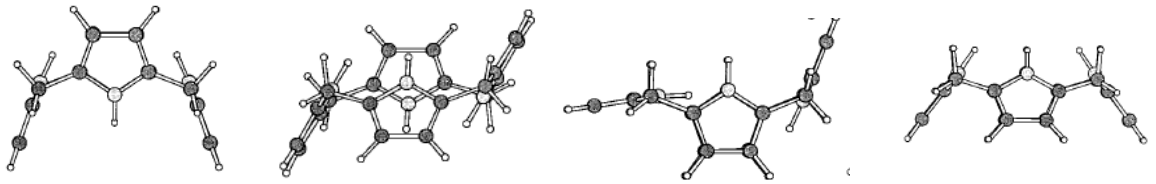

1,3-alternate 1,2-alternate partial cone cone

Figure 3.6. Conformations of calix[4]pyrrole

3.5 Binding of anions and neutral substrates

The calix[4]pyrroles have been extensively studied with regard to their capacity to function as anion sensors and neutral molecule receptors through the formation of four pyrrole NH–anion hydrogen bonds (Figure 3.5b) [Allen *et al*. 1996, [a]Gale *et al*. 1996, [b]Sessler and Gale 2000] and these receptors have been the subject of intense study [Gale *et al*. 1998, [a]Gale *et al*. 2001, [a]Sessler *et al*. 2003]. It has been highlighted that both sensitivity and selectivity exhibited by these macrocycles towards a wide range of guests is mainly governed by the harmonic synergism between their chemical and conformational properties. Indeed, while the (N–H) groups of the pyrrole moieties may act as receptors through H-bond interactions, the tetrahedral carbon bridges linking together the pyrrole units assure an adequate conformational flexibility during the binding event [Gale *et al*. 1998, [a]Gale *et al*.

2001]. A large number of derivatives have been reported in which the anion-binding properties were modulated by varying the size of the macrocycle. Sessler and co-workers reported that calix[4]pyrroles are not only effective anion-binding ligands but also selective ones. They showed that these receptors have a marked preference for fluoride ions relative to other halide guests [[a]Gale *et al*. 1996]. A detailed study carried out by Danil de Namor and Shehab [Namor and Shehab 2003, Namor and Shehab 2004] involving both the thermodynamics of anion-complexation of calix[4]pyrrole in dipolar aprotic media and the solution thermodynamics of the reactants and the products participating in the binding process, confirmed that this receptor interacts selectively with halide ions.

Subsequent studies have shown that members of this class of macrocycles can function both as anion sensors and anion separation agents [Sessler *et al*. 1997, [a]Sessler *et al*. 1998, [a]Sessler *et al*. 2000]. In contrast to typical Werner-type complexes, the nitrogen lone pairs of calix[4]pyrroles are a part of the aromatic π-system of the pyrrole ring and are therefore not available for the complexation of metal species. However, the metallation of calix[4]pyrroles to give the tetra-anion allows the introduction of metal ions [Jubb *et al*. 1992, Floriani 1996, Bonomo *et al*. 2001]. This procedure is experimentally challenging and requires the use of strong bases and strict exclusion of oxygen and water. In 2005, Sessler and co-workers discovered that calix[4]pyrroles can bind ion pairs such as cesium or 1,3-dialkylimidazolium halide salts with the anion bound to the pyrrole NH groups, locking the macrocycle into a cone conformation, and the large charge diffuse cation binding to the electron rich bowl-shaped cavity formed by the calix[4]pyrrole anion complex [Custelcean *et al*. 2005]. Subsequent studies in solution with a variety of salts have demonstrated a significant dependence of anion stability constants on both the nature of the solvent and cation used, indicating that complexation cannot be regarded as a simple 1 : 1 (anion :

calix[4]pyrrole) process but rather that the solvent and cation are intimately involved in the binding processes. This hypothesis is supported by evidence from a variety of solid-state structures showing cation inclusion in the calix[4]pyrrole cup [Lee *et al*. 2005, Sessler *et al*. 2006, [a]Bates *et al*. 2006 , Gross *et al*. 2008, Bates *et al*. 2008, Yoon *et al*. 2008]. It has also been shown that calixpyrroles can extract metal salts from aqueous solution [Wintergerst *et al*. 2008] and transport cesium chloride salts across lipid bilayer membranes [Tong *et al*. 2008, Fisher *et al*. 2009].

Sessler *et al*. in 1996 reported the binding of neutral substrates by calix[4]pyrroles in the solid state and solution state [Allen *et al*. 1996]. The authors have reported the binding of neutral molecules like methanol, N,N-dimethylformamide by calix[4]pyrrole. The calixpyrrole.methanol adduct adopts 1,3-alternate conformation in the solid state. Methanol form intermolecular hydrogen bonding with opposite pyrrolic NH groups. But, the calixpyrrole.N,N-dimethylformamide adduct is in 1,2-alternate conformation. Here also, intermolecular hydrogen bonding is present between N,N-dimethylformamide with adjacent pyrroles.

3.6 Modeling studies

By using Energy minimizations in the gas phase and Monte Carlo stimulations in CH_2Cl_2, van Hoorn and Jorgensen concluded that out of the four possible conformations, 1,3-alternate one is the most stable form of free base calix[4]pyrrole, while the cone conformer is the most stable one for anion bounded calix[4]pyrrole due to the four NH-halide hydrogen bonds [van Hoorn and Jorgensen 1999]. The calculated relative free

energies of binding of anions by **1** were found to be in excellent agreement with the experiment.

3.7 Functionalized systems

Calixpyrroles with functionalizable groups in the *meso*-positions (chloroalkyl or cyano) were reported recently by Lehn and co-workers. Although a major shortcoming of using the calix[4]pyrrole is the difficulty involved in detecting the absorption spectra, the

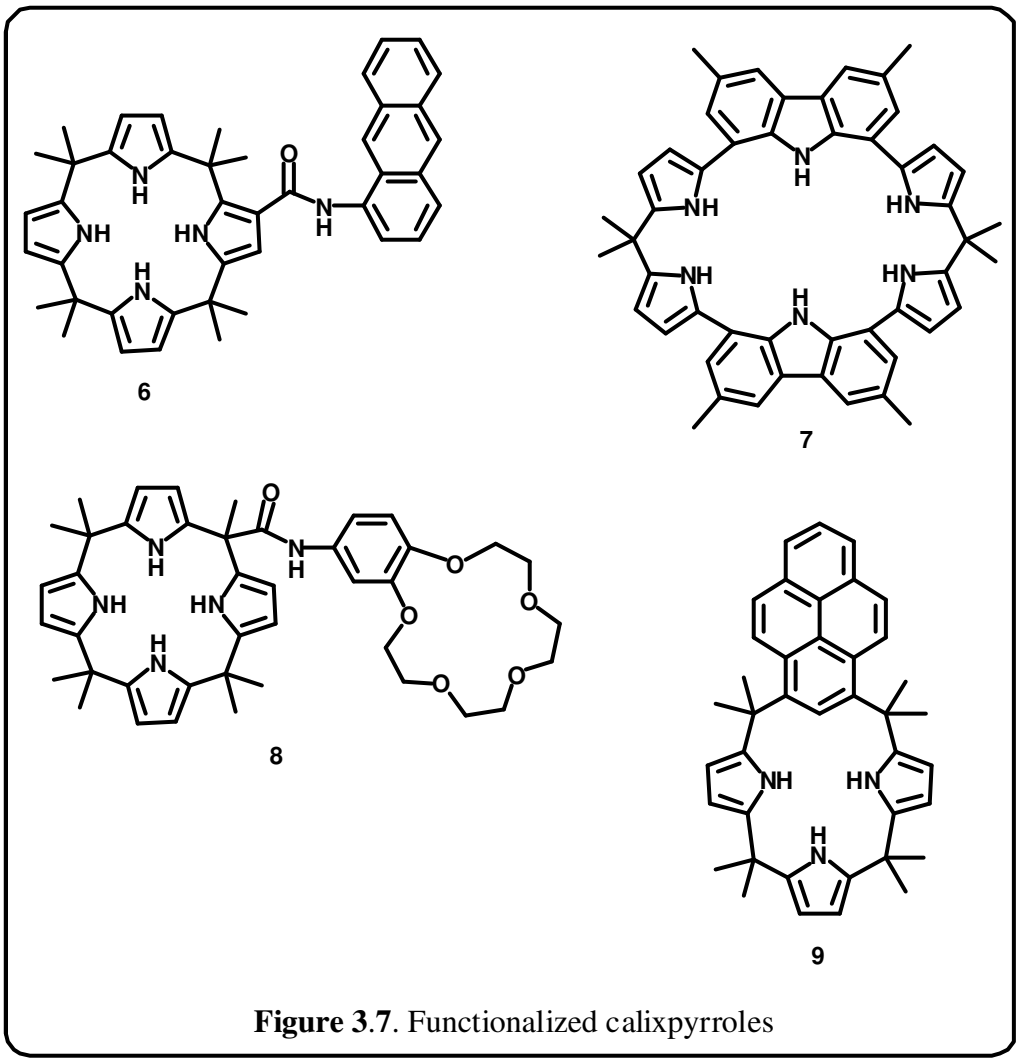

Figure 3.7. Functionalized calixpyrroles

absorption bands fall at energies that are too high to make them helpful in the binding process [Shriver 2002]. Hence, various research groups have created functionalized

calixpyrroles in which different varieties of optical-active species like anthracene **6** [[b]Sessler *et al*. 1998, [a]Sessler *et al*. 2000], carbazole **7** [Piatek *et al*. 2004], crown ethers **8** [[a]Aydogan *et al*. 2008] and pyrene **9** [Yoo *et al*. 2010] (Figure 3.7) have been attached to the calix[4]pyrrole rim to utilize them for anion recognition. The excellent recognition capability of these receptors in solution is widely documented and is currently the object of investigation by a number of research groups worldwide.

3.8 Calixpyrrole based optical and electrochemical sensors

3.8.1 Optical sensors

Two modifications have been done on calixpyrrole systems so that they can be used as optical sensors for different analytes. One method involves the covalent attachment of colorimetric or fluorescent reporter group to the calixpyrrole systems. After binding with anions, there occurs either color change or change in photophysical properties which clearly accounts for the binding properties. Sessler and co-workers synthesized β-(1-amido anthracene) substituted calix[4]pyrrole **6** and related systems [[b]Sessler *et al*. 1998, Miyaji *et al*. 1999] whose fluorescence was quenched significantly in the presence of anionic guests. These calixpyrrole-anthracene analogues possess conjugated and non-conjugated bond pathways of varying lengths between the anthracene reporter group and binding site of calixpyrrole. The second method is based on displacement assay [Metzger and Anslyn 1998, Gale *et al*. 1999] in which a colored anion forms colorless complex with calix[4]pyrroles to which the addition of another stronger binding anion restores the original color of the first anion by displacing it.

3.8.2 Electrochemical sensors

The different varieties of calixpyrrole based electrochemical sensors include the incorporation of calixpyrroles in ion-selective electrodes, discrete electrochemically active receptors and chemically modified electrodes. Sessler and co-workers prepared polyvinyl chloride derived ion-selective electrodes from **1** [Král *et al*. 1999] and they display a stronger anionic responses at lower pH. The attachment of redox-active reporters mainly ferrocene to the calixpyrrole systems [Sessler *et al*. 1997] forms the discrete electrochemically active receptors. Calixpyrroles bound to an electropolymerised

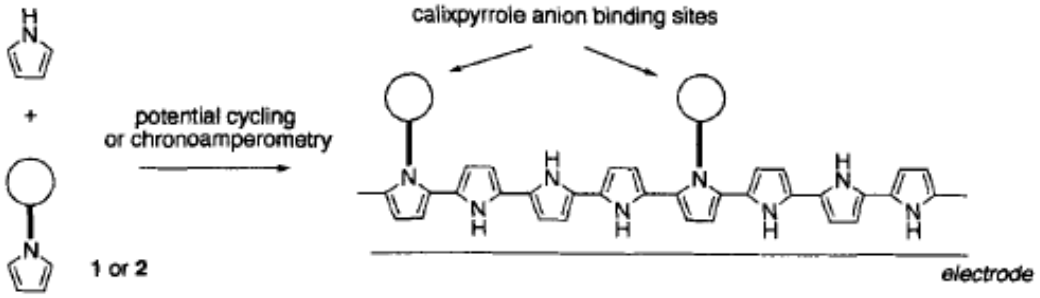

Scheme 3.2. Formation of electropolymerised calixpyrrole-pyrrole co-polymer

moiety [Chen *et al*. 1995] forms an matrix which results in the formation of chemically modified electrodes. Gale and co-workers reported the electropolymerised films by the electrochemical co-polymerisation of calix[4]pyrroles containing pendant *N*-substituted pyrrole moieties and pyrrole (Scheme 3.2) [[c]Gale *et al*. 2001]

3.9 Types of calixpyrrole systems

A large number of derivatives of calixpyrroles (Figure 3.8) have been reported in which the anion-binding properties were modulated by varying the size of the macrocycle, by synthesizing N-Confused calixpyrroles **10** [Depraetere *et al*. 1999, Chen *et al*. 2002, Gu *et al*. 2005, [b]Bates *et al*. 2006, Anzenbacher *et al*. 2006, Dehaen *et al*. 2007], the inclusion of

other aromatic rings like benzene **11** [Sessler *et al*. 2002, [b]Sessler *et al*. 2005, Cafeo *et al*. 2007, Ilango *et al*. 2010], carbazole **7** [Piatek *et al*. 2004], phosphole **12** [[a]Matano *et al*. 2006, Nakabuchi *et al*. 2008], by the use of substituents other than methyl at the *meso*-positions **13** [Camiolo and Gale 2000, Woods *et al*. 2002, Ji *et al*. 2005, Bruno *et al*. 2007] and by connecting two *meso* positions with an appropriate bridge **14** (strapped calixpyrroles) [Lee *et al*. 2003, Lee *et al*. 2005, Cafeo *et al*. 2006, Jeong *et al*. 2007, Lee *et al*. 2008].

Sessler and co-workers reported a newer class of calixpyrrole analogues in which they have used 2,2'-bipyrrole instead of pyrrole, there by synthesizing calix[3]bipyrrole **15** and calix[4]bipyrrole **16** [[c]Sessler *et al*. 2003, [c]Sessler *et al*. 2005], respectively.

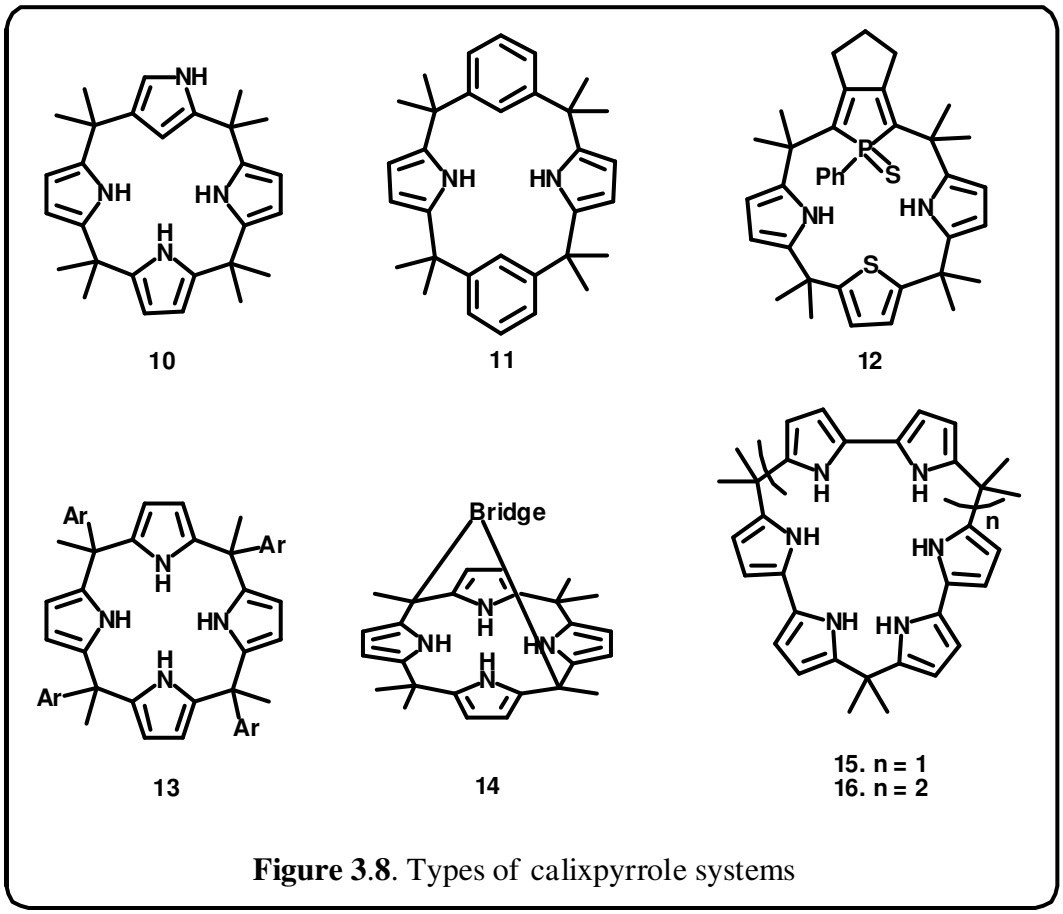

Figure 3.8. Types of calixpyrrole systems

3.10 Ferrocene – pyrrole systems

More germane to the current work are anion receptors containing redox groups that are covalently or non-covalently linked to the receptor moieties. These electrochemical responsive receptors are widely suitable in the areas of chemical sensors, redox catalysts and redox switchable ligands [Tendero *et al*. 1995, Kaifer and Mendoza 1996, [b]Gale *et al*. 2001]. The use of metallocenes, particularly, ferrocene and ruthenocene as an electrochemically active "reporter group" has been explored by a number of research groups [Plenio *et al*. 1998, [b]Beer *et al*. 1999, Beer *et al*. 2000, Collinson *et al*. 2001, Tomapatanaget *et al*. 2003, Reynes *et al*. 2005, Otón *et al*. 2006]. Currently, there are numerous examples of macrocycles in which ferrocenes are externally appended or attached to *meso* carbons to various anion binding porphyrin or porphyrin analog receptors and calixpyrroles **17-18** (Figure 3.9) are reported [Beer 1996, [a]Beer *et al*. 1997, Sessler *et al*. 1997, [b]Gale *et al.* 2001, Szymańska *et al*. 2006, Coman *et al*. 2008].

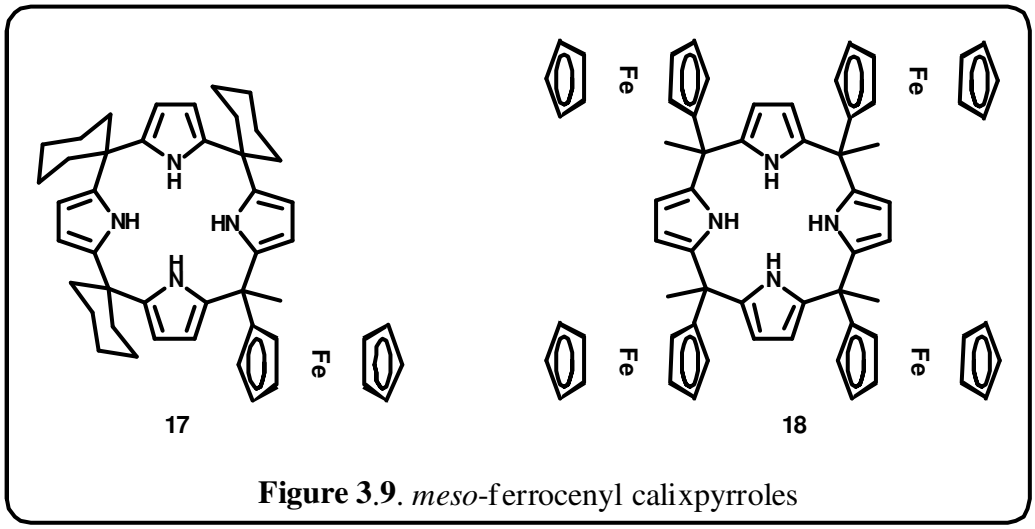

Figure 3.9. *meso*-ferrocenyl calixpyrroles

^{1}H NMR titration studies in acetonitrile-d_3 / DMSO-d_6 9:1 have revealed that **17** binds fluoride, chloride and dihydrogen phosphate in this solvent mixture. The downfield shift of one ferrocene CH proton clearly revealed the formation of CH---anion hydrogen

bonds in solution (Scheme 3.3). The electrochemical behavior of *meso*–tetraferrocenyl–tetramethylcalix[4]pyrrole modified graphite electrode (G/TFCP) **18** was investigated. Cyclic Voltammetry measurements were performed in order to examine the TFCP electrochemical response in various experimental conditions (different electrode materials, anion concentrations, pH and potential scan rates), and in the presence of the following anions: ClO_4^-, NO_3^-, F^-, Cl^-, Br^-, SO_4^{2-}, $H_2PO_4^-$.

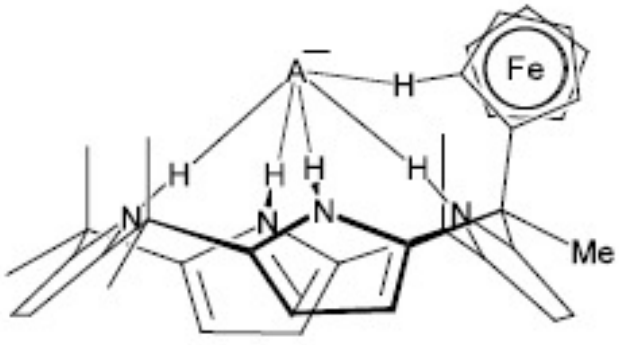

Scheme 3.3. Schematic representation of hydrogen bonding interaction between ferrocene CH and calixpyrrole NH with anion

Recently, Sessler has reported *ansa*-ferrocene type bridged pyrrolic systems **19** (Figure 3.10a) that shows significant perturbations in their electrochemical properties in the presence of anionic guests [Scherer *et al*. 1998, [b]Sessler *et al*. 2001]. ^{1}H-NMR binding studies of **19** in a 2% dimethylsulfoxide-d_6 solution of CH_2Cl_2-d_2 establish a correlation between the affinity for tetrabutylammonium dihydrogen phosphate and the number of heteroatoms in the diamine. Further support for this conclusion came from electrochemical analyses. A single crystal X-ray diffraction study (Figure 3.10b) revealed the presence of a water molecule inside the cavity, as well as a second water molecule not constrained in the cavity but hydrogen bonded to the encapsulated water molecule. The water molecule bound in the cavity was stabilized by NH---O hydrogen bonds from an amide NH and a pyrrole NH,

acting as hydrogen bond donors, as well as an OH---O hydrogen bond from the water to an ether oxygen of the linker, acting as a hydrogen bond acceptor.

a) b)

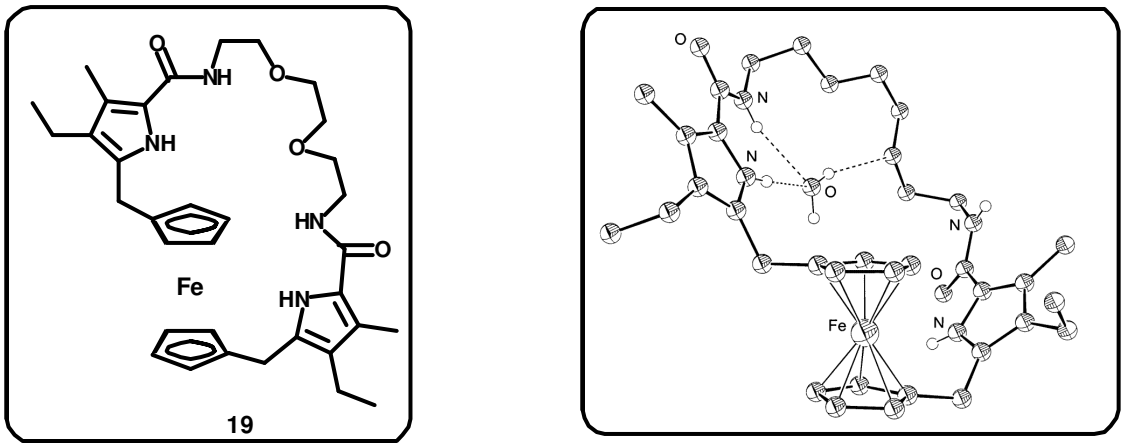

Figure 3.10. a) A bridged pyrrolic *ansa*-ferrocene **19**, b) Solid state structure of **19·2H$_2$O** (the second water molecule, which is outside the cavity, has been omitted for clarity)

3.11 Objective of our work

However, by incorporating metallocene into the backbone of calixpyrrole systems or incorporation of metallocenes in the mainframe work of calixpyrroles in an *ansa*-type way was not known. In this chapter, we were involved in the syntheses, spectral and structural characterization of *ansa*-ferrocene-based *normal* calixpyrroles (Scheme 3.4). The structure of these macrocycles were finally confirmed by single crystal X-ray analyses which clearly proves the linkage of dipyrrolyl moiety to 1 and 1' position of ferrocene through *meso* sp^3 hybridized carbons. Similar chemistry has been further extended into *ansa*-ruthenocene moiety (Scheme 3.4).

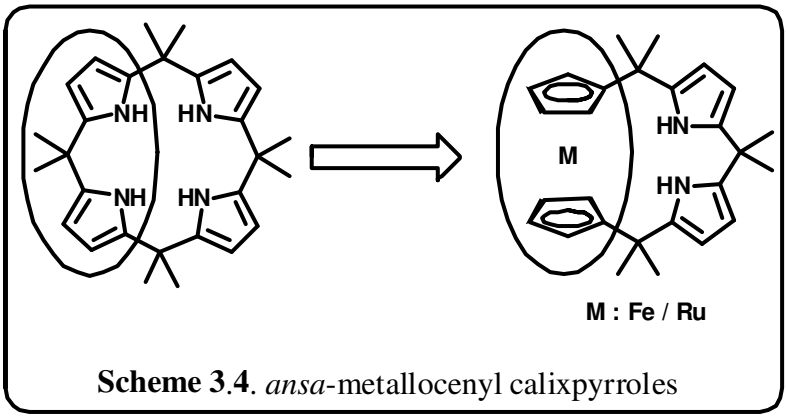

Scheme 3.4. *ansa*-metallocenyl calixpyrroles

3.12 Results and discussion

The syntheses of **30 - 37** are shown in Scheme 3.5a and 3.5b and the yields are mentioned in Table 3.1. In Scheme 3.5a, we used three different reaction conditions. (i) By varying the acid-catalyst, (ii) by using acetone as solvent as well as reactant and (iii) by mixing various ketones in CH_2Cl_2 solvent. The suitable acid-catalyst is identified from (i) and used as such in (ii) and (iii). Initially, in (i), we concentrated mainly on the synthesis of **30** by using 0.1 equiv of various catalysts such as Lewis to Protic acids. Thus, acid-catalyzed condensation of **25** with acetone (30 mL) using different acid catalysts afforded **30** and the observed yields are shown in Table 3.1. The yield was found to be dependent on the nature of the acid-catalyst used. The lower yield of **30** in the presence of Lewis acid indicates the partial acidolysis of **25**. Evidence of the acidolysis has come from the following observation, where the TLC (Silica gel G; EtOAc : Hexane [1 : 25]) analysis of **25** with 0.1 equiv of $BF_3.OEt_2$ indicated decrease in the concentration of **25**. Similar trend was observed by Lindsey and co-workers, wherein the dipyrromethanes undergo partial acidolysis depending on the Lewis acid concentration and nature of the *meso*-substituents [Lee and Lindsey 1994]. Overall, TFA was found to be well suited in (i) and employed for the syntheses of remaining macrocycles **31 - 37**. Thus, by using condition (ii), a series of 1,1'- ferrocenyl substituted

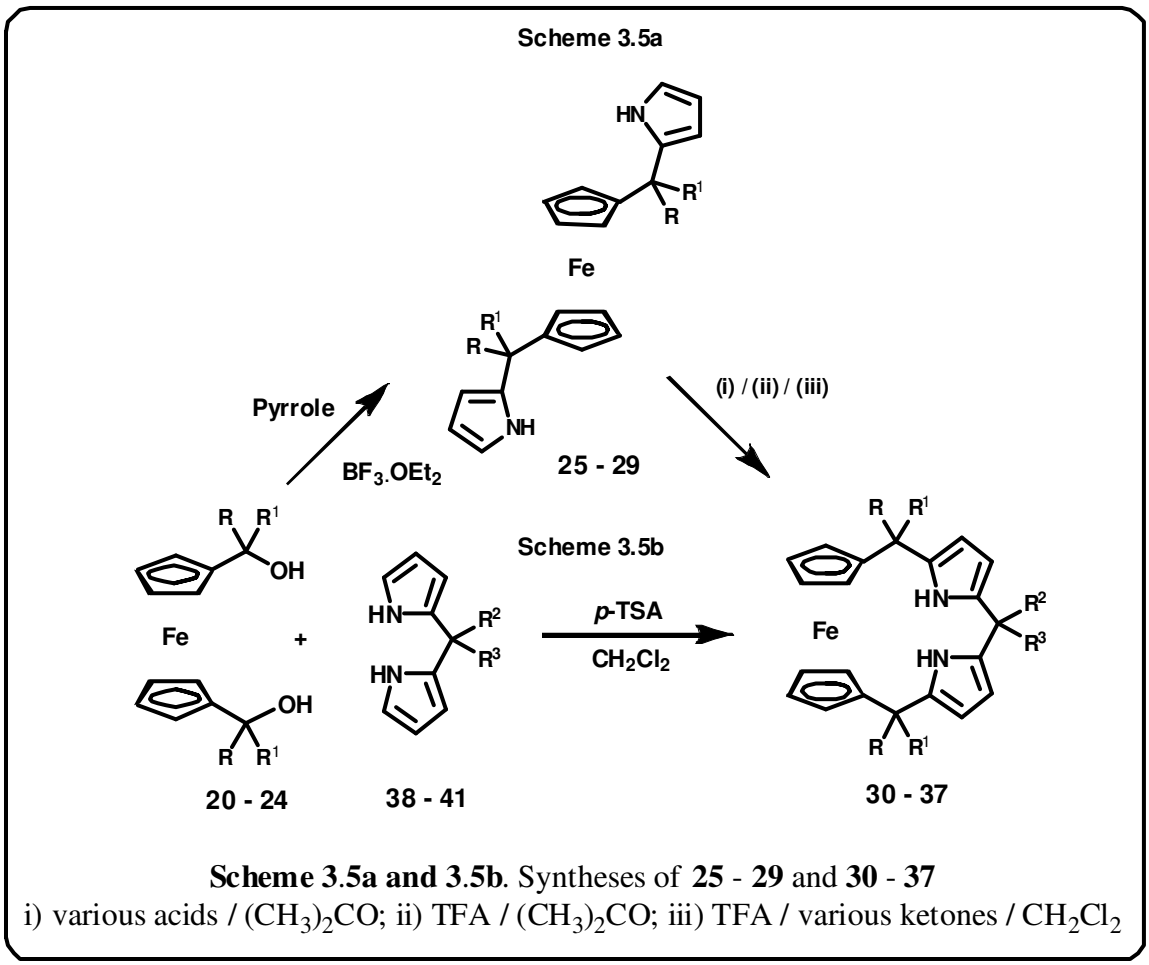

Scheme 3.5a and 3.5b. Syntheses of **25** - **29** and **30** - **37**
i) various acids / $(CH_3)_2CO$; ii) TFA / $(CH_3)_2CO$; iii) TFA / various ketones / CH_2Cl_2

dipyrromethanes (**26 - 29)** reacted with acetone in the presence of trifluoroacetic acid afforded **31 - 34** in 19 to 25% yield, respectively. On the other hand, in (iii), by using 30 mL of CH_2Cl_2, similar ketones, which are used for the synthesis of **21 - 23**, were condensed with the respective 1,1'- ferrocenyl dipyrromethanes (**26 - 28)** under identical reaction conditions yielded **35 - 37** in 17 – 25% yield, respectively (Table 3.1).

Table 3.1. Yields of **30** – **37**

acids	**30** (%)
$BF_3.OEt_2$	25
$SnCl_4$	28
TFA	48
p-TSA	46
MSA	41

no	R	R^1	R^2	R^3	Yield (%) Scheme 3.5a	Yield (%) Scheme 3.5b
30	C_6H_5	C_6H_5	CH_3	CH_3	48	23
31	CH_3	C_6H_5	CH_3	CH_3	19	18
32	cyclohexyl		CH_3	CH_3	22	20
33	C_2H_5	C_2H_5	CH_3	CH_3	19	17
34	CH_3	CH_3	CH_3	CH_3	25	22
35	CH_3	C_6H_5	CH_3	C_6H_5	23	19
36	cyclohexyl		cyclohexyl		25	22
37	C_2H_5	C_2H_5	C_2H_5	C_2H_5	17	16

Both the conditions mentioned here are straightforward with no side product formation. However, we observed trace amount of three more products along with **34**. The FAB mass analysis of the new products suggested the formation of the *higher* derivatives of **34**, calix[*n*]ferrocenyl[*m*]pyrroles where n = 2, 3, 4 and m = 4, 6, 8 (**42**, **43** and **44**) (Figure 3.11). In Scheme 3.5a, **30 - 34** were synthesized under the reaction conditions (ii), while **35 - 37** via (iii). In order to improve the yields of **30 - 37**, we adopted the different synthetic route which is shown in Scheme 3.5b. *p*-toluenesulphonic acid (*p*-TSA) catalyzed condensation of 1,1'-ferrocene diol with series of dipyrromethanes **38 - 41** [Lee and Lindsey 1994] afforded **30 - 37** in 16 to 23% yield, respectively. However, the obtained yields are comparable as mentioned in Scheme 3.5a. Thus, varying the synthetic methodology did not alter the yield of the macrocycle formation.

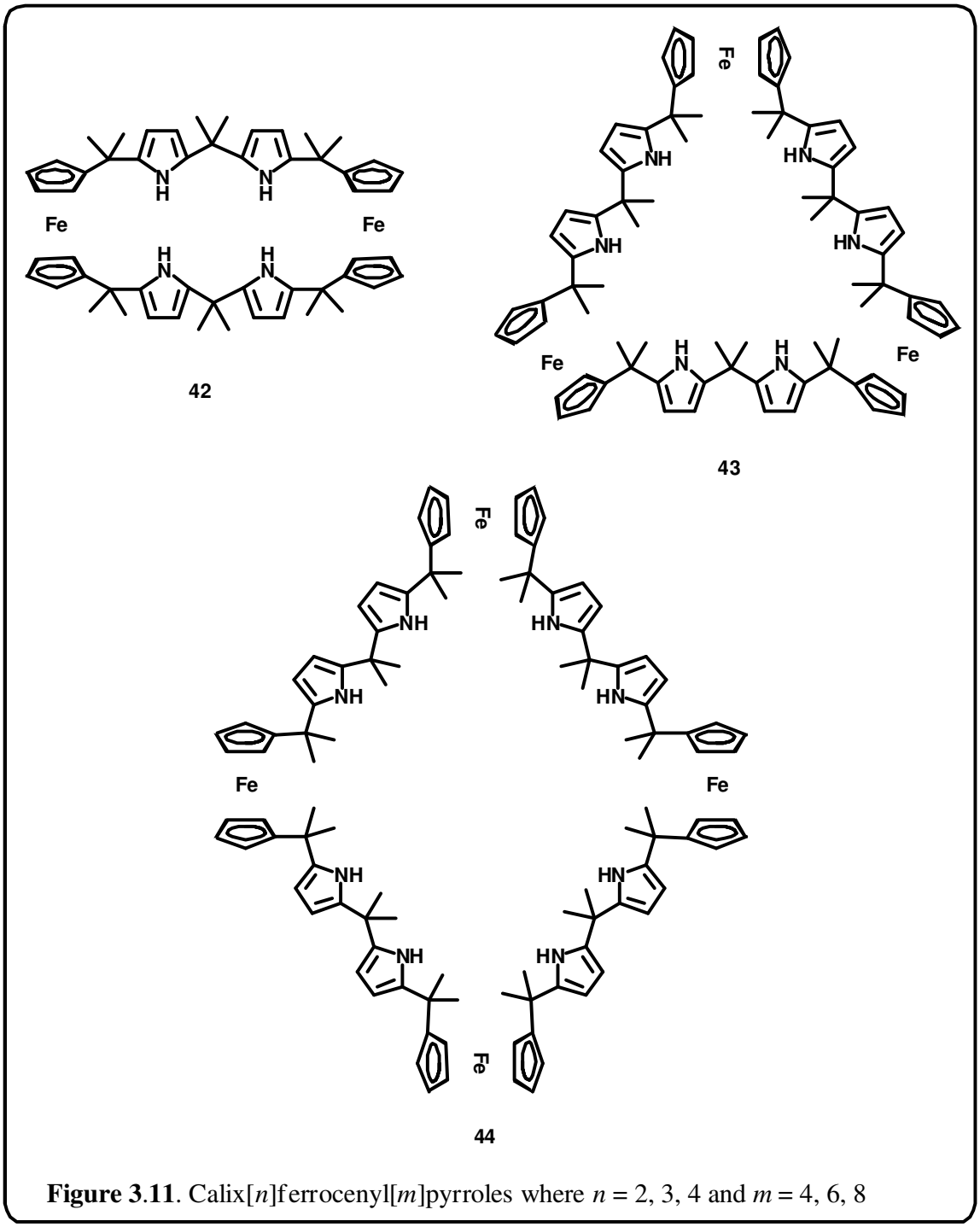

Figure 3.11. Calix[*n*]ferrocenyl[*m*]pyrroles where *n* = 2, 3, 4 and *m* = 4, 6, 8

The exact compositions of the macrocycles were confirmed by the FAB mass spectral analysis. The ^{1}H, ^{13}C NMR spectral analyses of all the macrocycles and ^{1}H – ^{1}H COSY spectrum of **30** were recorded at room temperature in $CDCl_3$.

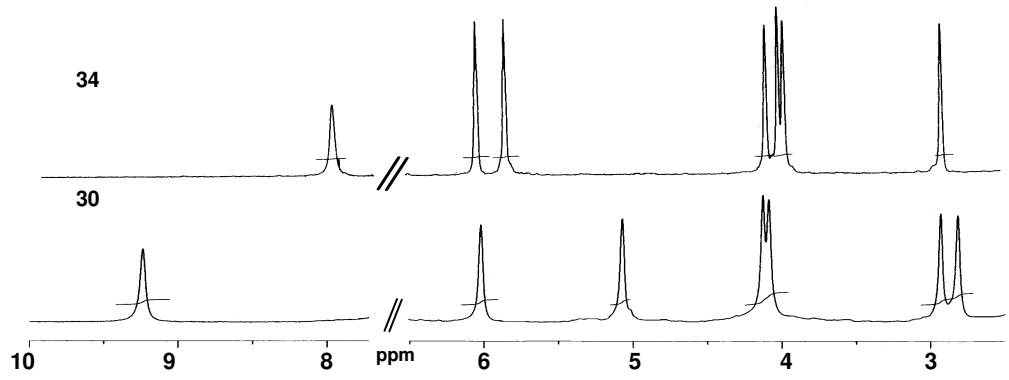

Figure 3.12. ^{1}H NMR spectra of **30** and **34**. The signals correspond to *meso*-groups and $CDCl_3$ are omitted for clarity.

As a representative example, ^{1}H NMR spectrum of **30** and **34** are shown in Figure 3.12. The NH protons of **30** and **34** resonate at 9.24 and 7.88 ppm, while the pyrrolic *β*-CH and ferrocenyl-CH protons resonated between 7 and 2.5 ppm, respectively. This suggested that NH protons in **30** are shifted downfield (1.36 ppm), while the pyrrolic *β*-CH and ferrocenyl-CH protons are 0.37 ppm upfield shifted as compared to **34** (Table 3.2). The D_2O exchangeable signals at 9.24 and 7.88 (**30** and **34**) ppm assigns the NH protons. Further, the absence of two *α*-CH protons in the pyrrolic rings, which are observed in **25** at 6.69 ppm, proved by ^{1}H and ^{1}H – ^{1}H COSY spectral analysis (Figure 3.13, Figure 3.14, Figure 3.15) of **30**, where the correlation between the pyrrolic NH with *β*-CH protons suggests the formation of the macrocycle. In addition, compared to the linear chains **25 - 29**, the pyrrolic *β*-CH and ferrocenyl-CH protons in **30 - 37** are upfield shifted with the shift difference of 0.05 to 0.53 ppm (Table 3.2), further supported the macrocyclic ring formation.

Table 3.2. The shift difference observed in the pyrrolic β-CH and ferrocenyl CH protons of macrocycles and dipyrromethanes.

No.	Pyrrolic β – CH*	Ferrocenyl – CH
30 – 25	5.55 – 5.93: (-0.38)	3.28 – 3.81: (-0.53)
31 – 26	5.71 – 6.05: (-0.34)	3.86 – 3.91: (-0.05)
32 – 27	6.00 – 6.09: (-0.09)	3.46 – 3.9: (-0.44)
33 – 28	5.98 – 6.10: (-0.12)	3.77 – 4.04: (-0.27)
34 – 29	5.92 – 5.93: (-0.01)	3.65 – 4.06: (-0.41)
35 – 26	5.99 – 6.05: (-0.06)	3.48 – 3.91: (-0.43)
36 – 27	6.04 – 6.09: (-0.05)	3.77 – 3.90: (-0.13)
37 – 28	5.95 – 6.10: (-0.15)	3.76 – 4.04: (-0.28)
47 – 46	5.57 – 5.84: (-0.27)	3.98 – 4.32: (-0.34)

*For calculation, pyrrolic α-CH protons of **25** – **29** and **46** are not included

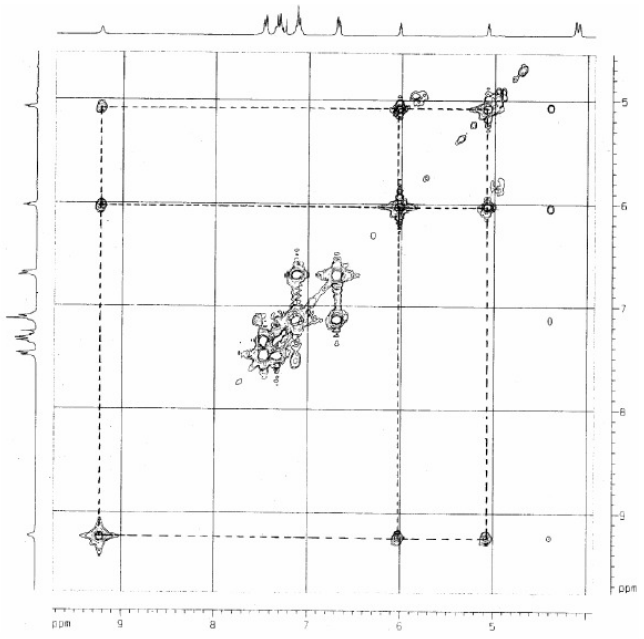

Figure 3.13. ^{1}H – ^{1}H COSY spectrum of **30** shows the correlation between pyrrolic NH and β-CH protons

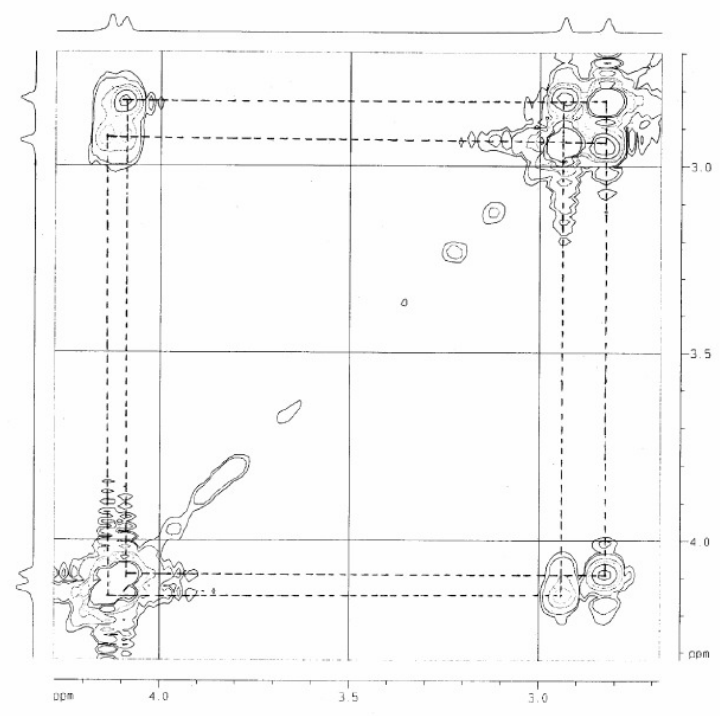

Figure 3.14. $^{1}H - {}^{1}H$ COSY spectrum of **30** shows the correlation in the ferrocenyl CH protons

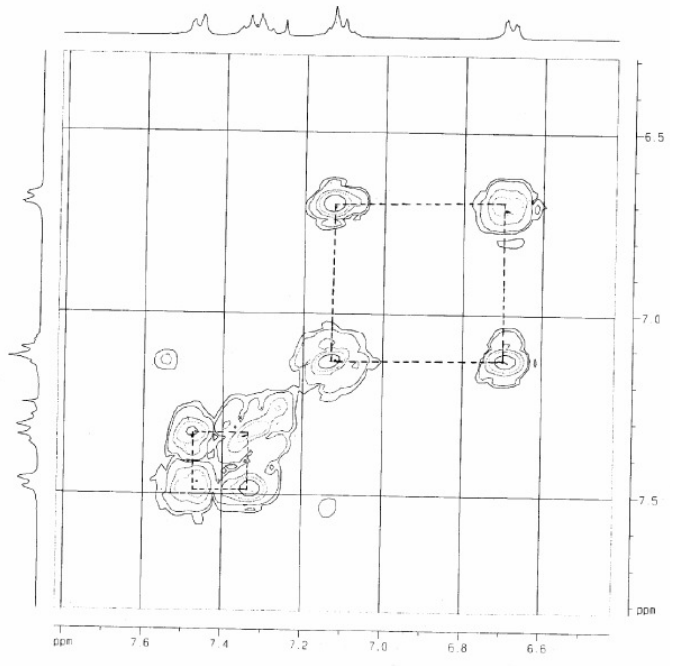

Figure 3.15. $^{1}H - {}^{1}H$ COSY spectrum of **30** shows the correlation in the phenyl CH protons

The confirmation of the proposed structure came from the single crystal X-ray analysis (Table 3.3) of **30** as shown in Figure 3.16. As suggested from the above observations, the pyrrole units are connected to 1 and 1' position of the ferrocenyl rings through the sp^3 hybridized *meso*-carbon bridges. The dihedral angles between the two planes (1 and 2; 3 and 4) in **30** are 68.43 and 68.37˚, respectively.

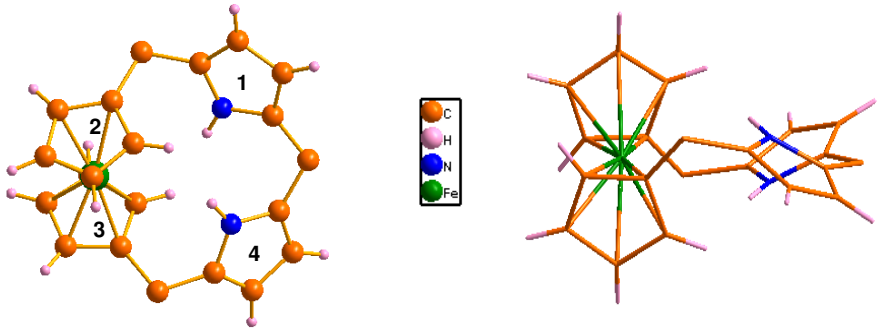

Figure 3.16. Single crystal X-ray structure of **30**. The *meso*-groups are omitted for clarity in the top and side view.

The pyrrole rings (1 and 4) in **25** (Figure 3.17) rotate in clockwise and anti-clockwise direction with the angle of 11.96 and 18.47˚ and condense with acetone in the presence of acid-catalyst to form the macrocycle **30**. This is achieved through the single bond rotation in **25** between C1 – C18 and C23 – C28. Further, the side view shows that both the pyrrole rings in the macrocycle adopts partial 1,2-alternate conformation in the solid state. The dihedral angle between the two planes (1 and 4) is 46.27˚ and the distance between the two pyrrole units is 4.45 Å. It is pertinent to point out here that the parent compound, calix[4]pyrrole adopts 1,2-alternate conformation in the solid state [[a]Gale *et al*. 1996].

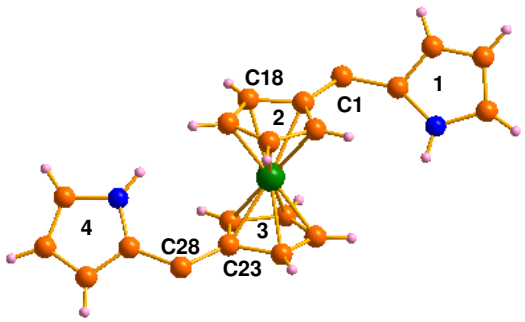

Figure 3.17. Single crystal X-ray structure of **25**. The *meso* groups are omitted for clarity.

The chemistry is further extended into the next higher metallocene, such as, ruthenocene. The diol **45** is achieved from the 1,1'-bislithiated salt of ruthenocene and benzophenone with the yield of 67%. **45** is condensed with pyrrole in the presence of $BF_3.OEt_2$ to form 1,1'-ruthenocenyl dipyrromethane **46** in 81% yield. The *ansa*-ruthenocene appended calix[2]pyrrole **47** is synthesized by the trifluoroacetic vacid catalyzed condensation of **46** with acetone as solvent as well as reactant, afforded **47** in 25% yield.

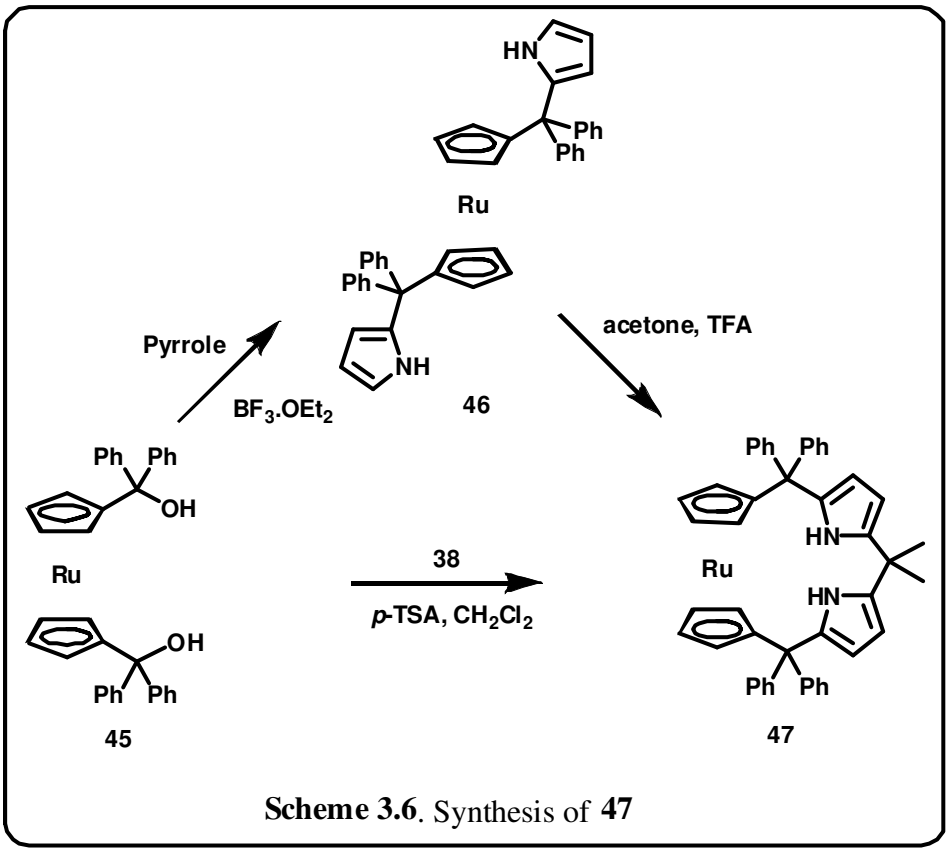

Scheme 3.6. Synthesis of **47**

Alternatively, **47** was synthesized by condensing **38** with **45** in the presence of *p*-TSA, in 18% yield (Scheme 3.6). The ^{1}H NMR analysis of **47** shows the pyrrolic NH, *β*-CH and ferrocenyl CH protons at 8.86, 5.57 and 3.98 ppm. As in **30**, the similar trend was observed in **47**, where the pyrrolic *β*-CH and ferrocenyl CH protons are upfield shifted, as compared to **46**, with the shift difference of 0.27 and 0.34 ppm, respectively. The macrocyclic ring formation is further confirmed by single crystal X-ray analysis (Table 3.3) of **47**, where the dihedral angle between the two pyrrolic rings (plane 1 and 2) is 45.96˚ with a distance of 4.48 (3) Å, respectively. The side view, further, confirms that the pyrrole rings in **47** maintains partial 1,2-alternate conformation in the solid state (Figure 3.18).

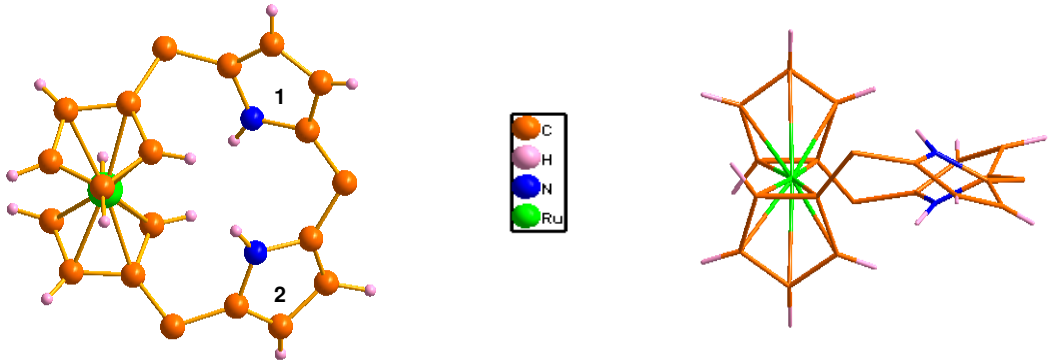

Figure 3.18. Single crystal X-ray structure of **47**. The *meso*-groups are omitted for clarity in the top and side view.

3.13 Conclusion

In conclusion, we have demonstrated the syntheses, spectral and structural characterization of *ansa*-metallocene-based calix[2]pyrroles. For the first time, metallocene units are incorporated into the backbone of the calixpyrrole frame work in an *ansa* type way. The partial 1,2- alternate conformation in the solid state proved that the macrocycle retains the calixpyrrole behavior. The synthetic methodology adopted here is simple and straightforward due to the absence of side products and easier purification.

3.14 Experimental Section

Synthesis of 30:

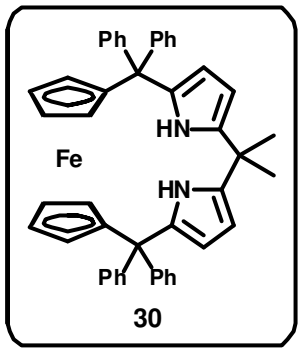

30

1,1'-bis(diphenylpyrrolylmethyl)ferrocene (**25**) (0.5 g, 0.77 mmol) and acetone (60 mL) were stirred under N_2 atm for 10 min at room temperature. Trifluoroacetic acid (0.006 mL, 0.077 mmol) was added to the above mixture and the solution was stirred at room temperature for 2 days. After removal of the solvent, the crude product was purified by silica gel column chromatography (100 – 200 mesh). The fraction eluted with EtOAc : petroleum ether (1 : 99) was identified as yellow solid **30**. Yield = 0.26 g, 48%; m.p : 145˚C; ^{1}H NMR (300 MHz, $CDCl_3$, 298 K) : δ = 9.24 (brs, 2H, pyrrole NH), 7.31 (m, 16H, phenyl CH), 6.58 (d, J = 9.2 Hz, 4H, phenyl CH), 6.02 (s, 2H, *β*-pyrrole CH), 5.07 (s, 2H, *β*-pyrrole CH), 4.10 (d, J = 11.8 Hz, 4H, ferrocenyl CH), 2.94 (s, 2H, ferrocenyl CH), 2.81 (s, 2H, ferrocenyl CH), 1.79 (s, 6H, methyl CH); ^{13}C NMR (100 MHz, $CDCl_3$, 298 K) : δ = 29.29, 33.45, 42.45, 55.80, 66.5, 71.80, 72.45, 99.58, 110.04, 111.57, 112.19, 119.55, 119.78, 124.76, 128.76, 130.75, 135.78; FT-IR (CH_2Cl_2) : 3431.36, 3065.93, 2924.00, 2853.25, 1597.45, 1492.09, 1443.09, 1415.66, 1275.75, 1220.88, 1048.43, 842.30 cm^{-1}; FAB-MS (m/z) : Calcd for $C_{47}H_{40}FeN_2$: 688.25; Found : 689.11.

The above macrocycle can also be obtained by the following method. 1,1'-bis(diphenylhydroxymethyl)ferrocene (**20**) (0.2 g, 0.36 mmol) and 5,5-dimethyldipyrromethane (**38**) (0.063 g, 0.36 mmol) were allowed to stir under N_2 atm in 30 mL dry CH_2Cl_2 for 10 min. Then *p*-TSA (0.017 g, 0.09 mmol) was added to the above reaction mixture and allowed to stir for 2 days. Then the purification was done as above. Yield = 0.056 g, 23%.

Synthesis of 31:

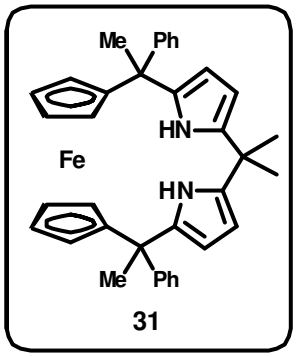

31

1,1'-bis(methylphenylpyrrolylmethyl)ferrocene (**26**) (0.26 g, 0.5 mmol) and acetone (37 mL) were stirred under N_2 atm for 10 min at room temperature Trifluoroacetic acid (0.004 mL, 0.05 mmol) was added to the above mixture and the solution was stirred at room temperature for 45 min. After removal of the solvent, the crude product was purified by silica gel column chromatography (100 – 200 mesh). The fraction eluted with EtOAc : petroleum ether (1 : 99) was identified as yellow solid **31**. Yield = 0.05 g, 19%; m.p : 140˚C; ^{1}H NMR (300 MHz, $CDCl_3$, 298 K) : δ = 7.75 (brs, 2H, pyrrole NH), 7.13 (d, J = 6.76 Hz, 6H, phenyl CH), 6.90 (d, J = 7.84 Hz, 4H, phenyl CH), 5.96 (t, 2H, *β*-pyrrole CH), 5.46 (t, 2H, *β*-pyrrole CH), 4.25 (s, 4H, ferrocenyl CH), 4.17 (s, 2H, ferrocenyl CH), 3.18 (s, 2H, ferrocenyl CH), 1.97 (s, 6H, methyl CH), 1.65 (s, 6H, methyl CH); ^{13}C NMR (100 MHz, $CDCl_3$, 298 K) : δ = 27.45, 29.47, 34.5, 41.5, 68.40, 68.69, 69.45, 69.76, 70.15, 99.15, 106.70, 107.05, 113.25, 127.11, 138.75; FT-IR (CH_2Cl_2) : 3428.57, 3313.18, 2917.58, 2851.64, 1596.43, 1445.84, 1119.38, 1086.46 cm^{-1}; FAB-MS (m/z) : Calcd for $C_{37}H_{36}FeN_2$: 564.22; Found : 564.37.

The above macrocycle can also be obtained by the following method. 1,1'-bis(methylphenylhydroxymethyl)ferrocene (**21**) (0.2 g, 0.47 mmol) and 5,5-dimethyldipyrromethane (**38**) (0.082 g, 0.47 mmol) were allowed to stir under N_2 atm in 30 mL dry CH_2Cl_2 for 10 min. Then *p*-TSA (0.022 g, 0.12 mmol) was added to the above reaction mixture and allowed to stir for 45 min. Then the purification was done as above. Yield = 0.046 g, 18%.

Synthesis of 32:

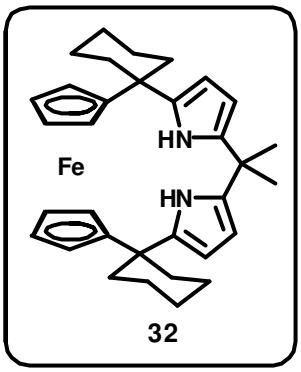

1,1'-bis(cyclohexylpyrrolylmethyl)ferrocene (**27**) (0.2 g, 0.42 mmol) and acetone (31 mL) were stirred under N_2 atm for 10 min at room temperature. Trifluoroacetic acid (0.003 mL, 0.042 mmol) was added to the above mixture and the solution was stirred at room temperature for 45 min. After removal of the solvent, the crude product was purified by silica gel column chromatography (100 – 200 mesh). The fraction eluted with EtOAc : petroleum ether (1 : 99) was identified as pale yellow solid **32**. Yield = 0.047 g, 22%; m.p: 123˚C; ^{1}H NMR (300 MHz, $CDCl_3$, 298 K) : δ = 7.70 (brs, 2H, pyrrole NH), 6.12 (t, 2H, *β*-pyrrole CH), 5.88 (q, 2H, *β*-pyrrole CH), 4.06 (m, 6H, ferrocenyl CH), 2.86 (d, J = 0.9 Hz, 2H, ferrocenyl CH), 2.15 (m, 5H, cyclohexyl CH), 1.74 (m, 5H, cyclohexyl CH), 1.6 (s, 6H, methyl CH), 1.38 (m, 6H, cyclohexyl CH), 0.87 (m, 4H, cyclohexyl CH); ^{13}C NMR (100 MHz, $CDCl_3$, 298 K) : δ = 21.15, 22.75, 23.16, 26.79, 28.95, 29.05, 29.75, 36.15, 36.27, 39.45, 42.75, 65.66, 66.17, 67.18, 68.25, 69.16, 127.15, 138.45; FT-IR (CH_2Cl_2) : 3456.04, 3093.40, 2925.44, 2854.50, 1574.77, 1446.97, 1415.66, 1264.77, 1187.96, 1042.56, 930.08 cm^{-1}; FAB-MS (m/z) : Calcd for $C_{33}H_{40}FeN_2$: 520.25; Found : 520.33.

The above macrocycle can also be obtained by the following method. 1,1'-bis(cyclohexylhydroxymethyl)ferrocene (**22**) (0.2 g, 0.52 mmol) and 5,5-dimethyldipyrromethane (**38**) (0.091 g, 0.52 mmol) were allowed to stir under N_2 atm in 30 mL dry CH_2Cl_2 for 10 min. Then *p*-TSA (0.025 g, 0.13 mmol) was added to the above reaction mixture and allowed to stir for 45 min. Then the purification was done as above. Yield = 0.054 g, 20%.

Synthesis of 33:

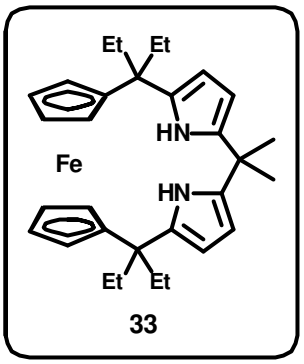

33

1,1'-bis(diethylpyrrolylmethyl)ferrocene (**28**) (0.45 g, 1 mmol) and acetone (73 mL) were stirred under N_2 atm for 10 min at room temperature. Trifluoroacetic acid (0.007 mL, 0.1 mmol) was added to the above mixture and the solution was stirred at room temperature for 45 min. After removal of the solvent, the crude product was purified by silica gel column chromatography (100 – 200 mesh). The fraction eluted with EtOAc : petroleum ether (1 : 99) was identified as yellow solid **33**. Yield = 0.094 g, 19%; m.p : 120˚C; ^{1}H NMR (300 MHz, $CDCl_3$, 298 K) : δ = 8.23 (brs, 2H, pyrrole NH), 6.06 (t, 2H, *β*-pyrrole CH), 5.90 (t, 2H, *β*-pyrrole CH), 4.19 (d, J = 1.16 Hz, 2H, ferrocenyl CH), 4.10 (m, 4H, ferrocenyl CH), 3.02 (s, 2H, ferrocenyl CH), 1.94 (m, 8H, ethyl CH), 1.66 (s, 6H, methyl CH), 0.79 (t, 6H, ethyl CH), 0.71 (t, 6H, ethyl CH); ^{13}C NMR (100 MHz, $CDCl_3$, 298 K) : δ = 9.18, 30.58, 31.51, 33.45, 36.23, 41.24, 65.57, 66.45, 67.45, 69.34, 102.59, 103.20, 105.84, 134.62, 136.94; FT-IR (CH_2Cl_2) : 3434.06, 3329.67, 2922.90, 2851.64, 1742.12, 1585.75, 1259.29, 1119.38, 1018.49 cm^{-1}; FAB-MS (m/z) : Calcd for $C_{31}H_{40}FeN_2$: 496.25; Found : 496.60.

The above macrocycle can also be obtained by the following method. 1,1'-bis(diethylhydroxymethyl)ferrocene (**23**) (0.2 g, 0.56 mmol) and 5,5-dimethyldipyrromethane (**38**) (0.097 g, 0.56 mmol) were allowed to stir under N_2 atm in 30 mL dry CH_2Cl_2 for 10 min. Then *p*-TSA (0.027 g, 0.14 mmol) was added to the above reaction mixture and allowed to stir for 45 min. Then the purification was done as above. Yield = 0.047 g, 17%.

Synthesis of 34:

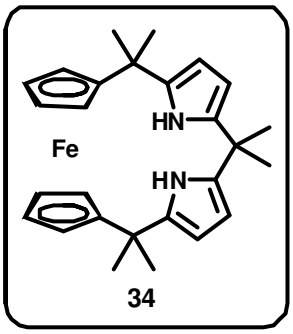

34

1,1'-bis(dimethylpyrrolylmethyl)ferrocene (**29**) (0.5 g, 1.25 mmol) and acetone (60 mL) were stirred under N_2 atm for 10 min at room temperature. Trifluoroacetic acid (0.01 mL, 0.125 mmol) was added to the above mixture and the solution was stirred at room temperature for 45 min. After removal of the solvent, the crude product was purified by silica gel column chromatography (100 – 200 mesh). The fraction eluted with EtOAc : petroleum ether (1 : 99) was identified as pale yellow solid **34**. Yield = 0.13 g, 25%; m.p : 115°C; ^{1}H NMR (300 MHz, $CDCl_3$, 298 K) : δ = 7.88 (brs, 2H, pyrrole NH), 6.02 (s, 2H, *β*-pyrrole CH), 5.82 (s, 2H, *β*-pyrrole CH), 4.07 (s, 2H, ferrocenyl CH), 3.97 (d, J = 11.3 Hz, 4H, ferrocenyl CH), 2.90 (s, 2H, ferrocenyl CH), 1.6 (s, 18H, methyl CH); ^{13}C NMR (100 MHz, $CDCl_3$, 298 K) : δ = 24.56, 26.75, 27.17, 29.15, 35.47, 68.15, 68.42, 98.45, 113.45, 114.55, 126.77, 137.11; FT-IR (CH_2Cl_2) : 3457.95, 3087.91, 2924.14, 2854.34, 1651.59, 1580.26, 1463.16, 1377.42, 1259.29, 1041.33, 828.58 cm^{-1}; FAB-MS (m/z) : Calcd for $C_{27}H_{32}FeN_2$: 440.19; Found : 439.98.

The above macrocycle can also be obtained by the following method. 1,1'-bis(dimethylhydroxymethyl)ferrocene (**24**) (0.2 g, 0.66 mmol) and 5,5-dimethyldipyrromethane (**38**) (0.12 g, 0.66 mmol) were allowed to stir under N_2 atm in 30 mL dry CH_2Cl_2 for 10 min. Then *p*-TSA (0.031 g, 0.17 mmol) was added to the above reaction mixture and allowed to stir for 45 min. Then the purification was done as above. Yield = 0.064 g, 22%.

Synthesis of 35:

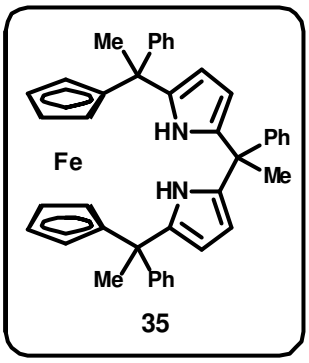

35

1,1'-bis(methylphenylpyrrolylmethyl)ferrocene (**26**) (0.235 g, 0.45 mmol) and acetophenone (0.05 mL, 0.45 mol) were dissolved in 30 mL dry CH_2Cl_2 and stirred under N_2 atm for 10 min at room temperature. Trifluoroacetic acid (0.003 mL, 0.045 mmol) was added to the above mixture and the solution was stirred at room temperature for 45 min. After removal of the solvent, the crude product was purified by silica gel column chromatography (100 – 200 mesh). The fraction eluted with EtOAc : petroleum ether (1 : 99) was identified as yellow solid **35**. Yield = 0.063 g, 23%; ^{1}H NMR (300 MHz, $CDCl_3$, 298 K) : δ = 8.03 (brs, 2H, pyrrole NH), 7.38 (d, J = 6.81 Hz, 8H, phenyl CH), 6.95 (d, J = 6.36 Hz, 3H, phenyl CH), 6.8 (d, J = 6.95 Hz, 4H, phenyl CH), 6.03 (t, 2H, *β*-pyrrole CH), 5.95 (t, 2H, *β*-pyrrole CH), 4.03 (s, 4H, ferrocenyl CH), 3.38 (s, 2H, ferrocenyl CH), 3.04 (s, 2H, ferrocenyl CH), 1.91 (s, 9H, methyl CH); ^{13}C NMR (100 MHz, $CDCl_3$, 298 K) : δ = 25.15, 26.17, 27.15, 35.15, 40.17, 66.70, 67.15, 67.45, 68.56, 69.15, 69.98, 98.15, 107.17, 108.05, 114.15, 128.11, 139.34; FT-IR (CH_2Cl_2): 3438.11, 2923.44, 2846.15, 1593.06, 1465.04, 1264.77, 1215.39, 1122.12, 1031.59 cm^{-1}; FAB-MS (m/z) : Calcd for $C_{42}H_{38}FeN_2$: 626.24; Found : 626.39.

The above macrocycle can also be obtained by the following method. 1,1'-bis(methylphenylhydroxymethyl)ferrocene (**21**) (0.2 g, 0.47 mmol) and 5-methyl-5-phenyldipyrromethane (**39**) (0.11 g, 0.47 mmol) were allowed to stir under N_2 atm in 30 mL dry CH_2Cl_2 for 10 min. Then *p*-TSA (0.022 g, 0.12 mmol) was added to the above reaction mixture and allowed to stir for 45 min. Then the purification was done as above. Yield = 0.056 g, 19%.

Synthesis of 36:

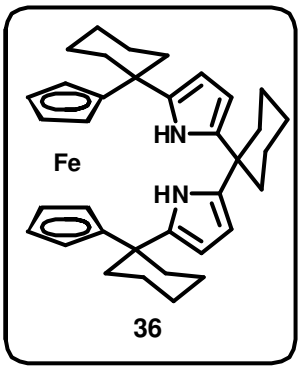

36

1,1'-bis(cyclohexylpyrrolylmethyl)ferrocene (**27**) (0.2 g, 0.42 mmol) and cyclohexanone (0.04 mL, 0.42 mmol) were dissolved in 30 mL dry CH_2Cl_2 and stirred under N_2 atm for 10 min at room temperature. Trifluoroacetic acid (0.003 mL, 0.042 mmol) was added to the above mixture and the solution was stirred at room temperature for 45 min. After removal of the solvent, the crude product was purified by silica gel column chromatography (100 – 200 mesh). The fraction eluted with EtOAc : petroleum ether (1 : 99) was identified as pale yellow solid **36**. Yield = 0.058 g, 25%; m.p : 205˚C; ^{1}H NMR (300 MHz, $CDCl_3$, 298 K) : δ = 7.50 (brs, 2H, pyrrole NH), 6.20 (t, 2H, *β*-pyrrole CH), 5.87 (t, 2H, *β*-pyrrole CH), 4.08 (s, 2H, ferrocenyl CH), 4.04 (s, 2H, ferrocenyl CH), 3.99 (s, 2H, ferrocenyl CH), 2.97 (s, 2H, ferrocenyl CH), 2.28 (m, 3H, cyclohexyl CH), 2.08 (t, 6H, cyclohexyl CH), 1.83 (m, 10H, cyclohexyl CH), 1.26 (m, 9H, cyclohexyl CH), 0.88 (m, 2H, cyclohexyl CH); ^{13}C NMR (100 MHz, $CDCl_3$, 298 K) : δ = 22.59, 22.78, 22.95, 23.15, 23.36, 25.94, 26.06, 26.14, 29.67, 37.88, 38.73, 39.01, 39.36, 39.78, 40.29, 40.84, 63.23, 65.10, 65.98, 66.16, 67.09, 68.55, 105.14, 105.32, 105.43, 106.37, 133.85, 136.44; FT-IR (CH_2Cl_2) : 3450.54, 2924.11, 2851.64, 1640.61, 1443.09, 1215.39, 1119.38, 1042.56, 930.08 cm^{-1}; FAB-MS (m/z) : Calcd for $C_{36}H_{44}FeN_2$: 560.29; Found : 560.06.

The above macrocycle can also be obtained by the following method. 1,1'-bis(cyclohexylhydroxymethyl)ferrocene (**22**) (0.2 g, 0.52 mmol) and 5,5-cyclohexyldipyrromethane (**40**) (0.11 g, 0.52 mmol) were allowed to stir under N_2 atm in 30 mL dry CH_2Cl_2 for 10 min. Then *p*-TSA (0.025 g, 0.13 mmol) was added to the above reaction mixture and allowed to stir for 45 min. Then the purification was done as above. Yield = 0.064 g, 22%.

Synthesis of 37:

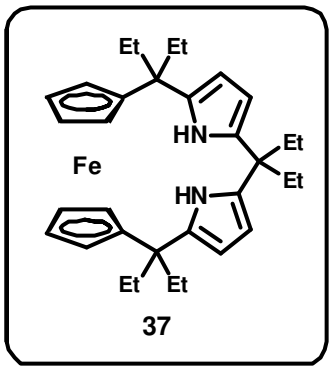

1,1'-bis(diethylpyrrolylmethyl)ferrocene (**28**) (0.2 g, 0.44 mmol) and 3-pentanone (0.046 mL, 0.44 mmol) were dissolved in 30 mL dry CH_2Cl_2 and stirred under N_2 atm for 10 min at room temperature. Trifluoroacetic acid (0.0034 mL, 0.044 mmol) was added to the above mixture and the solution was stirred at room temperature for 45 min. After removal of the solvent, the crude product was purified by silica gel column chromatography (100 – 200 mesh). The fraction eluted with EtOAc : petroleum ether (1 : 99) was identified as yellow solid **37**. Yield = 0.040 g, 17%; m.p : 115˚C; ^{1}H NMR (300 MHz, $CDCl_3$, 298 K) : δ = 8.33 (brs, 2H, pyrrole NH), 5.98 (t, 2H, *β*-pyrrole CH), 5.93 (t, 2H, *β*-pyrrole CH), 4.20 (s, 2H, ferrocenyl CH), 4.09 (d, J = 7.5 Hz, 4H, ferrocenyl CH), 2.99 (s, 2H, ferrocenyl CH), 1.97 (m, 12H, ethyl CH), 0.76 (t, 18 H, ethyl CH); ^{13}C NMR (100 MHz, $CDCl_3$, 298 K) : δ = 9.15, 10.15, 15.16, 31.15, 32.41, 35.15, 42.15, 66.78, 67.15, 68.11, 69.15, 104.15, 105.16, 133.15, 135.78; FT-IR (CH_2Cl_2) : 3429.52, 3321.25, 2947.16, 1676.87, 1560.08, 1260.00, 1085.15, 1040.87, 819.56 cm^{-1}; FAB-MS (m/z) : Calcd for $C_{33}H_{44}FeN_2$: 524.28; Found : 524.33.

The above macrocycle can also be obtained by the following method. 1,1'-bis(diethylhydroxymethyl)ferrocene (**23**) (0.2 g, 0.56 mmol) and 5,5-diethyldipyrromethane (**41**) (0.113 g, 0.56 mmol) were allowed to stir under N_2 atm in 30 mL dry CH_2Cl_2 for 10 min. Then *p*-TSA (0.026 g, 0.14 mmol) was added to the above reaction mixture and allowed to stir for 45 min. Then the purification was done as above. Yield = 0.047 g, 16%.

Synthesis of 47:

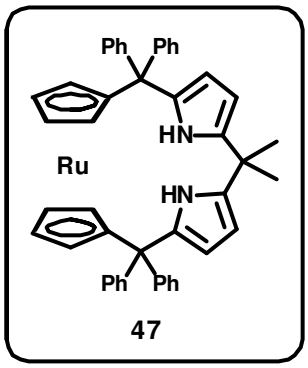

47

1,1'-bis(diphenylpyrrolylmethyl)ruthenocene (**46**) (0.2 g, 0.29 mmol) and acetone (21 mL) were stirred under N_2 atm for 10 min at room temperature. Trifluoroacetic acid (0.002 mL, 0.029 mmol) was added to the above mixture and the solution was stirred at room temperature for 2 days. After removal of the solvent, the crude product was purified by silica gel column chromatography (100 – 200 mesh). The fraction eluted with EtOAc : petroleum ether (1 : 99) was identified as white solid **47**. Yield = 0.05 g, 25%; m.p : 135˚C; ^{1}H NMR (300 MHz, $CDCl_3$, 298 K) : δ = 8.86 (brs, 2H, pyrrole NH), 7.31 (m, 16H, phenyl CH), 6.91 (m, 4H, phenyl CH), 5.96 (t, 2H, *β*-pyrrole CH), 5.17 (t, 2H, *β*-pyrrole CH), 4.44 (s, 2H, ferrocenyl CH), 4.38 (s, 2H, ferrocenyl CH), 3.66 (s, 2H, ferrocenyl CH), 3.43 (s, 2H, ferrocenyl CH); 1.72 (s, 6H, methyl CH); ^{13}C NMR (100 MHz, $CDCl_3$, 298 K) : δ = 25.45, 26.17, 28.17, 42.35, 69.15, 71.15, 72.46, 100.15, 108.91, 116.45, 127.15, 136.15; FT-IR (CH_2Cl_2) : 3372.49, 3049.45, 2920.67, 2846.15, 1596.87, 1486.99, 1443.09, 1273.00, 1217.96, 1037.07, 814.86 cm^{-1}; FAB-MS (m/z) : Calcd for $C_{47}H_{40}RuN_2$: 734.22; Found : 734.22.

The above macrocycle can also be obtained by the following method. 1,1'-bis(dimethylhydroxymethyl)ruthenocene (**45**) (0.2 g, 0.34 mmol) and 5,5-dimethyldipyrromethane (**38**) (0.059 g, 0.34 mmol) were allowed to stir under N_2 atm in 30 mL dry CH_2Cl_2 for 10 min. Then *p*-TSA (0.016 g, 0.09 mmol) was added to the above reaction mixture and allowed to stir for 2 days. Then the purification was done as above. Yield = 0.045 g, 18%.

3.15 Crystal data

Table 3.3. Crystallographic data for **30** and **47**

Parameters	**30**	**47**
Solvent of crystallization	CH_2Cl_2 / Pentane	CH_2Cl_2 / Pentane
Empirical formula	$C_{47}H_{40}N_2Fe$	$C_{47}H_{40}RuN_2$
M_w	688.66	733.88
T [K]	293(2)	293(2)
λ [Å]	0.71073	0.71073
Crystal system	Monoclinic	Monoclinic
Space group	$P2_{1/c}$	$P2_{1/c}$
a[Å]	17.8893(14)	17.9925(12)
b[Å]	10.0632(7)	10.1572(6)
c[Å]	19.1662(15)	19.0746(13)
α [˚]	90.00	90.00
β [˚]	92.893(4)	90.827(2)
γ [˚]	90.00	90.00
V[Å^3]	3446.0(5)	3485.6(4)
Z, ρ_{calcd} [Mg m^{-3}]	4, 1.327	4, 1.398
μ ($Mo_{K\alpha}$) [mm^{-1}]	0.475	0.487
F (000)	1448	1520
Crystal size [mm]	0.3 × 0.2 × 0.1	0.30 × 0.20 × 0.20
θ range for data collection [˚]	1.14 to 25.00	1.13 to 25.00
Limiting indices	$-20 \le h \le 21$, $-11 \le k \le 7$, $-22 \le l \le 22$	$-21 \le h \le 21$, $-12 \le k \le 12$, $-22 \le l \le 21$
Reflections collected	31078	32479
Refinement method	Full-matrix least-squares on F^2	Full-matrix least-squares on F^2
Data / restraints / parameters	6044 / 2 / 460	6133 / 0 / 467
Goodness-of- fit on F^2	1.183	1.315
Final R indices[I>2σ(I)]	R1 = 0.0722, wR2 = 0.1851	R1 = 0.1084, wR2 = 0.2581
R indices (all data)	R1 = 0.0830, wR2 = 0.1932	R1 = 0.1264, wR2 = 0.2717
Largest $\Delta\rho$ [e Å^{-3}]	0.761 and -0.583	2.385 and -2.316

Chapter 4

ansa-Metallocene-based *normal* and *expanded* Calixphyrins

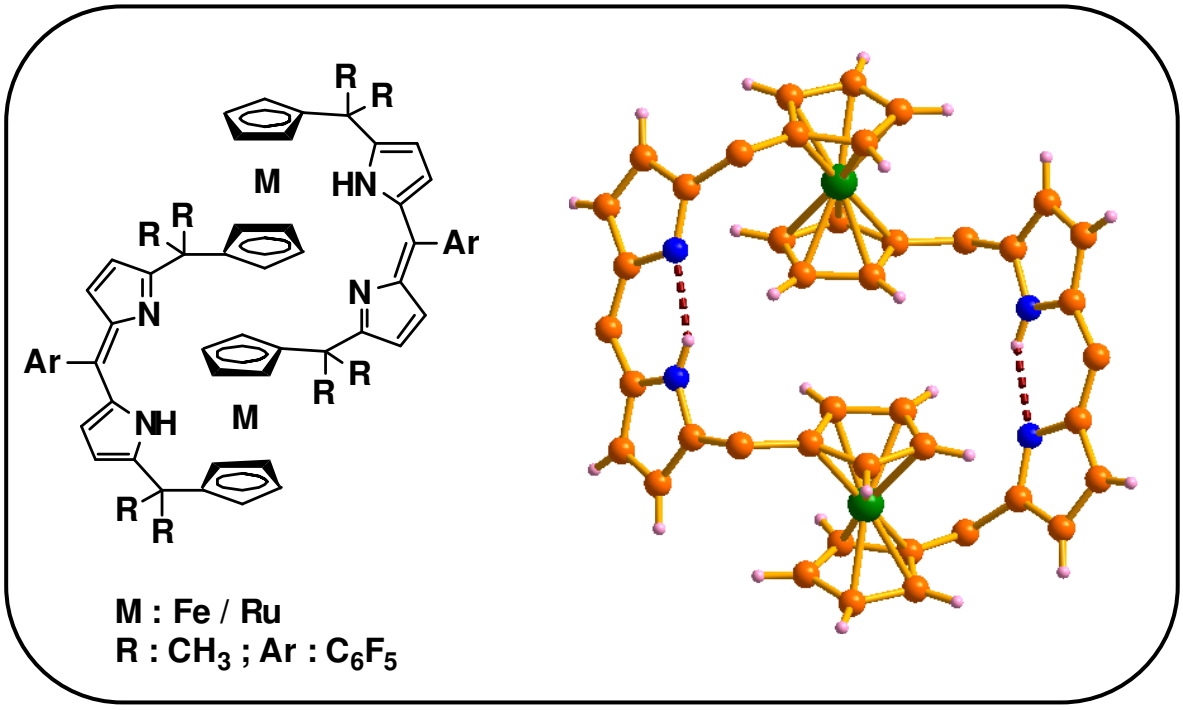

4.1 Abstract

Introduction of metallocenes in the calixphyrin framework as well as its expanded homologues are the highlights of this chapter. These are the largest metallocene incorporated porphyrinoids reported to date. The syntheses, spectral and structural characterization of metallocenes, mainly ferrocene/ruthenocene based macrocycles are reported. p-TSA catalysed condensation of 1,1'-ferrocenyl-bis-(gem-diphenylpyrrolyl)methane with electron withdrawing and electron donating aryl-aldehydes, followed by oxidation with 2,3-dichloro-5,6-dicyano-p-benzoquinone (DDQ) afforded the macrocycles in 15 to 19% yield. When changing the aryl substituted precursor to alkyl, to our surprise, apart from the normal derivatives, we observed expanded products in 4 to 5% yield, along with trace amounts of higher analogues. The NMR spectra and broad UV absorption band of these macrocycles clearly reveals its calixphyrin nature. The final confirmation of these macrocycles has come from single crystal X-ray structural analyses which form strong intramolecular hydrogen bonding interactions between the amine pyrrole NH and imine pyrrole N which are present in the dipyrrin unit. Self assembled dimer, one dimensional array and two dimensional arrays of these macrocycles in the solid state are also explained. The role of aryl vs alkyl is demonstrated to explain the formation of higher derivatives, where, in the case of the aryl groups, the pyrrole units forms only the normal derivatives, whereas the alkyl group assists the pyrrolic unit to bring it closer for further condensation with the aryl aldehydes to form the expanded derivatives. Similar results were obtained with the next higher metallocene, such as ruthenocene.

4.2 Introduction

Calixphyrins **1** (Figure 4.1) are pyrrole based macrocycles in which at least one of the *meso* carbon atom is sp^2 hybridized in addition to sp^3 hybridized carbon atoms. They form an intermediate between completely oxidized cation binding porphyrins **2** and completely non-oxidized anion or neutral electron rich molecule binding calixpyrroles **3**. As a consequence of this, there is an interruption in the conjugation pathway of the molecule

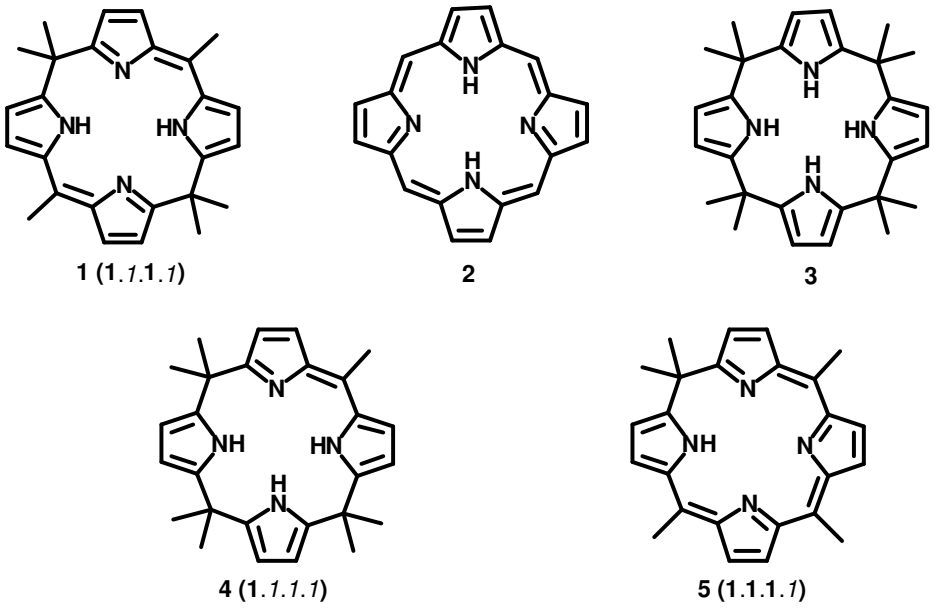

Figure 4.1. Different kinds of calixphyrins **1, 4** and **5**, porphyrin **2** and calixpyrrole **3**

which results in novel structural features and leads to interesting anion and cation recognition properties and they possess reasonably flexible frameworks as well as rather rigid π-conjugated networks. If these macrocycles contains only one sp^2 hybridized *meso* carbon atom, they are known as porphomonomethenes **4**. Those which contains two sp^2 hybridized *meso* carbon atoms are known as porphodimethenes **1** and three *meso* sp^2 hybridized carbon atoms are known as porphotrimethenes **5**.

Porphyrinogens are the partially oxidized intermediate products obtained during the acid catalysed condensation reactions of pyrrole and aldehyde followed by oxidation which

finally results in the formation of completely oxidized stable porphyrins. These intermediate products were more difficult to isolate, study and were relatively unstable due to its tendency to oxidize further to form porphyrins. The spectroscopic analyses which were carried out to study the porphyrin formation reactions clearly gave an evidence for the occurrence of these partially oxidized macrocycles. Acid catalysed condensation of pyrrole and aldehyde first resulted in completely reduced calixpyrroles [Lindsey book 1999] which were also obtained by the acid catalysed oligomerisation of pyrrole-2-hydroxymethyl derivatives [Uno *et al*. 2000], which upon stepwise oxidation resulted in the formation of porphomonomethene, porphodimethene etc. until complete oxidation is reached which resulted in the formation of porphyrins [Dolphin 1970, [a]Senge *et al*. 2000]. Many initial species were first isolated as metal complexes [Dwyer *et al*. 1974]. Then by suitably changing electronic and steric effects, stable nonmetallated calixphyrins were also synthesized.

In addition to sp^2 hybridized *meso* carbon, these macrocycles also contain sp^3 hybridized *meso* carbon due to which they adopt non-planar conformation which was very much evident from the single crystal X-ray structural analysis of **4** and **1** (Figure 4.2). From the crystal analysis, it is clear that **4** (Figure 4.2a) has a highly distorted conformation where as **1** has wing like conformation in the solid state (Figure 4.2b). But **4** and **1** displayed planarity corresponding to dipyrrolylmethene units [Dolphin 1970, Senge and Smith 1993, Runge and Senge 1998, Kalisch and Senge 1998, Benech *et al*. 1999, Král *et al*. 2000, Bucher *et al*. 2000, [b]Harmjanz *et al*. 2000, [a]Senge *et al*. 2000, [b]Senge and Feng 2000, Gill *et al*. 2004, Kojima *et al*. 2008]. But it should be noted that these free base forms were more bent and less planar when compared with the metal complexes of porphodimethene synthesized and characterized by Floriani and co-workers [Benech *et al*. 1999, Bonomo *et al*. 1999]. Metal complexation affects the local and long-range planarity; as a result, the pyrrole-

methene-pyrrole dihedral angle is considerably reduced. This non-planarity affects the photophysical properties of calixphyrins when compared with the planar analogues [Shelnutt *et al*. 1998, Chirvony *et al*. 2000].

a) b)

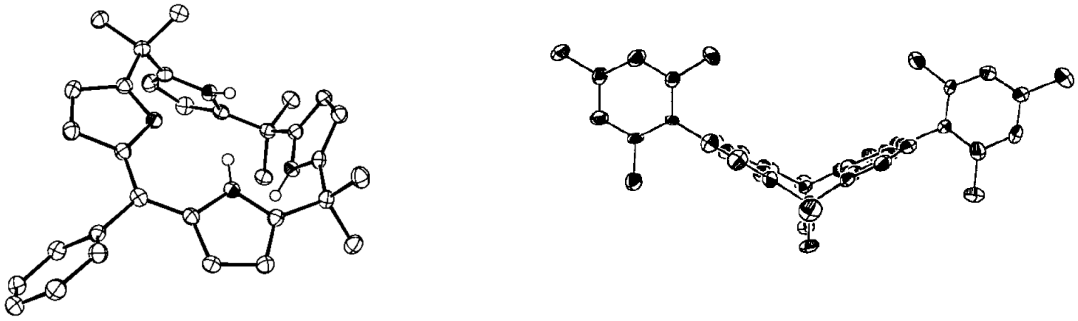

Figure 4.2. Single Crystal X-ray Structure of a) **4** and b) **1**

In general, the calixphyrins are orange or red-yellow colored solids, soluble in most of the organic solvents. They show broad UV-Vis absorption ranging between 400 to 500 nm mainly due to π - $\pi*$ transition within the dipyrrin moiety. Porphomonomethene usually absorbs at 460 to 470 nm, porphodimethenes show absorption peak roughly at 410 nm [Bucher *et al*. 2000] etc. ^{1}H NMR analysis of calixphyrins clearly reveals the presence of NH protons at high down field region ranging from 11 to 15 ppm. This high downfield shift of NH proton is mainly due to the delocalization of lone pair of electron of the amine N atom and also due to the intramolecular hydrogen bonding interaction between amine NH and imine N.

4.3 Nomenclature of calixphyrins:

The systematic name of **1** was proposed as calix[4]phyrin(**1**.*1*.**1**.*1*). Starting with the highest order sp^2 center, the molecule is named in the direction in which the nearest sp^2 center lies. The square bracketed number refers to the number of pyrroles in the macrocycle.

Each individual bold and italicized number in the circular bracket denotes the number of bridging *meso* centers between each pyrrole subunit. Bold numbers refer to sp^2 centers, and italicized numbers refer to sp^3 centers [[c]Sessler *et al*. 2001].

4.4 Types of calixphyrins:

4.4.1 Phlorins: Woodward, during his research towards the total synthesis of chlorophyll a, [Woodward 1962] discovered this class of calix[4]phyrin-(**1**.**1**.**1**.*1*) **6** (Figure 4.3) and Mauzerall and co-workers simultaneously contributed to these macrocycles during their work on the photoreduction of porphyrins [Mauzerall and Granick 1958, Mauzerall 1960].

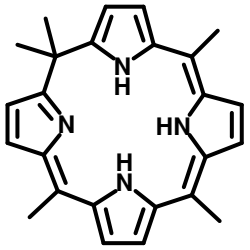

Figure 4.3. Phlorin **6** (**1**.**1**.**1**.*1*)

Upto recent years, several research groups have synthesized metal complexed phlorins like rhodium-phlorin complex [Setsune *et al*. 1980], trivalent gold complexed phlorins [Sugimoto 1982] etc. Metal-free phlorins were difficult to isolate. But the use of tetra-N-substituted phlorin cation [Pohl *et al*. 1991] and steric hindrance introduced by means of angular methyl groups [Liddell *et al*. 1990, Swanson *et al*. 1991] resulted in stabilization of these phlorin based systems. Later, callot synthesized stable phlorin by the electrochemical or $Na_2S_2O_4$ reduction of *N*-aryl porphyrin **7** to *N*-aryl phlorin **8** (Scheme 4.1) [Ruppert *et al*. 1999].

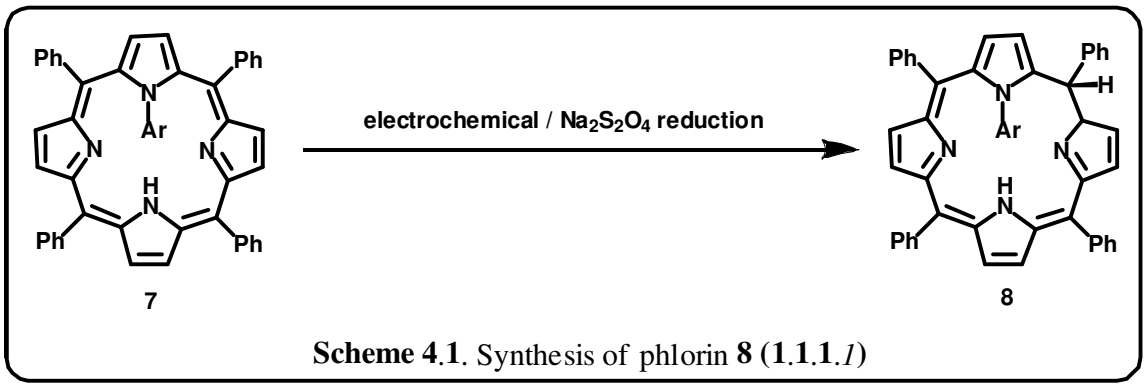

Scheme 4.1. Synthesis of phlorin **8** (**1**.**1**.**1**.*1*)

4.4.2 Isoporphyrins: These are another class of calix[4]phyrin-(**1**.**1**.**1**.*1*) system **9** (Figure 4.4) which was obtained as by-products of heme oxidation and intermediates in the biosynthesis of chlorophyll [Barkigia *et al*. 1993]. Isoporphyrins differ from phlorins mainly

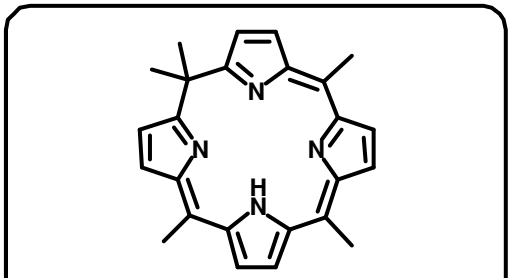

Figure 4.4. Isoporphyrin **9** (**1**.**1**.**1**.*1*)

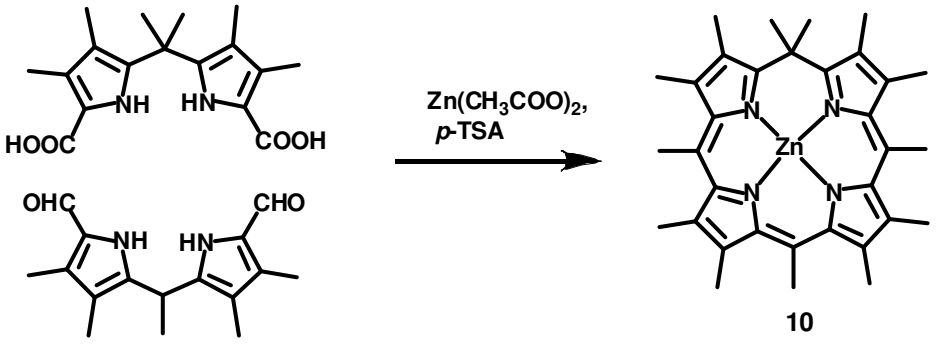

Scheme 4.2. Synthesis of **10**

in the number of NH protons. Smith and co-workers reported the first synthesis of stable metallated isoporphyrin derivative **10** through a MacDonald condensation involving a

dicarboxylic acid substituted dipyrromethane and a diformyl dipyrromethane in the presence of zinc acetate and *p*-TSA (Scheme 4.2) [Xie and Smith 1992, Barkigia *et al*. 1993].

4.4.3 Porphodimethenes: Recently, Floriani and co-workers have shown that through an unusual sequence of organometallic rearrangements, the partial (formal four-electron) oxidation of calix[4]pyrroles could be achieved to produce, among other products, hexaalkylporphodimethenes [Benech *et al*. 1999]. One of the well known intermediates which were formed during the stepwise oxidation process of porphyrinogens to porphyrins are porphodimethenes. Mainly there are two types of porphodimethenes. They are 5,15-porphodimethene type calix[4]phyrin-(**1**.*1*.**1**.*1*) (**1**) and 5,10-porphodimethene type calix[4]phyrin-(**1**.**1**.*1*.*1*) **(11)** (Figure 4.5). The first air stable di- or trivalent metallated porphodimethenes bearing alkyl substituents at the *meso* positions were isolated and

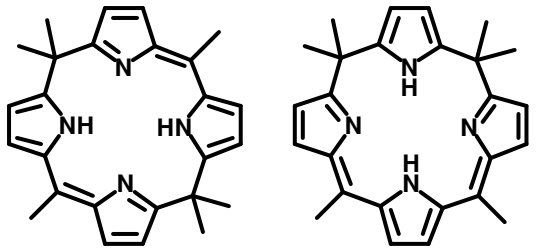

1 **11**

Figure 4.5. Porphodimethenes **1** (**1**.*1*.**1**.*1*) and **11** (**1**.**1**.*1*.*1*)

and characterized [Inhoffen *et al*. 1968, Buchler and Puppe 1970, Dolphin 1970, Dwyer *et al*. 1974, Botulinski *et al*. 1988]. This includes mainly of the type calix[4]phyrin-(**1**.*1*.**1**.*1*) systems. Earlier, Buchler's procedure was employed for the synthesis of symmetric metallated porphodimethenes which involved reductive alkylation at the *meso* position of the porphyrin [Buchler and Puppe 1970, Dwyer *et al*. 1974, Botulinski *et al*. 1984, Bischoff *et al*. 2001]. Recently, different methods for the synthesis of porphodimethene **12** which includes 2 + 2 Mac Donald-type condensation approaches [[a]Harmjanz and Scott 2000], acid-catalysed

condensation of oligo-calix[n]pyrroles with acetone (Scheme 4.3) followed by oxidation with DDQ [Král *et al*. 2000, Bucher *et al*. 2001] have been developed.

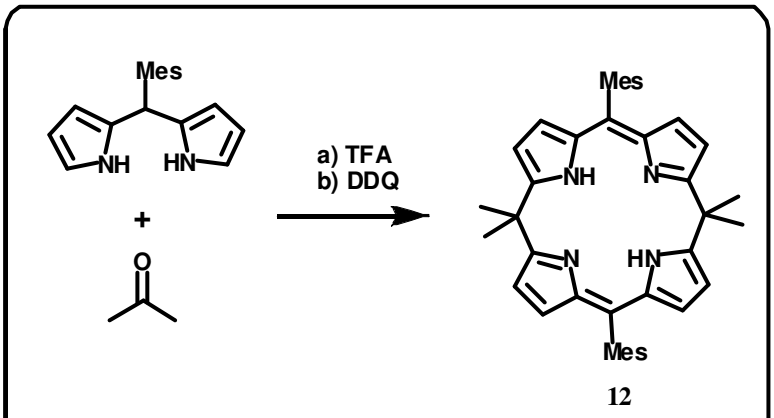

Scheme 4.3. Synthesis of **12** (**1**.*1*.**1**.*1*)

Since 5,15-disubstituted porphodimethenes appear in the biosynthetic pathway towards porphyrins, these have been thoroughly researched [Nayar *et al*. 1992, Belanzoni *et al*. 2001]. 5,10-porphodimethene is another type of calix[4]phyrin-(**1**.**1**.*1*.*1*) **13** which was first isolated (Scheme 4.4) and fully characterized by Callot *et al* [Krattinger and Callot 1996, Krattinger and Callot 1998]. The solid state structures of these porphodimethenes revealed a characteristic nonplanar tripyrrolic helical twisting that is most manifest between the two planes defined by the isolated "calix"-type pyrrole [Bucher *et al*. 2000].

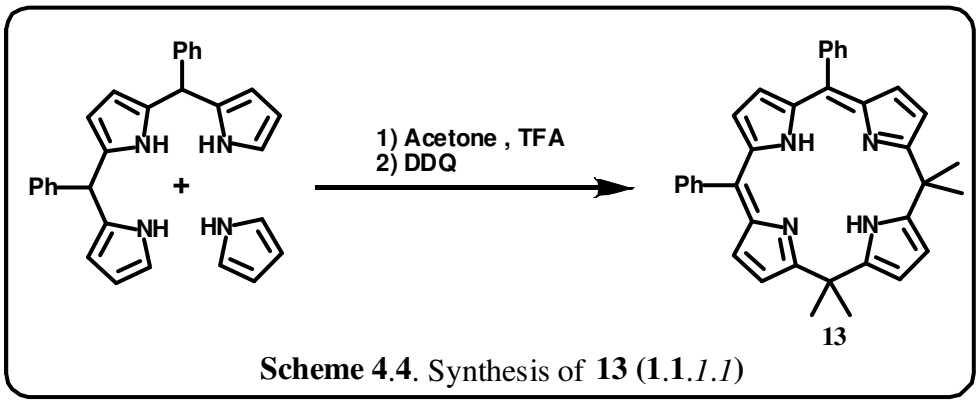

Scheme 4.4. Synthesis of **13** (**1**.**1**.*1*.*1*)

4.4.4 Three dimensional calixphyrin: These are cryptand like pyrrole containing system **14** (Figure 4.6) with sp^2 hybridized apical bridging carbon atoms [Bucher *et al*. 2003].

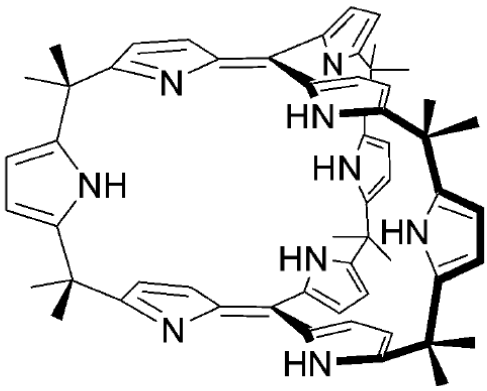

Figure 4.6. Three dimensional calixphyrin **14**

Bicyclic[3,3,3]nonapyrrole (**14**) was synthesized by the acid catalysed condensation of tripyrrane and its diformyl analogue in 15% yield. But these systems are relatively unstable and undergo color change from colorless to light red when exposed to air and light. These decomposed products contain sp^2 hybridized carbon atoms at the bridge head positions.

4.4.5 Hybrid calixphyrins: Core modification is a versatile methodology to drastically change the fundamental properties of the calixphyrin platform. Hybrid calixphyrins are those in which at least one of the pyrrole rings in these macrocycles is replaced by other aromatic rings. Matano and co-workers synthesized the first examples of P, S-containing hybrid calixphyrins of the 5,10-porphodimethene type **15** (Figure 4.7) [[b]Matano *et al*. 2006, [a]Matano *et al*. 2008]. **15** form reddish purple colored complexes **16** with palladium (Figure 4.7) and these complexes have been found to catalyze the Heck reaction with high efficiency at elevated temperatures. Another class of core modified calixphyrin is *m*-Benziporphodimethene **17** (Figure 4.7) i.e. introduction of benzene rings in the main framework of calixphyrins Hung *et al*. 2008, Chang *et al*. 2009, Huang *et al*. 2010]. **17** is non-fluorescent in its free base form and turn-on fluorescence is observed when bound with Zn^{2+} ions where the distorted *m*-benziporphodimethene core in the free base form becomes co-planar tripyrrin unit, as a consequence, there is an increase in the fluorescence.

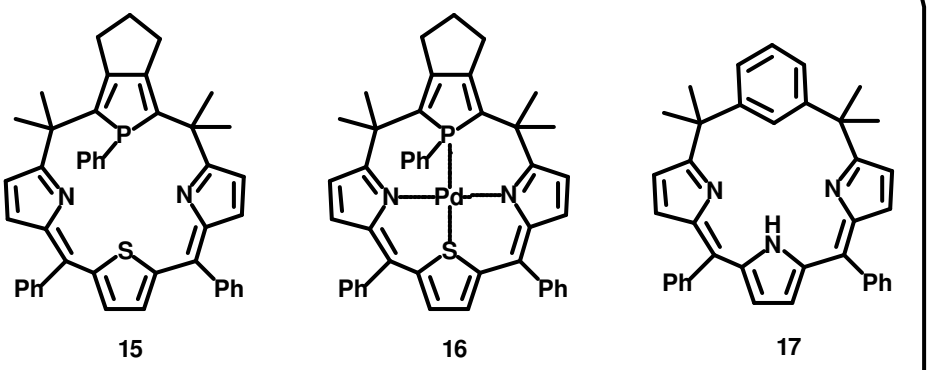

Figure 4.7. Hybrid calixphyrins

4.4.6 N-confused calixphyrins: N-confused calixphyrins **18** (Figure 4.8) are those in which α-α' (normal) and α-β' (confused) linkages of pyrrole rings exist in the calixphyrin framework. These compounds were synthesized by methanesulfonic acid catalysed cyclization of a mixture of pyrrole, aldehyde and acetone followed by oxidation with DDQ [Furuta *et al*. 2001]. The Ni and Cu complexes of this macrocycle were synthesized by refluxing **18** in $CHCl_3$ in the presence of $NiCl_2$ and $Cu(OAc)_2$. The Zinc complex was also synthesized with excess $Zn(OAc)_2.2H_2O$ in CH_2Cl_2, followed by treatment with isopropanol and aqueous NaCl, respectively, at room temperature [Furuta *et al*. 2003].

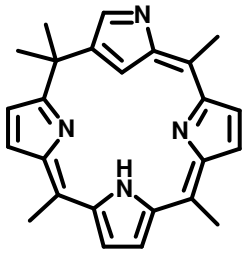

Figure 4.8. N-confused calixphyrin

4.4.7 *meso*-ferrocenyl calixphyrins: Bucher and co-workers reported the synthesis (Scheme 4.5), physico-chemical characterization, and electrochemical recognition properties of three novel *meso*-ferrocenyl calixphyrins **19**, **20** and **21** [Bucher *et al.* 2005]. The synthetic

methodology involved the acid catalysed condensation of *meso* dimethyldipyrromethane with ferrocenemonocarboxaldehyde followed by oxidation resulted in the formation of *meso* ferrocenyl calixphyrins **19**, **20** and **21**. The single crystal structure of **20** (Figure 4.9a) clearly revealed a roof like appearance and cyclopentadienyl units of ferrocene are eclipsed and almost parallel. They also synthesized and characterized the copper complex of **20** (Scheme 4.5 and Figure 4.9b).

a) b)

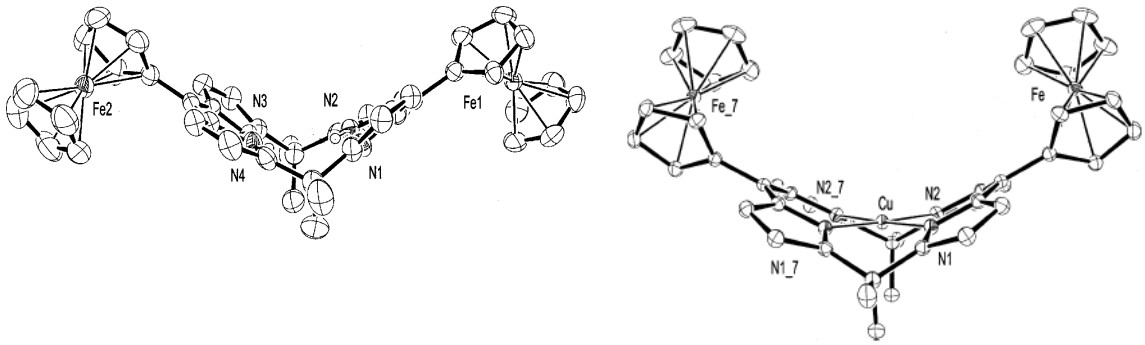

Figure 4.9. Single crystal X-ray structure of a) **20** and b) its copper complex

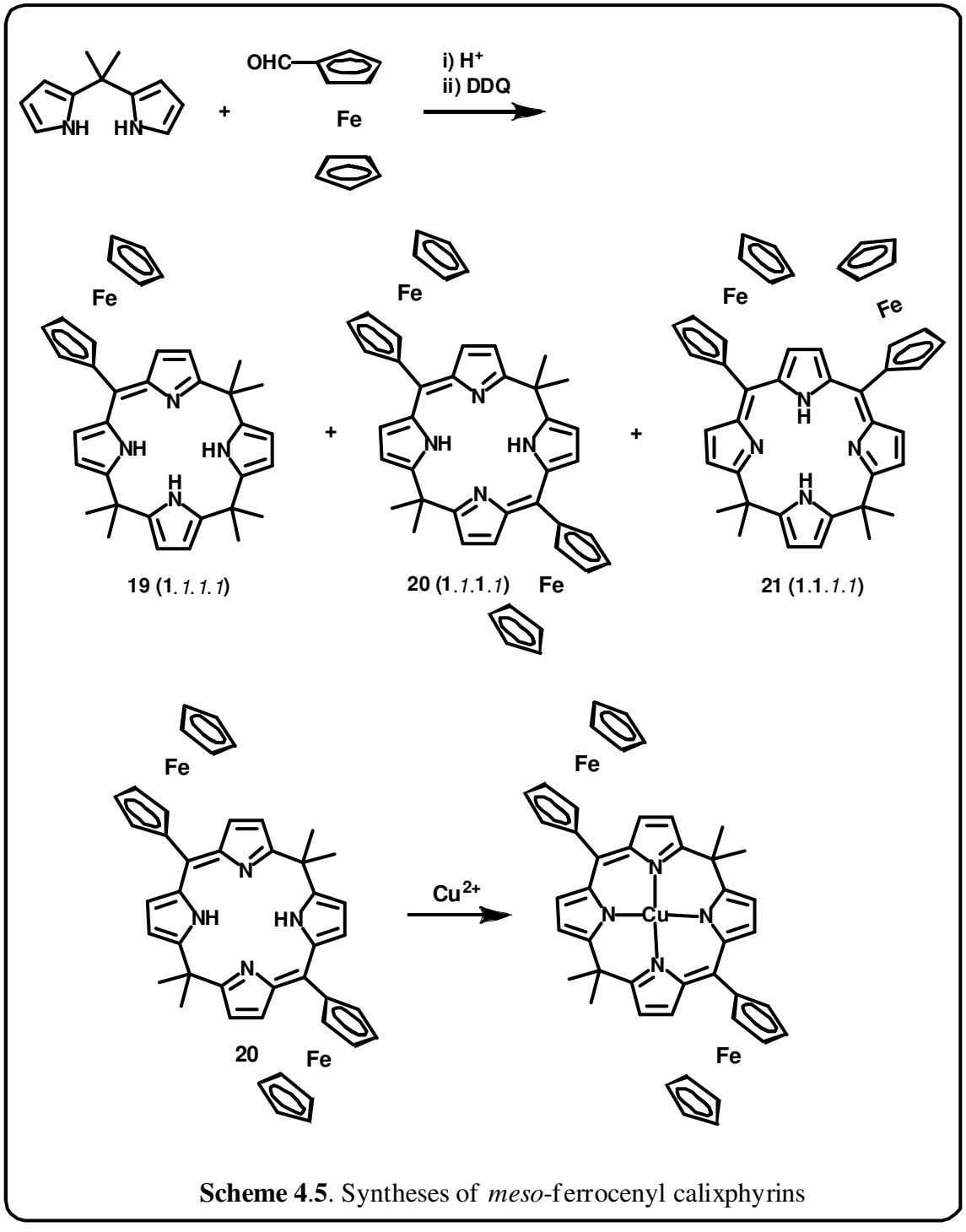

Scheme 4.5. Syntheses of *meso*-ferrocenyl calixphyrins

4.5 Objective of our work

Supramolecular assemblies with cyclic structures, particularly pyrrole receptors, have attracted considerable attention due to their potential application in the areas of host–guest chemistry, molecular recognition and catalysis [[a]Sessler and Davis 2001, [a]Sessler *et al*. 2003, Gale and Quesada 2006, Maeda 2007, [a]Matano *et al*. 2008]. Amongst various receptors, calix[n]phyrins (**A**) contain a mixture of both sp^2 and sp^3 hybridized *meso*-carbon bridges. This leads to partial interruptions in the conjugation pathway of the molecule, introduces novel structural features, and leads to interesting anion and cation recognition properties [Král *et al*. 2000, Bucher *et al*. 2001, [c]Sessler *et al*. 2001, Dolenský *et al*. 2004]. On the other hand, *ansa*-ferrocene type bridged pyrrolic systems [Scherer *et al*. 1998, [b]Sessler *et al*. 2001], metallocene appended porphyrins [Uosaki *et al*. 1997, Imahori *et al*. 2000, Bucher *et al*. 2004, Li *et al*. 2004, Suijkerbuijk and Gebbink 2008], *meso*-ferrocenyl calixpyrroles [[a]Gale *et al*. 2001] and calixphyrins [Bucher *et al*. 2005] have been found to be suitable for anionic guests, multiple electron transfer reactions and molecular electronic devices. However, incorporating metallocenes into the backbone of the fully/partially conjugated macrocycles are rare [Scherer *et al*. 1998, Sessler *et al*. 2001, Stępień *et al*. 2008]. So, in this chapter, we wish to discuss the syntheses, spectral and structural characterization of metallocenes, mainly ferrocene/ruthenocene, incorporated in the calixphyrin framework (**B**) as well as its higher-order homologues (**C**) (Figure 4.10). These molecules bear analogy to both calix[n]pyrroles and the porphyrin/*expanded* porphyrin series of macrocycles. To underscore this analogy, we propose that the compounds be referred to as calix[*n*]metallocenyl[*m*]phyrins (Figure 4.10) [Král *et al*. 1998, Arumugam *et al*. 2000, [b]Sessler *et al*. 2003, Piatek *et al*. 2004, Cafeo *et al*. 2007]. In addition to the two-dimensional

supramolecular assembly in the solid state, the role of aryl *vs*. alkyl is highlighted, in order to explain the formation of *expanded* macrocycles.

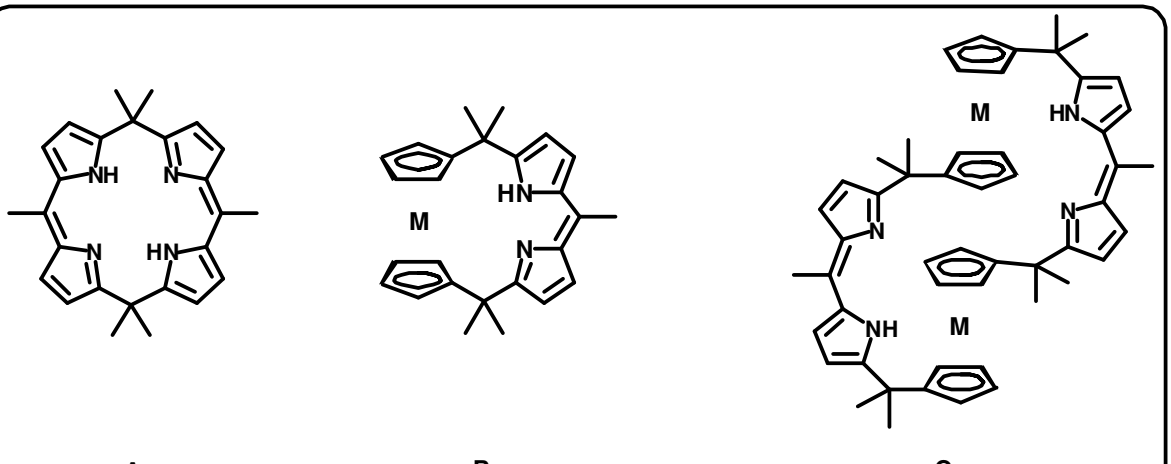

Figure 4.10. Calix[*n*]metallocenyl[*m*]phyrins (*n* = 1, 2 and *m* = 2, 4)

4.6 Results and Discussion

The syntheses of metallocene incorporated hybrid calixphyrins **25 - 40** are summarized in Scheme 4.6. The synthetic methodology adopted here is basically an acid catalysed condensation reaction [Ramakrishnan and Srinivasan 2007, Stępień *et al*. 2008]. Stirring a CH_2Cl_2 solution of **22** and electron withdrawing and electron donating aryl-aldehydes, in the presence of *p*-toluenesulfonic acid (*p*-TSA) as the catalyst, followed by 2,3-dichloro-5,6-dicyano-*p*-benzoquinone (DDQ) as an oxidizing agent afforded **25 - 30** in 15 to 19% yield, respectively. When changing the aryl substituted precursor (**22**) to alkyl (**23**), in addition to **31 - 36** in 14 to 19% yield, to our surprise, we observed *expanded* products **38 - 39** in 4 to 5% yield, along with trace amounts of higher analogues. Such *expanded* metallocenyl calixphyrins are, to the best of our knowledge, without precedent in the literature.

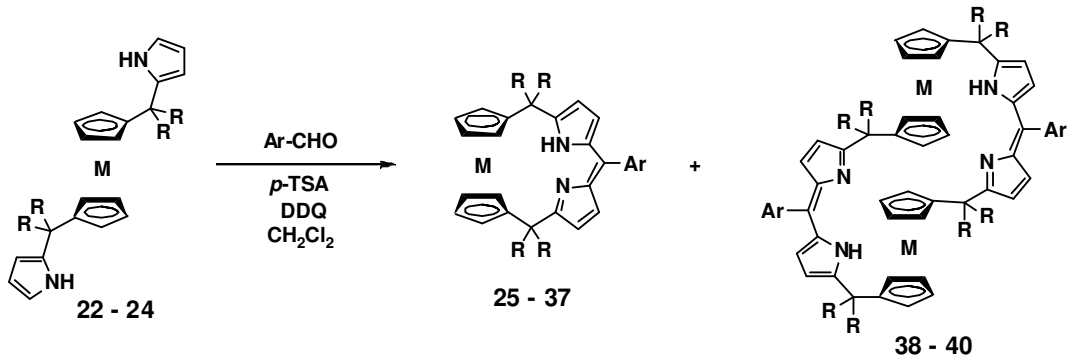

	R	M	Ar
22.	C_6H_5	Fe	4-CNC_6H_4
23.	CH_3	Fe	4-$NO_2C_6H_4$
24.	CH_3	Ru	4-$CH_3C_6H_4$
			4-$OCH_3C_6H_4$
			9-anthryl
			C_6F_5

	R	Ar	M
25.	C_6H_5	4-CNC_6H_4	Fe
26.	C_6H_5	4-$NO_2C_6H_4$	Fe
27.	C_6H_5	4-$CH_3C_6H_4$	Fe
28.	C_6H_5	4-$OCH_3C_6H_4$	Fe
29.	C_6H_5	9-anthryl	Fe
30.	C_6H_5	C_6F_5	Fe
31.	CH_3	4-CNC_6H_4	Fe
32.	CH_3	4-$NO_2C_6H_4$	Fe
33.	CH_3	4-$CH_3C_6H_4$	Fe
34.	CH_3	4-$OCH_3C_6H_4$	Fe
35.	CH_3	9-anthryl	Fe
36.	CH_3	C_6F_5	Fe
37.	CH_3	C_6F_5	Ru

	R	Ar	M
38.	CH_3	4-$NO_2C_6H_4$	Fe
39.	CH_3	C_6F_5	Fe
40.	CH_3	C_6F_5	Ru

Scheme 4.6. Syntheses of **25** - **40**

The FAB mass spectral analyses of all the new macrocycles (**25 - 36** and **38 - 39**) show the molecular ion signals, which proves the exact composition. The ^{1}H NMR spectra of **25 - 36** and **38 - 39** were recorded in $CDCl_3$ at room temperature, where the ferrocenyl CH in **25 - 30** are observed as four singlets from 2.93 to 4.58 ppm, while in **31 - 36**, the respective protons resonate at 4.28 ppm as a singlet, suggesting less *meso*-steric crowding in **31 - 36**. The pyrrolic β-CH signals in **25 - 36** are observed from 5.86 to 6.54 ppm, while the

NH proton resonates as broad signals from 15.62 to 16.19 ppm. On the other hand, the NH signals in **38 - 39** are at 12.74 and 12.33 ppm, which are upfield shifted with shift differences of 2.97 and 3.32 ppm as compared to **32** and **36**, suggesting the strong intramolecular hydrogen bonding interactions in the latter. The peaks due to NH protons were clearly confirmed by D_2O exchange experiments. The pyrrolic β-CH and ferrocenyl CH protons in **38 - 39** resonate from 6.28 to 3.9 ppm, respectively. The electronic spectral analysis of **26**, **29**, **30**, **32** and **36** (Figure 4.11a, Figure 4.11b, Figure 4.11c, Figure 4.11d, Figure 4.11e) shows the broad absorption band centered approximately at 480 nm, suggesting the π–π^* transition within the dipyrrin unit, instead of the traditional metal to ligand charge transfer band. The peaks due to $\pi \rightarrow \pi^*$ transitions of the anthracene moiety were observed at lower wavelength absorption bands between 332-386 nm with molar extinction coefficient values ranging from 96,000 to 49,000 $M^{-1}cm^{-1}$ respectively for **29** (Figure 4.11b). The similar trend is observed in **38** and **39** which shows the band at 445 nm (Figure 4.11c and Figure 4.11d) with the blue shift of 33 nm as compared to **32** and **36**. All the above macrocycles are non-fluorescent in its free base form.

a)

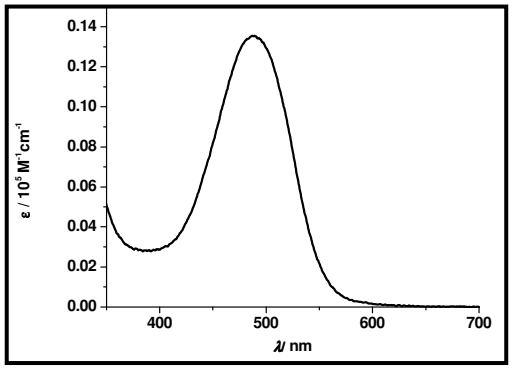

b)

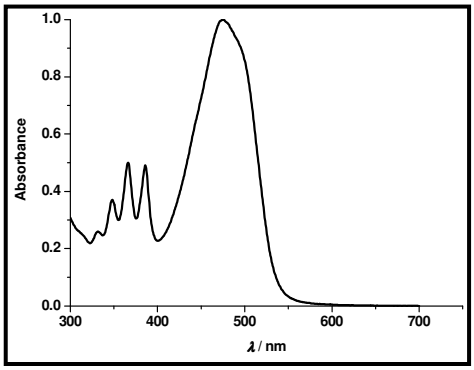

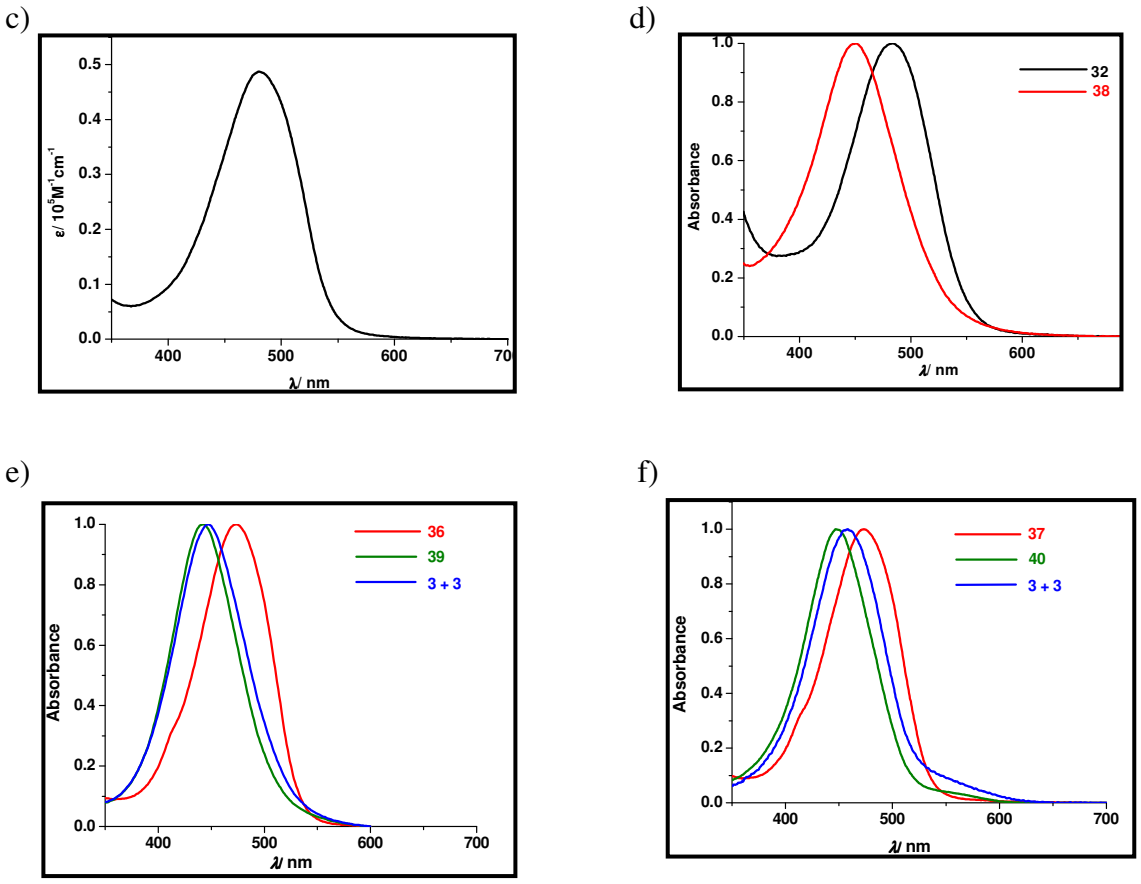

Figure 4.11. Electronic absorption spectrum of a) **26**, b) **29**, and c) **30** in $CHCl_3$. Normalised absorption spectrum of d) **32** and **38,** e) **36**, **39** and 3 + 3 derivative, f) Normalised electronic absorption spectrum of **37**, **40** and 3 + 3 derivative in $CHCl_3$.

As predicted from the above observations, the final confirmation of **25**, **26**, **27**, **29** and **36** have come from the single crystal X-ray structure analysis (Figure 4.12) (Table 4.1). The crystal structure clearly reveals the linkage of the dipyrrin moiety containing *meso* aryl group with 1 and 1'- position of the ferrocene unit through the sp^3 hybridized *meso* carbons. These macrocycles form strong intramolecular hydrogen bonding interactions between the amine pyrrole NH and imine pyrrole N which are present in the dipyrrin unit, with distances and angles for N1-H1C---N2 in **25** (Figure 4.12a), N1-H1A---N2 in **26** (Figure 4.12c), N2-H2C---N1 in **27** (Figure 4.12e), N1-H1C---N2 in **29** (Figure 4.12g) and N2-H2A---N1 in **36** (Figure 4.12i) of 2.03 Å, 122.32˚; 1.81 Å, 144˚; 1.89 Å, 137.41˚; 2 Å, 128.72˚ and 1.93 Å,

136˚. The *meso*-4-cyanophenyl and the cyclopentadienyl rings in **25** are deviated from the mean dipyrrin plane consisting of C11, C16, C21 atoms with angles of 50.52, 41.3 and 42.6˚ (Figure 4.12a). The *meso-p*-NO_2 phenyl group and the cyclopentadienyl rings in **26** are deviated from the mean dipyrrin plane consisting of C11, C28 and C33 atoms, with angles of 66.53, 43.27 and 43.04˚ respectively (Figure 4.12c). The *meso-p*-tolyl moiety and the cyclopentadienyl rings in **27**, are deviated from the mean dipyrrin plane consisting of C6, C11, C16 atoms with deviation of 37.76, 43.07 and 41.70˚ respectively (Figure 4.12e). The *meso*-9-anthryl part and the cyclopentadienyl rings in **29** are deviated from the mean dipyrrin plane consisting of C11, C16, C21 atoms with deviation of 62.83, 44.46 and 43.20˚ respectively (Figure 4.12g). Such deviation between the *meso*-pentafluorophenyl group and the cyclopentadienyl rings in **36** with the plane consisting of C11, C18 and C29 are 59.57, 45.73 and 45.13˚ respectively (Figure 4.12i).

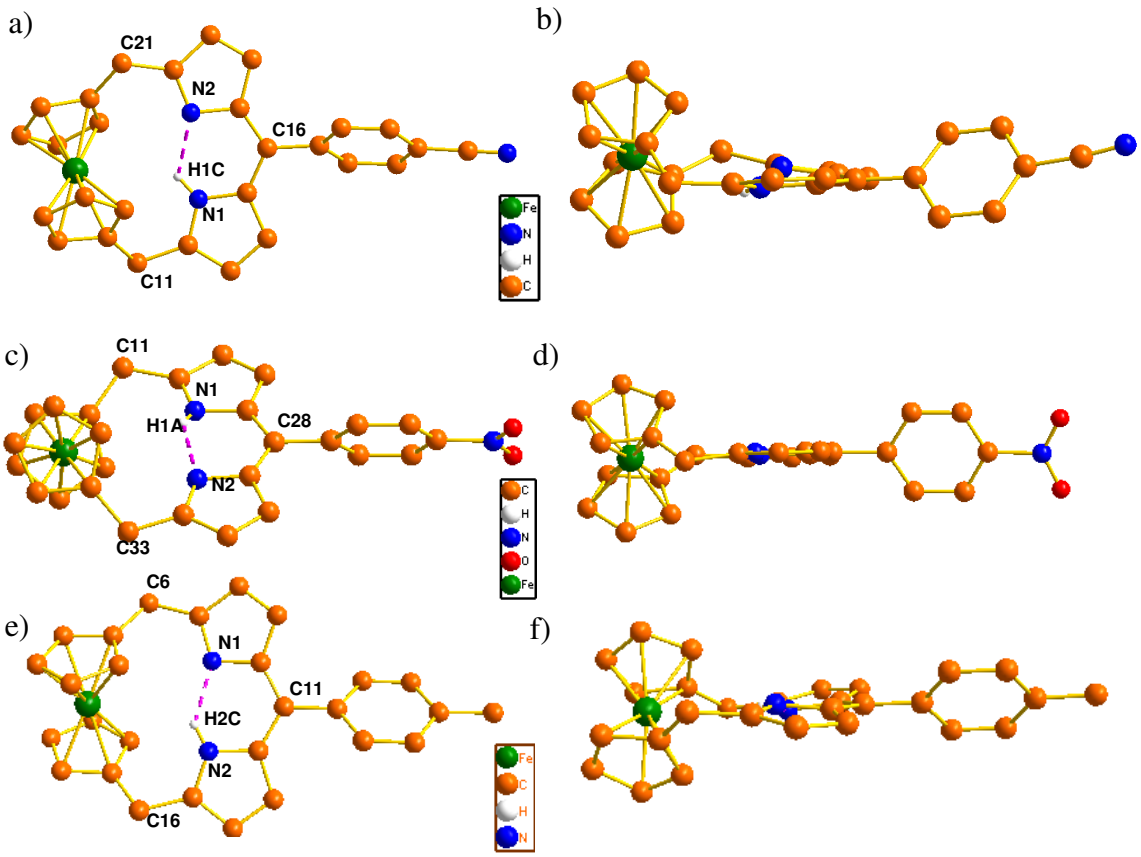

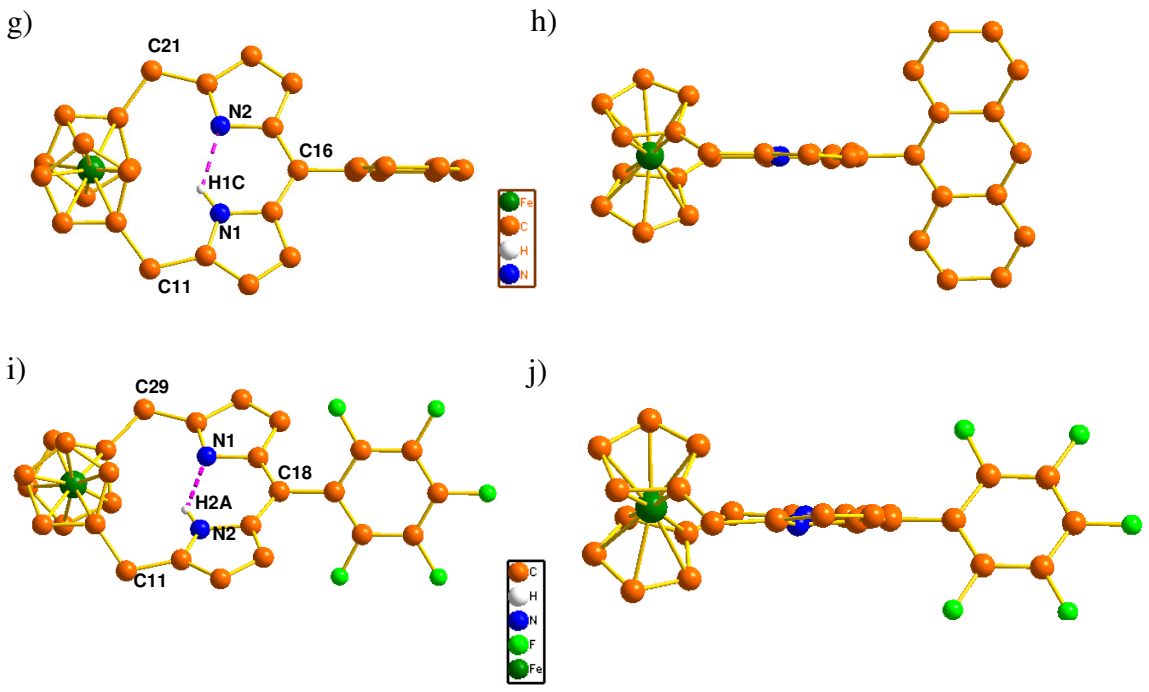

Figure 4.12. Single crystal X-ray structures and analysis of **25**, **26**, **27**, **29 and 36**. (a, b), (c, d), (e, f) (g, h) and (i, j) are the top and side views of **25**, **26**, **27**, **29** and **36** respectively with intramolecular hydrogen bonding interactions. The *meso* phenyl groups in **25**, **26**, **27** and **29** and *meso* methyl groups in **36** and hydrogens which are not involved in the hydrogen bonding interactions are omitted for clarity.

Further, the *meso*-*p*-cyano group in **25** interacts with *meso* *p*-CN phenyl CH of another molecule to form the self-assembled dimer with distance and angle of C38–H38---N3: 2.56 Å and 147.92˚ (Figure 4.13).

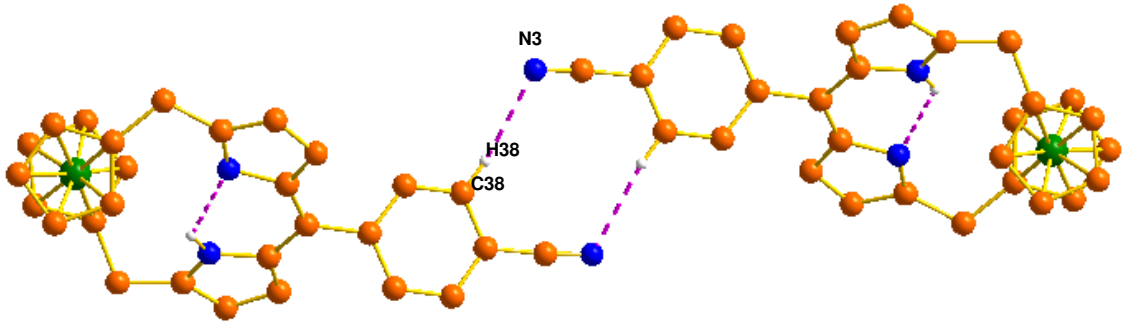

Figure 4.13. Self assembled dimer of **25**. The *meso* phenyl groups and hydrogens which are not involved in the interactions are omitted for clarity.

Further, the *meso-p*-NO_2 group in **26** interacts with pyrrolic β-CH of another molecule to form the self-assembled dimer (Figure 4.14a) with the distances and angles of C26-H26---O1: 2.81 Å, 151˚; C26-H26---O2: 2.8 Å, 163˚ and also forms 1-D array between the *meso*-phenyl CH and *meso-p*-NO_2 phenyl π cloud (Figure 4.14b) with distance and angle of C20-H20---Ph(π): 2.88 Å, 145˚.

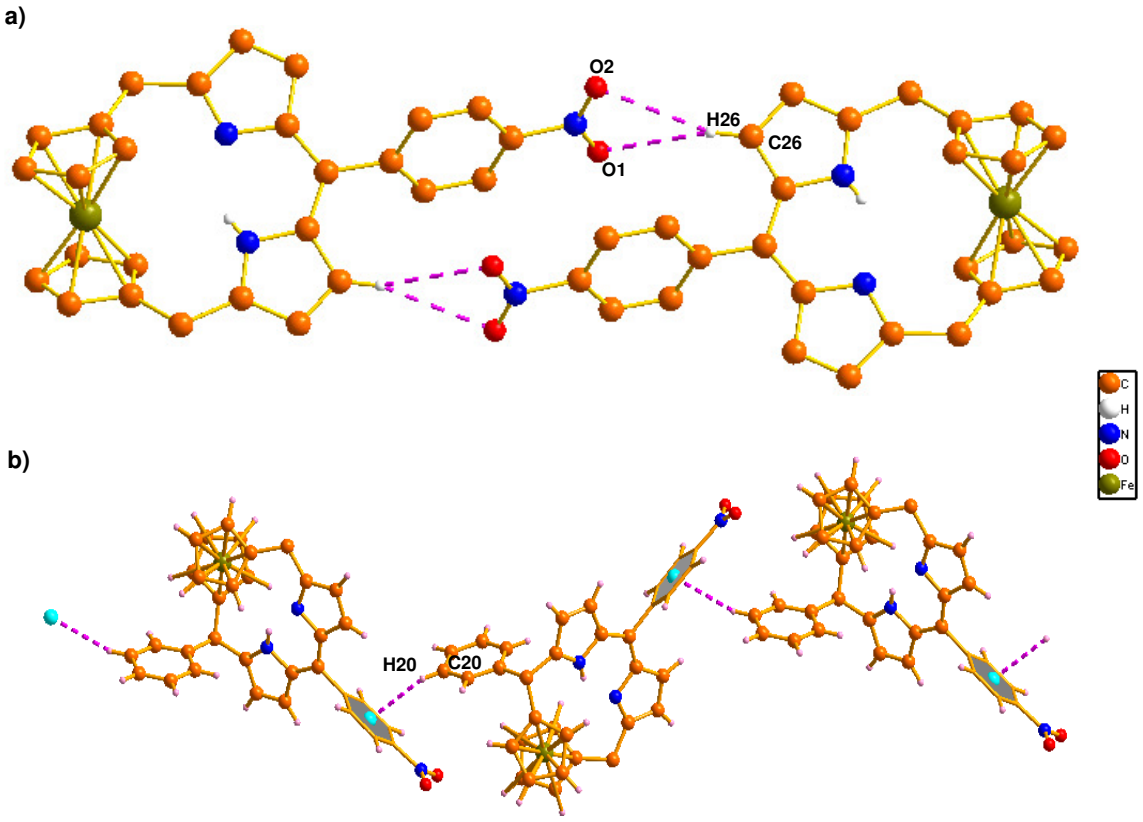

Figure 4.14. Single crystal X-ray analyses of **26**. a) Self-assembled dimer of **26** and b) 1-D array of **26**. The *meso*-diaryl groups and the groups which are not involved in the hydrogen bonding interactions are omitted for clarity.

Combining the above two assemblies, **26** forms a two-dimensional array (Figure 4.15).

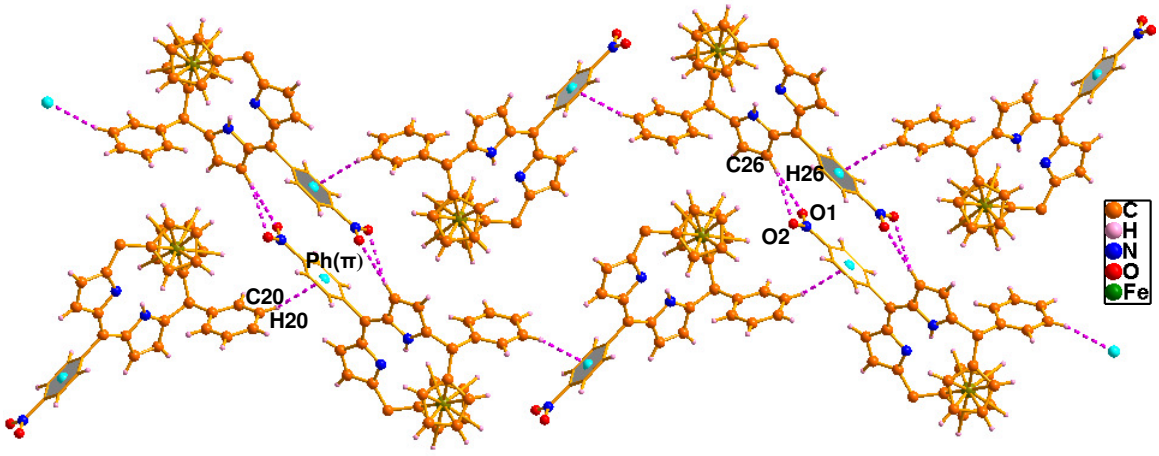

Figure 4.15. 2-D array of **26**. The groups which are not involved in the hydrogen bonding interactions are omitted for clarity.

In **29**, there are two pyrrolic C-H---phenyl(π) cloud interactions observed with distances and angles are i) C14-H14---phenyl(π): 2.85 Å, 152.25˚, ii) C18-H18---phenyl(π): 2.48 Å, 148.67˚ which forms 1-D array in the solid state (Figure 4.16).

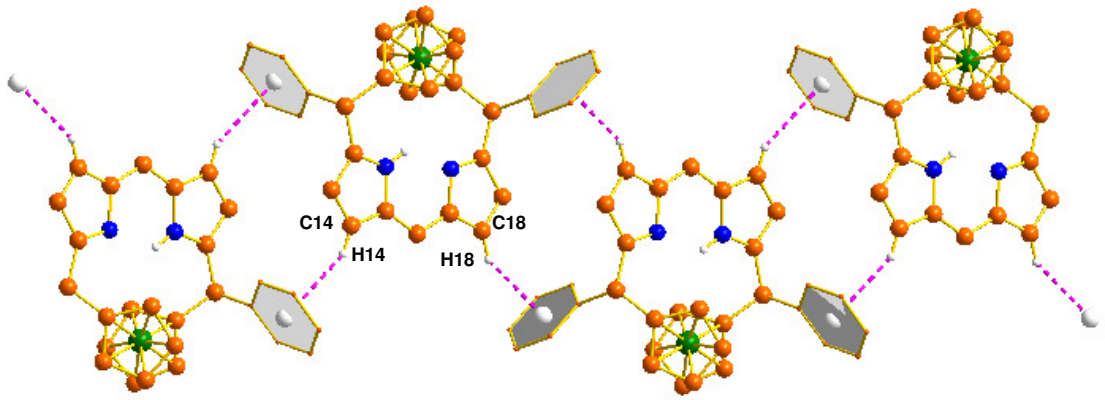

Figure 4.16. 1-D array of **29**. The phenyl groups and 9-anthryl groups which are not involved in interactions are omitted for clarity.

Due to the presence of fluorine atoms in the *meso*-pentafluorophenyl unit, **36** also generates self assembled dimer (Figure 4.17a) and 1-D array in the solid state (Figure 4.17b).

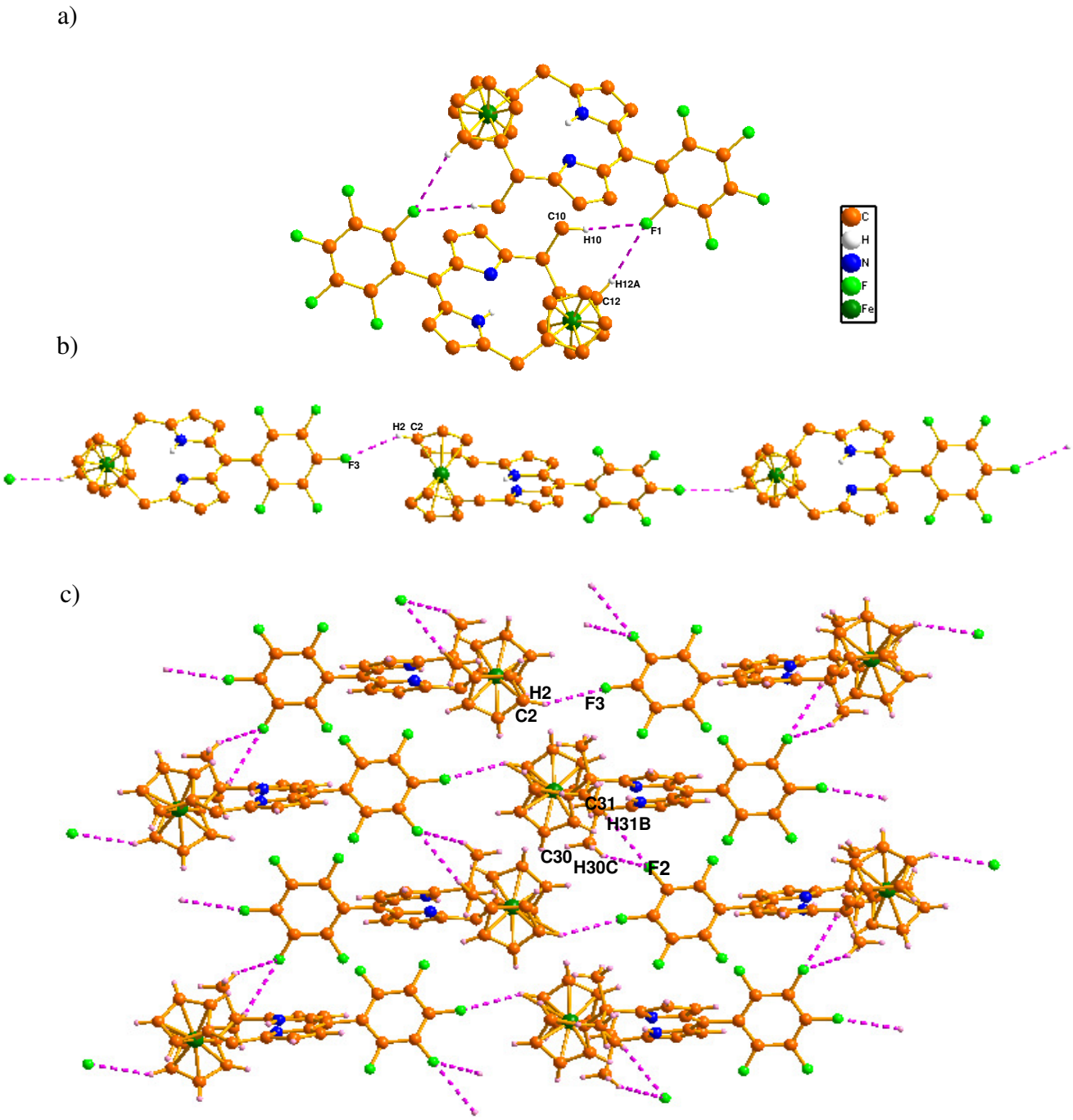

Figure 4.17. Single crystal X-ray analyses of **36**. a) Self-assembled dimer, b) 1-D array and c) 2-D array of **36**. The *meso*-dialkyl groups and the groups which are not involved in the hydrogen bonding interactions are omitted for clarity.

The single crystal X-ray structure of **39** (Table 4.1) is shown in Figure 4.18, where two pentafluorophenyl substituted dipyrrin units are linked to 1 and 1' position of the two

ferrocenyl units. As observed in **36**, **39** also forms intramolecular hydrogen bonding interactions between the dipyrrin pyrrole units with the distance and angle of N1–H1C---N2 being 2.05 Å and 132˚ (Figure 4.18a). Both the *meso*-pentafluorophenyl units and the cyclopentadienyl rings in **39** are deviated from the mean dipyrrin plane containing the C11, C16 and C21 atoms, with deviations of 65, 60.29 and 60.71˚ respectively, which is shown in the side view (Figure 4.18b).

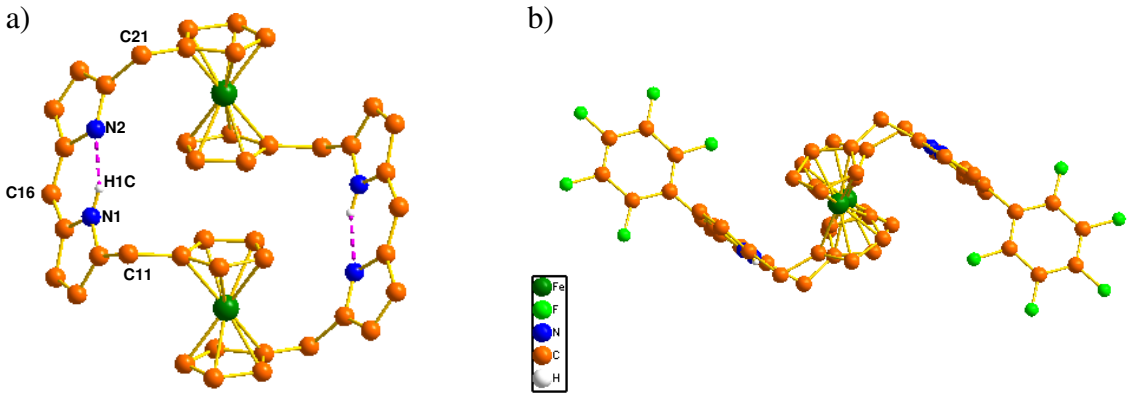

Figure 4.18. Single crystal X-ray structure of **39**. a) top view and b) side view. The *meso*-dialkyl groups in (a) and (b) and *meso* pentafluorophenyl groups in (a) are omitted for clarity.

As demonstrated in the precursor **23** (Figure 4.24b, Figure 4.24c), **39** also shows two different 1-D arrays, the first array was generated between the ferrocenyl C–H and one of the fluorine atoms of the *meso*-pentafluorophenyl group, with the distance and angle (C8–H8---F2) of 2.71 Å and 157˚, respectively (Figure 4.19a), while the second array was formed between the *meso*-methyl C-H and pyrrolic (N2) π-cloud, with the distance and angle (C28–H28---N2 (π)) of 2.73 Å and 153˚ (Figure 4.19b).

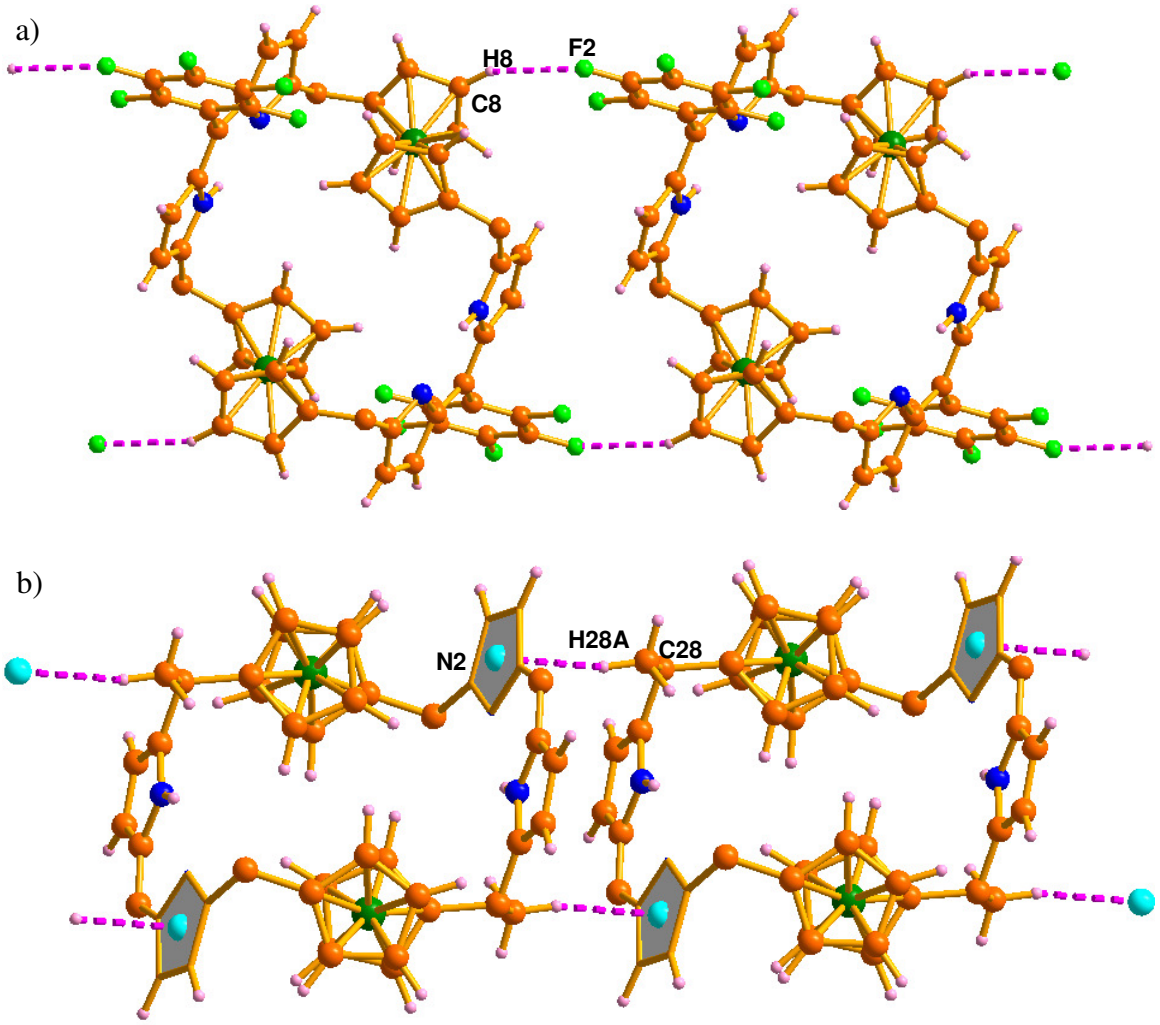

Figure 4.19. Single crystal X-ray analyses of **39**. a) and b) 1-D arrays. The groups which are not involved in the hydrogen bonding interactions are omitted for clarity.

Combining both the 1-D arrays, **39** forms a two-dimensional supramolecular assembly as shown in Figure 4.20.

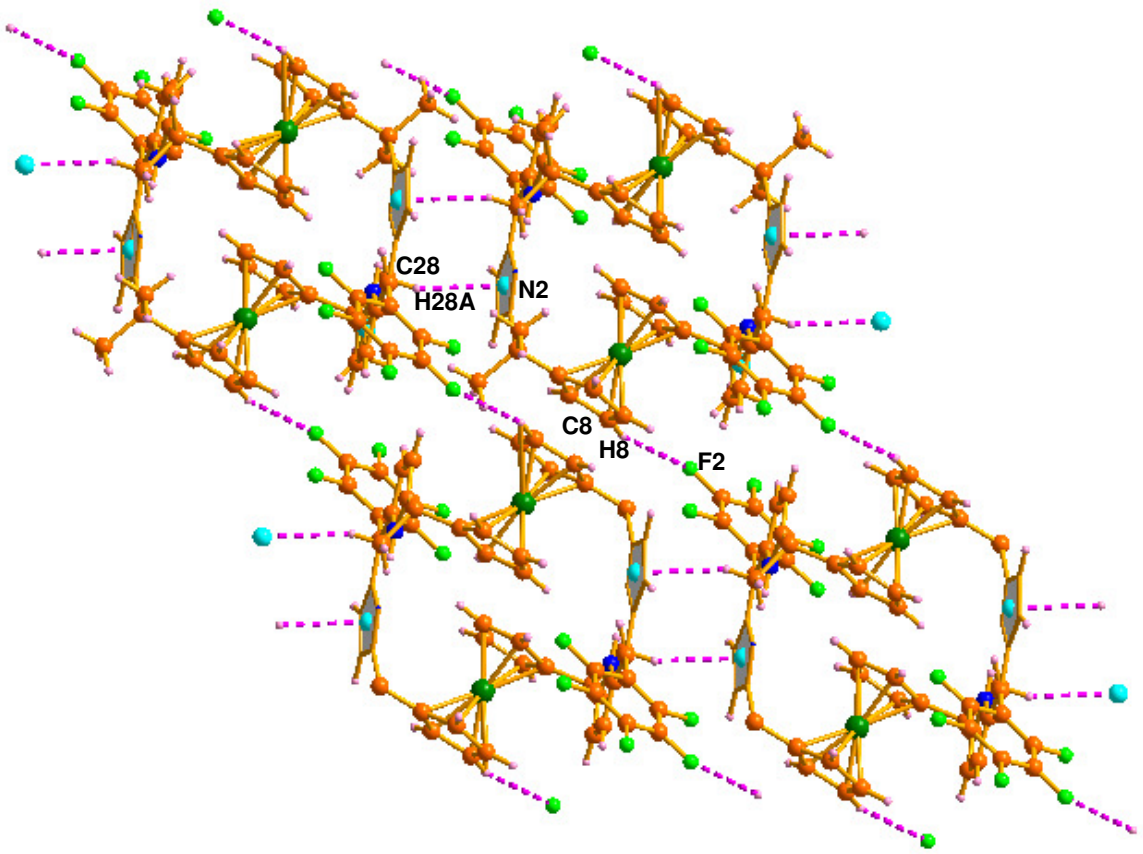

Figure 4.20. 2-D array of **39**.

The experiment was further performed with the next higher metallocene, such as ruthenocene. By using a similar synthetic methodology adopted earlier (Scheme 4.6), the treatment of **24** with pentafluorobenzaldehyde afforded **37** and **40** in 16.4 and 4% yield, respectively. Apart from standard spectroscopic techniques, the final confirmation of **40** has come from the single crystal X-ray analysis (Table 4.1), as shown in Figure 4.21. As observed in **39**, **40** also forms strong intramolecular H-bonding interactions between the pyrrole rings in dipyrrin units with the distance and angle N1–H1C---N2 of 2.00 Å and 141˚ (Figure 4.21a). As demonstrated in **39**, **40** also forms a two dimensional supramolecular assembly (Figure 4.23) in the solid state.

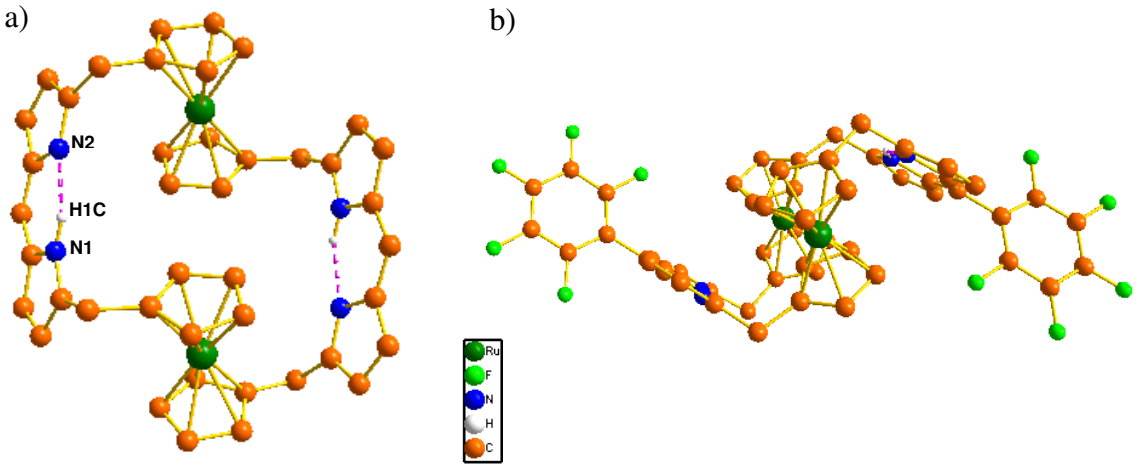

Figure 4.21. Single crystal X-ray structure of **40**. a) top view and b) side view. The *meso*-dialkyl groups in (a) and (b) and *meso* pentafluorophenyl groups in (a) are omitted for clarity.

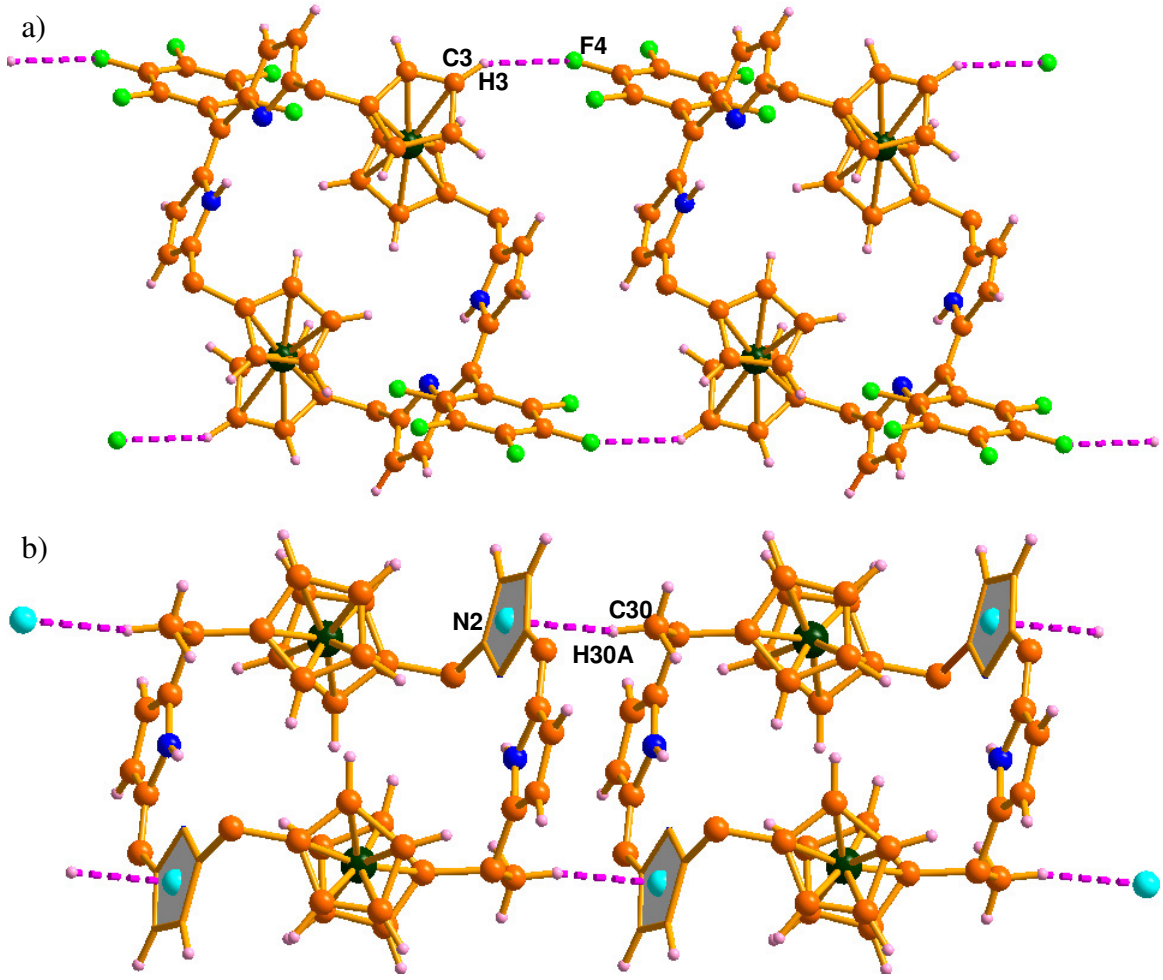

Figure 4.22. Single crystal X-ray analyses of **40**. a) and b) 1-D arrays. The groups which are not involved in the hydrogen bonding interactions are omitted for clarity.

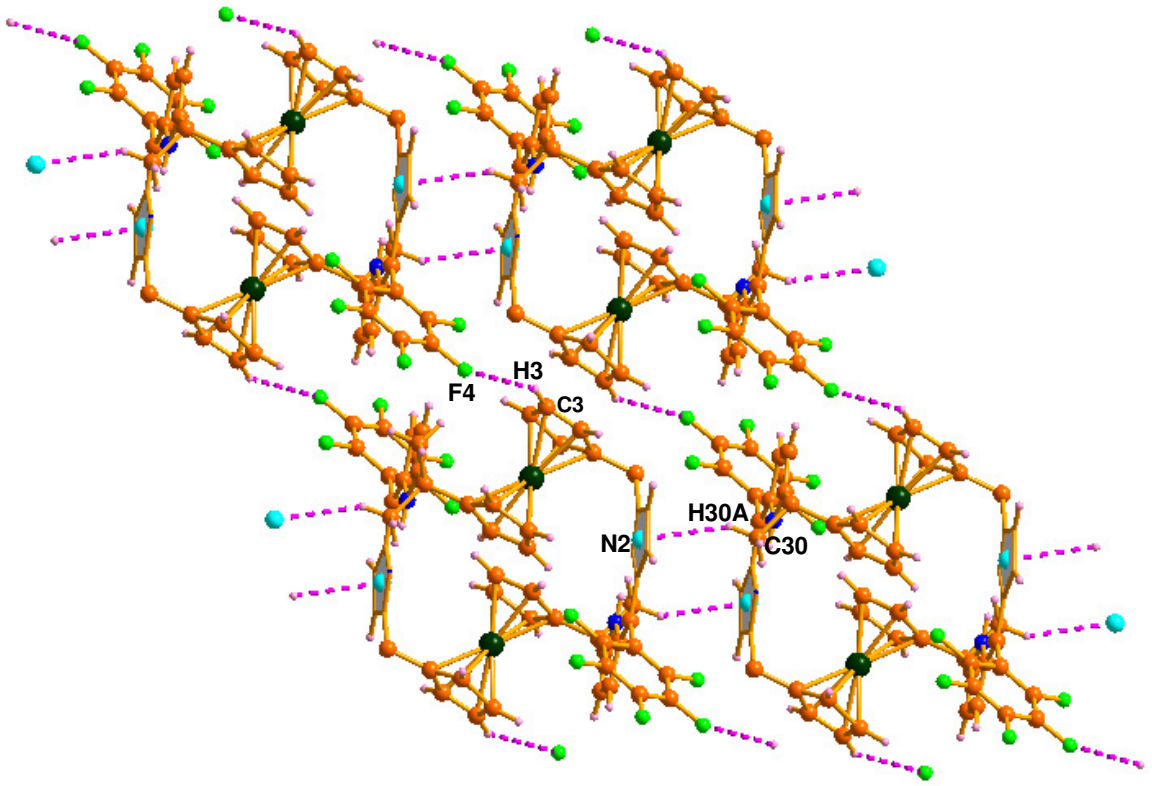

Figure 4.23. 2-D array of **40**.

Furthermore, the role of aryl *vs*. alkyl is demonstrated as follows. The intermolecular distance between the two closest pyrrolic π clouds in **22** is 8.76 Å (Figure 4.24a) and the respective distances in **23** are 5.07 and 4.93 Å (Figure 4.24b and Figure 4.24c) which are 3.69 and 3.83 Å lower than **22**, suggesting that pyrrole rings in **23** are arranged in such a way to form the *expanded* macrocycle. This is further confirmed from the single crystal X-ray analyses of **39** and **40**, where the minimum distance required for the dipyrrin unit formation is 4.47 Å (Figure 4.24d). These distances are obtained between the two pyrrolic π-clouds which are present in the dipyrrin unit in **39** and **40**. The observed distance in the precursor **23** falls close to dipyrrin unit formation, however, which is not possible from **22**. Hence, the aryl group in **22** obstructs the pyrrole unit preventing it coming closer; whereas the alkyl group in **23** assists the pyrrolic unit to bring it closer for further condensation with

the aryl aldehydes. Overall, the alkyl group plays a vital role in synthesizing the higher derivatives.

a)

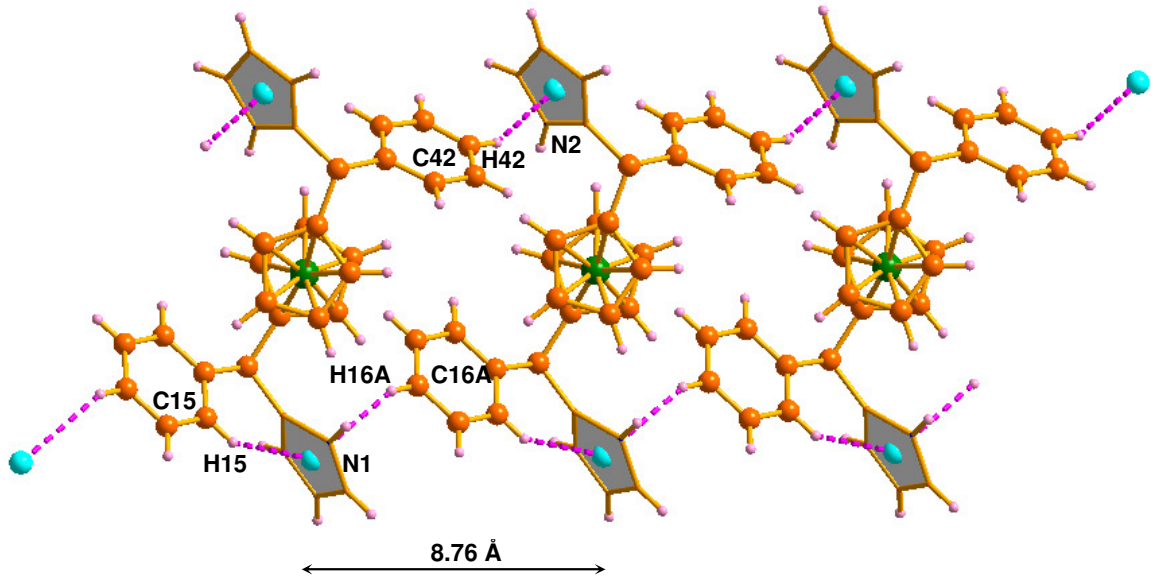

b)

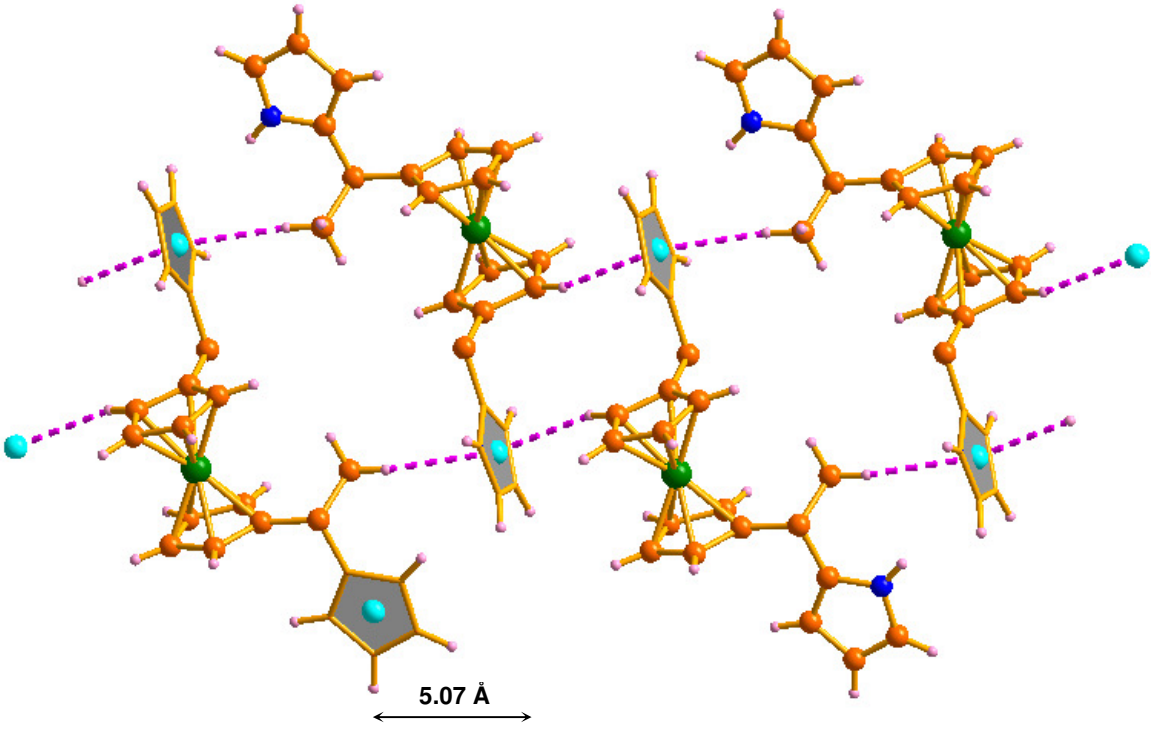

c)

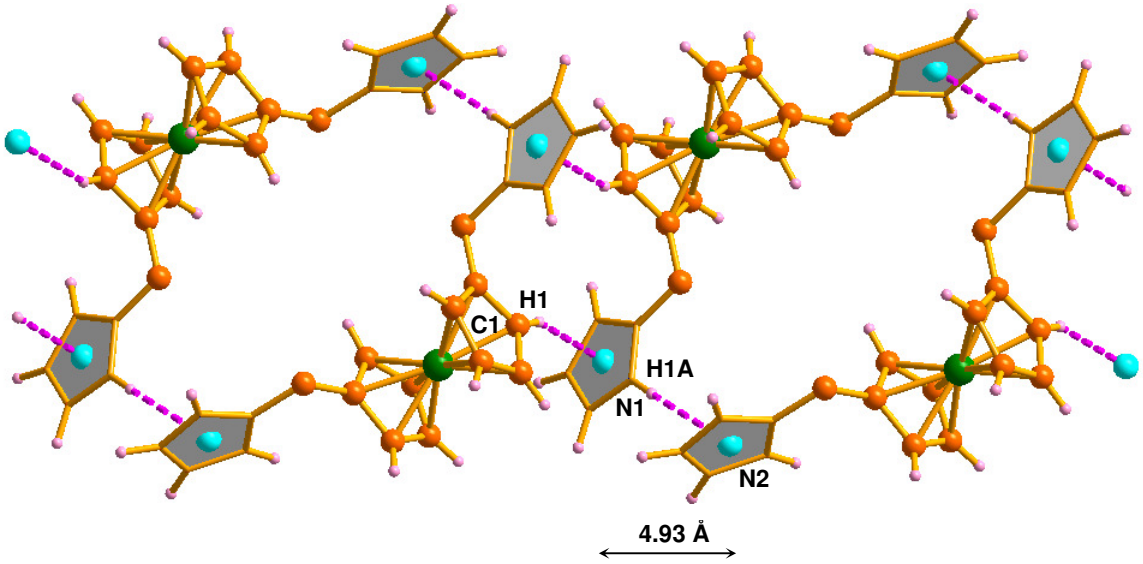

d)

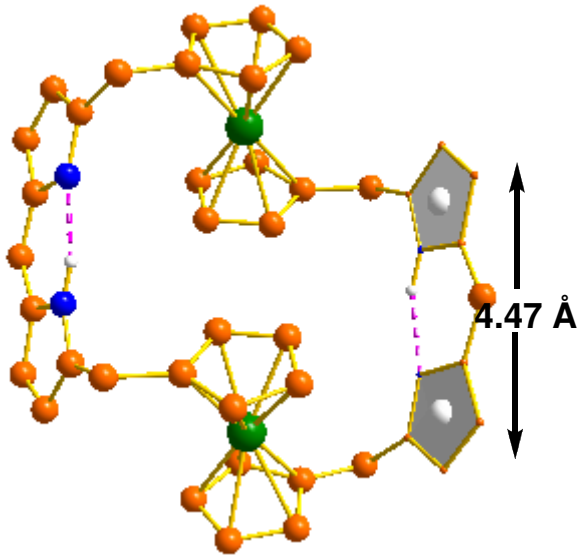

Figure 4.24. a) 1-D array of **22**; (b), (c) are two different 1-D arrays of **23** and d) top view of **40** showing the distance between the two pyrrolic units in the dipyrrin moiety.

4.7 Conclusion

In conclusion, we have demonstrated the syntheses and supramolecular assemblies of a series of calix[*n*]metallocenyl[*m*]phyrins. The synthetic methodology adopted here is simple and straightforward. Introduction of the alkyl group at the *meso*-position assists the *expanded* macrocycle formation and are considered as potential candidates for the synthesis of higher homologues. To the best of our knowledge, the macrocycles discussed here are the largest metallocene incorporated porphyrinoids reported to date.

4.8 Experimental Section

Synthesis of 25:

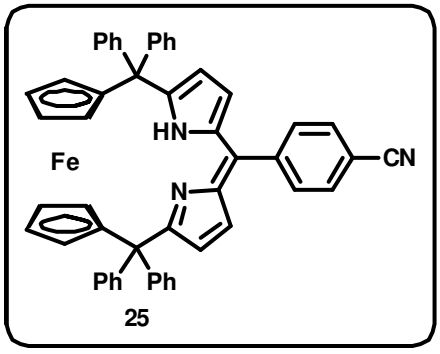

25

1,1'-bis(diphenylpyrrolylmethyl)ferrocene (**22**) (0.2 g, 0.3 mmol) and 4-cyanobenzaldehyde (0.04 g, 0.3 mmol) were dissolved in 100 mL of dry CH_2Cl_2 under inert conditions and allowed to stir for 10 min at room temperature. *p*-TSA (0.002 g, 0.01 mmol) was added to the above reaction mixture and allowed to stir for 2 hr. DDQ (0.136 g, 0.6 mmol) was added to the above reaction mixture, solution was opened to air and stirring was continued for further 2 hr. The solvent was removed using rotary evaporator. The crude product was purified by silica gel column chromatography (100 – 200 mesh) and the red fraction eluted with CH_2Cl_2 : petroleum ether (40 : 60) was identified as **25**. Yield = 0.04 g, 17%. ^{1}H NMR (300MHz, $CDCl_3$, 298 K): δ = 16.18 (brs, 1H, pyrrole NH), 7.78 (s, 4H, phenyl CH), 7.38 (s, 10H, phenyl CH), 7.17-7.15 (t, 6H, phenyl CH), 6.96-6.95 (m, 4H, phenyl CH), 6.48-6.47 (d, J = 4.04 Hz, 2H, β-pyrrolyl CH), 5.87-5.85 (d, J = 3.8 Hz, 2H, β-pyrrolyl CH), 4.57 (s, 2H,

ferrocenyl CH), 3.97 (s, 2H, ferrocenyl CH), 3.86 (s, 2H, ferrocenyl CH), 2.93 (s, 2H, ferrocenyl CH); UV-Vis ($CHCl_3$): λ_{max}/nm ($\varepsilon/M^{-1}cm^{-1}$) = 467.4 (38000); FAB mass (m/z) : Calcd. for $C_{52}H_{37}FeN_3$: 759.23; Found : 758.80 (100%, M^+).

Synthesis of 26:

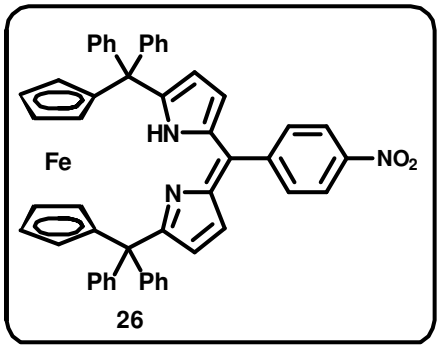

26

The above procedure was followed by using 4-nitro benzaldehyde (0.046 g, 0.3 mmol). The crude product was purified by silica gel column chromatography (100 – 200 mesh) and the red fraction eluted with CH_2Cl_2 : petroleum ether (40 : 60) was identified as **26**. Yield = 0.04 g, 18%. ^{1}H NMR (300 MHz, $CDCl_3$, 298K) : δ = 16.19 (brs, 1H, pyrrolyl NH), 8.36-8.33 (d, J = 8.65 Hz, 2H, phenyl H), 7.86-7.83 (d, J = 8.7 Hz, 2H, phenyl H), 7.39-7.35 (m, 10H, phenyl CH), 7.18-7.16 (m, 6H, phenyl CH), 6.97-6.91 (m, 4H, phenyl CH), 6.5-6.48 (d, J = 4 Hz, 2H, *β*-pyrrolyl CH), 5.9-5.87 (d, J = 4 Hz, 2H, *β*-pyrrolyl CH), 4.58 (s, 2H, ferrocenyl CH), 3.97 (s, 2H, ferrocenyl CH), 3.87 (s, 2H, ferrocenyl CH), 2.93 (s, 2H, ferrocenyl CH); UV-Vis ($CHCl_3$): λ_{max}/nm ($\varepsilon/M^{-1}cm^{-1}$) = 489 (14000); FAB mass (m/z) : Calcd for $C_{51}H_{37}FeN_3O_2$ = 779.22; Observed = 778.59 (100%, M^+).

Synthesis of 27:

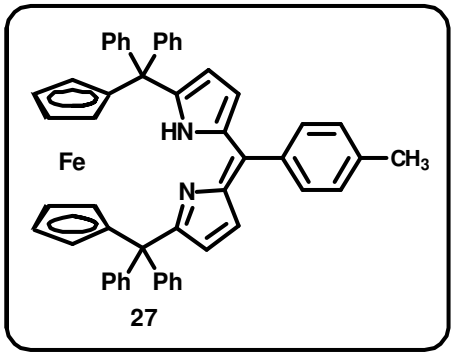

27

The above procedure was followed by using *p*-tolualdehyde (0.036 mL, 0.3 mmol). The crude product was purified by silica gel column chromatography (100 – 200 mesh) and the red fraction eluted with CH_2Cl_2 : petroleum ether (15 : 85) was identified as **27**. Yield = 0.043 g, 18.5%. ^{1}H NMR (300MHz, $CDCl_3$, 298 K): δ = 16.26 (brs, 1H, pyrrolyl NH), 7.61 (m, 2H, phenyl CH), 7.4-7.38 (m, 9H, phenyl CH), 7.17-7.14 (m, 8H, phenyl CH), 6.96-6.93

(m, 5H, phenyl CH), 6.62-6.61 (d, J = 3.92 Hz, 2H, β-pyrrolyl CH), 5.81-5.8 (d, J = 4Hz, 2H, β-pyrrolyl CH), 4.59 (s, 2H, ferrocenyl CH), 3.94 (s, 2H, ferrocenyl CH), 3.86 (s, 2H, ferrocenyl CH), 2.89 (s, 2H, ferrocenyl CH), 2.45 (s, 3H, methyl CH); UV-Vis ($CHCl_3$): λ_{max}/nm ($\varepsilon/M^{-1}cm^{-1}$) = 468.5 (33000); FAB mass (m/z): Calcd for $C_{52}H_{40}FeN_2$: 748.25; Found : 748.22 (100%, M^+).

Synthesis of 28:

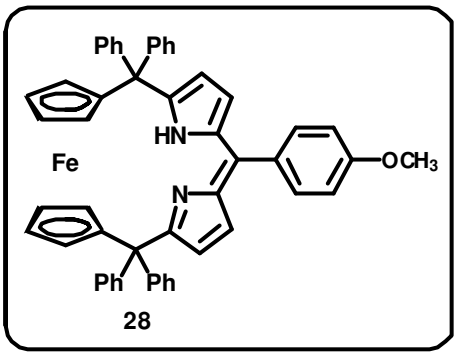

28

The above procedure was followed by using *p*-methoxybenzaldehyde (0.036 mL, 0.3 mmol). The crude product was purified by silica gel column chromatography (100 – 200 mesh) and the red fraction eluted with CH_2Cl_2 : petroleum ether (15 : 85) was identified as **28**. Yield = 0.04 g, 17%. ^{1}H NMR (300MHz, $CDCl_3$, 298 K): δ = 16.24 (brs, 1H, pyrrolyl NH), 7.61 (m, 2H, phenyl CH), 7.40-7.38 (m, 9H, phenyl CH), 7.16-7.14 (m, 8H, phenyl CH), 7.01-6.91 (m, 5H, phenyl CH), 6.63-6.62 (d, J = 4 Hz, 2H, β-pyrrolyl CH), 5.81-5.80 (d, J = 4Hz, 2H, β-pyrrolyl CH), 4.58 (s, 2H, ferrocenyl CH), 3.89 (s, 2H, ferrocenyl CH), 3.85 (s, 3H, methoxy CH), 3.82 (s, 2H, ferrocenyl CH), 2.86 (s, 2H, ferrocenyl CH). UV-Vis ($CHCl_3$): λ_{max}/nm ($\varepsilon/M^{-1}cm^{-1}$) = 464.5 (33000). FAB mass (m/z) : Calcd for $C_{52}H_{40}FeN_2O$: 764.25; Found : 764.67 (100%, M^+).

Synthesis of 29:

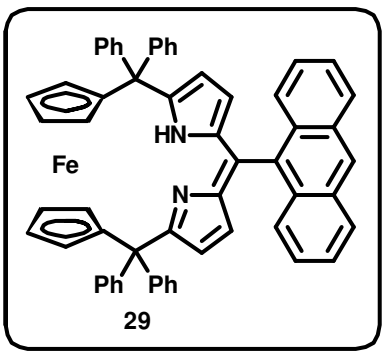

29

The above procedure was followed by using 9-anthraldehyde (0.62 g, 0.3 mmol). The crude product was purified by silica gel column chromatography (100 – 200 mesh) and the red fraction eluted with CH_2Cl_2 : petroleum

ether (20 : 80) was identified as **29**. Yield = 0.07 g, 19%. ^{1}H NMR (300 MHz, $CDCl_3$, 298 K): δ = 16.41 (brs, 1H, pyrrolyl NH), 8.55 (s, 1H, phenyl CH), 8.17-8.05 (m, 4H, phenyl CH), 7.48-7.39 (m, 14H, phenyl CH), 7.14-7.12 (m, 6H, phenyl CH), 6.96-6.93 (m, 4H, phenyl CH), 5.98-5.97 (d, J = 4 Hz, 2H, *β*-pyrrolyl CH), 5.69-5.67 (d, J = 4 Hz, 2H, *β*-pyrrolyl CH), 4.76 (s, 2H, ferrocenyl CH), 4.01 (s, 2H, ferrocenyl CH), 3.90 (s, 2H, ferrocenyl CH), 3.02 (s, 2H, ferrocenyl CH); UV-Vis ($CHCl_3$): λ_{max}/nm (ε/$M^{-1}cm^{-1}$) = 474.5 (190000), 386 (94000), 366.5 (95700), 348.5 (71000), 332 (49700); FAB mass (m/z): Calcd for $C_{59}H_{42}FeN_2$: 834.23; Found : 834.08 (100%, M^+).

Synthesis of 30:

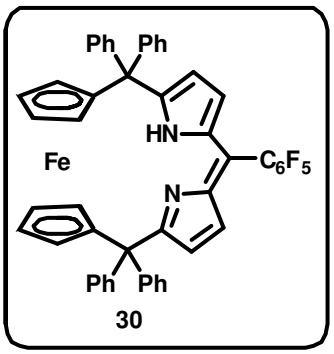

30

The above procedure was followed by using pentafluorobenzaldehyde (0.04 mL, 0.31 mmol). The crude product was purified by silica gel column chromatography (100 – 200 mesh) and the red fraction eluted with CH_2Cl_2 : petroleum ether (30 : 70) was identified as **30**. Yield = 0.047 g, 19%. ^{1}H NMR (300 MHz, $CDCl_3$, 298 K) : δ = 16.03 (brs, 1H, pyrrolyl NH), 7.4-7.37 (m, 11H, phenyl CH), 7.17-7.16 (d, J = 3.13 Hz, 5H, phenyl CH), 6.95-6.91 (m, 4H, phenyl CH), 6.43-6.42 (d, J = 4 Hz, 2H, *β*-pyrrolyl CH), 5.88-5.86 (d, J = 4 Hz, 2H, *β*-pyrrolyl CH), 4.58 (s, 2H, ferrocenyl CH), 3.97 (s, 2H, ferrocenyl CH), 3.85 (s, 2H, ferrocenyl CH), 2.94 (s, 2H, ferrocenyl CH); λ_{max}/nm (ε/$M^{-1}cm^{-1}$) = 480 (49000); FAB mass (m/z) : Calcd for $C_{51}H_{33}F_5FeN_2$: 824.19; Found : 824.86 (100%, M^+).

Synthesis of 31:

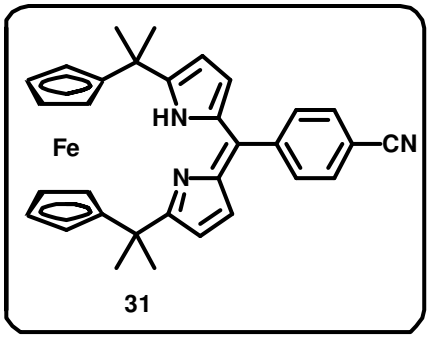

31

The above procedure was followed by using 1,1'-bis(dimethylpyrrolylmethyl)ferrocene (**23**) (0.2 g, 0.5 mmol) and 4-cyanobenzaldehyde (0.066 g, 0.5 mmol). The crude product was purified by silica gel column chromatography (100 – 200 mesh) and the red fraction eluted with CH_2Cl_2 : petroleum ether (30 : 70) was identified as **31**. Yield = 0.045 g, 17.5%. ^{1}H NMR (300 MHz, $CDCl_3$, 298 K) : δ = 15.61 (brs, 1H, pyrrolyl NH), 8.25-8.23 (m, 2H, phenyl CH), 8.09-8.01 (m, 2H, phenyl CH), 6.68-6.66 (d, J = 3.92 Hz, 2H, *β*-pyrrolyl CH), 6.39-6.35 (d, J = 4 Hz, 2H, *β*-pyrrolyl CH), 4.22 (s, 8H, ferrocenyl CH), 1.57 (s, 12H, methyl CH); UV-Vis ($CHCl_3$): λ_{max}/nm (ε/$M^{-1}cm^{-1}$) = 481.5 (16500); FAB mass (m/z) : Calcd for $C_{32}H_{29}FeN_3$: 511.17; Found : 511.68 (100%, M^+).

Synthesis of 32 and 38:

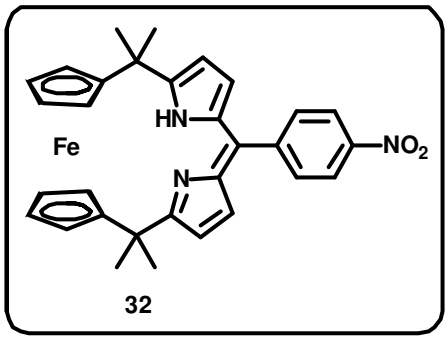

32

The above procedure was followed by using 4-nitro benzaldehyde (0.076 g, 0.5 mmol). The crude product was purified by silica gel column chromatography (100 – 200 mesh) and the red fraction eluted with CH_2Cl_2 : petroleum ether (20 : 80) was identified as **32**. Yield = 0.05 g, 18%. ^{1}H NMR (300 MHz, $CDCl_3$, 298 K) : δ = 15.71 (brs, 1H, pyrrolyl NH), 8.35-8.32 (d, J = 8.68 Hz, 2H, phenyl CH), 7.81-7.78 (d, J = 8.67 Hz, 2H, phenyl CH), 6.54-6.53 (d, J = 4 Hz, 2H, *β*-pyrrolyl CH), 6.34-6.33 (d, J = 4 Hz, 2H, *β*-pyrrolyl CH), 4.29 (s, 8H, ferrocenyl CH), 1.55 (s, 12H, methyl CH); λ_{max}/nm (ε/$M^{-1}cm^{-1}$) = 483.5 (16800); FAB mass (m/z) : Calcd for $C_{31}H_{29}FeN_3O_2$: 531.16; Found : 532.37 (100%, M + 1^+).

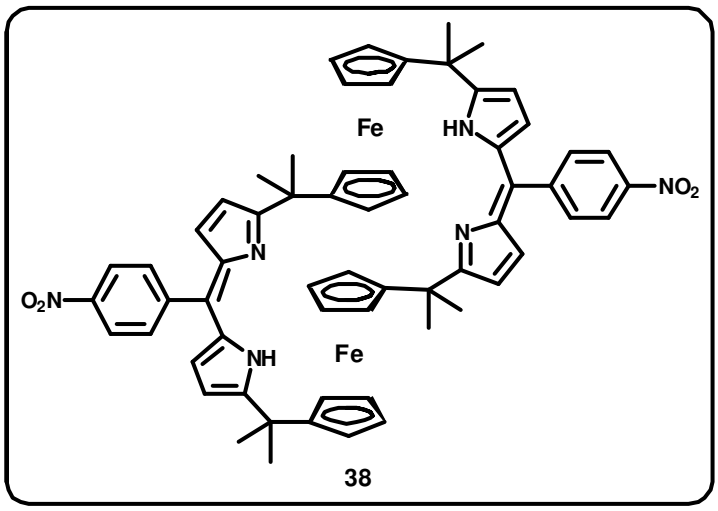

38

The second red fraction eluted with CH_2Cl_2 : petroleum ether (40 : 60) was identified as **38** in 4% yield. ^{1}H NMR (300 MHz, $CDCl_3$, 298 K) : δ = 12.74 (brs, 2H, pyrrolyl NH), 8.25-8.23 (d, J = 8.63 Hz, 4H, phenyl CH), 7.59-7.54 (m, 4H, phenyl CH), 6.28 (s, 8H, *β*-pyrrolyl CH), 4.18 (s, 10H, ferrocenyl CH), 3.98 (s, 6H, ferrocenyl CH), 1.75 (s, 12H, methyl CH), 1.57 (s, 12H, methyl CH); λ_{max}/nm (ε/$M^{-1}cm^{-1}$) = 450 (39900); FAB mass (m/z) : Calcd for $C_{62}H_{58}Fe_2N_6O_4$: 1062.32; Found : 1062.80 (80%, M^+).

Synthesis of 33:

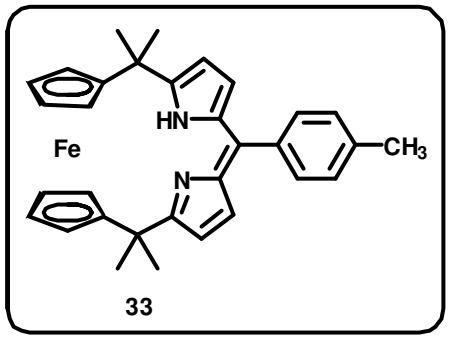

33

The above procedure was followed by using *p*-tolualdehyde (0.06 mL, 0.5 mmol). The crude product was purified by silica gel column chromatography (100 – 200 mesh) and the red fraction eluted with CH_2Cl_2 : petroleum ether (15 : 85) was identified as **33**. Yield = 0.05 g, 18%. ^{1}H NMR (300 MHz, $CDCl_3$, 298 K) : δ = 15.83 (brs, 1H, pyrrolyl NH), 7.5-7.49 (m, 2H, phenyl CH), 7.39-7.36 (m, 2H, phenyl CH), 6.49-6.46 (d, J = 4 Hz, 2H, *β*-pyrrolyl CH), 6.38-6.37 (d, J = 4 Hz, 2H, *β*-pyrrolyl CH), 4.31 (s, 8H, ferrocenyl CH), 2.39 (s, 3H, methyl CH) 1.61 (s, 12H, methyl CH); λ_{max}/nm (ε/$M^{-1}cm^{-1}$) = 481.5 (15300); FAB mass (m/z) : Calcd for $C_{32}H_{32}FeN_2$: 500.19; Found : 502.19 (100%, M + 2^+).

Synthesis of 34:

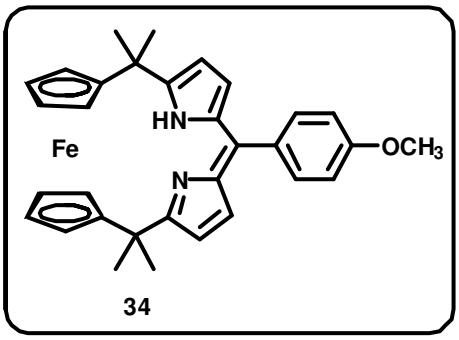

34

The above procedure was followed by using *p*-methoxybenzaldehyde (0.06 mL, 0.5 mmol). The crude product was purified by silica gel column chromatography (100 – 200 mesh) and the red fraction eluted with CH_2Cl_2 : petroleum ether (15 : 85) was identified as **34**. Yield = 0.044 g, 16.5%. ^{1}H NMR (300 MHz, $CDCl_3$, 298 K): δ = 15.77 (brs, 1H, pyrrolyl NH), 7.39-7.36 (m, 2H, phenyl CH), 7.27-7.24 (m, 2H, phenyl CH), 6.59-6.57 (d, J = 4 Hz, 2H, β-pyrrolyl CH), 6.41-6.38 (d, J = 4Hz, 2H, β-pyrrolyl CH), 4.21 (s, 8H, ferrocenyl CH), 3.76 (s, 3H, methoxy CH), 1.63 (s, 12H, methyl CH); UV-Vis ($CHCl_3$): λ_{max}/nm (ε/$M^{-1}cm^{-1}$) = 478.5 (15600); FAB mass (m/z) : Calcd for $C_{32}H_{32}FeN_2O$: 516.19; Found : 516.56 (100%, M^+).

Synthesis of 35:

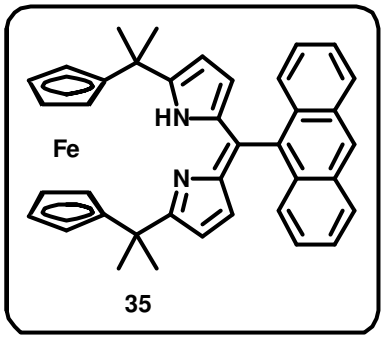

35

The above procedure was followed by using 9-anthraldehyde (0.1 g, 0.5 mmol). The crude product was purified by silica gel column chromatography (100 – 200 mesh) and the red fraction eluted with CH_2Cl_2 : petroleum ether (20 : 80) was identified as **35**. Yield = 0.07 g, 17%. ^{1}H NMR (500 MHz, $CDCl_3$, 298 K): δ = 16.08 (brs, 1H, pyrrolyl NH), 8.57 (s, 1H, phenyl CH), 8.09-8.05 (t, 4H, phenyl CH), 7.5-7.42 (m, 4H, phenyl CH), 6.14-6.13 (d, J = 4 Hz, 2H, β-pyrrolyl CH), 6.03-6.02 (d, J = 4 Hz, 2H, β-pyrrolyl CH), 4.36 (s, 8H, ferrocenyl CH), 1.59 (s, 12H, methyl CH); UV/Vis ($CHCl_3$): λ_{max}/nm (ε/$M^{-1}cm^{-1}$) = 468.5 (33000), 386 (17300), 366.5 (17700), 348.5 (13000), 332.5 (8600); FAB mass (m/z): Calcd for $C_{39}H_{34}FeN_2$: 586.21; Found : 586.55 (62.5%, M^+).

Synthesis of 36 and 39:

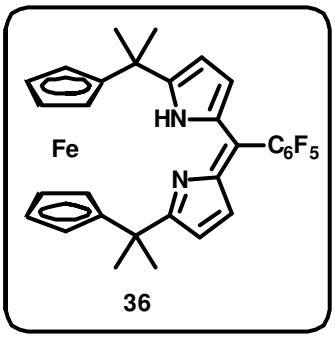

36

The above procedure was followed by using pentafluorobenzaldehyde (0.07 mL, 0.5 mmol). The crude product was purified by silica gel column chromatography (100 – 200 mesh) and the red fraction eluted with CH_2Cl_2 : petroleum ether (20 : 80) was identified as **36**. Yield = 0.047 g, 16%. ^{1}H NMR (500 MHz, $CDCl_3$, 298K): δ = 15.65 (brs, 1H, pyrrolyl NH), 6.46-6.45 (d, J = 4 Hz, 2H, *β*-pyrrolyl CH), 6.3-6.29 (m, 2H, *β*-pyrrolyl CH), 4.28 (s, 8H, ferrocenyl CH), 1.55 (s, 12H, methyl CH); UV-Vis (CH_2Cl_2): λ_{max}/nm (ε/$M^{-1}cm^{-1}$) = 473 (22000); FAB mass (m/z) : Calcd for $C_{31}H_{25}F_5FeN_2$: 576.13; Found : 576.49 (100%, M^+).

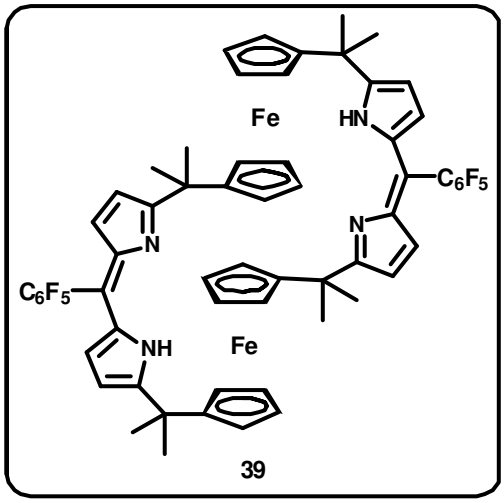

39

The second red fraction eluted with CH_2Cl_2 : petroleum ether (40 : 60) was identified as **39** in 4% yield. ^{1}H NMR (500 MHz, $CDCl_3$, 298K): δ = 12.33 (brs, 2H, pyrrolyl NH), 6.2 (s, 8H, *β*-pyrrolyl CH), 4.07 (t, 8H, ferrocenyl CH), 3.9 (t, 8H, ferrocenyl CH), 1.64 (s, 24H, methyl CH); UV-Vis (CH_2Cl_2): λ_{max}/nm (ε/$M^{-1}cm^{-1}$) = 441 (21000); FAB mass (m/z) : Calcd for $C_{62}H_{50}F_{10}Fe_2N_4$: 1152.26; Found : 1151.57 (80%, M^+).

Synthesis of 37 and 40:

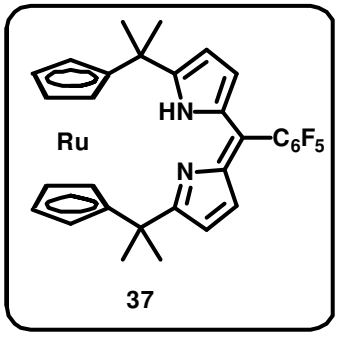

37

The above procedure was followed by using 1,1'-bis(dimethylpyrrolylmethyl)ruthenocene (**24**) (0.3 g, 0.45 mmol) and pentafluorobenzaldehyde (0.05 mL, 0.45 mmol). The crude product was purified by silica gel column chromatography

(100 – 200 mesh) and the red fraction eluted with CH_2Cl_2 : petroleum ether (20 : 80) was identified as **37**. Yield = 0.047 g, 16.4%. ^{1}H NMR (300 MHz, $CDCl_3$, 298 K) : δ = 15.62 (brs, 1H, pyrrolyl NH), 6.4-6.38 (d, J = 4 Hz, 2H, *β*-pyrrolyl CH), 6.26-6.24 (d, J = 4 Hz, 2H, *β*-pyrrolyl CH), 4.27 (s, 8H, ferrocenyl CH), 1.65 (s, 12H, methyl CH); λ_{max}/nm (ε/$M^{-1}cm^{-1}$) = 473 (28000); FAB mass (m/z) = Calcd for $C_{31}H_{25}F_5RuN_2$ = 622.09; Observed = 622.44 (100%, M^+).

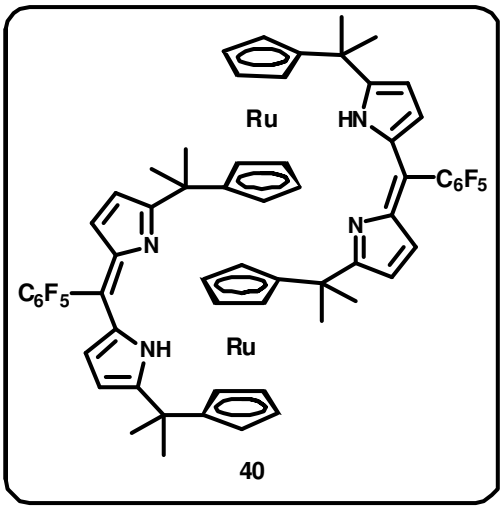

40

The second red fraction eluted with CH_2Cl_2 : petroleum ether (40 : 60) was identified as **40**. Yield = 0.02 g, 4%. ^{1}H NMR (300 MHz, $CDCl_3$, 298 K) : δ = 12.34 (brs, 2H, pyrrolyl NH), 6.29-6.27 (t, 8H, *β*-pyrrolyl CH), 4.6 (t, 8H, ferrocenyl CH), 4.35-4.34 (t, 8H, ferrocenyl CH), 1.62 (s, 24H, methyl CH); λ_{max}/nm (ε/$M^{-1}cm^{-1}$) = 447 (25000); FAB mass (m/z) = Calcd for $C_{62}H_{50}F_{10}Ru_2N_4$ = 1244.19; Observed = 1244.48 (80%, M^+).

4.9 Crystal Data

Table 4.1. Crystallographic data for **25, 26** and **27**

Parameters	**25**	**26**	**27**
Solvent of crystallization	$CHCl_3$/Heptane	$CHCl_3$/Heptane	$CHCl_3$/Heptane
Empirical formula	$C_{52}H_{37}FeN_3$	$C_{59}H_{54}Cl_3FeN_3O_2$	$C_{52}H_{40}FeN_2$
M_w	759.70	999.25	748.71
T [K]	100(2)	293(2)	100(2)
λ [Å]	0.71073	0.71073	0.71073
Crystal system	Monoclinic	Monoclinic	Monoclinic
Space group	P21/c	P21/n	P21/n
a[Å]	18.3257(17)	10.8374(12)	16.4365(15)
b[Å]	15.9064(15)	25.707(3)	9.8425(9)
c[Å]	12.7614(11)	18.728(2)	23.296(2)
α [˚]	90.00	90.00	90.00
β [˚]	93.401(2)	105.443(3)	91.443(2)
γ [˚]	90.00	90.00	90.00
V[Å^3]	3713.3(6)	5029.2(9)	3767.5(6)
Z, ρ_{calcd}[Mg m^{-3}]	4, 1.359	4, 1.320	4, 1.320
μ ($Mo_{K\alpha}$) [mm^{-1}]	0.449	0.506	0.441
F (000)	1584	2088	1568
Crystal size [mm]	0.40 × 0.24 × 0.14	0.30 × 0.20 × 0.20	0.42 × 0.32 × 0.19
θ range for data collection [˚]	1.70 to 25.00	1.94 to 25.00	1.50 to 28.26
Limiting indices	-21≤ h ≤ 16, -18 ≤ k ≤ 18, -11 ≤ l ≤15	-10 ≤ h ≤ 12 -30 ≤ k ≤ 30 -22 ≤ l ≤ 21	-21 ≤ h ≤ 21, -12 ≤ k ≤ 13, -30 ≤ l ≤ 30
Reflections collected	18392	46958	31454
Refinement method	Full-matrix least-squares on F^2	Full-matrix least-squares on F^2	Full-matrix least-squares on F^2
Data / restraints / parameters	6524 / 0 / 505	8846 / 0 / 618	8910 / 0 / 501
Goodness-of- fit on F^2	1.131	1.069	1.129
Final R indices[I>2σ(I)]	R1 = 0.0694, wR2 = 0.1286	R1 = 0.0716, wR2 = 0.2079	R1 = 0.0642, wR2 = 0.1305
R indices (all data)	R1 = 0.0942, wR2 = 0.1379	R1 = 0.0889, wR2 = 0.2236	R1 = 0.0841, wR2 = 0.1383
Largest Δρ [e Å^{-3}]	0.612 and -0.447	0.774 and -0.952	0.588 and -0.545

Table 4.1. Crystallographic data for **29** and **36**

Parameters	**29**	**36**
Solvent of crystallization	$CHCl_3$/Heptane	$CHCl_3$/Heptane
Empirical formula	$C_{59}H_{41}FeN_2$	$C_{31}H_{25}F_5FeN_2$
M_w	833.79	576.38
T [K]	100(2)	293(2)
λ [Å]	0.71073	0.71073
Crystal system	Triclinic	Monoclinic
Space group	P-1	P21/c
a[Å]	10.7256(16)	11.1820(2)
b[Å]	13.681(2)	10.4371(2)
c[Å]	17.613(2)	21.7536(4)
α [˚]	112.668(2)	90.00
β [˚]	93.344(3)	90.4690(10)
γ [˚]	105.922(2)	90.00
V[Å^3]	2253.8(5)	2538.73(8)
Z, ρ_{calcd}[Mg m^{-3}]	2, 1.229	4, 1.508
μ ($Mo_{K\alpha}$) [mm^{-1}]	0.376	0.655
F (000)	870	1184
Crystal size [mm]	0.35 × 0.20 × 0.15	0.30 × 0.20 × 0.20
θ range for data collection [˚]	1.65 to 25.00	1.82 to 30.25
Limiting indices	-12 ≤ h ≤ 12, -16 ≤ k ≤ 15, -20 ≤ l ≤ 20	-15 ≤ h ≤ 15 -14 ≤ k ≤ 14 -30 ≤ l ≤ 30
Reflections collected	16106	32605
Refinement method	Full-matrix least-squares on F^2	Full-matrix least-squares on F^2
Data / restraints / parameters	7866 / 0 / 560	7550 / 0 / 356
Goodness-of- fit on F^2	1.043	1.053
Final R indices[I>2σ(I)]	R1 = 0.0715, wR2 = 0.1830	R1 = 0.0391, wR2 = 0.1035
R indices (all data)	R1 = 0.0960, wR2 = 0.1944	R1 = 0.0625, wR2 = 0.1212
Largest Δρ[e Å^{-3}]	0.700 and -0.604	0.341 and -0.300

Table 4.1. Crystallographic data for **39** and **40**

Parameters	**39**	**40**
Solvent of crystallization	$CHCl_3$/Heptane	$CHCl_3$/Heptane
Empirical formula	$C_{62}H_{50}F_{10}Fe_2N_4$	$C_{62}H_{50}F_{10}N_4Ru_2$
M_w	1152.76	1243.20
T [K]	100(2)	100(2)
λ [Å]	0.71073	0.71073
Crystal system	Triclinic	Triclinic
Space group	P-1	P-1
a[Å]	11.0784(17)	11.2539(10)
b[Å]	11.4123(17)	11.5076(10)
c[Å]	12.3519(19)	12.2368(11)
α [˚]	117.468(2)	117.3260(10)
β [˚]	99.411(2)	99.1430(10)
γ [˚]	106.469(2)	107.6930(10)
V[Å^3]	1246.8(3)	1255.16(19)
Z, ρ_{calcd}[Mg m^{-3}]	1, 1.535	1, 1.629
μ ($Mo_{K\alpha}$) [mm^{-1}]	0.667	0.687
F (000)	592	628
Crystal size [mm]	0.30 × 0.22 × 0.12	0.60 × 0.50 × 0.45
θ range for data collection [˚]	1.98 to 28.26	2.27 to 26.28
Limiting indices	$-14 \le h \le 14$ $-15 \le k \le 14$ $-16 \le l \le 16$	$-12 \le h \le 12$ $-13 \le k \le 13$ $-13 \le l \le 13$
Reflections collected	10763	8098
Refinement method	Full-matrix least-squares on F^2	Full-matrix least-squares on F^2
Data / restraints / parameters	5645 / 0 / 360	3902 / 0 / 360
Goodness-of- fit on F^2	1.085	1.207
Final R indices[I>2σ(I)]	R1 = 0.0524, wR2 = 0.1162	R1 = 0.1092, wR2 = 0.2284
R indices (all data)	R1 = 0.0625, wR2 = 0.1210	R1 = 0.1162, wR2 = 0.2328
Largest $\Delta\rho$[e Å^{-3}]	0.809 and -0.339	2.924 and -4.493

Chapter 5

ansa-Metallocene-based core-modified *expanded* Calixpyrroles and Calixphyrins

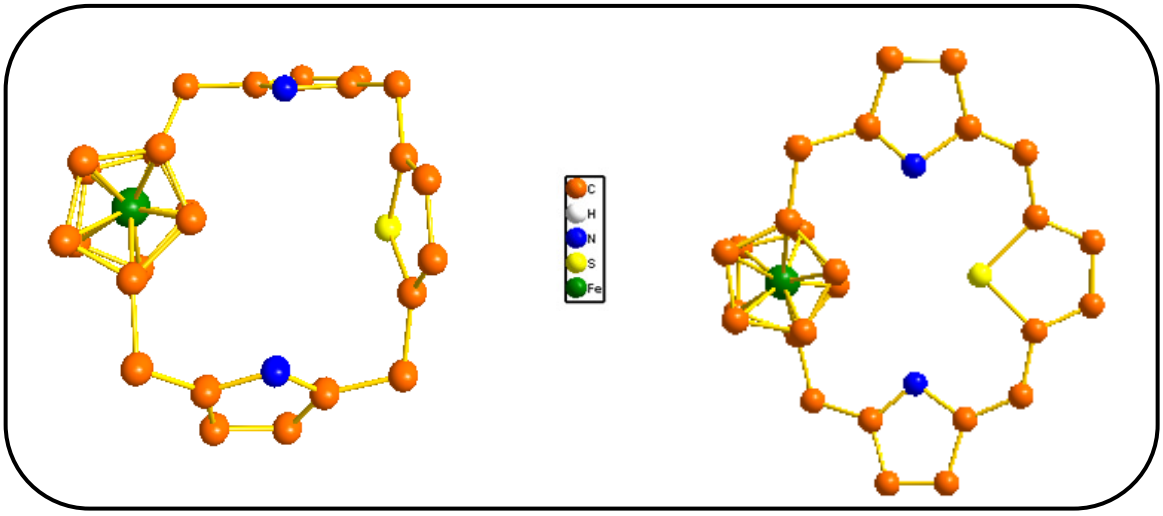

5.1 Abstract

As an one step extension of the previously reported ansa-metallocene-based normal calixpyrroles and calixphyrins, we have incorporated thiophene/furan in the main framework of these macrocycles which results in the formation of ansa-metallocene based core-modified expanded calixpyrroles and calixphyrins i.e. ansa-metallocene-based calix[2]pyrrole[1]thiophene/furan and calix[2]phyrin[1]thiophene. So the present chapter deals with the syntheses, spectral and structural characterization of these macrocycles. Acid promoted dehydrative condensation of 1,1'-bis(dimethylpyrrolylmethyl)ferrocene with 2,5-bis(dimethylhydroxymethyl)thiophene yielded ansa ferrocene based calix[2]pyrrole[1]thiophene while the acid catalysed dehydrative condensation of 1,1'-bis(diphenylpyrrolylmethyl)ferrocene with 2,5-bis(hydroxyphenylmethyl)thiophene followed by DDQ oxidation yielded ansa-ferrocene- based calix[2]phyrin[1]thiophene. The newly synthesised ansa ferrocenyl macrocycles were characterized by FAB mass, UV- Vis, NMR spectral analyses and finally by single crystal X-ray structural analysis. All these studies clearly revealed the introduction of ferrocene in the main framework of the corresponding macrocycles in an ansa type way. It is worth noting that ansa-ferrocene-based calix[2]pyrrole[1]thiophene and calix[2]phyrin[1]thiophene adopts 1,3-alternate and curved staircase conformation respectively in the solid state. It is also clear that ansa-ferrocene-based calix[2]pyrrole[1]thiophene is highly non-planar where as ansa-ferrocene-based calix[2]phyrin[1]thiophene are partially planar systems. Due to the presence of ferrocene in the main frame work in an ansa type way, the above macrocycles are highly rigid in the solid state.

5.2 Introduction

5.2.1 *Expanded* calixpyrroles

Initial analyses of the reaction mixtures that were used to produce calix[4]pyrroles revealed some other products which were analysed and found to be *expanded* derivatives of calix[4]pyrrole systems i.e. these macrocycles contain more than four pyrrole rings in the main framework. Sessler and co-workers initially attempted a template based strategy [[b]Gale *et al*. 1997] by using *p-tert*-butylcalix[5]arene pentaketone both as reactant and template and thereby obtaining calix[5]arene-calix[5]pyrrole pseudo dimer **1** (Figure 5.1) in 10% yield. But they were unsuccessful in separating free calix[5]pyrrole.

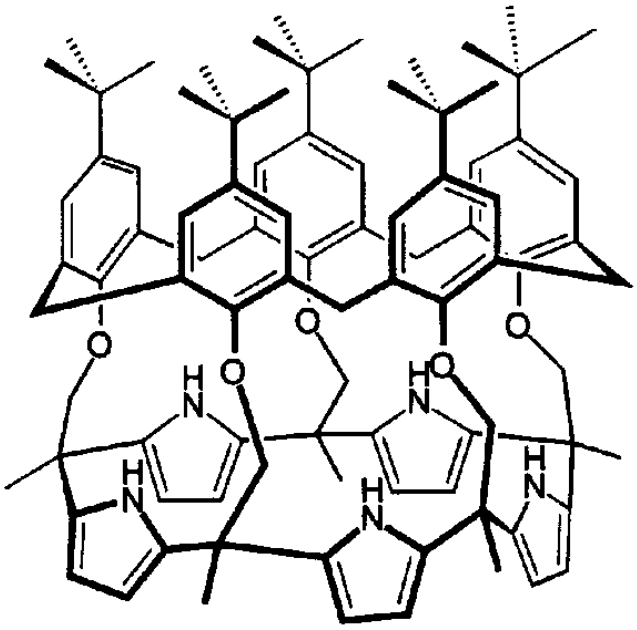

Figure 5.1. Calix[5]arenecalix[5]pyrrole pseudo dimer **1**

Later, Eichen and co-workers achieved the first synthesis of *expanded* calixpyrrole mainly calix[6]pyrroles **2** and **3** (Figure 5.2) which differ in their *meso* substituents [Turner *et al*. 1998]. They condensed diaryldi-(2-pyrrolyl)methanes with acetone using trifluoroacetic acid as the acid catalyst to yield **2** and **3** respectively. Single crystal X-ray

analysis revealed that **2** adopt an asymmetric cone like conformation and the three diphenylmethylene bridges point above the macrocyclic plane. They showed that these *expanded* calixpyrroles have binding modes to different substrates ranging from simple anions to aromatic derivatives. The axial *meso* phenyl groups form a genuine preorganized cavity and actively participate in binding with halogenated compounds [Turner *et al*. 2001, [a]Turner *et al*. 2002, [b]Turner *et al*. 2002].

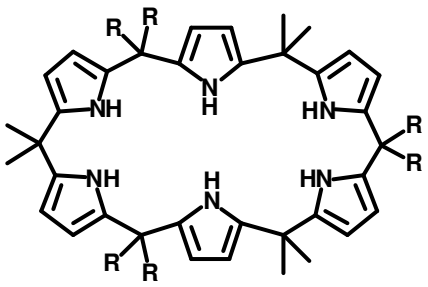

2. R = phenyl
3. R = 2-pyridyl

Figure 5.2. Calix[6]pyrroles **2** and **3**

Sessler and co-workers synthesized β-substituted calix[5]- **4** and calix[8]pyrroles **5** (Figure 5.3) by the methanesulphonic acid catalysed condensation of 3,4-difluoropyrrole as the starting material with acetone. In contrast to parent calix[4]pyrrole**, 4** and **5** showed enhanced affinities for various anionic substrates and also improved selectivities for phosphate and chloride ions. Analyses of these fluorinated calix[*n*]pyrroles revealed an increase in the relative affinity for higher halide ions with increasing macrocycle size [[c]Sessler *et al*. 2000, Levitskaia *et al*. 2003, [d]Sessler *et al*. 2005]. In another work, Kohnke and co-workers described the conversion of calix[6]furan to calix[6]pyrrole **6**, calix[3]furan[3]pyrrole **7** and calix[2]furan[4]pyrrole **8** (Figure 5.4) and studied the complexation of halide ions by these calix[6]pyrrole systems [[a]Cafeo *et al*. 2000, [b]Cafeo *et al*. 2000, [b]Cafeo *et al*. 2002, Bruno *et al*. 2007]. They also demonstrated the efficient binding of paraquat dichloride in organic solvents, as well as its extraction from water into CH_2Cl_2

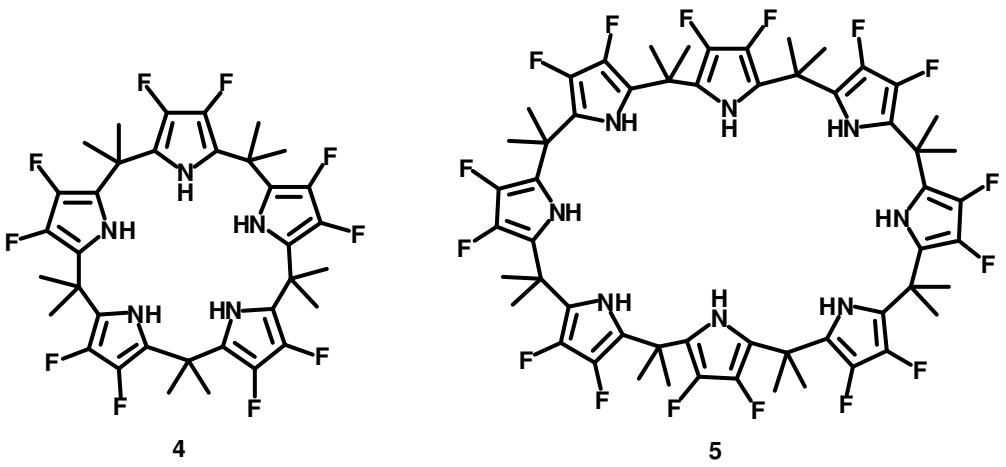

Figure 5.3. Calix[5]pyrrole **4** and calix[8]pyrrole **5**

by the use of cyclodextrin/calix[6]pyrrole binary host systems [[c]Cafeo *et al*. 2002]. Kohnke and co-workers obtained β-unsubstituted calix[5]pyrrole **9** (Figure 5.4) from the furan analogue via the homologation of the furan rings to pyrrole [[a]Cafeo *et al*. 2002].

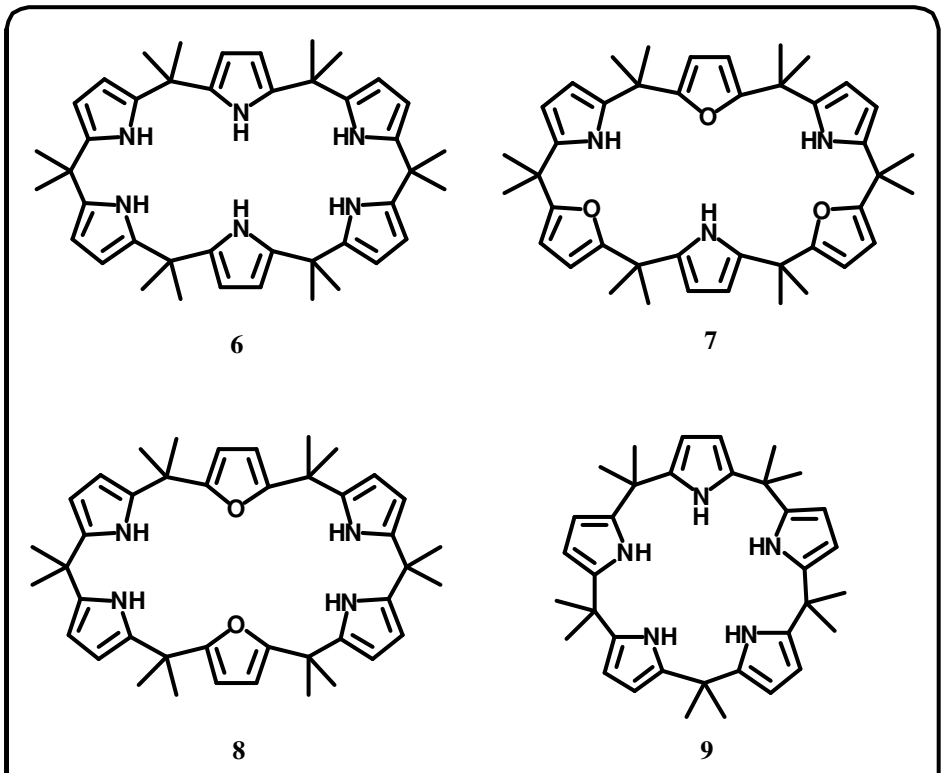

Figure 5.4. Calix[6] and [5]pyrroles and core-modified derivatives

Simultaneously, Lee and co-workers synthesized *meso*-alkylporphyrinogen-like cyclic oligomers "Calix[*n*]furano[*m*]pyrroles" by the "3 + 2" and "4 + 2" approaches [Nagarajan *et al*. 2000, Nagarajan *et al*. 2001]. They were also involved in the synthesis of calix[6]pyrrole capped with 1,3,5-trisubstituted benzene **10** (Figure 5.5) [Yoon *et al*. 2007]. The synthesis involved the acid-catalyzed cyclization of ester/ether-functionalized tripodal dipyrromethanes. The ^{1}H NMR anion binding studies of **10** indicated 1 : 1 binding with fluoride ion and also revealed that **10** becomes more symmetric upon binding with fluoride anion.

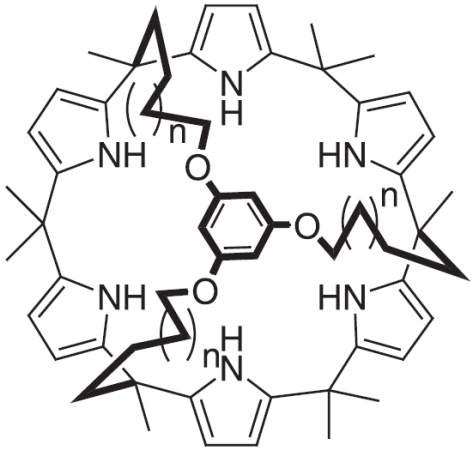

Figure 5.5. Calix[6]pyrrole capped with 1,3,5-trisubstituted benzene **10**

5.2.2 Thiophene based calixpyrroles

A large number of derivatives of calixpyrroles have been synthesized in which the pyrrole rings were substituted by thiophene **11** or furan **12** which resulted in the formation of hybrid calixpyrroles (Figure 5.6) [Jang *et al*. 2000, Nagarajan *et al*. 2000, Nagarajan *et al*. 2001, Lee *et al*. 2002, Song *et al*. 2004, [a]Sessler *et al*. 2005, Namor *et al*. 2006, [a]Namor *et al*. 2007, [b]Namor and Abbas 2007, Poulsen *et al*. 2007]. In addition to this, Sessler and co-workers were also successful in synthesizing calix[2]bipyrrole[2]thiophene **13** and

calix[2]bipyrrole[2]furan **14** (Figure 5.6) [[b]Sessler *et al*. 2003] respectively where they used bipyrrole as the starting material instead of pyrrole.

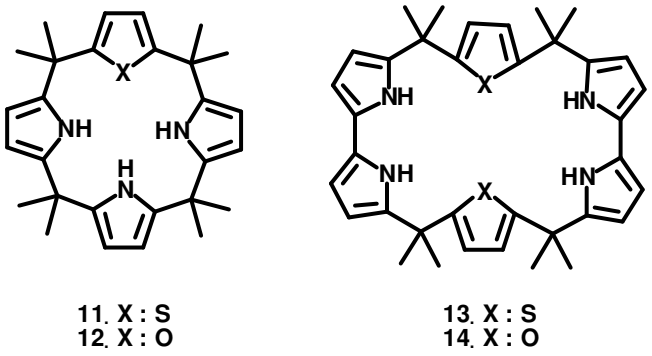

Figure 5.6. Thiophene and furan substituted calixpyrroles

5.2.3 *Expanded* calixphyrins

Calixphyrins which contain more than 4 pyrrole rings in the main frame work are generally regarded as *expanded* calixphyrins. Sessler and co-workers found that acid-catalysed condensation reaction of mesityldipyrrylmethane with acetone followed by DDQ oxidation resulted in not only the expected 5,15-disubstituted porphodimethene, but also the unprecedented higher-order calix[6]phyrin-(**1***.1*.**1***.1*.**1**.1) **15** and calix[8]phyrin-(**1***.1*.**1***.1*.**1***.1*.**1***.1*) **16** derivatives (Scheme 5.1) [Král *et al*. 2000]. *Expanded* calixphyrins are orange to red-yellow colored solids and have maximal UV/Vis absorption ranging from 400 to 440 nm. Single crystal X-ray diffraction studies revealed that these are highly non-planar systems and display regions of local planarity corresponding to dipyrrolylmethene links. Molecular modeling studies suggested that these might be fluxional in solution. As expected for a fully fluxional molecule, no significant broadening of any signals was seen in either the ^{1}H or ^{13}C NMR spectra of calix[8]phyrin **16** at room temperature. However at low temperature, fully resolved sharp signals were observed for this *expanded* calixphyrin.

In another report, Sessler and co-workers have done the synthesis of calix[6]phyrin-(**1***.1.1*.**1***.1.1*) **17** by condensing *gem*-dimethyl substituted tripyrrane with pentafluorobenzaldehyde followed by DDQ oxidation (Scheme 5.1) [Bucher *et al*. 2001,

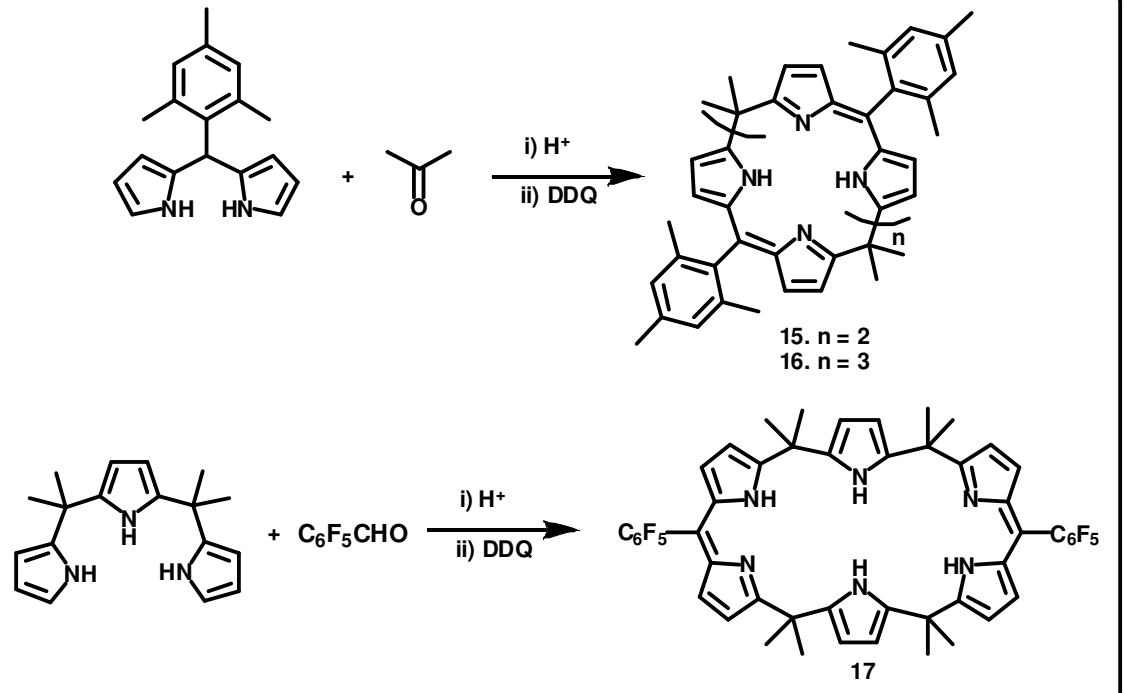

Scheme 5.1. Syntheses of *expanded* calixphyrins **15, 16, 17**

Chen and Liu 2008]. In addition to **17**, calix[9]phyrin, a higher derivative was also obtained. They observed that by using appropriate acyclic polypyrrolic precursors, it is possible to modify the ratio of oxidized to non-oxidized *meso*-like carbon atoms in higher order calix[*n*]phyrins as well as the distribution of these bridging centers within the macrocyclic skeleton. Initial attempts to react tripyrrane with benzaldehyde in the presence of various Brønsted or Lewis acids proved unproductive. Compound **17** displayed spectroscopic properties in accord with the proposed structure and was characterized by single crystal X-ray diffraction analysis.

Another type of *expanded* calixphyrins were reported by Osuka and co-workers in 2007 where they explained the synthesis of calix[3]dipyrrins in modest yields by a modified

Lindsey protocol in the presence of small amount of water [Inuoe *et al*. 2007]. Calix[3]dipyrrins have preorganized coordination sites that can accommodate three cations in a symmetric triangular fashion. Metallated calix[3]dipyrrin **18** (Figure 5.7) was obtained as a red colored side product during the TFA catalysed condensation of pyrrole and 4-methoxycarbonylbenzaldehyde followed by oxidation with DDQ, then subsequent metallation with [Ni(acac)$_2$]. The structure of this calix[3]dipyrrin was confirmed by the single crystal X-ray diffraction analysis which revealed a trimetallated calix[3]dipyrrin macrocycle consisting of three planar dipyrrin segments connected by aryl- and hydroxy-substituted methylene units. The three Ni(II) atoms are located at the apexes of an equilateral triangle and were bridged by three *m*-alkoxo oxygen atoms to form a Ni_3O_3 hexagonal core. Each Ni(II) atoms are coordinated by two pyrrolic N atoms.

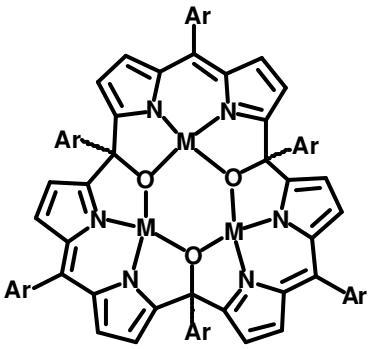

18

Figure 5.7. Metallated calix[3]dipyrrin **18**

In 2008, Furuta and co-workers reported the syntheses of new type of doubly N-confused calix[6]phyrin **19** and its metal complex **20** (Figure 5.8) which displayed phosphorescence in the near-IR region around 1000 nm [Won *et al*. 2008]. The explicit structural assignment, especially on the configurations of the confused pyrrole rings have come from the X-ray single-crystal diffraction analyses of free base **19** and its Pt^{II} complex (Figure 5.9), the arrangement of the confused pyrrole rings was verified to be NNNC,NNNC

for **19**. This macrocycle adopts a rooflike (L-shaped) conformation bending along the axis defined by the two sp^3-hybridized *meso*-carbon atoms. The roof angle of **19** is 103.88˚. In contrast, **20** displayed ruffled molecular structures. The distance between two Pt metals is 3.86 Å. Direct interactions between the Pt metals are, thus, not expected.

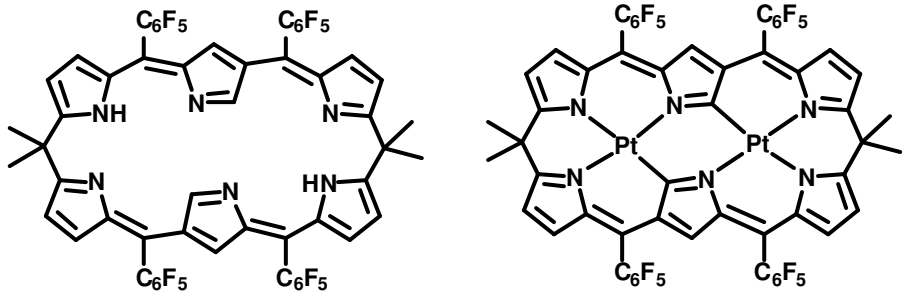

Figure 5.8. N-Confused calix[6]phyrin **19** and its metal complex **20**

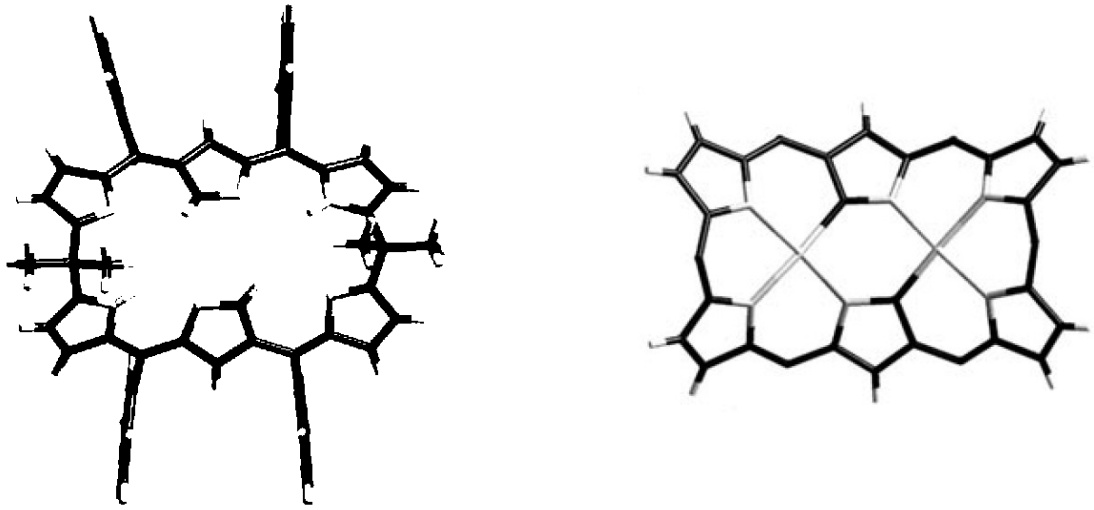

Figure 5.9. Single crystal X-ray structures of **19** and **20**

5.2.4 Thiophene based calixphyrins

Matano and co-workers reported the synthesis, structural, optical and electrochemical properties of thiophene-containing hybrid calixphyrin **21** (Figure 5.10) [[b]Matano *et al.* 2008] and its Zinc complex [Matano *et al*. 2010].

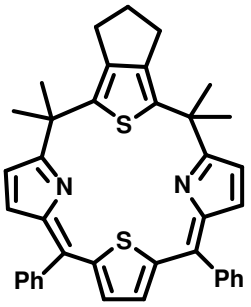

21

Figure 5.10. Thiophene based calixphyrin

5.3 Objective of our work

In the third and fourth chapters, we have explained the syntheses, spectral and single crystal X-ray structural analyses of *ansa*-Metallocene based *normal* Calixpyrroles [Ramakrishnan and Srinivasan 2007] and *ansa*-Metallocene based *normal* Calixphyrins [Ramakrishnan *et al*. 2010]. These type of macrocycles contain one ferrocene and two pyrroles in the mainframe work joined by either sp^3 hybridized or sp^2 or both hybridized *meso* carbons. As a one step expansion of these kind of macrocycles, we incorporated another heterocyclic ring mainly thiophene and furan in the main frame work which resulted in the formation of *ansa*-ferrocene-based *expanded* calixpyrroles i.e. *ansa*-ferrocene-based calix[2]pyrrole[1]thiophene/furan and *ansa*-ferrocene based *expanded* calixphyrins i.e. *ansa*-ferrocene-based calix[2]phyrin[1]thiophene (Figure 5.11). So, this chapter is dealt with syntheses, spectral and single crystal X-ray structural analyses of these *ansa*-ferrocene-based *expanded* calixpyrroles and calixphyrins.

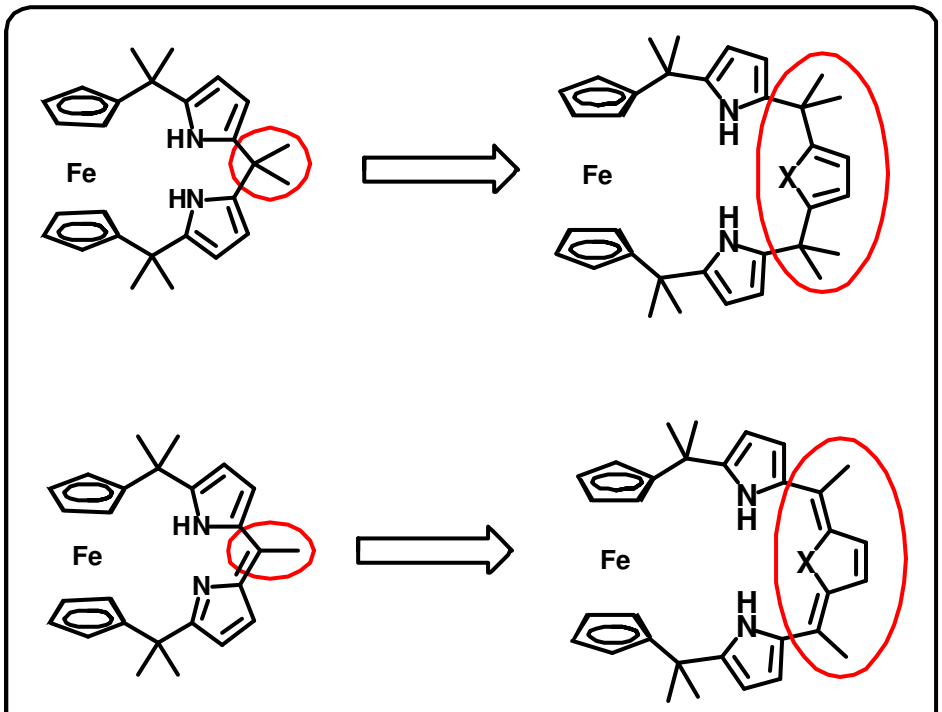

Figure 5.11. *ansa*-metallocene based core-modified *expanded* calixpyrroles and calixphyrins

5.4 Results and Discussion

5.4.1 Syntheses, Spectral and Structural Analyses of *ansa*-ferrocene-based core-modified *expanded* calixpyrrole

The syntheses of *ansa*-ferrocene-based *expanded* calixpyrrole i.e. *ansa*-ferrocene-based "calix[2]pyrrole[1]thiophene **22** and calix[2]pyrrole[1]furan **23**" is depicted in Scheme 5.2. The Scheme utilizes trifluoroacetic acid catalysed condensation of **24** [Ramakrishnan and Srinivasan 2007] with **25** and **26** [Chadwick and Willbe 1977] in CH_2Cl_2 followed by column chromatographic separation resulted in stable yellow colored macrocycles **22** and **23** in 26- 28% yield, respectively. The above macrocycles are soluble in almost all the organic solvents like CH_2Cl_2, $CHCl_3$, CH_3CN etc.

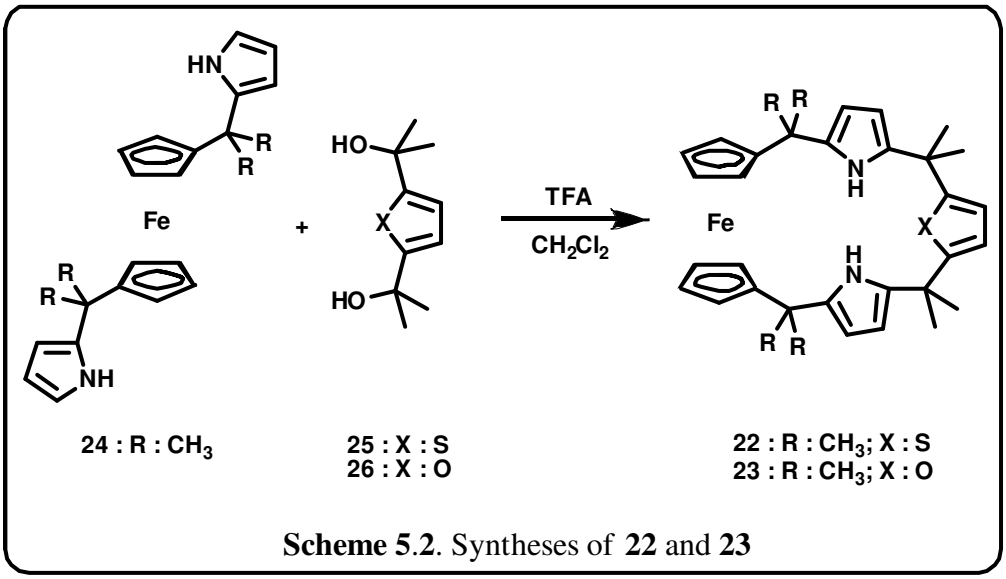

Scheme 5.2. Syntheses of **22** and **23**

The FAB mass spectral analyses of **22** and **23** shows the right molecular ion signals at 564.87 and 548.60 which clearly prove the exact composition of the macrocycles. The ^{1}H NMR analyses of the macrocycles **22** (Figure 5.12) and **23** (Figure 5.13) shows the presence of NH proton as a broad singlet at 8.21 and 8.36 ppm respectively which were clearly confirmed by D_2O exchange experiments. The thiophene β-CH protons of **22** are observed as singlet at 6.78 ppm while the furan β-CH protons in **23** resonated as a singlet at 6.05 ppm. The pyrrolic β-CH protons of **22** are resonated as two multiplets at 5.97 and 5.86 ppm, while for that of **23**, pyrrolic β-CH protons are observed as a doublet at 5.96 ppm. Due to the heteroatom effect, the ferrocenyl CH protons of **22** and **23** split into two different sets and resonated as a multiplet and singlet at 4.19-3.97 and 3.35 ppm. The *meso*-methyl units of **22** and **23** are observed between 1.73 & 1.26 ppm; 2.15 & 1.65 ppm respectively. Further, the absence of the two α–CH protons in the pyrrolic rings in **24** at 6.48 ppm supports the formation of the macrocycle. Overall, introduction of the heteroaromatics like thiophene and furan, in the *ansa*-ferrocenyl based calixpyrroles leads to the downfield shift of the NH protons, while the ferrocenyl CH protons are resonated as a multiplet in furan incorporated

macrocycle and split into multiplet as well as singlet in the thiophene incorporated macrocycle.

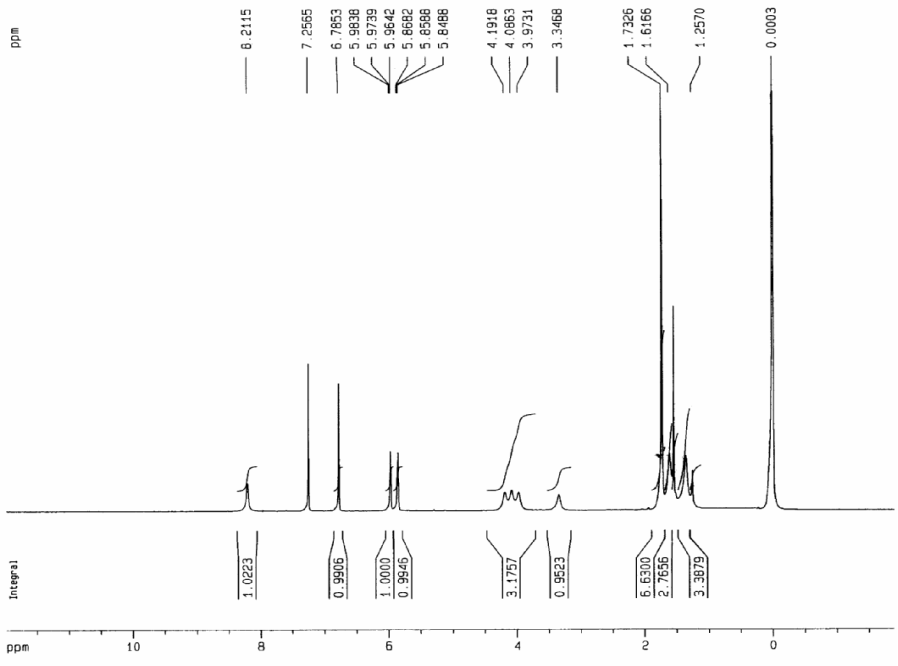

Figure 5.12. ^{1}H NMR spectrum of **22** in $CDCl_3$

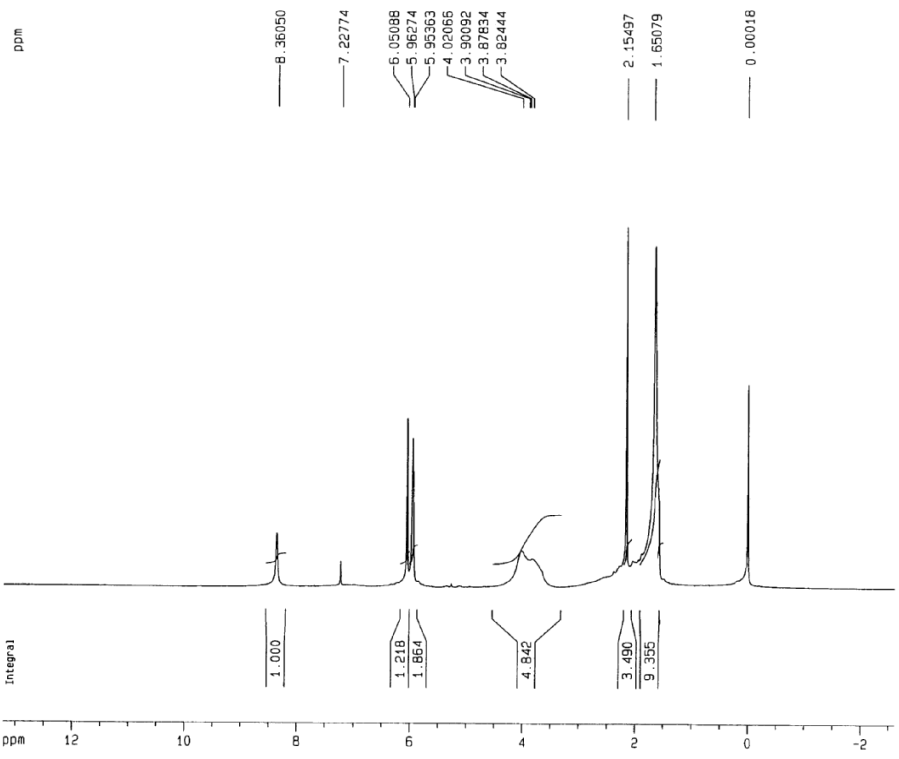

Figure 5.13. ^{1}H NMR spectrum of **23** in $CDCl_3$

The final confirmation of **22** has come from single crystal X-ray structural analysis (Table 5.1) which is shown in Figure 5.14. Good quality X-ray crystals of **22** were grown by slow diffusion of heptane into its $CHCl_3$ solution. As predicted from the above observations, the crystal structure of **22** contains one ferrocene unit, two pyrrole units, one thiophene unit and four *meso* sp^3 hybridized carbons each containing two methyl groups. It is clear that two pyrrole units are connected to 1 and 1' position of ferrocene by two sp^3 hybridized *meso* carbons. It is worth noting that the above macrocycle adopts 1,3-alternate conformation in the solid state as in the parent calix[4]pyrrole [Wu *et al*. 2001]. In fact, recent theoretical studies have shown that octaalkylcalix[4]pyrroles are conformationally flexible molecules. But due to the presence of ferrocene in the main frame work of *ansa* calixpyrrole, **22** is highly rigid in the solid state.

a) b)

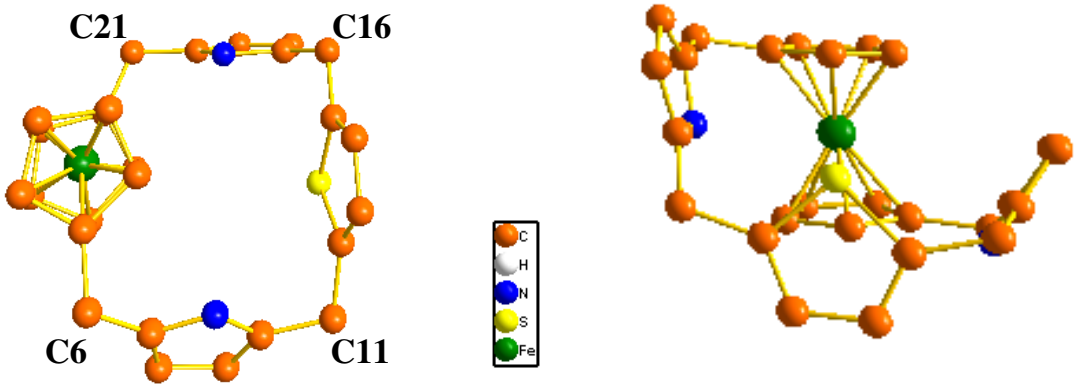

Figure 5.14. Single crystal X-ray structure of **22**. a) top view, b) side view. *meso* methyl groups and all the hydrogens are omitted for clarity.

The two alternate pyrroles are situated in a head-on manner with an N–N distance of 5.61 Å and with a dihedral angle of 44.15˚ indicating that both are nearly coplanar. From the side view (Figure 5.14b), it is clear that since two pyrroles are attached to 1 and 1' position of ferrocene, one pyrrole unit lies in a plane above than the other. The resulting structure

thus bears direct analogy as in the case of parent calix[4]pyrrole. The distance between C6 and C11 is 4.99 Å, C11 and C16 is 5.41 Å, C16 and C21 is 4.99 Å, C6 and C21 is 6.46 Å (Figure 5.14a). From these values it is clear that the presence of ferrocene or thiophene other than pyrrole in the main framework increases the distance between the *meso* carbons. The crystal structure also resembles the structural behavior of calix[2]benzene[2]pyrrole [Sessler *et al*. 2002]. The dihedral angle between two cyclopentadienyl rings and the corresponding pyrrolic units in **22** are 54.5˚ and 78.4˚ respectively, pyrrolic and thiophene moiety is 87.7˚, thiophene and pyrrolic plane is 83.61˚. Another interesting observation is that the dihedral angle between the two opposite pyrrolic planes in **22** is 44.15˚ which is entirely different from the dihedral angle between the two opposite pyrrolic planes in calix[4]pyrrole and calix[2]benzene[2]pyrrole in which the corresponding angles are approximately 90˚. The distance between the two opposite pyrrolic π-clouds is 6.46 Å.

5.4.2 Syntheses, Spectral and Structural Analyses of *ansa*-ferrocene-based core-modified *expanded* calixphyrin

As a one step expansion of the *ansa*-ferrocene-based *normal* calix[2]phyrins, we also concentrated in introducing another heterocyclic ring namely thiophene in the main frame work of these macrocycles which resulted in the formation of *ansa*-ferrocene-based *expanded* calixphyrin i.e. *ansa*-ferrocene-based calix[2]phyrin[1]thiophene. The synthesis of *ansa*-ferrocene-based calix[2]phyrin[1]thiophene **27** is demonstrated in Scheme 5.3. The above macrocycle is obtained by the trifluoroacetic acid catalysed condensation of **28** with **29** in CH_2Cl_2 followed by 2,3-dichloro-5,6-dicyano-*p*-benzoquinone (DDQ) oxidation resulted in stable red colored macrocycle **27** in quantitative yields. The above macrocycle is soluble in almost all the organic solvents like CH_2Cl_2, $CHCl_3$, CH_3CN etc.

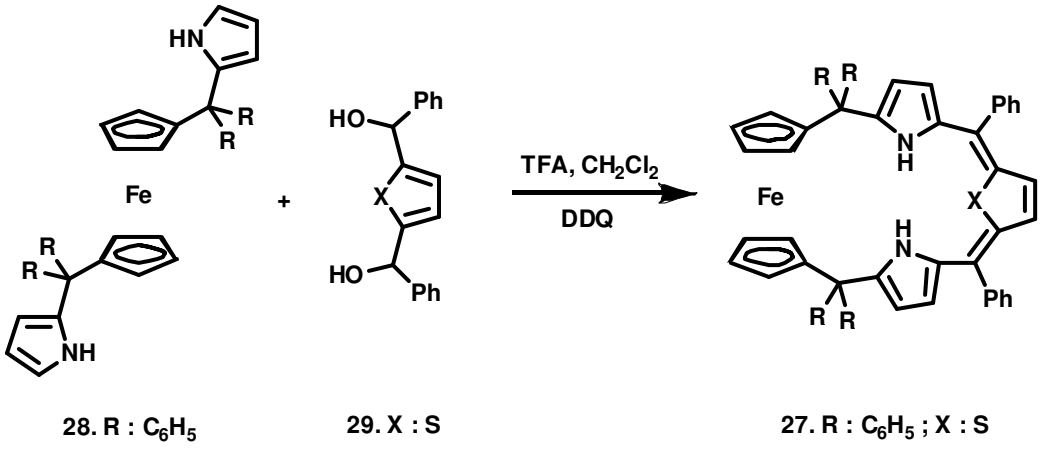

Scheme 5.3. Synthesis of **27**

The FAB mass spectral analysis of **27** shows the molecular ion signal at 906.68 which clearly proves the exact composition. The ^{1}H NMR spectra of **27** were recorded in $CDCl_3$ at room temperature. The *β*-pyrrolic CH protons of the macrocycle **27** resonated as two doublets between 6.78-6.77 and 6.64-6.63 ppm. The *β*-thiophene CH protons appeared as a singlet at 6.74 ppm. The six ferrocenyl protons of macrocycle **27** resonated as a set of three singlets at 5.86, 4.14 and 3.01 ppm while the remaining two protons appeared as a doublet at 3.66 ppm.

The UV-Vis spectral characteristics of the macrocycle **27** were turned out to be generally comparable to those of calix[n]phyrin type macrocycles. In the electronic spectral analysis of the macrocycle **27** in $CHCl_3$, broad absorption maximum which were originated due to $\pi \rightarrow \pi^*$ transitions in the dipyrrin moiety were observed at 494 and 521 nm (Figure 5.15) respectively with molar extinction coefficient values of 38000 and 41000 $M^{-1}cm^{-1}$. The above macrocycle is nonfluorescent in its free base form.

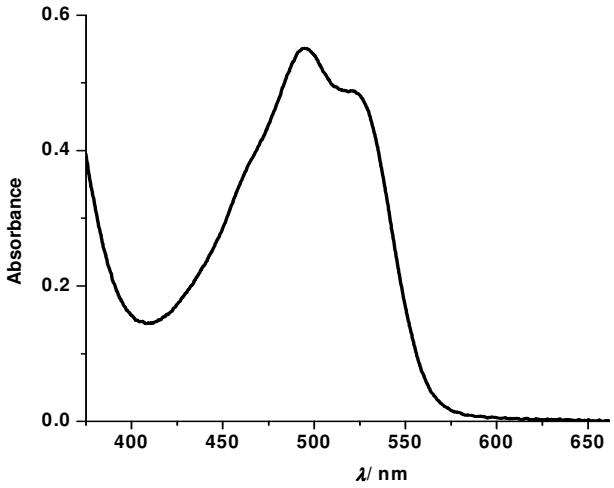

Figure 5.15. UV-Vis absorption spectrum of **27**

The final confirmation of **27** has come from single crystal X-ray analysis (Table 5.1) which is shown in Figure 5.16. X-ray quality single crystals were obtained by slow evaporation of heptane into $CHCl_3$ solution of **27**. As predicted from the above observations, the crystal structure of **27** contains one ferrocene unit, two pyrrole units, one thiophene unit, two *meso* sp^3 hybridized carbons each containing two phenyl groups which is connected to 1 and 1' position of ferrocene and two *meso* sp^2 hybridized carbons each containing one phenyl group which is connected to 2^{nd} and 5^{th} position of thiophene. From the side view, (Figure 5.16b) it is clear that the structure adopts a curved stair case like conformation in the solid state. The clear observation of the crystal structure reveals the partial planarity of the system along the 2,5-dipyrrolylthiophenyl part. Further, the *meso* phenyl carbon interacts with β-thiophene CH to form the self assembled dimer with distance and angle of C19–H19---C37: 2.83 Å and 129.84˚ (Figure 5.16c).

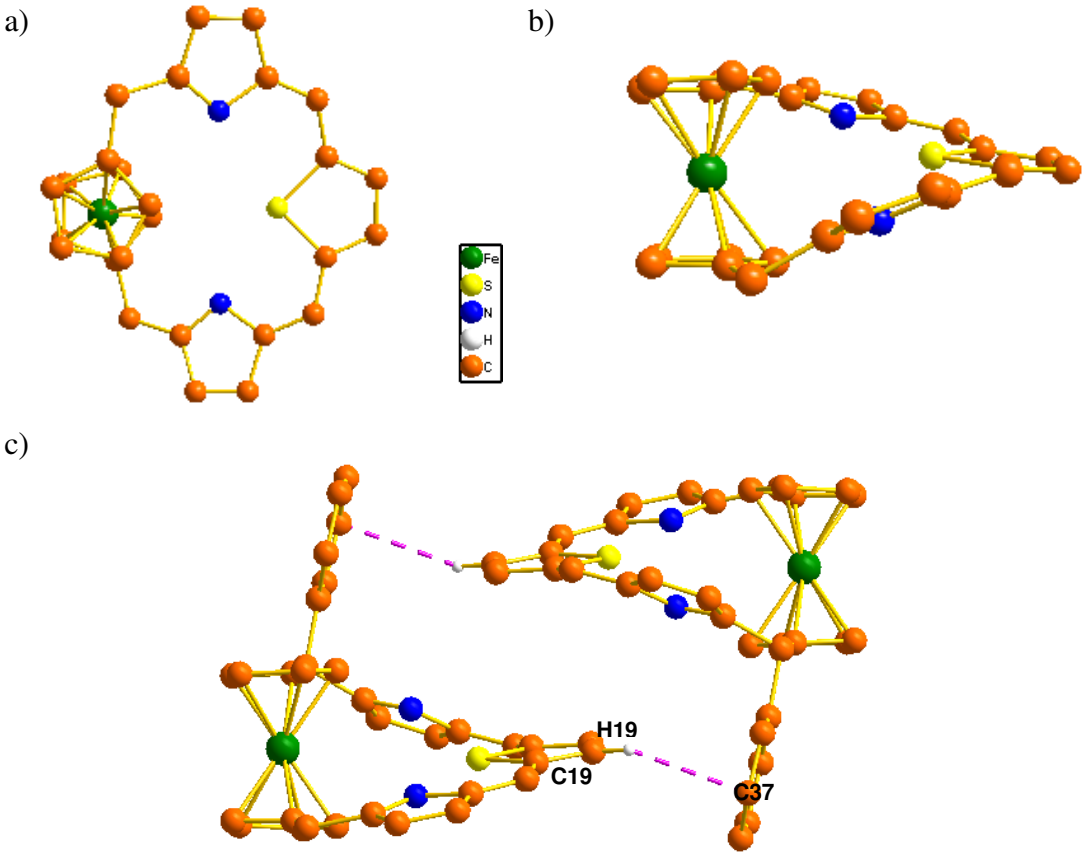

Figure 5.16. Single crystal X-ray structure of **27**. a) top view, b) side view, c) self assembled dimer. *meso*-phenyl groups, solvent molecules and all the hydrogens are omitted for clarity.

5.5 Conclusion

In summary, we have developed an efficient and easy synthetic protocol for *ansa*-ferrocene-based "calix[2]pyrrole[1]thiophene, and calix[2]phyrin[1]thiophene". To the best of our knowledge, this is the first report of *ansa*-ferrocene-based core-modified systems. The present work clearly points out the incorporation of both ferrocene and thiophene/furan simultaneously in the main frame work of calixpyrroles and calixphyrins.. UV-Vis absorption studies clearly show the peaks due to dipyrrin moiety. Finally, single crystal X-ray structures of these *ansa*-ferrocene-based macrocycles have been clearly elucidated. From

the single crystal X-ray structure analyses, it is clear that *ansa*-ferrocene-based calix[2]pyrrole[1]thiophene is highly non-planar where as calix[2]phyrin[1]thiophene is partially planar system. *ansa*-ferrocene-based calix[2]pyrrole[1]thiophene adopts 1,3-alternate conformation in the solid state and retains the parent calix[4]pyrrole behavior. Due to the presence of ferrocene in *ansa* type way, these macrocycles are highly rigid in the solid state.

5.6 Experimental Section

Synthesis of 22:

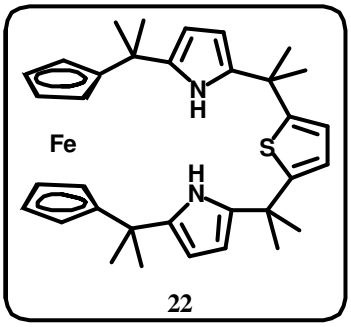

22

1,1'-bis(dimethylpyrrolylmethyl)ferrocene (**24**) (0.2 g, 0.5 mmol) and 2,5-bis(dimethylhydroxymethyl)thiophene (**25**) (0.092 g, 0.5 mmol) were dissolved in CH_2Cl_2 (60 mL) and allowed to stir for 10 min at room temperature under N_2 atm. Then TFA (0.01 mL, 0.1 mmol) was added as acid catalyst and allowed to stir for 45 min. After removal of the solvent, the crude product was purified by silica gel column chromatography (100 - 200 mesh). The first fraction eluted with EtOAc : petroleum ether (3 : 97) was identified as a yellow solid **22**. Yield = 0.08 g, 28%. ^{1}H NMR (300 MHz, $CDCl_3$, 298 K) : δ = 8.21 (brs, 2H, pyrrole NH), 6.78 (s, 2H, β-thiophene CH), 5.98-5.96 (m, 2H, β-pyrrole CH), 5.87-5.85 (m, 2H, β-pyrrole CH), 4.19-3.97 (m, 6H, ferrocenyl CH), 3.35 (s, 2H, ferrocenyl CH), 1.73 (s, 12H, methyl CH), 1.62 (s, 6H, methyl CH), 1.26 (s, 6H, methyl CH). FAB mass (m/z) = Calcd for $C_{34}H_{40}FeN_2S$: 564.22; Found : 564.87 (100%, M^+).

Synthesis of 23:

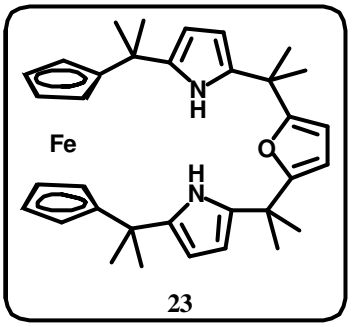

23

1,1'-bis(dimethylpyrrolylmethyl)ferrocene (**24**) (0.2 g, 0.5 mmol) and 2,5-bis(dimethylhydroxymethyl)furan (**26**) (0.092 g, 0.5 mmol) were dissolved in CH_2Cl_2 (60 mL) and allowed to stir for 10 min at room temperature under N_2 atm. Then TFA (0.01 mL, 0.1 mmol) was added as acid catalyst and allowed to stir for 45 min. After removal of the solvent, the crude product was purified by silica gel column chromatography (100 - 200 mesh). The first fraction eluted with EtOAc : petroleum ether (3 : 97) was identified as a yellow solid **23**. Yield = 0.076 g, 26.5%. ^{1}H NMR (300 MHz, $CDCl_3$, 298 K) : δ = 8.36 (brs, 2H, pyrrole NH), 6.05 (s, 2H, *β*-furan CH), 5.96 (d, J = 2.7 Hz, 4H, *β*-pyrrole CH), 4.02-3.82 (m, 8H, ferrocenyl CH), 2.15 (s, 6H, methyl CH), 1.65 (s, 18H, methyl CH). FAB mass (m/z) = Calcd for $C_{34}H_{40}FeN_2O$: 548.25; Found : 548.60 (100%, M^+).

Synthesis of 27:

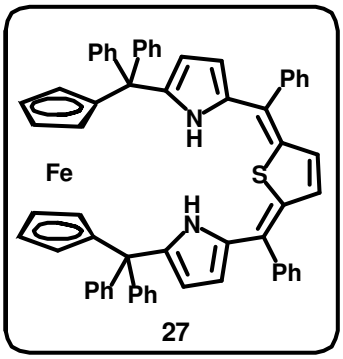

27

1,1'-bis(diphenylpyrrolylmethyl)ferrocene (**28**) (0.2 g, 0.3 mmol) and 2,5-bis(phenylhydroxymethyl)thiophene (**29**) (0.091 g, 0.3 mmol) were dissolved in 120 mL CH_2Cl_2 and allowed to stir for 10 min at room temperature under N_2 atm. Then TFA (0.005 mL, 0.06 mmol) was added as acid catalyst and allowed to stir for further 2 hrs. DDQ (0.136 g, 0.6 mmol) was added to the above reaction mixture, solution was opened to air and stirring was continued for further 2 hrs. After removal of the solvent, the crude product was purified by silica gel column chromatography (100 - 200 mesh). The first fraction eluted with CH_2Cl_2 : petroleum ether (50 : 50) was identified as a red solid **27**. Yield = 0.011 g, 4%. ^{1}H NMR (500 MHz, $CDCl_3$, 298 K) : δ = 7.41-7.37 (m,

10H, phenyl CH), 7.26-7.22 (m, 10H, phenyl CH), 7.06-7.05 (m, 6H, phenyl CH), 6.84-6.83 (m, 4H, phenyl CH), 6.78-6.77 (d, J = 4.5 Hz, 2H, pyrrolic CH), 6.74 (s, 2H, thiophene CH), 6.64-6.63 (d, J = 4.5 Hz, 2H, pyrrolic CH), 5.86 (s, 2H, ferrocenyl CH), 4.14 (s, 2H, ferrocenyl CH), 3.66-3.65 (d, J = 1 Hz, 2H, ferrocenyl CH), 3.01 (s, 2H, ferrocenyl CH). UV-Vis ($CHCl_3$): λ_{max}/nm ($\varepsilon/M^{-1}cm^{-1}$) = 494.8 (38000), 520 (41000). FAB mass (m/z) = Calcd for $C_{62}H_{46}FeN_2S$: 906.27; Found : 906.68 (100%, M^+).

5.7 Crystal data

Table 5.1. Crystallographic data for **22** and **27**

Parameters	**22**	**27**
Solvent of crystallization	$CHCl_3$/Heptane	$CHCl_3$/Heptane
Empirical formula	$C_{34}H_{40}FeN_2S$	$C_{63}H_{47}Cl_3FeN_2S$
M_w	564.59	1026.29
T [K]	293(2)	110(2)
λ [Å]	0.71073	0.71073
Crystal system	Monoclinic	Triclinic
Space group	Cc	P-1
a[Å]	10.8142(6)	10.8554(14)
b[Å]	22.5198(14)	13.2066(17)
c[Å]	13.0638(7)	17.776(2)
α [°]	90.00	99.425(2)
β [°]	113.378(3)	101.517(2)
γ [°]	90.00	94.053(2)
V[Å^3]	2920.3(3)	2449.3(5)
Z, ρ_{calcd} [Mg m^{-3}]	4, 1.284	2, 1.392
μ ($Mo_{K\alpha}$) [mm^{-1}]	0.613	0.559
F (000)	1200	1064
Crystal size [mm]	0.30 × 0.20 × 0.20	0.32 × 0.21 × 0.11
θ range for data collection [°]	1.81 to 30.99	1.19 to 28.27
Limiting indices	-15≤h≤15, -32≤k≤32, -18≤l≤17	-14≤h≤14, -17≤k≤17, -23≤l≤23
Reflections collected	37453	21017
Refinement method	Full-matrix least-squares on F^2	Full-matrix least-squares on F^2
Data / restraints / parameters	8676 / 4 / 359	11082 / 0 / 631
Goodness-of- fit on F^2	1.007	1.135
Final R indices[I>2σ(I)]	R1 = 0.0320, wR2 = 0.0849	R1 = 0.0614, wR2 = 0.1472
R indices (all data)	R1 = 0.0400, wR2 = 0.0936	R1 = 0.0680, wR2 = 0.1512
Largest $\Delta\rho$[e Å^{-3}]	0.335 and -0.214	0.807 and -0.774

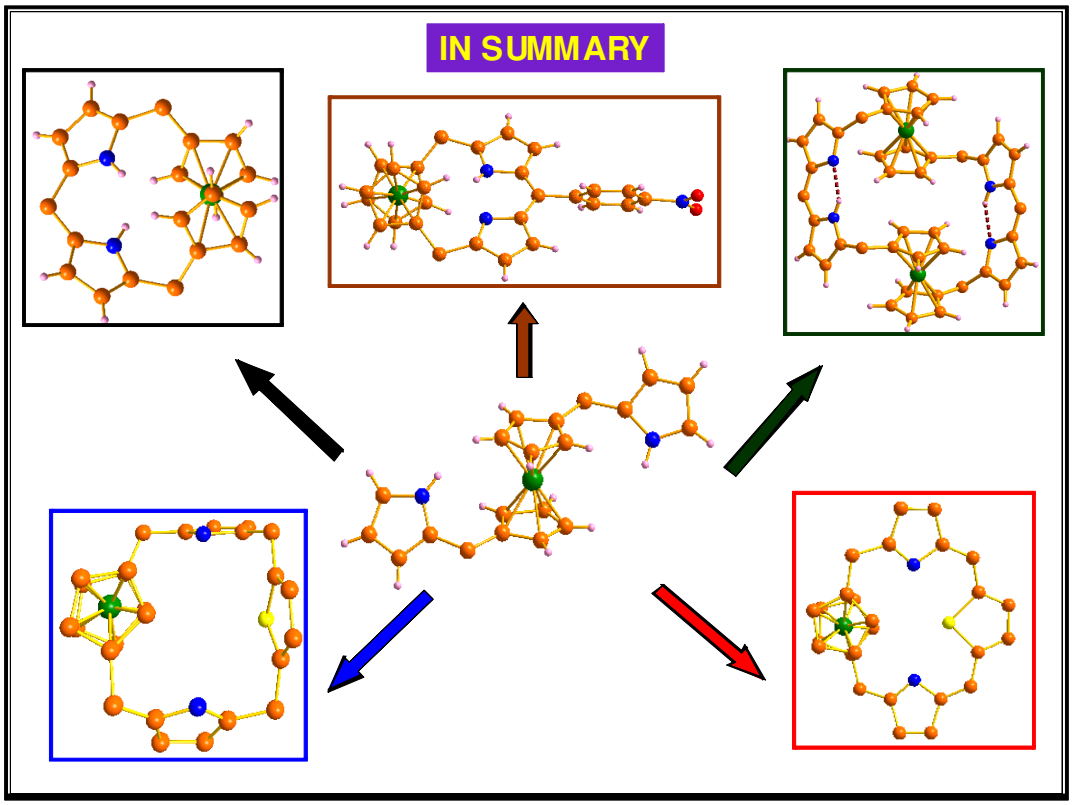
IN SUMMARY

List of Publications

1) *Calix[*n*]metallocenyl[*m*]phyrins (*n* = 1, 2 and *m* = 2, 4): aryl *vs*. alkyl: **S. Ramakrishnan**, K. S. Anju, Ajesh P. Thomas, E. Suresh and A. Srinivasan, *Chem. Commun*. **2010**, *46*, 4746-4748.

2) **ansa*-Metallocene-Based Cyclic[2]pyrroles: **S. Ramakrishnan** and A. Srinivasan, *Org. Lett*. **2007**, *9*, 4769-4772.

3) 9,10,19,20-Tetraarylporphycenes: K. S. Anju, **S. Ramakrishnan**, Ajesh P. Thomas, E. Suresh and A. Srinivasan, *Org. Lett*. **2008**, *10*, 5545-5548.

4) Calix[2]-*m*-benzo-[4]phyrin with Aggregation-Induced Enhanced Emission Characteristics: Application as Hg^{2+} Chemosensor: P. S. Salini, Ajesh P. Thomas, R. Sabarinathan, **S. Ramakrishnan**, K. C. Gowri Sreedevi, M. L. P. Reddy and A. Srinivasan, *Chem. Eur. J*. **2011**, accepted for publication.

5) **ansa*-ferrocene incorporated core-modified calixpyrroles and calixphyrins: syntheses, spectral and structural characterization: **S. Ramakrishnan**, K. S. Anju, Ajesh P. Thomas, K. C. Gowri Sreedevi, P. S. Salini, M. G. Derry Holaday, E. Suresh and A. Srinivasan, *Chem. Eur. J*. **2011**, communicated.

6) An improved synthetic methodology for 5,5-diaryldipyrromethanes with anion binding properties: K. C. Gowri Sreedevi, Ajesh P. Thomas, P. S. Salini, **S. Ramakrishnan**, K. S. Anju, M. G. Derry Holaday, M. L. P. Reddy and A. Srinivasan. *J. Org. Chem*. **2011**. communicated.

7) *meso*-Aryl triphyrin(2.1.1): K. S. Anju, **S. Ramakrishnan**, and A. Srinivasan, *Org. Lett*. **2011**. communicated.

*pertaining to thesis

List of Poster Presentations

1. International Conference on Advanced Materials and Composites (ICAMC – 2007) October 24-26, 2007. Organized by National Institute for Interdisciplinary Science and Technology (NIIST-CSIR) (Formerly Regional Research Laboratory, CSIR) Trivandrum.
2. Symposium on Advanced Biological Inorganic Chemistry (SABIC – 2009), November 04-07, 2009. Organised by Tata Institute of Fundamental Research, Mumbai.
3. Modern Trends in Inorganic Chemistry (MTIC-XIII), December 07-10, 2009, conducted by Department of Inorganic & Physical Chemistry, Indian Institute of Science, Bangalore.
4. Mid Chemical Research Society of India (MCRSI), July 23-24, 2010, conducted by Photosciences and Photonics Section, Chemical Sciences and Technology Division, National Institute for Interdisciplinary Science and Technology (NIIST – CSIR), Trivandrum.

References

Allen, W. E.; Gale, P. A.; Brown, C. T.; Lynch, V. M.; Sessler, J. L. "Binding of Neutral Substrates by Calix[4]pyrroles" *J. Am. Chem. Soc*. 118, **1996**, 12471.

Altomare, A.; Cascarano, G.; Giacovazzo, C.; Guagliardi, A. "Completion and refinement of crystal structures with SIR92" *J. Appl. Cryst*. 26, **1993**, 343.

Amako, M.; Schinkel, J.; Brook, M. A.; McGlinchey, M. J.; Britten, J. F. "*Rac/meso* Transformations of Disiloxane-bis(1-indenyl)-*ansa*-ferrocenes: An X-ray Crystallographic and NMR Study" *Organometallics* 24, **2005**, 1533.

[a]Anzenbacher, P. Jr.; Jursíková, K.; Sessler, J. L. "Second Generation Calixpyrrole Anion Sensors" *J. Am. Chem. Soc*. 122, **2000**, 9350.

[b]Anzenbacher, P. Jr.; Try, A. C.; Miyaji, H.; Jursíková, K.; Lynch, V. M.; Marquez, M.; Sessler, J. L. "Fluorinated Calix[4]pyrrole and Dipyrrolylquinoxaline: Neutral Anion Receptors with Augmented Affinities and Enhanced Selectivities" *J. Am. Chem. Soc*. 122, **2000**, 10268.

[c]Anzenbacher, P. Jr.; Jursíková, K.; Shriver, J. A.; Miyaji, H.; Lynch, V. M.; Sessler, J. L.; Gale, P. A. "Lithiation of *meso*-Octamethylcalix[4]pyrrole: A General Route to *C*-Rim Monosubstituted Calix[4]pyrroles" *J. Org. Chem*. 65, **2000**, 7641.

Anzenbacher, P. Jr.; Nishiyabu, R.; Palacios, M. A. "N-confused calix[4]pyrroles" *Coord. Chem. Rev*. 250, **2006**, 2929.

Archer, R. D. *Inorganic and Organometallic Polymer*; Wiley-VCH: New York, **2001**.

Arumugam, N.; Jang, Y. -S.; Lee, C. -H. "Convenient Route to Super-Expanded Calixpyrroles: Synthesis of Calix[*n*]furano[*m*]pyrroles (*n* = 3, 4, 6, 8 and *m* = 2, 4)" *Org. Lett*. 2, **2000**, 3115.

Ashe III, A. J.; Al-Ahmad, S.; Fang, X.; Kampf, J. W. "Conformational Properties of Boron-Bridged Dimethylethylenediamino Bis(boratabenzene) Zirconium(IV) and Iron(II) Complexes" *Organometallics* 20, **2001**, 468.

Ashe, III. A. J.; Fang, X.; Hokky, A.; Kampf, J. W. "The C_s-Symmetric Aminoboranediyl-Bridged Zirconocene Dichloride [(η^9-$C_{13}H_8$)- BN(^{i}Pr)$_2$(η-C_5H_4)]$ZrCl_2$: Its Synthesis, Structure, and Behavior as an Olefin Polymerization Catalyst" *Organometallics* 23, **2004**, 2197.

[a]Aydogan, A.; Coady, D. J.; Kim, S. K.; Akar, A.; Bielawski, C. W.; Marquez, M.; Sessler, J. L. "Poly (methyl methacrylate)s with Pendant Calixpyrroles and Crown Ethers: Polymeric Extractants for Potassium Halides" *Angew. Chem. Int. Ed*. 47, **2008**, 9648.

Baeyer, A. "Ueber ein Condensationsproduct von Pyrrol mit Aceton" *Ber. Dtsch. Chem. Ges*. 19, **1886**, 2184.

Bagh, B.; Gilroy, J. B.; Staubitz, A.; Müller, J. "Ring-Opening Polymerization of a Galla[1]ferrocenophane: A Gallium-Bridged Polyferrocene with Observable Tacticity" *J. Am.Chem. Soc*. 132, **2010**, 1794.

Bajgur, C. S.; Tikkanen, W.; Petersen, J. L. "Synthesis, structural characterization, and electrochemistry of [1]Metallocenophane Complexes, [Si(alkyl)$_2$(C_5H_4)$_2$]MCl_2, M = Ti, Zr" *Inorg. Chem*. 24, **1985**, 2539.

Barkigia, K. M.; Renner, M. W.; Xie, H.; Smith, K. M.; Fajer, J. "Structural consequences of porphyrin tautomerization. Molecular structure of a zinc isoporphyrin" *J. Am. Chem. Soc*. 115, **1993**, 7894.

[a]Bates, G. W.; Gale, P. A.; Light, M. E. "Ionic liquid-calix[4]pyrrole complexes: pyridinium inclusion in the calixpyrrole cup" *CrystEngComm*. 8, **2006**, 300.

[b]Bates, G. W.; Kostermans, M.; Dehaen, W.; Gale, P. A.; Light, M. E. "Organic salt inclusion: the first crystal structures of anion complexes of *N*-confused calix[4]pyrrole" *CrystEngComm*. 8, **2006**, 444.

Bates, G. W.; Gale, P. A.; Light, M. E. "Interactions of Organic Halide and Nitrate Salts with *meso*-Octamethylcalix[4]pyrrole" *Supramol. Chem*. 20, **2008**, 23.

Bauer, F.; Braunschweig, H.; Schwab, K. "1,1-Diboration of Isocyanides with [2]Borametalloarenophanes" *Organometallics* 29, **2010**, 934.

Beer, P. D. "Anion selective recognition and optical/electrochemical sensing by novel transition-metal receptor systems" *Chem. Commun*. **1996**, 689.

[a]Beer, P. D.; Drew, M. G. B.; Jagessar, R. "Selective anion recognition by novel 5,10,15,20- tetrakis(*o*-ferrocenylcarbonylaminophenyl-substituted) zinc metalloporphyrin receptors" *J. Chem. Soc., Dalton Trans*. **1997**, 881.

[b]Beer, P. D.; Szemes, F.; Balzani, V.; Salá, C. M.; Drew, M. G. B.; Dent, S. W.; Maestri, M. "Anion Selective Recognition and Sensing by Novel Macrocyclic Transition Metal Receptor Systems. ^{1}H NMR, Electrochemical, and Photophysical Investigations" *J. Am. Chem. Soc*. 119, **1997**, 11864.

[a]Beer, P. D.; Cadman, J.; Lloris, J. M.; Martínez-Mañez, R.; Padilla, M. E.; Pardo, T.; Smith, D. K.; Soto, J. "Selective electrochemical recognition of sulfate over phosphate and phosphate over sulfate using polyaza ferrocene macrocyclic receptors in aqueous solution" *J. Chem. Soc. Dalton Trans*. **1999**, 127.

[b]Beer, P. D.; Gale, P. A.; Chen, G. Z. "Electrochemical molecular recognition: pathways between complexation and signalling" *J. Chem. Soc., Dalton Trans*. **1999**, 1897.

Beer, P. D.; Cadman, J. "Electrochemical and optical sensing of anions by transition metal based receptors" *Coord. Chem. Rev*. 205, **2000**, 131.

Belanzoni, P.; Rosi, M.; Sgamellotti, A.; Bonomo, L.; Floriani, C. "A theoretical analysis of the fundamental stepwise six-electron oxidation of porphyrinogen to porphyrins: the energetics of porphodimethene and artificial porphyrin intermediates" *J. Chem. Soc., Dalton Trans*. **2001**, 1492.

Benech, J. -M.; Bonomo, L.; Solari, E.; Scopelliti, R.; Floriani, C. "Porphomethenes and Porphodimethenes Synthesized by the Two- and Four-Electron Oxidation of the *meso*-Octaethylporphyrinogen" *Angew. Chem. Int. Ed.* 38, **1999**, 1957.

Berenbaum, A.; Braunschweig, H.; Dirk, R.; Englert, U.; Green, J. C.; Jäkle, F.; Lough, A. J.; Manners, I. "Synthesis, Electronic Structure, and Novel Reactivity of Strained, Boron-Bridged [1]Ferrocenophanes" *J. Am. Chem. Soc*. 122, **2000**, 5765.

Bischoff, I.; Feng, X.; Senge, M. O. "One-pot synthesis of functionalized, highly substituted porphodimethenes" *Tetrahedron* 57, **2001**, 5573.

Blessing, R. "An empirical correction for absorption anisotropy" *Acta Cryst.* A51, **1995**, 33.

Bonomo, L.; Toraman, G.; Solari, E.; Scopelliti, R.; Floriani, C. "Porphodimethene–Zirconium: A New Entry into Zirconium Macrocycle Organometallic Chemistry" *Organometallics* 18, **1999**, 5198.

Bonomo, L.; Solari, E.; Scopelliti, R.; Floriani, C. "The π Complexation of Alkali and Alkaline Earth Ions by the Use of *meso*-Octaalkylporphyrinogen and Aromatic Hydrocarbons" *Chem. Eur. J*. 7, **2001**, 1322.

Botulinski, A.; Buchler, J. W.; Lay, K. -L.; Stoppa, H. "Metallkomplexe mit Tetrapurrol-Liganden, XXXV. Synthese weiterer, zum Teil sterisch gehinderter 5,15-Dialkyloctaethyl porphodimethene durch reduzierende Alkylierung von Octaethylporphyrinatozink" *Liebigs Ann. Chem*. **1984**, 1259.

Botulinski, A.; Buchler, J. W.; Lee, Y. J.; Scheidt, W. R.; Wicholas, M. "Metal Complexes with tetrapyrrole ligands. 49. Solid-state and solution structures of iron(III) porphodimethenes. Effects of steric hindrance" *Inorg. Chem*. 27, **1988**, 927.

Brandenburg, K. Diamond Version 3.1.

Brandt, P. F.; Compton, D. L.; Rauchfuss, T. B. "*ansa*-Ferrocenes with both Trisulfide and Hydrocarbon Straps" *Organometallics* 17, **1998**, 2702.

Braunschweig, H.; Dirk, R.; Müller, M.; Nguyen, P.; Resendes, R.; Gates, D. P.; Manners, I. "Incorporation of a First Row Element into the Bridge of a Strained Metallocenophane: Synthesis of a Boron-Bridged [1]Ferrocenophane" *Angew. Chem. Int. Ed. Eng*. 36, **1997**, 2338.

Braunschweig, H.; Breitling, F. M.; Gullo, E.; Kraft, M. "The chemistry of [1]borametallocenophanes and related compounds" *J. Organomet. Chem*. 680, **2003**, 31.

Braunschweig, H.; Kupfer, T.; Lutz, M.; Radacki, K.; Seeler, F.; Sigritz, R. "Metal-Mediated Diboration of Alkynes with [2]Borametalloarenophanes under Stoichiometric, Homogeneous, and Heterogeneous Conditions" *Angew. Chem. Int. Ed*. 45, **2006**, 8048.

Braunschweig, H.; Kupfer, T. "Transition-Metal-Catalyzed Bis-Silylation of Propyne by [2]Chromoarenophanes" *Organometallics* 26, **2007**, 4634.

Braunschweig, H.; Kupfer, T. "Non-iron [n]Metalloarenophanes" *Acc. Chem. Res*. 43, **2010**, 455.

Brintzinger, H. H.; Fischer, D.; Mülhaupt, R.; Rieger, B.; Waymouth, R. M. "Stereospecific OlefinPolymerization with Chiral Metallocene Catalysts" *Angew. Chem. Int. Ed. Eng*. 34, **1995**, 1143.

Brown, W. H.; Hutchinson, B. J.; Mackinnon, M. H. "The Condensation of Cyclohexanone with Furan and Pyrrole" *Can. J. Chem.* 49, **1971**, 4017.

Bruker (**1999**). SADABS, Bruker AXS Inc., Madison, Wisconsin, USA.

Bruker (**2004**). APEX-II and SAINT-Plus (Version 7.06a), Bruker AXS Inc., Madison, Wisconsin, USA.

Bruno, G.; Cafeo, G.; Kohnke, F. H.; Nicolò, F. "Tuning the anion binding properties of calixpyrroles by means of *p*-nitrophenyl substituents at their *meso*-positions" *Tetrahedron* 63, **2007**, 10003.

Bucher, C.; Seidel, D.; Lynch, V.; Král, V.; Sessler, J. L. "Novel Synthesis of Hybrid Calixphyrin Macrocycles" *Org. Lett*. 2, **2000**, 3103.

Bucher, C.; Zimmerman, R. S.; Lynch, V.; Král, V.; Sessler, J. L. "Synthesis of Novel Expanded Calixphyrins: Anion Binding Properties of a Calix[6]phyrin with a Deep Cavity" *J. Am. Chem. Soc*. 123, **2001**, 2099.

Bucher, C.; Zimmerman, R. S.; Lynch, V.; Sessler, J. L. "Synthesis and X-ray structure of three dimensional calixphyrin" *Chem. Commun*. **2003**, 1646.

Bucher, C.; Devillers, C. H.; Moutet, J. -C.; Royal, G; Aman, E. S. "Anion recognition and redox sensing by a metalloporphyrin–ferrocene–alkylammonium conjugate" *New J. Chem*. 28, **2004**, 1584.

Bucher, C.; Devillers, C. H.; Moutet, J. -C.; Pécaut, J.; Royal, G.; Aman, E. S.; Thomas, F. "Calix[4]phyrin based redox architectures: towards new molecular tools for electrochemical sensing" *Dalton Trans*. **2005**, 3620.

Buchler. J. W.; Puppe, L. "Metallkomplexe mit Tetrapyrrol-Liganden, II1) Metallchelate des α.γ-Dimethyl-α.γ-dihydro-octaäthylporphins durch reduzierende Methylierung von Octaäthylporphinato-zink" *Justus Liebigs Ann. Chem.* 740, **1970**, 142.

Butler, I. R.; Cullen, W. R.; Einstein, F. W. B.; Rettig, S. J.; Willis, A. J. "Synthesis of some ring-substituted [1]ferrocenophanes and the structure of four representative examples" *Organometallics* 2, **1983**, 128.

Buretea, M. A.; Tilley, T. D. "Poly(ferrocenylenevinylene) from Ring-Opening Metathesis Polymerization of *ansa*-(Vinylene)ferrocene" *Organometallics* 16, **1997**, 1507.

[a]Cafeo, G.; Kohnke, F. H.; Torre, G. L. L.; White, A. J. P.; Williams, D. J. "From Large Furan-Based Calixarenes to Calixpyrroles and Calix[*n*]furan[*m*]pyrroles: Syntheses and Structures" *Angew. Chem. Int. Ed.* 39, **2000**, 1496.

[b]Cafeo, G.; Kohnke, F. H.; Torre, G. L. L.; White, A. J. P.; Williams, D. J. "The complexation of halide ions by a calix[6]pyrrole" *Chem. Commun*. **2000**, 1207.

[a]Cafeo, G.; Kohnke, F. H.; Parisi, M. F.; Nascone, R. P.; La Torre, G. L.; Williams, D. J. "The Elusive *β*-Unsubstituted Calix[5]pyrrole Finally Captured" *Org. Lett*. 4, **2002**, 2695.

[b]Cafeo, G.; Kohnke, F. H.; La Torre, G. L.; Parisi, M. F.; Nascone, R. P.; White, A. J. P.; Williams, D. J. "Calix[6]pyrrole and Hybrid Calix[*n*]furan[*m*]pyrroles (n + m = 6): Syntheses and Host – Guest Chemistry" *Chem. Eur. J*. 8, **2002**, 3148.

[c]Cafeo, G.; Gargiulli, C.; Gattuso, G.; Kohnke, F. H.; Notti, A.; Occhipinti, S.; Pappalardo, S.; Parisi, M. F. "Recognition and binding of paraquat dichloride by cyclodextrin/calix[6]pyrrole binary host systems" *Tetrahedron Lett*. 43, **2002**, 8103.

Cafeo, G.; Kaledkowski, A.; Kohnke, F. H.; Messina, A. "Strapped Calix[2]furan[4]pyrroles, Novel Examples of Ditopic Molecular Receptors" *Supramol. Chem*. 18, **2006**, 273.

Cafeo, G.; Kohnke, F. H.; White, A. J. P.; Garozzo, D.; Messina, A. "Syntheses, Structures, and Anion-Binding Properties of Two Novel Calix[2]benzo[4]pyrroles" *Chem. Eur. J*. 13, **2007**, 649.

Camiolo, S.; Gale, P. A. "Fluoride recognition in 'super-extended cavity' calix[4]pyrroles" *Chem. Commun*. **2000**, 1129.

Carroll, M. A.; Widdowson, D. A.; Williams, D. J. "A Short Efficient Route to C2 Symmetric 1,1',2,2'-Tetrasubstituted Ferrocenes" *Synlett* **1994**, 1025.

Chadha, P.; Dutton, J. L.; Sgro, M. J.; Ragogna, P. J. "Synthesis of Neutral Mixed Sandwich CH_2-SiR_2 Bridged [2]Cobaltoarenophanes from the Dilithiation of Cb*CoCp [Co(η^4-C_4Me_4)(η^5-C_5H_5)]" *Organometallics* 26, **2007**, 6063.

Chadwick, D. J.; Willbe, C. "High-yield syntheses of dilithio-derivatives of furan, thiophen, N-methylpyrrole, 3-methylfuran, and 3-methylthiophen. Application of the method to 2-methylfuran, 2-methylthiophen, 2,5-dimethylfuran, 2,5-dimethylthiophen, benzo[b]furan, benzo[b]thiophen, pyrrole, and indole" *J. Chem. Soc. Perkin Trans. I*. **1977**, 887.

Chang, G. -F.; Kumar, A.; Ching, W. -M.; Chu, H. -W.; Hung, C. -H. "Tetramethyl-*m*-benziporphodimethene and Isomeric α,β-Unsaturated γ-Lactam Embedded N-Confused Tetramethyl-*m*-benziporphodimethenes" *Chem. Asian J*. 4, **2009**, 164.

[a]Chelintzev, V. V.; Tronov, B. V. "Process of condensation of pyrrole and acetone. Constitution of the resulting products," *J. Russ. Phy. Chem. Soc*. 48, **1916**, 105.

[b]Chelintzev, V. V.; Tronov, B. V.; Karmanov, S. G. "Simple condensation of pyrrole with cyclohexanone and other cyclic ketones in mixed condensation with acetone

and cyclohexanone, and conclusions in respect to the ability of different ketones to condense with pyrrole," *J. Russ. Phys. Chem. Soc*. 48, **1916**, 1210.

Chen, Q.; Wang, T.; Zhang, Y.; Wang, Q.; Ma, J. "DOUBLY N-CONFUSED CALIX[4]PYRROLE PREPARED BY RATIONAL SYNTHESIS" *Syn. Commun*. 32, **2002**, 1051.

Chen, W.; Liu, T. J. "Synthesis and characterization of novel calix[6]phyrin derivatives" *Chin. Chem. Lett*. 19, **2008**, 1199.

Chen, Y. -X.; Fu, P. -F.; Stern, C. L.; Marks, T. J. "A Novel Phenolate "Constrained Geometry" Catalyst System. Efficient Synthesis, Structural Characterization, and α-Olefin Polymerization Catalysis" *Organometallics* 16, **1997**, 5958.

Chen, Z.; Gale, P. A.; Beer, P. D. "Synthesis and electrochemical polymerization of calix[4]arenes containing N-substituted pyrrole moieties" *J. Electroanal. Chem*. 393, **1995**, 113.

Chirvony, V. S.; van Hoek, A.; Galievsky, V. A.; Sazanovich, I. V.; Schaafsma, T. J.; Holten, D. "Comparative Study of the Photophysical Properties of Nonplanar Tetraphenylporphyrin and Octaethylporphyrin Diacids" *J. Phys. Chem. B* 104, **2000**, 9909.

Chowdhury, S.; Schatte, G.; Kraatz, H. -B. "Synthesis, structure and electrochemistry of ferrocene–peptide macrocycles" *Dalton Trans*. **2004**, 1726.

Coates, G. W. "Precise Control of Polyolefin Stereochemistry Using Single-Site Metal Catalysts" *Chem. Rev*. 100, **2000**, 1223.

Collinson, S. R.; Gelbrich, T.; Hursthouse, M. B.; Tucker, J. H. R. "Novel ferrocene receptors for barbiturates and ureas" *Chem. Commun*. **2001**, 555.

Coman, V.; Mureşan, L. M.; Lozovanu, S.; Silaghi-Dumitrescu, L.; Popescu, I. C. "MESO–TETRAFERROCENYL–TETRAMETHYL CALIX[4]PYRROLE-

MODIFIED GRAPHITE ELECTRODE WITH ANION RECOGNITION PROPERTIES" *Revue Roumaine de Chimie*, 53, **2008**, 119.

Comba, P.; Linti, G.; Merz, K.; Pritzkow, H.; Renz, F. "Electronic Interactions in Ferrocene- and Ruthenocene-Functionalized Tetraazamacrcocyclic Ligand Complexes of $Fe^{II/III}$, Co^{II}, Ni^{II}, Cu^{II} and Zn^{II}," *Eur. J. Inorg. Chem.* **2005**, 383.

Custelcean, R.; Delmau, L. H.; Moyer, B. A.; Sessler, J. L.; Cho, W. -S.; Gross, D.; Bates, G. W.; Brooks, S. J.; Light, M. E.; Gale, P. A. "Calix[4]pyrrole: An Old yet New Ion-Pair Receptor" *Angew. Chem. Int. Ed*. 44, **2005**, 2537.

Dahlmann, M.; Erker, G.; Nissinen, M.; Fröhlich, R. "Direct Experimental Observation of the Stereochemistry of the First Propene Insertion Step at an Active Homogeneous Single-Component Metallocene Ziegler Catalyst" *J. Am. Chem. Soc*. 121, **1999**, 2820.

Dang, V. A.; Yu, L. -C.; Balboni, D.; Dall'Occo, T.; Resconi, L.; Mercandelli, P.; Moret, M.; Sironi, A. "Simple Route to Bis(3-indenyl)methanes and the Synthesis, Characterization, and Polymerization Performance of Selected *racemic*-Dichloro[methylenebis(R_n-1-indenyl)]- zirconium Complexes" *Organometallics* 18, **1999**, 3781.

Danil de Namor, A. F.; Shehab, M. "Selective Recognition of Halide Anions by Calix[4]pyrrole: A Detailed Thermodynamic Study" *J. Phys. Chem. B* 107, **2003**, 6462.

Danil de Namor, A. F.; Shehab, M. "Recognition of Biologically and Environmentally Important Phosphate Anions by Calix[4]pyrrole: Thermodynamic Aspects" *J. Phys. Chem. A* 108, **2004**, 7324.

Davis, B. R.; Bernal, I. "The crystal and molecular structure of (1,1'-trimethylenedicyclopentadienyl)titanium dichloride" *J. Organomet. Chem*. 30, **1971**, 75.

Deckers, P. J. W.; van der Linden, A. J.; Meetsma, A.; Hessen, B. Cationic *ansa*-(η^5-Cyclopentadienyl)(η^6-arene) Complexes of Titanium" *Eur. J. Inorg. Chem*. **2000**, 929.

Dehaen, W.; Gale, P. A.; García-Garrido, S. E.; Kostermans, M.; Light, M. E. "Anion recognition by N-confused calix[4]pyrrole-α-carbaldehyde and its Knoevenagel reaction derivatives" *New J. Chem.* 31, **2007**, 691.

Dennstedt, M.; Zimmerman. J. "Ueber die Einwirkung des Acetons auf das Pyrrol" *Chem. Ber*. 20, **1887**, 850.

Dennstedt, M. "Ueber die Einwirkung des Acetons auf das Pyrrol" *Ber. Dtsch. Chem. Ges*. 23, **1890**, 1370.

Depraetere, S.; Smet, M.; Dehaen, W. "N-Confused Calix[4]pyrroles" *Angew. Chem. Int. Ed*. 38, **1999**, 3359.

Ding, L.; Ma, K.; Fabrizi de Biani, F.; Bolte, M.; Zanello, P.; Wagner, M. "Electronic Communication in a Novel Five-Step Redox System" *Organometallics* 20, **2001**, 1041.

Dolenský , B.; Kroulík, J.; Král, V.; Sessler, J. L.; Dvořákova, H.; Bouř, P.; Bernátková, M.; Bucher, C.; Lynch, V. "Calix[4]phyrins. Effect of Peripheral Substituents on Conformational Mobility and Structure within a Series of Related Systems" *J. Am. Chem. Soc*. 126, **2004**, 13714.

Dolphin, D. "Porphyrinogens and porphodimethenes, intermediates in the synthesis of *meso*-tetraphenylporphins from pyrroles and benzaldehyde" *J. Heterocycl. Chem*. 7, **1970**, 275.

Dormund, A.; Khan, O.; Tirouflet, J. "Synthese et etude des complexes $[C_5H_4(CH_2)_3C_5H_4]Ti(C_5H_5)_2$ presentant un pont entre deux ligands cyclopentadienyles" *J. Organomet. Chem*. 110, **1976**, 321.

Dwyer, P. N.; Buchler, J. W.; Scheidt, W. R. "Crystal Structure and Molecular Stereochemistry of α,γ-Dimethyl-α,γ-dihydrooctaethylporphinatonickel(II)" *J. Am. Chem. Soc*. 96, **1974**, 2789.

Elschenbroich, C.; Hurley, J.; Metz, B.; Massa, W.; Baum, G. "Metal π-complexes of benzene derivatives. 34. Tetraphenylsilane as a chelating ligand: synthesis, structural characterization, and reactivity of the tilted bis(arene) metal complexes $[(C_6H_5)_2Si(\eta^6\text{-}C_6H_5)_2]M$ (M = V, Cr)" *Organometallics* 9, **1990**, 889.

Elschenbroich, C.; Schmidt, E.; Gondrum, R.; Metz, B.; Burghaus, O.; Massa, W.; Wocadlo, S. "Metal π Complexes of Benzene Derivatives. Germanium in the Periphery of Bis(benzene)vanadium and Bis(benzene)chromium. Synthesis and Structure of New Heterametallocyclophanes" *Organometallics* 16, **1997**, 4589.

Farrugia, L. J. "*ORTEP-3* for Windows - a version of *ORTEP-III* with a Graphical User Interface (GUI)" *J. Appl. Cryst*. 30, **1997**, 565.

Farrugia, L. J. "*WinGX* suite for small-molecule single-crystal crystallography" *J. Appl. Cryst*. 32, **1999**, 837.

Finckh, W.; Tang, B. Z.; Lough, A.; Manners, I. "Synthesis and properties of organometallic rings and macrocycles containing ferrocene, silicon, and unsaturated hydrocarbon units: x-ray crystal structures of the novel ferrocenophanes $Fe(\eta\text{-}C_5H_4)_2(SiMe_2)_2(CH{=}CH)$ and *trans*,*trans*-$Fe(\eta\text{-}C_5H_4)_2(SiMe_2)_2(CH_2CH{=}CHCH_2)_2$" *Organometallics* 11, **1992**, 2904.

Finckh, W.; Tang, B. Z.; Foucher, D. A.; Zamble, D. B.; Ziembinski, R.; Lough, A.; Manners, I. "The polymerization behavior of [1]- and [2]ferrocenophanes

containing silicon atoms in the bridge: comparison of the molecular structure of the strained, polymerizable cyclic ferrocenylsilane $Fe(\eta\text{-}C_5H_4)_2(SiMe_2)$ with that of the cyclic ferrocenyldisilane $Fe(\eta\text{-}C_5H_4)_2(SiMe_2)_2$" *Organometallics* 12, **1993**, 823.

Fischer, E. O.; Pfab, W. *Z. Naturforch. Teil b*. "CYCLOPENTADIEN-METALLKOMPLEXE, EIN NEUER TYP METALLORGANISCHER VERBINDUNGEN" 7, **1952**, 377.

Fischer, H.; Orth, H. "Die Chemie des Pyrrols," Akademische Verlagsgesellschaft m.b.H., Leipzig, **1934**, 20.

Fisher, M. G.; Gale, P. A.; Hiscock, J. R.; Hursthouse, M. B.; Light, M. E.; Schmidtchen, F. P.; Tong, C. C. "1,2,3-Triazole-strapped calix[4]pyrrole: a new membrane transporter for chloride" *Chem. Commun*. **2009**, 3017.

Floriani, C. "The porphyrinogen–porphyrin relationship: the discovery of artificial porphyrins" *Chem. Commun*. **1996**, 1257.

Floriani, C.; Solari, E.; Solari, G.; Chiesi-Villa, A.; Rizzoli, C. "The π-Pyrrole Complexation of Alkali Metal Ions by Zirconium *meso*-Octaalkylporphyrinogens: Encapsulation of Li_4H_4 and Li_2O in Sandwich Structures" *Angew. Chem. Int. Ed*. 37, **1998**, 2245.

Foucher, D. A.; Tang, B. Z.; Manners, I. "Ring-opening polymerization of strained, ring-tilted ferrocenophanes: a route to high-molecular-weight poly(ferrocenylsilanes)" *J. Am. Chem. Soc*. 114, **1992**, 6246.

Foucher, D. A.; Edwards, M.; Burrow, R. A.; Lough, A. J.; Manners, I. "Ring-Opening Polymerization of Strained, Ring-Tilted [1]Ferrocenophanes with Germanium in the Bridge: Structures of the [1]Germaferrocenophane $Fe(\eta\text{-}C_5H_4)_2GeMe_2$ and

the Ferrocenylgermane Fe(η-$C_5H_4GeEt_2Cl$)(η-C_5H_5)" *Organometallics* 13, **1994**, 4959.

Franck, B. "Topical Problems in the Biosynthesis of Red Blood Pigment" *Angew. Chem. Int. Ed. Engl*. 21, **1982**, 343.

Furusho, Y.; Kawasaki, H.; Nakanishi, S.; Aida, T.; Takata, T. "Design of Multidentate Pyrrolic Ligands by *N*-Modification: Synthesis of *N*-Monomethyl, Monoethyl, Dimethyl, Trimethyl, and Tetramethylporphyrinogens" *Tetrahedron Lett.* 39, **1998**, 3537.

Furuta, H.; Ishizuka, T.; Osuka, A.; Uwatoko, Y.; Ishikawa, Y. "Metal Complexes of an N-Confused Calix[4]phyrin Derivative–The First X-ray Structure of an Organometallic Compound of Divalent Copper" *Angew. Chem. Int. Ed*. 40, **2001**, 2323.

Furuta, H.; Ishizuka, T.; Osuka, A. "Zinc complex of N-confused calix[4]phyrin" *Inorg. Chem. Commun*. 6, **2003**, 398.

[a]Gale, P. A.; Sessler, J. L.; Král, V.; Lynch, V. "Calix[4]pyrroles: Old Yet New Anion-Binding agents" *J. Am. Chem. Soc*. 118, **1996**, 5140.

[b]Gale, P. A.; Sessler, J. L.; Lynch, V.; Sansom, P. I. "Synthesis of a New Cylindrical Calix[4]arene-Calix[4]pyrrole Pseudo Dimer" *Tetrahedron Lett*. 37, **1996**, 7881.

[a]Gale, P. A.; Sessler. J. L.; Allen, W. E.; Tvermoes, N. A.; Lynch. V. "Calix[4]pyrroles: *C*-rim substitution and tunability of anion binding strength" *Chem. Commun*. **1997**, 665.

[b]Gale, P. A.; Genge, J. W.; Král, V.; McKervey, M. A.; Sessler, J. L.; Walker, A. "First Synthesis of an Expanded Calixpyrrole" *Tetrahedron Lett*. 38, **1997**, 8443.

Gale, P. A.; Sessler, J. L.; Král, V. "Calixpyrroles" *Chem. Commun*. **1998**, 1.

Gale, P. A.; Twyman, L. J.; Handlin, C. I.; Sessler, J. L. "A colourimetric calix[4]pyrrole–4-nitrophenolate based anion sensor" *Chem. Commun*. **1999**, 1851.

Gale, P. A. "Anion coordination and anion-directed assembly: highlights from 1997 and 1998" *Coord. Chem. Rev*. 199, **2000**, 181.

[a]Gale, P. A.; Anzenbacher, P. Jr.; Sessler, J. L. "Calixpyrroles II" *Coord. Chem. Rev*. 222, **2001**, 57.

[b]Gale, P. A.; Hursthouse, M. B.; Light, M. E.; Sessler, J. L.; Warriner, C. N.; Zimmerman, R. S. "Ferrocene-substituted calix[4]pyrrole: a new electrochemical sensor for anions involving CH---anion hydrogen bonds" *Tetrahedron Lett*. 42, **2001**, 6759.

[c]Gale, P. A.; Bleasdale, E. R.; Chen, G. Z. "Synthesis and Electrochemical Polymerisation of Calix[4]pyrroles Containing *N*-substituted Pyrrole Moieties" *Supramol. Chem*. 13, **2001**, 557.

Gale, P. A.; Quesada, R. "Anion coordination and anion-templated assembly: Highlights from 2002 to 2004" *Coord. Chem. Rev*. 250, **2006**, 3219.

Gale, P. A.; Tong, C. C.; Haynes, C. J. E.; Adeosun, O.; Gross, D. E.; Karnas, E.; Sedenberg, E. M.; Quesada, R.; Sessler, J. L. "Octafluorocalix[4]pyrrole: A Chloride/Bicarbonate Antiport Agent" *J. Am. Chem. Soc*. 132, **2010**, 3240.

Gill, H. S.; Harmjanz, M.; Santamaría, J.; Finger, I.; Scott, M. J. "Facile Oxidative Rearrangement of Dispiro-Porphodimethenes to Nonplanar and Sheetlike Porphyrins with Intense Absorptions in the Near-IR Region" *Angew. Chem. Int. Ed*. 43, **2004**, 485.

Gross, D. E.; Schmidtchen, F. P.; Antonius, W.; Gale, P. A.; Lynch, V. M.; Sessler, J. L. "Cooperative Binding of Calix[4]pyrrole-Anion Complexes and

Alkylammonium Cations in Halogenated Solvents" *Chem. Eur. J*. 14, **2008**, 7822.

Gu, R.; Depraetere, S.; Kotek, J.; Budka, J.; -Wysiecka, E. W.; Biernat, J. F.; Dehaen, W. "Anion recognition by α-arylazo-*N*-confused calix[4]pyrroles" *Org. Biomol. Chem*. 3, **2005**, 2921.

Hall, C. D.; Chu, S. Y. F. "Cyclic voltammetry of cryptands and cryptates containing the ferrocene unit" *J. Organomet. Chem*. 498, **1995**, 221.

[a]Harmjanz, M.; Scott, M. J. "A convenient synthesis of porphodimethenes and their conversion to trans-porphyrins with two functionalized *meso*-naphthyl substituents" *Chem. Commun*. **2000**, 397.

[b]Harmjanz, M.; Gill, H. S.; Scott, M. J. "Porphodimethene–Porphyrin Interconversion: A Tetrapyrrolic Redox-Switchable Macrocycle" *J. Am. Chem. Soc*. 122, **2000**, 10476.

Helten, H.; Beckmann, M.; Schnakenburg, G.; Streubel, R. "Synthesis and Reactivity of an Unusual Ferrocenophane Bis(carbene complex)" *Eur. J. Inorg. Chem*. **2010**, 2337.

Herberhold, M.; Steffl, U.; Milius, W.; Wrackmeyer, B. "1,2-Distanna[2]- and 1,2,3-Tristanna[3]-ferrocenophanes" *Angew. Chem. Int. Ed. Eng*. 35, **1996**, 1803.

Herbert, D. E.; Gilroy, J. B.; Staubitz, A.; Haddow, M. F.; Harvey, J. N.; Manners, I. "Strain-Induced Cleavage of Carbon-Carbon Bonds: Bridge Rupture Reactions of Group 8 Dicarba[2]metallocenophanes" *J. Am. Chem. Soc*. 132, **2010**, 1988.

Hlatky, G. G. "Metallocene catalysts for olefin polymerization: Annual review for 1996" *Coord. Chem. Rev*. 181, **1999**, 243.

Huang, C.; Li, Y.; Yang, J.; Cheng, N.; Liu, H.; Li. Y. "Construction of multi dimensional nanostructures by self-assembly of a porphyrin analogue" *Chem.*

Commun. 46, **2010**, 3161.

Hultzsch, K. C.; Nelson, J. M.; Lough, A. J.; Manners, I. "Synthesis, Characterization, and Homopolymerization and Copolymerization Behavior of the Silicon-Bridged [1]Chromarenophane $Cr(\eta\text{-}C_6H_5)_2SiMe$" *Organometallics* 14, **1995**, 5496.

Hung, C. -H.; Chang, G. -F.; Kumar, A.; Lin, G. -F.; Luo, L. -Y.; Ching, W. -M.; Diau, E. W. -G. "*m*-Benziporphodimethene: a new porphyrin analogue fluorescence zinc(II)sensor" *Chem. Commun*. **2008**, 978.

Ilango, S.; Vidjayacoumar, B.; Gambarotta, S. "Samarium complexes of a σ-/π-pyrrolide/arene based macrocyclic ligand" *Dalton Trans*. 39, **2010**, 6853.

Imahori, H.; Yamada, H.; Nishimura, Y.; Yamazaki, I.; Sakata, Y. "Vectorial Multistep Electron Transfer at the Gold Electrodes Modified with Self-Assembled Monolayers of Ferrocene−Porphyrin−Fullerene Triads" *J. Phys. Chem. B* 104, **2000**, 2099.

Inhoffen, H. H.; Buchler, J. W.; Jager. P. "Chemistry of chlorine and porphyrins [Chemie der Chlorine und Porphyrine.]" *Fortschr. Chem. Org. Natur*. 26, **1968**, 284.

Inoue, M.; Ikeda, C.; Kawata, Y.; Venkataraman, S.; Furukawa, K.; Osuka, A. "Synthesis of Calix[3]dipyrrins by a Modified Lindsey Protocol" *Angew. Chem. Int. Ed.* 46, **2007**, 2306.

Jäkle, F.; Priermeier, T.; Wagner, M. "Synthesis, Structure, and Dynamic Behavior of *ansa*-Ferrocenes with Pyrazabole Bridges" *Organometallics* 15, **1996**, 2033.

Jäkle, F.; Rulkens, R.; Zech, G.; Foucher, D. A.; Lough, A. J.; Manners, I. "Synthesis, Reactivity, and Ring-Opening Polymerization (ROP) of Tin-Bridged [1]Ferrocenophanes" *Chem. Eur. J*. 4, **1998**, 2117.

Jang, Y. -S.; Kim, H. -J.; Lee, P. -H.; Lee, C. -H. "Synthesis of calix[*n*]furano[*n*]pyrroles and calix[*n*]thieno[*n*]pyrroles (n=2,3,4) by '3+1' approach" *Tetrahedron Lett*. 41, **2000**, 2919.

Jeong, S. -D.; Yoo, J.; Na, H. -K.; Chi, D. Y.; Lee, C. -H. "Strapped-calix[4]pyrroles Bearing Acridine Moiety" *Supramol. Chem*. 19, **2007**, 271.

Ji, X. K.; Black, D. St. C.; Colbran, S. B.; Craig, D. C.; Edbey, K. M.; Harper, J. B.; Willett, G. D. "*meso*-Indanyl calix[4]pyrrole receptors" *Tetrahedron* 61, **2005**, 10705.

Jin, J.; Uozumi, T.; Sano, T.; Teranishi, T.; Soga, K.; Shiono, T. "Alternating copolymerization of ethylene and propene with the [ethylene(1-indenyl)(9-fluorenyl)]zirconium dichloridemethylaluminoxane catalyst system" *Macromol. Rapid Commun*. 19, **1998**, 337.

Jing, S.; Morley, C. P.; Gu, C. -Y.; Vaira, M. D. "1,5,9,13-Tetraselena[13]ferrocenophane: synthesis, complexation, crystallographic and electrochemical study" *Dalton Trans*. 39, **2010**, 8812.

Jubb, J.; Jacoby, D.; Floriani, C.; Chiesi-Villa, A.; Rizzoli, C. "Lithium-transition metal complexes derived from *meso*-octaethylporphyrinogen which display σ- and π-bonding modes" *Inorg. Chem*. 31, **1992**, 1306.

Kaifer, A. E.; Mendoza, S. In *Comprehensive Supramolecular Chemistry*; Gokel, G. W., Ed.; Pergamon: Oxford, **1996**; Vol. 1.

Kalisch, W. W.; Senge, M. O. "Facile *meso* Functionalization of Porphyrins by Nucleophilic Substitution with Organolithium Reagents" *Angew. Chem. Int. Ed*. 37, **1998**, 1107.

Kaminsky, W.; Külper, K.; Brintzinger, H. H.; Wild, F. R. W. P. "Polymerization of Propene and Butene with a Chiral Zirconocene and Methylalumoxane as Cocatalyst" *Angew. Chem. Int. Ed. Eng*. 24, **1985**, 507.

Kaminsky, W. "Highly active metallocene catalysts for olefin polymerization" *J. Chem. Soc., Dalton Trans*. **1998**, 1413.

Kealy, T. J.; Pauson, P. L. "A New Type of Organo-Iron Compound" *Nature* 168, **1951**, 1039.

Kettenback, R. T.; Butenschön, H. "(Cyclopentadienylalkyl)phosphane Cobalt(I) Chelate Complexes" *New J. Chem*. 14, **1990**, 599.

Khramov, D. M.; Rosen, E. L.; Lynch, V. M.; Bielawski, C. W. "Diaminocarbene[3]ferrocenophanes and Their Transition-Metal Complexes" *Angew. Chem. Int. Ed*. 47, **2008**, 2267.

Kojima, T.; Hanabusa, K.; Ohkubo, K.; Shiro, M.; Fukuzumi, S. "Formation of dodecaphenylporphodimethene via facile protonation of saddle-distorted dodecaphenylporphyrin" *Chem. Commun*. **2008**, 6513.

Král, V.; Gale, P. A.; Anzenbacher, P. Jr.; Jursíková, K.; Lynch, V.; Sessler, J. L. "Calix[4]pyridine: a new arrival in the heterocalixarene family" *Chem. Commun*. **1998**, 9.

Král, V.; Sessler, J. L.; Shishkanova, T. V.; Gale, P. A.; Volf, R. "Molecular Recognition at an organic-Aqueous Interface: Heterocalixarenes as Anion Binding Agents in Liquid Polymeric Membrane Ion-Selective Electrodes" *J. Am. Chem. Soc*. 121, **1999**, 8771.

Král, V.; Sessler, J. L.; Zimmerman, R. S.; Seidel, D.; Lynch, V.; Andrioletti, B. "Calixphyrins: Novel Macrocycles at the Intersection between Porphyrins and Calixpyrroles" *Angew. Chem. Int. Ed*. 39, **2000**, 1055.

Krattinger, B.; Callot, H. J. "New routes from porphyrins to stable phlorins. *Meso*-alkylation and reduction of *meso*-tetraphenyl- and octaalkylporphyrins" *Tetrahedron Lett*. 37, **1996**, 7699.

Krattinger, B.; Callot, H. J. "Addition of sterically hindered organolithium compounds to *meso*-tetraphenylporphyrin" *Tetrahedron Lett*. 39, **1998**, 1165.

Kunz, K.; Erker, G.; Döring, S.; Fröhlich, R.; Kehr, G. "Generation of Homogeneous (sp^3-C_1)-Bridged Cp/Amido and Cp/Phosphido Group 4 Metal Ziegler–Natta Catalyst Systems" *J. Am. Chem. Soc*. 123, **2001**, 6181.

Lee, B. Y.; Kim, Y. H.; Won, Y. C.; Shim, C. B.; Shin, D. M.; Chung, Y. K. "Synthesis, molecular structure, and polymerization reactivity of ethylenebis(1,3-dimethylcyclopentadienyl)zirconium dichloride" *J. Organomet. Chem.* 660, **2002**, 161.

Lee, C. -H.; Lindsey, J. S. "One-flask synthesis of *meso*-substituted dipyrromethanes and their application in the synthesis of *trans*-substituted porphyrin building blocks" *Tetrahedron* 50, **1994**, 11427.

Lee, C. -H.; Na, H. -K.; Yoon, D. -W.; Won, D. -H.; Cho, W. -S.; Lynch, V. M.; Shevchuk, S. V.; Sessler, J. L. "Single Side Strapping: A New Approach to Fine Tuning the Anion Recognition Properties of Calix[4]pyrroles" *J. Am. Chem. Soc*. 125, **2003**, 7301.

Lee, C. -H.; Lee, J. -S.; Na, H. -K.; Yoon, D. -W.; Miyaji, H.; Cho, W. -S.; Sessler, J. L. "Cis- and Trans-Strapped Calix[4]pyrroles Bearing Phthalamide Linkers: Synthesis and Anion-Binding Properties" *J. Org. Chem*. 70, **2005**, 2067.

Lee, C. -H.; Miyaji, H.; Yoon, D. -W.; Sessler, J. L. "Strapped and other topographically nonplanar calixpyrrole analogues. Improved anion receptors" *Chem. Commun*. **2008**, 24.

Lee, E. C.; Park, Y. -K.; Kim, J. -H.; Hwang, H.; Kim, Y. -R.; Lee, C. -H. "Bithiophene-containing super-expanded calixpyrrole analogues" *Tetrahedron Lett.* 43, **2002**, 9493.

Lee, M. H.; Park, J. -W.; Hong, C. S.; Woo, S. I.; Do, Y. "Ethylene-bridged pseudo-C_s symmetric *ansa*-zirconocene complexes: synthesis, structures and propylene polymerization behavior" *J. Organomet. Chem.* 561, **1998**, 37.

Levitskaia, T. G.; Marquez, M.; Sessler, J. L.; Shriver, J. A.; Vercouter, T.; Moyer, B. A. "Fluorinated calixpyrroles: anion-binding extractants that reduce the Hofmeister bias" *Chem. Commun*. **2003**, 2248.

Li, Q.; Mathur, G.; Gowda, S.; Surthi, S.; Zhao, Q.; Yu, L.; Lindsey, J. S.; Bocian, D. F.; Misra, V. "Multibit Memory Using Self-Assembly of Mixed Ferrocene/Porphyrin Monolayers on Silicon" *Adv. Mater.* 16, **2004**, 133.

Liddell, P. A.; Olmstead, M. M.; Smith, K. M. "Porphyrin synthesis from a,c-biladienes. Evidence for a common mechanistic pathway in the electrochemical and chemical routes: formation of novel macrocycles possessing the homoporphyrin carbon skeleton" *J. Am. Chem. Soc*. 112, **1990**, 2038.

Lindsey, J. S. In the porphyrin handbook, Kadish, K.; Smith, K. M.; Guilard, R. (Eds.), Vol 1, p. 45, Academic Press, San Diego, **1999**.

Lund, C. L.; Hanson, S. S.; Schatte, G.; Quail, J. W.; Müller, J. "*ansa*-Zirconocenes with Aluminum or Gallium in Bridging Positions" *Organometallics* 29, **2010**, 6038.

Lüttringhaus, A.; Kullick, W. "Ansa-ferrocene" *Angew. Chem.* 70, **1958**, 438.

Lüttringhaus, V. A.; Kullick, W. "Oligomethylenferrocene. Monomere („Ansa-Ferrocene"), Dimere und höhere Polymere" *Macromol. Chem*. 44-46, **1961**, 669.

Ma, K.; Fabrizi de Biani, F.; Bolte, M.; Zanello, P.; Wagner, M. "Electronic Communication in a series of Novel Multistep Redox Systems" *Organometallics* 21, **2002**, 3979.

Maeda, H. "Supramolecular Chemistry of Acyclic Oligopyrroles" *Eur. J. Org. Chem*. **2007**, 5313.

[a]Matano, Y.; Nakabuchi, T.; Miyajima, T.; Imahori, H. "Phosphole-Containing Hybrid Calixpyrroles: New Multifunctional Macrocyclic Ligands for Platinum(II) Ions" *Organometallics* 25, **2006**, 3105.

[b]Matano, Y.; Miyajima, T.; Nakabuchi, T.; Imahori, H.; Ochi, N.; Sakaki, S. "Phosphorus-Containing Hybrid Calixphyrins: Promising Mixed-Donor Ligands for Visible and Efficient Palladium Catalysts" *J. Am. Chem. Soc*. 128, **2006**, 11760.

[a]Matano, Y.; Miyajima, T.; Ochi, N.; Nakabuchi, T.; Shiro, M.; Nakao, Y.; Sakaki, S.; Imahori, H. "Syntheses, Structures, and Coordination Chemistry of Phosphole-Containing Hybrid Calixphyrins: Promising Macrocyclic P,N_2,X-Mixed Donor Ligands for Designing Reactive Transition-Metal Complexes" *J. Am. Chem. Soc*. 130, **2008**, 990.

[b]Matano, Y.; Miyajima, T.; Ochi, N.; Nakao, Y.; Sakaki, S.; Imahori, H. "Synthesis of Thiophene-Containing Hybrid Calixphyrins of the 5,10-Porphodimethene Type" *J. Org. Chem*. 73, **2008**, 5139.

Matano, Y.; Fujita, M.; Miyajima, T.; Imahori, H. "ZINC-INDUCED FLUORESCENCE ENHANCEMENT OF THE 5,10-PORPHODIMETHENE-TYPE THIOPHENE-CONTAINING CALIXPHYRINS" *Phos. Sul. Si*. 185, **2010**, 1098.

Matas, I.; Whittell, G. R.; Partridge, B. M.; Holland, J. P.; Haddow, M. F.; Green, J. C.; Manners. I. "Synthesis, Electronic Structure, and Reactivity of Strained Nickel-,

Palladium-, and Platinum-Bridged [1]Ferrocenophanes" *J. Am. Chem. Soc*. 132, **2010**, 13279.

Mauzerall, D.; Granick, S. "PORPHYRIN BIOSYNTHESIS IN ERYTHROCYTES: III. UROPORPHYRINOGEN AND ITS DECARBOXYLASE" *J. Biol. Che*. 232, **1958**, 1141.

Mauzerall, D. "THE PHOTOREDUCTION OF PORPHYRINS AND THE OXIDATION OF AMINES BY PHOTO-EXCITED DYES" *J. Am. Chem. Soc*. 82, **1960**, 1832.

McKnight, A. L.; Waymouth, R. M. "Group 4 *ansa*-Cyclopentadienyl-Amido Catalysts for Olefin Polymerization" *Chem. Rev*. 98, **1998**, 2587.

Medina, J. C.; Goodnow, T. T.; Rojas, M. T.; Atwood, J. L.; Lynn, B. C.; Kaifer, A. E.; Gokel, G. W. "Ferrocenyl iron as a donor group for complexed silver in ferrocenyldimethyl[2.2]cryptand: a redox-switched receptor effective in water" *J. Am. Chem. Soc*. 114, **1992**, 10583.

Metzger, A.; Anslyn, E. V. "A Chemosensor for Citrate in Beverages" *Angew. Chem. Int. Ed*. 37, **1998**, 649.

Miller, S. A.; Tebboth, J. A.; Tremaine, J. F. "*Dicyclopentadienyliron*" *J. Chem. Soc*. **1952**, 632.

Miyaji, H.; Anzenbacher, P. Jr.; Sessler, J. L.; Bleasdale, E. R.; Gale, P. A. "Anthracene-linked calix[4]pyrroles: fluorescent chemosensors for anions" *Chem. Commun*. **1999**, 1723.

Mizuta, T.; Onishi, M.; Miyoshi, K. "Photolytic Ring-Opening Polymerization of Phosphorus-Bridged [1]Ferrocenophane Coordinating to an Organometallic Fragment" *Organometallics* 19, **2000**, 5005.

Nagarajan, A.; Jang, Y. -S.; Lee, C. -H. "Convenient Route to Super-Expanded Calixpyrroles: Synthesis of Calix[*n*]furano[*m*]pyrroles (*n* = 3, 4, 6, 8 and *m* = 2, 4)" *Org. Lett*. 2, **2000**, 3115.

Nagarajan, A.; Ka, J. -W.; Lee, C. -H. "Synthesis of expanded calix[*n*]pyrroles and their furan or thiophene analogues" *Tetrahedron* 57, **2001**, 7323.

Nakabuchi, T.; Matano, Y.; Imahori, H. "Synthesis, Structures, and Coordinating Properties of Phosphole-Containing Hybrid Calixpyrroles" *Organometallics* 27, **2008**, 3142.

Namor, A. F. D.; Shehab, M. "Selective Recognition of Halide Anions by Calix[4]pyrrole: A Detailed Thermodynamic Study" *J. Phys. Chem. B* 107, **2003**, 6462.

Namor, A. F. D.; Shehab, M. "Recognition of Biologically and Environmentally Important Phosphate Anions by Calix[4]pyrrole: Thermodynamic Aspects" *J. Phys. Chem. A* 108, **2004**, 7324.

Namor, A. F. D.; Abbas, I.; Hammud, H. H. "Anion Complexation by Calix[3]thieno[1]pyrrole: The Medium Effect" *J. Phys. Chem. B* 110, **2006**, 2142.

[a]Namor, A. F. D.; Abbas, I.; Hammud, H. H. "A New Calix[4]pyrrole Derivative and Its Anion (Fluoride)/Cation (Mercury and Silver) Recognition" *J. Phys. Chem. B* 111, **2007**, 3098.

[b]Namor, A. F. D.; Abbas, I. "Sulfur-Containing Hetero-Calix[4]pyrroles as Mercury(II) Cation-Selective Receptors: Thermodynamic Aspects" *J. Phys. Chem. B* 111, **2007**, 5803.

Nayar, P.; Brun, A. M.; Harriman, A.; Begley, T. P. "Mechanistic studies on proto chlorophyllide reductase: a model system for the enzymatic reaction" *J. Chem. Soc., Chem. Commun*. **1992**, 395.

Ogasawara, M.; Nagano, T.; Hayashi, T. "Metathesis Route to Bridged Metallocenes" *J. Am. Chem. Soc.* 124, **2002**, 9068.

Osborne, A. G.; Whiteley, R. H. "Silicon Bridged [1] ferrocenophanes" *J. Organomet. Chem*. 101, **1975**, C27.

Osborne, A. G.; Whiteley, R. H.; Meads, R. E. "[1] Ferrocenophanes. synthesis and spectroscopic properties of [1] ferrocenophanes with group IV and V elements as bridge atoms" *J. Organomet. Chem*. 193, **1980**, 345.

Otón, F.; Tórraga, A.; Espinosa, A.; Velasco, M. D.; Molina, P. "Ferrocene-Based Ureas as Multisignalling Receptors for Anions" *J. Org. Chem*. 71, **2006**, 4590.

Peckham, T. J.; Foucher, D. A.; Lough, A. J.; Manners, I. "The synthesis and polymerization behaviour of silicon-bridged [1]- and [2]ferrocenophanes with sterically demanding trimethylsilyl substituents attached to the cyclopentadienyl rings" *Can. J. Chem*. 73, **1995**, 2069.

Piatek, P.; Lynch, V. M.; Sessler, J. L. "Calix[4]pyrrole[2]carbazole: A New Kind of Expanded Calixpyrrole" *J. Am. Chem. Soc*. 126, **2004**, 16073.

Plenio, H.; Diodone, R. "Complexation of Na^+ in Redox-Active Ferrocene Crown Ethers, a Structural Investigation, and an Unexpected Case of Li^+ Selectivity" *Inorg. Chem*. 34, **1995**, 3964.

Plenio, H.; Aberle, C. "An Artificial Regulatory System with Coupled Molecular Switches" *Angew. Chem. Int. Ed*. 37, **1998**, 1397.

Plenio, H.; Aberle, C.; Shihadeh, Y. A.; Lloris, J. M.; Martínez-Máñez, R.; Pardo, T.; Soto, J. "Ferrocene - Cyclam: A Redox-Active Macrocycle for the Complexation of Transition Metal Ions and a Study on the Influence of the Relative Permittivity on the Coulombic Interaction between Metal Cations" *Chem. Eur. J*. 7, **2001**, 2848.

Pohl, M.; Schmickler, H.; Lex, J.; Vogel, E. "Isophlorins: Molecules at the Crossroads of Porphyrin and Annulene Chemistry" *Angew. Chem. Int. Ed.* 30, **1991**, 1693.

Poulsen, T.; Nielsen, K. A.; Bond, A. D.; Jeppesen, J. O. "Bis(tetrathiafulvalene)-Calix[2]pyrrole[2]-thiophene and Its Complexation with TCNQ" *Org. Lett*. 9, **2007**, 5485.

Pudelski, J. K.; Gates, D. P.; Rulkens, R.; Lough, A. J.; Manners, I. "Synthesis and Structure of the First Sulfur-Bridged [1]Ferrocenophane" *Angew. Chem. Int. Ed. Eng*. 34, **1995**, 1506.

Qian, C.; Zou, G.; Sun, J. "Chiral lanthanocene complexes with an ether-functionalized indene ligand: synthesis and structure of bis{1-(2-methoxyethyl)indenyl}lanthanocene chlorides" *J. Organomet. Chem*. 566, **1998**, 21.

Ramakrishnan, S.; Srinivasan, A. "*ansa*-Metallocene-Based Cyclic[2]pyrroles" *Org. Lett*. 9, **2007**, 4769.

Ramakrishnan, S.; Anju, K. S.; Thomas, A. P.; Suresh, E.; Srinivasan, A. "Calix[*n*]metallocenyl[*m*]phyrins (n = 1, 2 and m = 2, 4): aryl *vs*. alkyl" *Chem. Commun*. 46, **2010**, 4746

Reetz, M. T.; Willuhn, M.; Psiorz, C.; Goddard, R. "Donor complexes of bis(1-indenyl)phenylborane dichlorozirconium as isospecific catalysts in propene polymerization" *Chem. Commun*. **1999**, 1105.

Reynes, O.; Bucher, C.; Moutet, J. -C.; Royal, G.; Aman, E. S.; Ungureanu, E. -M. "Electrochemical sensing of anions by redox-active receptors built on the ferrocenyl cyclam framework" *J. Electroanal. Chem*. 580, **2005**, 291.

Rieger, B. "Preparation and some properties of chiral *ansa*-mono(η5-fluorenyl)zirconium(IV) complexes" *J. Organomet. Chem*. 420, **1991**, C17.

Rothemund, P.; Gage, C. L. "Concerning the Structure of "Acetonepyrrole" " *J. Am. Chem. Soc*. 77, **1955**, 3340.

Rulkens, R.; Lough, A. J.; Manners, I. "Synthesis and Ring-Opening Polymerization of a Tin-Bridged [1]Ferrocenophane" *Angew. Chem. Int. Ed. Engl*. 35, **1996**, 1805.

Rulkens, R.; Gates, D. P.; Balaishis, D.; Pudelski, J. K.; McIntosh, D. F.; Lough, A. J.; Manners, I. "Highly Strained, Ring-Tilted [1]Ferrocenophanes Containing Group 16 Elements in the Bridge: Synthesis, Structures, and Ring-Opening Oligomerization and Polymerization of [1]Thia- and [1]Selenaferrocenophanes" *J. Am. Chem. Soc*. 119, **1997**, 10976.

Runge, S.; Senge, M. O. "Electron Donor-Acceptor Compounds. Synthesis and Structure of 5-(1,4-Benzoquinone-2-yl)-10,15,20-trialkylporphyrins" *Z. Naturforsch*. 53b, **1998**, 1021.

Ruppert, R.; Jeandon, C.; Sgambati, A.; Callot, H. J. "Reduction of *N*-arylporphyrins to *N*-arylphlorins: opposite stereochemical courses as a function of the reducing agent" *Chem. Commun*. **1999**, 2123.

Saji, T. "ELECTROCHEMICALLY SWITCHED CATION BINDING IN PENTAOXA[13] FERROCENOPHANE" *Chem. Lett*. **1986**, 275.

Schachner, J. A.; Lund, C. L.; Quail, J. W.; Müller, J. "Synthesis and Characterization of the First Aluminum-Bridged [1]Ferrocenophane" *Organometallics* 24, **2005**, 785.

Scherer, M.; Sessler, J. L.; Gebauer, A.; Lynch, V. "A bridged pyrrolic *ansa*-ferrocene. A new type of anion receptor" *Chem. Commun*. **1998**, 85.

Schnutenhaus, H.; Brintzinger, H. H. "1,1'-Trimethylenebis(η^5-3-*tert*-butylcyclopentadienyl)-titanium(IV)Dichloride, a Chiral *ansa*-Titanocene Derivative" *Angew. Chem. Int. Ed. Engl*. 18, **1979**, 777.

Senge, M. O.; Smith, K. M. "Metal Complexes of Dioxo-Porphyrins - Zinc(II) Complexes of 5,15-Dioxo-2,3,7,8,12,13,17,18-octaethyl-porphyrin and 5,15-dioxo-etioporphyrin I" *Z. Naturforsch*. 48b, **1993**, 991.

[a]Senge, M. O.; Runge, S.; Speck, M.; Ruhlandt-Senge, K. "Identification of Stable Porphomethenes and Porphodimethenes from the Reaction of Sterically Hindered Aldehydes with Pyrrole" *Tetrahedron* 56, **2000**, 8927.

[b]Senge, M. O.; Feng, X. "Regioselective reaction of 5,15-disubstituted porphyrins with organolithium reagents—synthetic access to 5,10,15-trisubstituted porphyrins and directly *meso-meso*-linked bisporphyrins" *J. Chem. Soc., Perkin Trans*. 1, **2000**, 3615.

Sessler, J. L.; Weghorn, S. J.; Hiseada, Y.; Lynch, V. "Hexaalkyl Terpyrrole: A New Building Block for the Preparation of Expanded Porphyrins" *Chem. Eur. J*. 1, **1995**, 56.

Sessler, J. L.; Andrievsky, A.; Gale, P. A.; Lynch, V. "Anion Binding: Self-Assembly of Polypyrrolic Macrocycles" *Angew. Chem. Int. Ed. Engl*. 35, **1996**, 2782.

Sessler, J. L.; Gebauer, A.; Gale, P. A. "Anion Binding and Electrochemical Properties Of Calix[4]pyrrole Ferrocene Conjugates" *Gazz. Chim. Ital*. 127, **1997**, 723.

[a]Sessler, J. L.; Gale, P. A.; Genge, J. W. "Calix[4]pyrroles: New Solid-Phase HPLC Supports for the Separation of Anions" *Chem. Eur. J*. 4, **1998**, 1095.

[b]Sessler, J. L.; Anzenbacher, P. Jr.; Jursiková, K.; Miyaji, H.; Genge, J. W.; Tvermoes, N. A.; Allen, W. E.; Shriver, J. A.; Gale, P. A.; Král, V. "Functionalized calix[4]pyrroles" *Pure Appl. Chem*. 70, **1998**, 2401.

[a]Sessler, J. L.; Anzenbacher, P. Jr.; Miyaji, H.; Jursíková, K.; Bleasdale, E. R.; Gale, P. A. "Modified Calix[4]pyrroles" *Ind. Eng. Chem. Res*. 39, **2000**, 3471.

[b]Sessler, J. L.; Gale, P. A.; in The Porphyrin Handbook, *Vol. 6* (Eds.: K. M. Kadish, K. M. Smith, R. Guilard), Academic Press, San Diego, **2000**, 257.

[c]Sessler, J. L.; Anzenbacher, P. Jr.; Shriver, J. A.; Jursíkova, K.; Lynch, V. M.; Marquez, M. "Direct Synthesis of Expanded Fluorinated Calix[*n*]pyrroles: Decafluorocalix[5]pyrrole and Hexadecafluorocalix[8]pyrrole" *J. Am. Chem. Soc*. 122, **2000**, 12061.

[a]Sessler, J. L.; Davis, J. M. "Sapphyrins: Versatile Anion Binding Agents" *Acc. Chem. Res*. 34, **2001**, 989.

[b]Sessler, J. L.; Zimmerman, R. S.; Kirkovits, G. J.; Gebauer, A.; Scherer. M. "Synthesis and hydrogen phosphate binding properties of pyrrole containing *ansa*-ferrocenes" *J. Organometallic Chem*. 637–639, **2001**, 343.

[c]Sessler, J. L.; Zimmerman, R. S.; Bucher, C.; Král, V.; Andrioletti, B. "Calixphyrins Hybrid macrocycles at the structural crossroads between porphyrins and calixpyrroles" *Pure Appl. Chem.* 73, **2001**, 1041.

Sessler, J. L.; Cho, W. -S.; Lynch, V.; Král, V. "Missing-Link Macrocycles: Hybrid Heterocalixarene Analogues Formed from Several Different Building Blocks" *Chem. Eur. J*. 8, **2002**, 1134.

[a]Sessler, J. L.; Camiolo, S.; Gale, P. A. "Pyrrolic and polypyrrolic anion binding agents" *Coord. Chem. Rev*. 240, **2003**, 17.

[b]Sessler, J. L.; An, D.; Cho, W. -S.; Lynch, V. M. "Calix[2]bipyrrole[2]furan and Calix[2]bipyrrole[2]thiophene: New Pyrrolic Receptors Exhibiting a Preference for Carboxylate Anions" *J. Am. Chem. Soc*. 125, **2003**, 13646.

[c]Sessler, J. L.; An, D.; Cho, W. -S.; Lynch, V. "Calix[*n*]bipyrroles: Synthesis, Characterization, and Anion-Binding Studies" *Angew. Chem. Int. Ed*. 42, **2003**, 2278.

[a]Sessler, J. L.; An, D.; Cho, W. -S.; Lynch, V.; Yoon, D. -W.; Hong, S. -J.; Lee, C. -H. "Anion-Binding Behavior of Hybrid Calixpyrroles" *J. Org. Chem*. 70, **2005**, 1511.

[b]Sessler, J. L.; An, D.; Cho, W. -S.; Lynch, V.; Marquez, M. "Calix[*n*]bispyrrolylbenzenes: Synthesis, Characterization, and Preliminary Anion Binding Studies" *Chem. Eur. J*. 11, **2005**, 2001.

[c]Sessler, J. L.; An, D.; Cho, W. -S.; Lynch, V.; Marquez, M. "Calix[4]bipyrrole–a big, flexible, yet effective chloride-selective anion receptor" *Chem. Commun*. **2005**, 540.

[d]Sessler, J. L.; Cho, W. -S.; Gross, D. E.; Shriver, J. A.; Lynch, V. M.; Marquez, M. "Anion Binding Studies of Fluorinated Expanded Calixpyrroles" *J. Org. Chem*. 70, **2005**, 5982.

Sessler, J. L.; Gross, D. E.; Cho, W. -S.; Lynch, V. M.; Schmidtchen, F. P.; Bates, G. W.; Light, M. E.; Gale, P. A. "Calix[4]pyrrole as a Chloride Anion Receptor: Solvent and Countercation Effects" *J. Am. Chem. Soc.* 128, **2006**, 12281.

Sessler, J. L.; Roznyatovskiy, W.; Lynch, V. M. "Novel β-substituted calix[4]pyrroles" *J. Porphyrins Phthalocyanines* 13, **2009**, 322.

Setsune, J.; Yazawa, T.; Ogoshi, H.; Yoshida, Z. "Meso-substitution reactions of rhodium(III)–octaethylporphyrins with organolithium reagents" *J. Chem. Soc., Perkin Trans. 1*. **1980**, 1641.

Seyferth, D.; Withers, H. P. Jr. "Phosphorus- and arsenic-bridged [1]ferrocenophanes. 1. Synthesis and characterization" *Organometallics* 1, **1982**, 1275.

Shapiro, P. J. " Boron-Bridged Group-4 *ansa*-Metallocene Complexes" *Eur. J. Inorg. Chem*. **2001**, 321.

Shapiro, P. J. "The evolution of the *ansa*-bridge and its effect on the scope of metallocene chemistry" *Coord. Chem. Rev*. 231, **2002**, 67.

Shapiro, P. J.; Jiang, F.; Jin, X.; Twamley, B.; Patton, J. T.; Rheingold, A. L. "Zwitterionic Phosphorus Ylide Adducts of Boron-Bridged *ansa*-Zirconocene Complexes as Precatalysts for Olefin Polymerization" *Eur. J. Inorg. Chem*. **2004**, 3370.

Sheldrick, G. M. (**1997**). SHELXL97. University of Göttingen, Germany.

Shelnutt, J. A.; Song, X. -Z.; Ma, J. -G.; Jia, S. -L.; Jentzen, W.; Medforth, C. J. "Nonplanar porphyrins and their significance in proteins" *Chem. Soc. Rev*. 27, **1998**, 31.

SHELXL-97: Programs for Crystal Structure Analysis, G. M. Sheldrick, University of Göttingen (Germany), **1998**.

Shriver, J. A. Ph.D. Dissertation, The University of Texas at Austin, **2002**.

Smith, J. A.; Seyerl, J. V.; Huttner, G.; Brintzinger, H. H. "*ansa*-Metallocene derivatives : Molecular structure and proton magnetic resonance spectra or methylene- and ethylene-bridged dicyclopentadienyltitanium compounds" *J. Organomet. Chem*. 173, **1979**, 175.

Sobral, A. J. F. N.; Rebanda, N. G. C. L.; da Silva, M.; Lampreia, S. H.; Silva, M. R.; Beja, A. M.; Paixão, J. A.; Gonsalves, A. M. A. R. "One-step synthesis of dipyrromethanes in water" *Tetrahedron Lett*. 44, **2003**, 3971.

Song, M. -Y.; Na, H. K.; Kim, E. -Y.; Lee, S. -J.; Kim, K. I.; Baek, E. -M.; Kim, H. -S.; An, D. K.; Lee, C. -H. "Hetero-calix[4]pyrroles: incorporation of furans, thiophenes, thiazoles or fluorenes as a part of the macrocycle" *Tetrahedron Lett*. 45, **2004**, 299.

Spaleck, W.; Antberg, M.; Dolle, V.; Klein, R.; Rohrmann, J.; Winter, A. "Stereorigid Metallocenes: Correlations Between Structure and Behaviour in Homopolymerizations of Propylene" *New J. Chem.* 14, **1990**, 499.

Spek, A. L. "Single-crystal structure validation with the program PLATON" *J. Appl. Cryst.* 36, **2003**, 7.

Srinivasan, A.; Mahajan, S.; Pushpan, S. K.; Kumar, M. R.; Chandrashekar, T. K. "Synthesis of *meso*-substituted core modified expanded porphyrins; effect of acid catalysts on the cyclization" *Tetrahedron Lett.* 39, **1998**, 1961.

[a]Srinivasan, A.; Pushpan, S. K.; Kumar, M. R.; Mahajan, S.; Chandrashekar, T. K.; Roy, R.; Ramamurthy, P. "*meso*-Aryl sapphyrins with heteroatoms; synthesis, characterization, spectral and electrochemical properties" *J. Chem. Soc. Perkin. Trans. 2*. **1999**, 961.

[b]Srinivasan, A.; Anand, V. G.; Narayanan, S. J.; Pushpan, S. K.; Kumar, M. R.; Chandrashekar, T. K.; Sugiura, K. -I.; Sakata, Y. "Structural Characterization of Meso Aryl Sapphyrins" *J. Org. Chem.* 64, **1999**, 8693.

Stehling, U.; Diebold, J.; Kirsten, R.; Roell, W.; Brintzinger, H. H.; Juengling, S.; Muelhaupt, R.; Langhauser, F. "ansa-Zirconocene Polymerization Catalysts with Anelated Ring Ligands -Effects on Catalytic Activity and Polymer Chain Length" *Organometallics* 13, **1994**, 964.

Stępień, M.; Simkowa, I.; Grażyński, L. L. "Helical Porphyrinoids: Incorporation of Ferrocene Subunits into Macrocyclic Structures" *Eur. J. Org. Chem.* **2008**, 2601.

Stoeckli-Evans, H.; Osborne, A. G.; Whiteley, R. H. "Ring-tilted ferrocenophanes. the crystal and molecular structures of (1,1'-ferrocenediyl)diphenylgermane and (1,1'-ferrocenediyl)phenylphosphine" *J. Organomet. Chem.* 194, **1980**, 91.

Sugimoto, H. "Phlorin complex of gold(III)" *J. Chem. Soc., Dalton tans.* **1982**, 1169.

Suijkerbuijk, B. M. J. M.; Gebbink, R. J. M. K. "Merging Porphyrins with Organo metallics: Synthesis and Applications" *Angew. Chem. Int. Ed*. 47, **2008**, 7396.

Swanson, K. L.; Snow, K. M.; Jeyakumar, D.; Smith, K. M. "Tetrapyrrole products from electrochemical cyclization of 1′,8′-Disubstituted-a,c-biladiene salts" *Tetrahedron* 47, **1991**, 685.

Szymańska, I.; Radecka, H.; Radecki, J.; Gale, P. A.; Warriner, C. N. "Ferrocenyl-substituted calix[4]pyrrole modified carbon paste electrodes for anion detection in water" *J. Elec. Chem*. 591, **2006**, 223.

Tendero, M. J. L.; Benito, A.; Cano, J.; Lloris, J. M.; Martínez-Máñez, R.; Soto, J.; Edwards, A. J.; Raithby, P. R.; Rennie, A. "Host molecules containing electroactive cavities obtained by the molecular assembly of redox-active ligands and metal ions" *J. Chem. Soc., Chem. Commun*. **1995**, 1643.

Tian, G.; Wang, B.; Dai, X.; Xu, S.; Zhou, X.; Sun, J. "Synthesis, structures and catalytic properties of Group 4 metallocenes based upon $[Me_2E(C_5H_4)(C_5Me_4)]_2$ (E=Si, Ge) supporting coordination" *J. Organomet. Chem*. 634, **2001**, 145.

Tietze, L. F.; Geissler, H. "Investigations in the Biosynthesis of the Pigments of Life: Calculations on the Formation of Uroporphyrinogen III from Hydroxymethylbilan and Description of a New Mechanism for the D-Ring Inversion" *Angew. Chem. Int. Ed. Engl*. 32, **1993**, 1040.

Tomapatanaget, B.; Tuntulani, T.; Chailapakul, O. "Calix[4]arenes Containing Ferrocene Amide as Carboxylate Anion Receptors and Sensors" *Org. Lett*. 5, **2003**, 1539.

Tong, C. C.; Quesada, R.; Sessler, J. L.; Gale, P. A. "*meso*-Octamethylcalix[4]pyrrole: an old yet new transmembrane ion-pair transporter" *Chem. Commun*. **2008**, 6321.

Turner, B.; Botoshansky, M.; Eichen, Y. "Extended Calixpyrroles: *meso*-Substituted Calix[6]pyrroles" *Angew. Chem. Int. Ed*. 37, **1998**, 2475.

Turner, B.; Shterenberg, A.; Kapon, M.; Suwinska, K.; Eichen, Y. "Selective anion binding and solid-state host-guest chemistry of an extended cavity calix[6]pyrrole" *Chem. Commun*. **2001**, 13.

[a]Turner, B.; Shterenberg, A.; Kapon, M.; Suwinska, K.; Eichen, Y. "The role of template in the synthesis of *meso*-hexamethyl-*meso*-hexaphenyl-calix[6]pyrrole: trihalogenated compounds as templates for the assembly of a host with a trigonal cavity" *Chem. Commun*. **2002**, 404.

[b]Turner, B.; Shterenberg, A.; Kapon, M.; Botoshansky, M.; Suwinska, K.; Eichen, Y. "Self-assembled calix[6]pyrrole capsules: solid-state encapsulation of different guests in preorganised calix[6]pyrrole capsules" *Chem. Commun*. **2002**, 726.

Yoon, D. -W.; Jeong, S. -D.; Song, M. -Y.; Lee. C. -H. "Calix[6]pyrroles Capped with 1,3,5-Trisubstituted Benzene" *Supramol. Chemistry*, 19, **2007**, 265.

Ulman, A.; Manassen, J. "Synthesis of new tetraphenylporphyrin molecules containing heteroatoms other than nitrogen. I. Tetraphenyl-21,23-dithiaporphyrin" *J. Am. Chem. Soc*. 97, **1975**, 6540.

Ulman, A.; Manassen, J. " Synthesis of tetraphenylporphyrin molecules containing heteroatoms other than nitrogen. Part 4. Symmetrically and unsymmetrically substituted tetra phenyl-21,23-dithiaporphyrins" *J. Chem. Soc. Perkin Trans. 1.* **1979**, 1066.

Uno, H.; Inoue, T.; Fumoto, Y.; Shiro, M.; Ono, N. "*meso*-Unsubstituted Porphyrinogens and Hexaphyrinogens: The First X-ray Characterization" *J. Am. Chem. Soc*. 122, **2000**, 6773.

Uosaki, K.; Kondo, T.; Zhang, X. -Q.; Yanagida, M. "Very Efficient Visible-Light-Induced Uphill Electron Transfer at a Self-Assembled Monolayer with a

Porphyrin–Ferrocene–Thiol Linked Molecule" *J. Am. Chem. Soc*. 119, **1997**, 8367.

van Hoorn, W. P.; Jorgensen, W. L. "Selective Anion Complexation by a Calix[4]pyrrole Investigated by Monte Carlo Simulations" *J. Org. Chem*. 64, **1999**, 7439.

Varadarajan, A.; Johnson, S. E.; Gomez, F. A.; Chakrabarti, S.; Knobler, C. B.; Hawthorne, M. F. "Synthesis and structural characterization of pyrazole-bridged metalla-bis(dicarbollide) derivatives of cobalt, nickel, copper, and iron: models for venus flytrap cluster reagents" *J. Am. Chem. Soc*. 114, **1992**, 9003.

Vogel's Textbook of Practical Organic Chemistry, Furniss, B. S. Ed: ELBS and Longmann: 4th edition, **1978**, Chapter 2. (b) Weissberger, A.; Proskraner, E. S.: Riddick, J. A.; Toppos Jr., E. F. *Organic Solvents in Techniques of Organic Chemistry*, *Vol. IV*, 3rd edition, Inc. New York, **1970**.

Wagner, H.; Baumgartner, J.; Marschner, C. "1,1'-Oligosilylferrocene Compounds" *Organometallics* 26, **2007**, 1762.

Wang, B.; Mu, B.; Deng, X.; Cui, H.; Xu, S.; Zhou, X.; Zou, F.; Li, Y.; Yang, L.; Li, Y.; Hu, Y. "Synthesis and Structures of Cycloalkylidene-Bridged Cyclopentadienyl Metallocene Catalysts: Effects of the Bridges of *Ansa*-Metallocene Complexes on the Catalytic Activity for Ethylene Polymerization" *Chem. Eur. J*. 11, **2005**, 669.

Wang, B. "*Ansa*-metallocene polymerization catalysts: Effects of the bridges on the catalytic activities" *Coord. Chem. Rev*. 250, **2006**, 242.

Whittell, G. R.; Partridge, B. M.; Presly, O. C.; Adams, C. J.; Manners, I. "Strained Metallocenophanes with Late Transition Metals in the Bridge: Syntheses and Structures of Nickel- and Platinum-Bridged [1]Ferrocenophanes" *Angew. Chem. Int. Ed*. 47, **2008**, 4354.

Wild, F. R. W. P.; Zsolnai, L.; Huttner, G.; Brintzinger, H. H. "*ansa*-Metallocene Derivatives : IV. Synthesis and molecular structures of chiral *ansa*-titanocene derivatives with bridged tetrahydroindenyl ligands*" J. Organomet. Chem*. 232, **1982**, 233.

Wild, F. R. W.P.; Wasiucionek, M.; Huttner, G.; Brintzinger, H. H. "*ansa*-Metallocene derivatives : VII. Synthesis and crystal structure of a chiral *ansa*-zirconocene derivative with ethylene-bridged tetrahydroindenyl ligands" *J. Organomet. Chem.* 288, **1985**, 63.

Wilkinson, G.; Rosenblum, M.; Whiting, M. C.; Woodward, R. B. "THE STRUCTURE OF IRON BIS-CYCLOPENTADIENYL" *J. Am. Chem. Soc*. 74, **1952**, 2125.

Wintergerst, M. P.; Levitskaia, T. G.; Moyer, B. A.; Sessler, J. L.; Delmau, L. H. "Calix[4]pyrrole: A New Ion-Pair Receptor As Demonstrated by Liquid-Liquid Extraction" *J. Am. Chem. Soc*. 130, **2008**, 4129.

Wochner, F.; Zsolnai, L.; Huttner, G.; Brintzinger, H. H. "*ansa*-Metallocene derivatives : VIII. Syntheses and crystal structures of ethylene-bridged titanocene and zirconocene derivatives with permethylated ring ligands" *J. Organomet. Chem*. 288, **1985**, 69.

Won, D. -H.; Toganoh, M.; Terada, Y.; Fukatsu, S.; Uno, H.; Furuta, H. "Near-Infrared Emission from Bis-Pt^{II} Complexes of Doubly N-Confused Calix[6]phyrins (**1**.**1**.*1*.**1**.**1**.*1*)" *Angew. Chem. Int. Ed.* 47, **2008**, 5438.

Woods, C. J.; Camiolo, S.; Light, M. E.; Coles, S. J.; Hursthouse, M. B.; King, M. A.; Gale, P. A.; Essex, J. W. "Fluoride-Selective Binding in a New Deep Cavity Calix[4]pyrrole: Experiment and Theory" *J. Am. Chem. Soc*. 124, **2002**, 8644.

Woodward, R. B. *Ind. Chim. Belge*. 27, **1962**, 1293.

Wu, Y. -D.; Wang, D. -F.; Sessler, J. L. "Conformational Features and Anion-Binding Properties of Calix[4]pyrrole: A Theoretical Study" *J. Org. Chem.* 66, **2001**, 3739.

Xie, H.; Smith. K. M. "Stable isoporphyrin chromophores: synthesis" *Tetrahedron Lett.* 33, **1992**, 1197.

Xu, S.; Deng, X.; Wang, B.; Zhou, X.; Yang, L.; Li, Y.; Hu, Y.; Zou, F.; Li, Y. "Ethylene Polymerization with Cycloalkylidene-Bridged Cyclopentadienyl Metallocene Catalysts" *Macromol. Rapid Commun.* 22, **2001**, 708.

Xu, S.; Dai, X.; Wang, B.; Zhou, X. "Synthesis, structures and polymerization catalytic properties of germyl-bridged bis(cyclopentadienyl) metallocenes" *J. Organomet. Chem.* 645, **2002**, 262.

Yoo, J.; Kim, Y.; Kim, S. -J.; Lee, C. -H. "Anion-modulated, highly sensitive supramolecular fluorescence chemosensor for C_{70}" *Chem. Commun.* 46, **2010**, 5449.

Yoon, D. -W.; Jeong, S. -D.; Song, M. -Y.; Lee. C. -H. "Calix[6]pyrroles Capped with 1,3,5-Trisubstituted Benzene" *Supramolecular Chemistry*, 19, **2007**, 265.

Yoon, D. -W.; Gross, D. E.; Lynch, V. M.; Sessler, J. L.; Hay, B. P.; Lee, C. -H. "Benzene-, Pyrrole-, and Furan-Containing Diametrically Strapped Calix[4]pyrroles–An Experimental and Theoretical Study of Hydrogen-Bonding Effects in Chloride Anion Recognition" *Angew. Chem. Int. Ed.* 47, **2008**, 5038.